

N67-33893

NASA CR-66437

FACILITY FORM 802

(ACCESSION NUMBER)	(THRU)
144	0
(PAGES)	(CODE)
CR-66437	31
(NASA CR OR TMX OR AD NUMBER)	(CATEGORY)

LUNAR ORBITER II

VOLUME III

MISSION SYSTEM PERFORMANCE

Prepared for the
NATIONAL AERONAUTICS AND SPACE ADMINISTRATION
Langley Research Center

by

THE **BOEING** COMPANY

Contract No. NAS1-3800

April 24, 1967

BOEING DOCUMENT NO. D2-100752-3 (VOL. III)

Distribution of this report is provided in the interest of information exchange. Responsibility for the contents resides in the author or organization that prepared it.

FOREWORD

The Lunar Orbiter II final report is divided into six volumes as follows.

Volume I	Mission Summary
Volume II	Photography
Volume III	Mission System Performance
Volume IV	Extended-Mission Operations
Volume V	Extended-Mission Spacecraft Subsystem Performance
Volume VI	Appendices

Volume I summarizes the photographic mission concepts and conduct, system performance, and results. Volume II contains the mission photographic planning and conduct and a description and analysis of the photos obtained during Mission II together with photo supporting data. Volume III contains a discussion and performance analysis of the Lunar Orbiter and its subsystems. It also includes launch operations, flight conduct and flight path control information, as well as discussions of the anomalies encountered during the mission. Volume IV summarizes the operational reports covering the extended mission. Volume V contains a discussion and analysis of the spacecraft performance and of the experiments conducted and anomalies encountered during the extended mission. Volume VI contains selected detail data and information in support of the analyses presented in Volumes II and III.

Descriptions of the Lunar Orbiter hardware will be found in the Lunar Orbiter I Final Report, Boeing Documents D2-100727-1 through -6.

CONTENTS

	Page No
* 3.0 MISSION SYSTEM PERFORMANCE	1
3.1 LAUNCH OPERATIONS	1
3.1.1 Spacecraft Processing	1
3.1.1.1 Hangar "S"	1
3.1.1.2 Explosive Safe Area (ESA)	4
3.1.1.3 Launch Pad 13	5
3.1.2 Launch Conduct	6
3.1.2.1 Launch Criteria	6
3.1.2.2 Countdown and Launch	7
3.1.2.3 Weather	8
3.1.2.4 Tracking Coverage	8
3.1.2.5 Telemetry Coverage	9
3.1.3 Launch Vehicle Performance	15
3.1.3.1 Atlas Performance	19
3.1.3.2 Agena Performance	19
3.2 FLIGHT OPERATIONS	20
3.2.1 Flight Plan	21
3.2.1.1 Introduction	21
3.2.1.2 Preparation	22
3.2.1.3 Mission I/Mission II comparisons	22
3.2.1.4 Significant Events Summary	23
3.2.2 Flight Conduct	25
3.2.2.1 Spacecraft Control	25
3.2.2.1.1 Command Programming	25
3.2.2.1.2 Photography Control	26
3.2.2.2 Flight Path Control	27
3.2.2.2.1 Countdown, Launch, and Acquisition Phase	28
3.2.2.2.2 Injection through Midcourse	30
3.2.2.2.3 Midcourse through Deboost	34
3.2.2.2.4 Initial Ellipse	39
3.2.2.2.5 Photo Ellipse	51
3.2.3 Spacecraft Performance Summary	59
3.2.3.1 Photographic Subsystem	63
3.2.3.2 Power Subsystem	66
3.2.3.3 Communications Subsystem	74
3.2.3.4 Attitude Control Subsystem	80
3.2.3.5 Velocity Control Subsystem	92
3.2.3.6 Structures and Mechanisms Subsystem	102

CONTENTS

	Page No
3.2.4 Data System Performance	110
3.2.4.1 Ground Equipment at DSS-12, -41, and -61	110
3.2.4.1.1 DSS Antenna Problems	110
3.2.4.1.2 Ground Reconstruction (GRE) Problems	110
3.2.4.1.3 Processing and Film Evaluation Problems	114
3.2.4.2 Ground Communication System	115
3.2.4.2.1 DSS-12 Ground Communications	115
3.2.4.2.2 DSS-41 Ground Communications	115
3.2.4.2.3 DSS-61 Ground Communications	115
3.2.4.3 SFOF	116
3.2.4.3.1 Central Computing Complex	116
3.2.4.3.2 GRE and Photo Processor	116
3.2.4.4 Software	117
3.2.4.4.1 System Software	117
3.2.4.4.2 FPAC Software System Performance	118
3.2.4.4.3 SPAC Software System Performance	118
3.2.5 Lunar Environmental Data	118
3.2.5.1 Radiation Data	118
3.2.5.2 Micrometeoroid Data	120
Appendix A Summary of Lunar Orbiter II Anomalies	126

ILLUSTRATIONS

Figure No	Title	Page No
3.1-1:	Spacecraft Transporter	5
3.1-2:	Lunar Orbiter Uprange Radar Coverage	10
3.1-3:	Tracking Coverage	11
3.1-4:	Earth Track for Nov. 6-7, 1966	13
3.1-5:	Telemetry Coverage	14
3.1-6:	Lunar Orbiter Space Vehicle	16
3.1-7:	SLV Configuration	17
3.1-8:	Lunar Orbiter Agena Basic Configuration	18
3.2-1:	Early Orbit Determination Results	30
3.2-2:	Effect of Midcourse Time on ΔV Required	32
3.2-3:	Effect of Time of Flight on Total ΔV Requirements	33
3.2-4:	Pre-Midcourse Encounter Parameter Summary	35
3.2-5:	Midcourse Geometry	36
3.2-6:	Midcourse Doppler Shift	36
3.2-7:	Deboost Doppler Shift	40
3.2-8:	Geometry at Deboost	41
3.2-9:	Initial-Ellipse Argument of Perilune History	42
3.2-10:	Initial-Ellipse Orbit Inclination History	42
3.2-11:	Initial-Ellipse Perilune Altitude History	43
3.2-12:	Initial-Ellipse Longitude of Ascending Node History	43
3.2-13:	Transfer Doppler Shift	45
3.2-14:	Orbital Geometry at Transfer	47
3.2-15:	Perilune Altitude vs Longitude of Descending Node — Photo Ellipse Prediction at Transfer	48
3.2-16:	Photo Orbit Traces for Primary Targets	49
3.2-17:	Predicted Primary Photo Altitudes based on Transfer Design LRC 9-4-66 Harmonics.	50
3.2-18:	Photo Ellipse — Perilune Radius History	53

ILLUSTRATIONS

Figure No	Title	Page No
3.2-19:	Photo Ellipse—Apolune Radius History	53
3.2-20:	Photo Ellipse—Argument of Perilune History	54
3.2-21:	Photo Ellipse—Orbit Inclination History	54
3.2-22:	Photo Ellipse—Longitude of Ascending Node History	55
3.2-23:	Predicted Primary Photo Altitudes (Based on Real-Time Eval Runs LRC 9-4-66 Harmonics)	58
3.2-24:	Predicted vs Actual Perilune Altitudes	59
3.2-25:	Spacecraft Block Diagram	62
3.2-26:	Array Output vs Temperature	67
3.2-27:	Battery Characteristics	68
3.2-28:	Array Characteristics During Initial (High) Orbit	72
3.2-29:	Battery Characteristics Orbit 8-9	73
3.2-30:	Battery Characteristics Orbit 108-109	73
3.2-31:	Transponder Output Power and Temperature Variations During Lunar Orbit	77
3.2-32:	Transponder Data	78
3.2-33:	Attitude Control Subsystem Nitrogen Usage	87
3.2-34:	Velocity Control Subsystem Available Nitrogen History	96
3.2-35:	Velocity Control Subsystem Pressure-Time Histories	97
3.2-36:	Velocity Control Subsystem Temperature-Time Histories	98
3.2-37:	Velocity Control Subsystem—Orbit Injection Maneuver—System Pressures and Temperatures	100
3.2-38:	Velocity Control Subsystem—Orbit Injection Maneuver—System Dynamics	100
3.2-39:	Thermal Coating Absorptivity Degradation from Solar Radiation	104
3.2-40:	Thermal Coating Coupon Performance	106
3.2-41:	ST04 Thermistor Anomaly in Orbit 29	106
3.2-42:	Selected Telemetry Measurement Locations	111
3.2-43:	SFOF Data Processing (Typical Computer String)	112

ILLUSTRATIONS

Figure No	Title	Page No
3.2-44:	Deep Space Station Data Flow Operation	113
3.2-45:	DSS-SFOF Ground Communications	114
3.2-46:	Micrometeoroid Detector Locations	120
3.2-47:	L.O. II Location at Meteoroid Collision—Detector 4	121
3.2-48:	L.O. II Location at Meteoroid Collision—Detector 5	122
3.2-49:	L.O. II Location at Meteoroid Collision—Detector 13	123
3.2-50:	L.O. II Location at Suspected Meteoroid Collision—ST04 Thermistor	124
3.2-51:	True Anomaly vs Time—Mission II Orbits	125

TABLES

	Page No
3.1-1: Hangar S and ESA Spacecraft Retests	2
3.1-2: Spacecraft Special Tests	2
3.1-3: Summary of Differences from Standard Flight Spacecraft	3
3.1-4: Explosive Safe Area Tests	4
3.1-5: Launch Area Tests	6
3.1-6: Spacecraft Prelaunch Milestones	6
3.1-7: Ascent Trajectory Event Times	15
3.2-1: Photographic Site Locations	21
3.2-2: Significant Events Summary	23
3.2-3: Trajectory Sequence of Events	28
3.2-4: Powered Flight Trajectory Events	29
3.2-5: Pre-Midcourse Orbit Determination Encounter Parameter Summary	31
3.2-6: Encounter Conditions	37
3.2-7: Orbit Determinations used for Photo Site Command Conferences	52
3.2-8: Frame Numbers vs Photo Sites	56
3.2-9: Site vs Orbit Number	57
3.2-10: Key Events	61
3.2-11: Shutter Count PB-04 Data	64
3.2-12: Typical Current by Mode	70
3.2-13: Attitude Data for Photo Sites	83
3.2-14: Velocity Control Subsystem Maneuver Performance—Mission II	
3.2-15: Propellant and Nitrogen Servicing Summary—VCS	94
3.2-16: Velocity Control Subsystem Telemetry Resolution	95
3.2-17: Engine Valve Temperature Maximum Soak-Back	101
3.2-18: Gimbal Actuator Position	101
3.2-19: Thermal Coating Properties (Selected Orbits)	105
3.2-20: Orbital Peak Temperatures	107
3.2-21: Lunar Orbiter II SPAC Program Execution	119
3.2-22: Radiation Data Record	119

LUNAR ORBITER II

3.0 MISSION SYSTEM PERFORMANCE

3.1 LAUNCH OPERATIONS

The Launch Operations Plan (LOP), Lockheed Missiles and Space Company Document LMSC-A751901A, provided the primary planning for overall space vehicle program direction through the lunar preinjection phase of Lunar Orbiter II flight. This document served as the basis for directing the activities required to achieve and evaluate the flight objectives, launch criteria and constraints, and implementation of preflight tests, checkouts, and launch of the space vehicle.

The launch operations plan followed during Mission II was identical to that used in the Mission I launch. A description of the Launch Operation organization and supporting launch/postlaunch tracking and communication facilities is contained in the Lunar Orbiter Mission I Final Report, Section 3.3.1, "Launch Operation Plans" and 3.3.2, "Base Facilities."

3.1.1 SPACECRAFT PROCESSING

Spacecraft 5 arrived at Cape Kennedy on June 10, 1966, to serve as backup for the Mission I flight article, Spacecraft 4. Upon arrival it was moved to Hanger "S" to initiate processing of the spacecraft for the backup function. On July 6, the spacecraft was moved to the Explosive Safe Area (ESA) where processing continued until August 5. At that time, it was returned to Hanger "S" for storage until required for Mission II.

On August 26, Spacecraft 6 arrived at Cape Kennedy for testing as a backup to Spacecraft 5.

On August 30, Spacecraft 5 was removed from storage to perform rework required to satisfy flight acceptance requirements and to incorporate modifications to preclude recurrence of anomalies experienced in Spacecraft 4. On October 31, the spacecraft was transferred to Launch Pad 13 and mated to the Agena. The simulated launch countdown was performed on November 3, 1966, with launch readiness confirmed at 1330 EST. No operations readiness test (ORT) was performed for this mission.

3.1.1.1 Hangar "S"


The standard sequence of tests as outlined in the Mission I report was performed on Spacecraft 5 during Mission I preparation. On August 30, the spacecraft was removed from storage and retested (Figure 3.1-1) as indicated in Table 3.1-1. In addition, special tests in accordance with Table 3.1-2 were performed. The purpose of these tests was twofold: to determine if interim degradation had occurred and to test the subsystems which had been changed as a result of Mission I experience. Refer to Table 3.1-3 for a summary of differences from Spacecraft 4. A detailed listing of the retests performed is contained in Boeing Document D2-100389-5, Volume V, Technical Compliance Review Summary Report, Spacecraft 5.

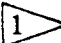
The retests disclosed that the star map output had apparently shifted; accordingly the star tracker was returned to the vendor. The difficulty was in the star tracker test set. The star tracker was reinstalled and successfully tested.

All retests and special tests were satisfactorily concluded.

Table 3.1-1: Hangar "S" And ESA Spacecraft Retests	
Location	Test Title
Hangar "S"	Spacecraft Alignment Verification
Hangar "S"	Pre-Power "ON" Check
Hangar "S"	Initial Test Setup
Hangar "S"	Initial Conditions/Readiness Test
Hangar "S"	Radiation Dosage Measurement System
Hangar "S"	Attitude Control Functional Test
Hangar "S"	Velocity Control Subsystem
Hangar "S"	Power Subsystem Performance
Hangar "S"	High-Gain Antenna Position Control Camera Thermal Door Operation, and Antenna Deployment
Hangar "S"	Solar Panel Test and Low-Gain Antenna Alignment
Hangar "S"	EMD Reflectance Test
Hangar "S"	Spacecraft/Hangar "S"/DSIF-71 Checkout
ESA	Spacecraft Regulator and Leak Test

Table 3.1-2: Spacecraft Special Tests	
Location	Test Title
Hangar "S"	Ranging Mode II and R. F. Probe
Hangar "S"	Connector Pin Verification
Hangar "S"	Camera Thermal Door Test
Hangar "S"	Attitude Control Functional Test
Hangar "S"	High-Gain Antenna Position Control
Hangar "S"	Canopus Tracker Field of View
Hangar "S"	Command Time Delay
Hangar "S"	Engineering Model Photo Subsystem Test
Hangar "S"	Spacecraft Command Sequence Test
Hangar "S"	Command Decoder Plug Retest
ESA	Spacecraft Regulator and Leak Test
Hangar "S"	Transistor Panel and Power Resistor Test
Hangar "S"	Fuel Fill Valve Leak Rate Test
Hangar "S"	Solar Panel Illumination Test
Hangar "S"	CST/STTS Star Map Test
Hangar "S"	Modulation Index Test
Hangar "S"	High-Gain Antenna Operation and Plug Continuity
Hangar "S"	Photo Subsystem (P/S No. 6)/Spacecraft V/H Test
Hangar "S"	EMD Paint Coupon Test
Hangar "S"	Camera Thermal Door (Open/Close) Test
Hangar "S"	Programmer Memory Core Verification Test
Hangar "S"	TWTA Power Outout Test
ESA	Pressure Transducer Checks
Hangar "S"	Camera Thermal Door Star Wheel Check
ESA	Accelerometer Aliveness Check

Table 3.1-3: Summary Of Differences From Standard Flight Spacecraft			
Subsystem	Part Number		Remarks 
	(Lunar Orbiter II)	(Lunar Orbiter I)	
Photo Subsystem	1200-100	1200-100	Ref. EK Data Package for P/S No. 6 and meeting minutes 2-1572-02-2908 dated 10/8/66 and 2-1572-02-2934 dated 10/14/66.
Camera			
Structure and Mechanisms			
Thermal Coating Coupon Installation	25-55211-1		Incorporated ECM-LO-I-0556, "Thermal Coating Coupon Test"
Equipment Mounting Deck	No Part Number Change		Incorporated ECM-LO-I-0558, "EMD Painting"
Paint Coupon	25-51848-4	25-51848-1	Added Paint Coupons-Ref. LO-I-0556, "Painting"
Attitude Control Subsystem			
IRU	1512469-906 (10-70053-1)	1512469-905 (10-70053-1)	Incorporated ECM-LO-I-0544, "Elimination of Noise Spikes in IRU, RIM"
Canopus Tracker	No Part Number Change		Conducted test per ECM-LO-I-0557, "Stray Light Test"
Communications Subsystem			
Low-Gain Antenna	25-50937-12	25-50937-11	Incorporated ECM-LO-I-0557, "Stray Light Test"
Power Subsystem			
Solar Panels	No Part Number Change		Incorporated ECM-LO-I-0557, "Stray Light Test"

 The items noted in the "Remarks" column are either physical differences between Lunar Orbiter I and Lunar Orbiter II which have resulted from design changes, or equipment that is to be installed at a later date. The part number noted under the "Lunar Orbiter I" and "Lunar Orbiter II" part number columns are part number differences, if a part number difference exists.

3.1.1.2 Explosive Safe Area (ESA)

On October 17, the spacecraft was moved to the Explosive Safe Area (ESA 5/6). This area is so designated because it is away from the main industrial area and provides minimum hazard to personnel and equipment during potentially hazardous operations on the spacecraft. The layout of the fuel servicing building and the entire ESA are shown in the final report for Mission I. Table 3.1-4 lists tests performed at the ESA.

The fuel system was rechecked for leaks and the regulator system pressure was verified. The fuel, oxidizer, and nitrogen loading was accomplished on October 18 and 19 without incident.

On October 23, the photo subsystem - - which had been purged, loaded with flight film, pressurized, and tested as a component - - was loaded and aligned on the spacecraft.

Flight batteries were installed and final weight and balance checks were completed on the spacecraft.

Table 3.1-4: Explosive Safe Area Tests	
Test Title	
	Photo Subsystem Launch Preparation Spacecraft Regulator and Leak Test Propellant Servicing Nitrogen Servicing Photo System Installation and Alignment Weight and Balance Verification Battery Verification Camera Thermal Door Verification Pressure Transducer Checks Accelerometer Aliveness Test Spacecraft Operational Check with DSIF-71 Ordnance Check and Hook-Up Agena Adapter Installation Thermal Barrier Installation Nose Fairing Installation Spacecraft Operational Check with DSIF-71 Transport Spacecraft (ESA to Pad)

On October 25, a test was run to verify spacecraft operation compatibility between DSIF-71 and ESA. The test was satisfactorily completed; however, it was noted via telemetry that the nitrogen gas (N_2), fuel, and oxidizer tank pressures were below the recorded pressures following initial tank pressurization. These pressure differences were attributed to the temperature change that had occurred following pressurization and "topping." The N_2 tank was "topped off" again and the pressure remained within established limits through launch. The oxidizer and fuel tanks were not repressurized since the pressure remained constant and was within launch requirements.

The Agena adapter, thermal barrier, and spacecraft shroud (nose fairing) were installed in preparation for the second DSIF-71 to ESA test. During the DSIF test on October 28 and 29, the photo subsystem pressure read 15.2 psia instead of the previously noted 16.6 psia. All other tests were completed satisfactorily. The shroud, thermal barrier,

and photo subsystem P/S were then removed so that the P/S could be transported to Hangar "S." A leak was found in the photo system pressure shell, the shell was repaired, rechecked, and the P/S was reinstalled in the spacecraft.

On October 31, the shroud was again installed. The encapsulated spacecraft was transported from the ESA to the launch pad and installed on the launch vehicle.

During the entire period after October 23 when the flight film was loaded in the photo subsystem, it was necessary to maintain the P/S temperature at below 55°F. Figure 3.1-1 shows the encapsulated spacecraft, its thermal blanket, and spacecraft cooler en-route to the launch pad from the ESA.

3.1.1.3 Launch Pad 13

Spacecraft processing continued normally after shroud reinstallation. The move from the ESA to the launch pad was made during the evening without incident. Table 3.1-5 lists tests performed at Pad 13.

The spacecraft was mated to the Agena and tests were run to verify impedance and interface compatibility. Control was checked from the blockhouse with ground power in the base of the launch pad applied to the spacecraft. Two-way phase lock from the van to the spacecraft was satisfactorily obtained. After demonstration of spacecraft

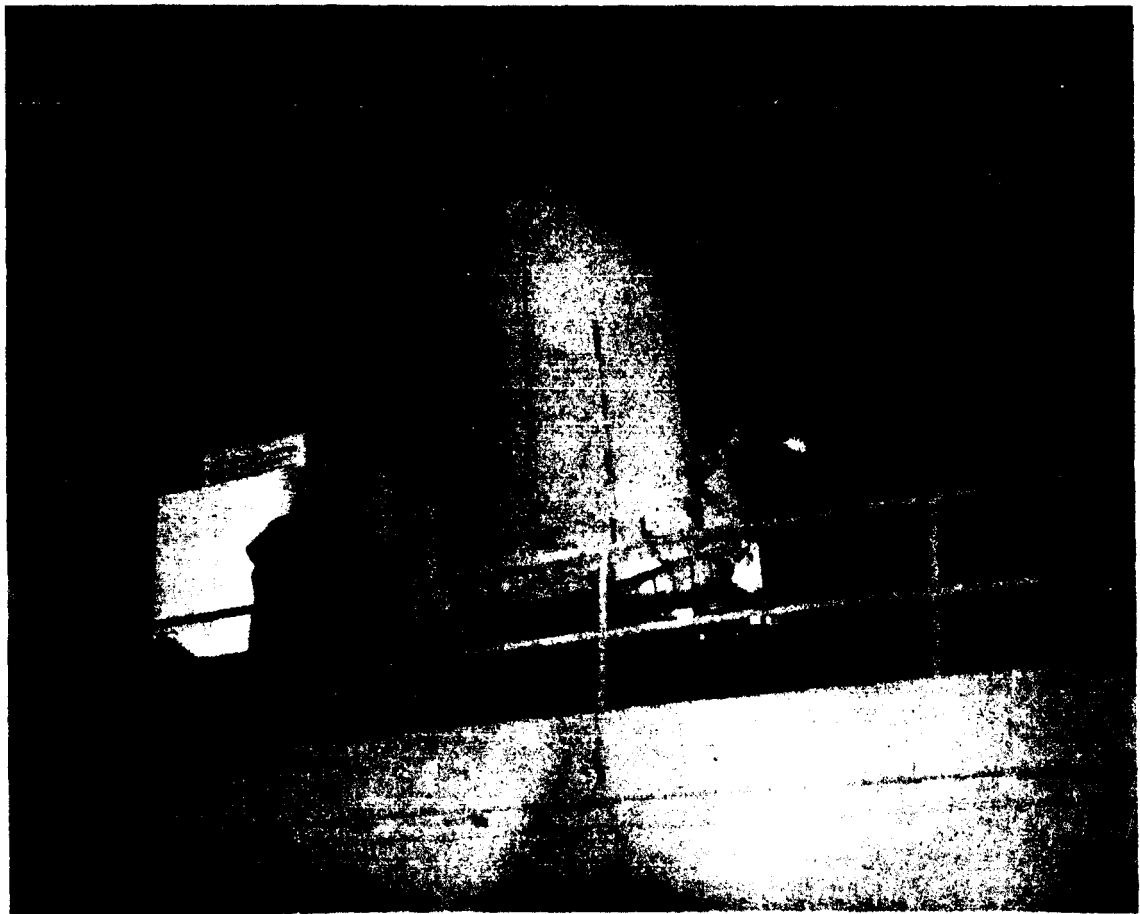


Figure 3.1-1: Spacecraft Transporter

operational compatibility with DSIF-71, the flight vehicle was deemed ready for simulated launch on November 3, 1966.

Table 3.1-5: Launch Area Tests
Test Title
Spacecraft to Adapter and Agena Matchmate
Van, Blockhouse, and Spacecraft Interface Verification
Lunar Orbiter Spacecraft - - Second Flight Spacecraft - - Initial Pat Tests
Lunar Orbiter Spacecraft - - Second Flight Spacecraft - - Simulated Launch

3.1.2 LAUNCH CONDUCT

The launch plan, activities, facilities, and participating organizations were similar to that for Mission I (Spacecraft 4). Specific information may be obtained from Paragraph 3.3, "Launch Operations," of the Mission I final report.

3.1.2.1 Launch Criteria

Launch criteria and space vehicle preparation were governed by the Launch Operations Plan LMSC A751901a. Although Spacecraft 5 had been tested and used as a backup to Spacecraft 4, it was necessary to retest it for Mission II in accordance with the requirement of Section 5.0 of Boeing Document D2-100111-3, Spacecraft Test Specification - - Eastern Test Range - - Lunar Orbiter.

Significant milestones described in Table 3.1-6 were satisfactorily completed by Spacecraft 5 in preparation for launch.

Table 3.1-6: Spacecraft Prelaunch Milestones	
Date Complete	Event
October 4, 1966	Spacecraft-DSIF-71 Compatibility Retest
October 7, 1966	Install EMD Paint Coupons and Retest
October 12, 1966	EMD Repainted
October 13, 1966	Spacecraft Fueling Cart Preps
October 17, 1966	Transfer Spacecraft to ESA
October 18-19, 1966	Spacecraft Fueling
October 23, 1966	P/S Installation in Spacecraft
October 25, 1966	DSIF Check without Shroud
October 26, 1966	Spacecraft-to-Agena Adapter Matchmate
October 28, 1966	Spacecraft Encapsulation in Shroud
October 28-29, 1966	Spacecraft Checkout
October 29, 1966	Shroud Demate
October 31, 1966	Re-encapsulation of Spacecraft
October 31, 1966	Transfer Spacecraft to Launch Pad
October 31, 1966	Spacecraft-to-Agena Mate
November 3, 1966	Simulated Launch
November 7, 1966	Launch

3.1.2.2 Countdown And Launch

JOINT FLIGHT ACCEPTANCE COMPOSITE TESTS (J-FACT) October 31, 1966

The spacecraft did not participate in the J-FACT for Mission II. During the test, the Agena velocity display meter in the blockhouse did not work properly, but a satisfactory readout was confirmed by means of the backup recorders and telemetry. The test was conducted satisfactorily and all test objectives were met.

SIMULATED LAUNCH TEST NOVEMBER 3, 1966

The simulated launch test commenced as planned at 10:36 EST (T- 460 minutes), and terminated at 18:54 EST. There were 34 minutes of unplanned hold time and a planned recycle to T - 7 minutes at T- 19 seconds. The following problems were encountered.

- The Atlas sustainer engine LOX reference regulator was indicating a high regulating pressure, necessitating replacement of the regulator.
- A small leak developed at the Atlas B1 fuel pump outlet flange, necessitating replacement of the seals.
- A pinhole leak in a weld seam on the Atlas sustainer low-pressure duct was observed.
- During guidance command test (GCT) No. 1, a no-go was given when disturbances appeared on the V1 and V2 pitch, B1 and B2 yaw engine traces. This anomaly was the result of saturation of the roll gyro nulling loop due to the 11-degree roll program called for in Launch Plan 6-C. When the normal test configuration of 5-degree roll program was substituted for the 11-degree program, satisfactory data was obtained.
- The Agena C-band beacon was no-go for the test because its radiated power was under range minimum requirements for downrange metric data acquisition. This beacon was replaced.

The spacecraft simulated countdown began at T - 530 minutes, as governed by requirements in Boeing Document D2-100626-2, Lunar Orbiter Spacecraft Countdown, Volume III. A problem with the printer at DSIF-71 caused a delay in acquiring two-way lock between the spacecraft and DSIF-71 until T - 401.

During checks of the star tracker at T- 455 minutes, a slight amount of noise was observed on the Canopus star map telemetry channel. Light reflection into the star tracker from the Sun was believed to be the cause of this anomaly. Positioning of the service tower outer doors to block all light transmission eliminated the star map noise. Evaluation of the anomaly indicated light was entering through the air conditioning exhaust vent located in the nose shroud. Elimination of the light source produced a satisfactory checkout.

At T - 352 minutes there was an inadvertent firing of the ACS yaw thruster. This was attributed to activity around the launch vehicle on the service tower.

During traveling wave tube amplifier (TWTA) checkout, a fluctuation of power occurred. This had not been seen before, but was similar to a condition that had been noted at the ESA after installation of the shroud on Spacecraft 4 where the apparent TWTA output had increased. On Spacecraft 5 an apparent decrease had resulted. These effects were determined to be caused by reflections from the shroud and surrounding environment which changed the VSWR and resultant output power. The evaluation was later veri-

fied when, after shroud ejection, stable TWTA power was noted via telemetry.

The remainder of the spacecraft simulated countdown proceeded without incident.

LAUNCH, NOVEMBER 6, 1966

The spacecraft countdown, governed by Volume IV of Boeing Document D2-100626-2, was initiated at T - 530 minutes. In attempting to acquire a two-way lock between the spacecraft and DSIF-71 at T - 424 minutes, there was a problem with the range in receiving Agena Channel F data from Tel-2 to DSIF-71. During this period, spacecraft power was shut down as there was no telemetry monitor available. A work-around method was incorporated and two-way lock was established at T - 396 minutes. Lost time was made up by T - 320 minutes.

At T - 285 minutes spacecraft performance analysis and command (SPAC) personnel noticed that the photo system film takeup reel contents telemetry readout indication was noisy. The Eastman representative suggested that the potentiometer indicator might be dirty at the extreme end of its rotation. A decision was made, with NASA concurrence, to run a short test to try to resolve the problem. A "wing forward" command was sent and the takeup reel contents indication became stable. No other spacecraft problem developed during the countdown.

Tower removal and Agena oxidizer tanking were late due to the special check on the Atlas LOX reference regulator. Since prelaunch testing indicated the LOX reference regulator was regulating on the high side, the airborne helium bottles were pressurized to 2500 psig, which was within specification.

Air conditioning supplied to the spacecraft was stable and the equipment mounting deck temperature was 42.8°F at liftoff, well within the specified range of 35 to 85°F.

3.1.2.3 Weather

Weather during the launch operation was favorable. A light rain occurred at T - 115 but did not delay the launch. Upper wind shears were within acceptable limits. At liftoff, the following weather parameters were recorded:

Temperature	72°F
Relative humidity	79%
Visibility	10 miles
Dew point	65°F
Surface winds	7 knots at 065 degrees
Clouds	Cloudy skies (almost overcast)
Sea-level atmosphere	30.170 inches of Hg

3.1.2.4 Tracking Coverage

The Air Force Eastern Test Range (AFETR), Deep Space Network (DSN), and Manned Space Flight Network (MSFN) are the elements of the tracking and data system (TDS) that together support the tracking and telemetry requirements for the Lunar Orbiter II launch.

Tracking during the launch phase consisted of C-band tracking of the launch vehicle and reception of VHF and S-band telemetry from the launch vehicle and spacecraft respectively. Figure 3.1-2 shows AFETR and MSFN uprange coverage for any launch day.

Tracking data provided to AFETR during the launch phase established (1) the Agena orbit and the normalcy of spacecraft cislunar injection in real time, and (2) launch vehicle performance evaluation. This was done by first tracking the Agena stage and then, after separation, both the spacecraft and Agena. Since the separation velocity was small, tracking of the Agena stage both prior to and subsequent to separation was valuable in determining an early spacecraft trajectory.

Other elements of the TDS received the tracking data to prepare acquisition and prediction data for the Deep Space Stations. Prediction data based upon actual launch vehicle performance was used during initial acquisition by all stations. The tracking data supplied by the uprange AFETR and Manned Space Flight Network (MSFN) radars were processed by the real-time computer system (RTCS) at the AFETR and station predictions were generated in real time for the AFETR, MSFN, and Deep Space Stations farther downrange. The AFETR forwarded the tracking data directly to Goddard Space Flight Center (GSFC) so that GSFC would generate prediction data for the MSFN stations. These data were also relayed to the Space Flight Operations Facility (SFOF) for use with Deep Space Station data in calculating the spacecraft trajectory. The MSFN transmitted Bermuda and Carnarvon tracking data to the AFETR. The AFETR retransmitted their raw tracking data and that of the MSFN stations to the SFOF in near-real time.

Tracking coverage for various portions of the near-Earth phase of the launch trajectory is shown in Figure 3.1-3.

The ability to satisfy the near-Earth phase tracking and telemetry requirements was strongly dependent upon trajectory characteristics and tracking and data system (TDS) facilities during that phase. The most dominant trajectory characteristic was the variable location of the cislunar orbit injection point. With the injection taking place uprange, i.e., in the Atlantic Ocean, the support problems were quite different than for an injection far downrange in the Indian Ocean as experienced during Mission I. An Earth map with injection loci for the November launch period is presented in Figure 3.1-4. The injection point for the launch of November 6, 1966, on azimuth 92.9 was near the western edge of Africa in the Atlantic Ocean.

3.1.2.5 Telemetry Coverage

Elements of the TDS received and recorded spacecraft and launch vehicle telemetry during the near-Earth phase of the mission (see Figure 3.1-5). Spacecraft telemetry was received and recorded at both S-band and VHF via the Agena link.

Launch vehicle telemetry received by downrange AFETR stations was retransmitted to Kennedy Space Center, in real time except for Channels 17 and 18, which were subsequently retransmitted to KSC within 1 hour of reception.

Spacecraft telemetry was received at the land stations and ships via the Agena link and was retransmitted to DSS-71 and the SFOF in real time. S-band telemetry received directly from the spacecraft was also transmitted in real time.

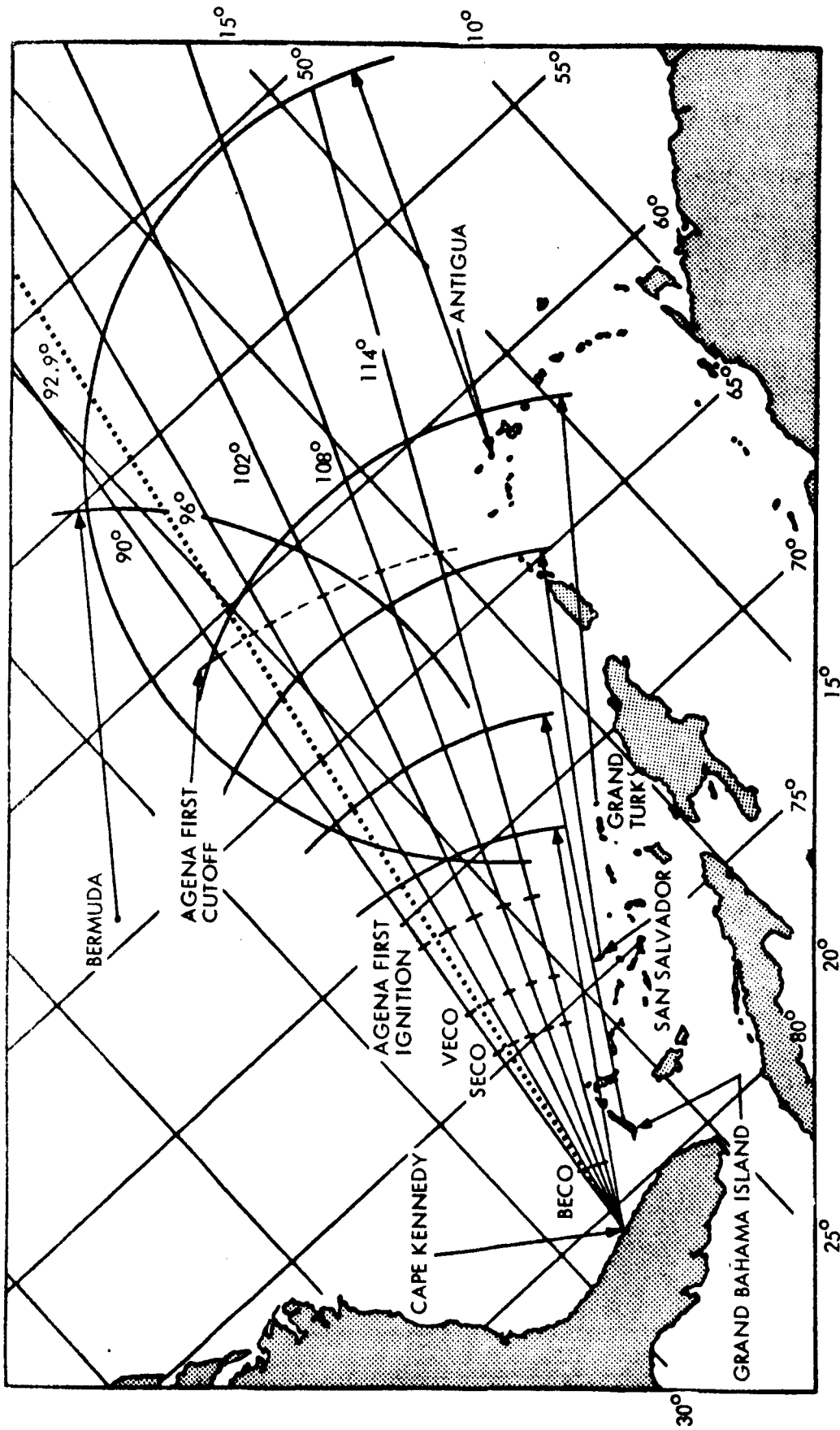


Figure 3.1-2: Lunar Orbiter Uprange Radar Coverage

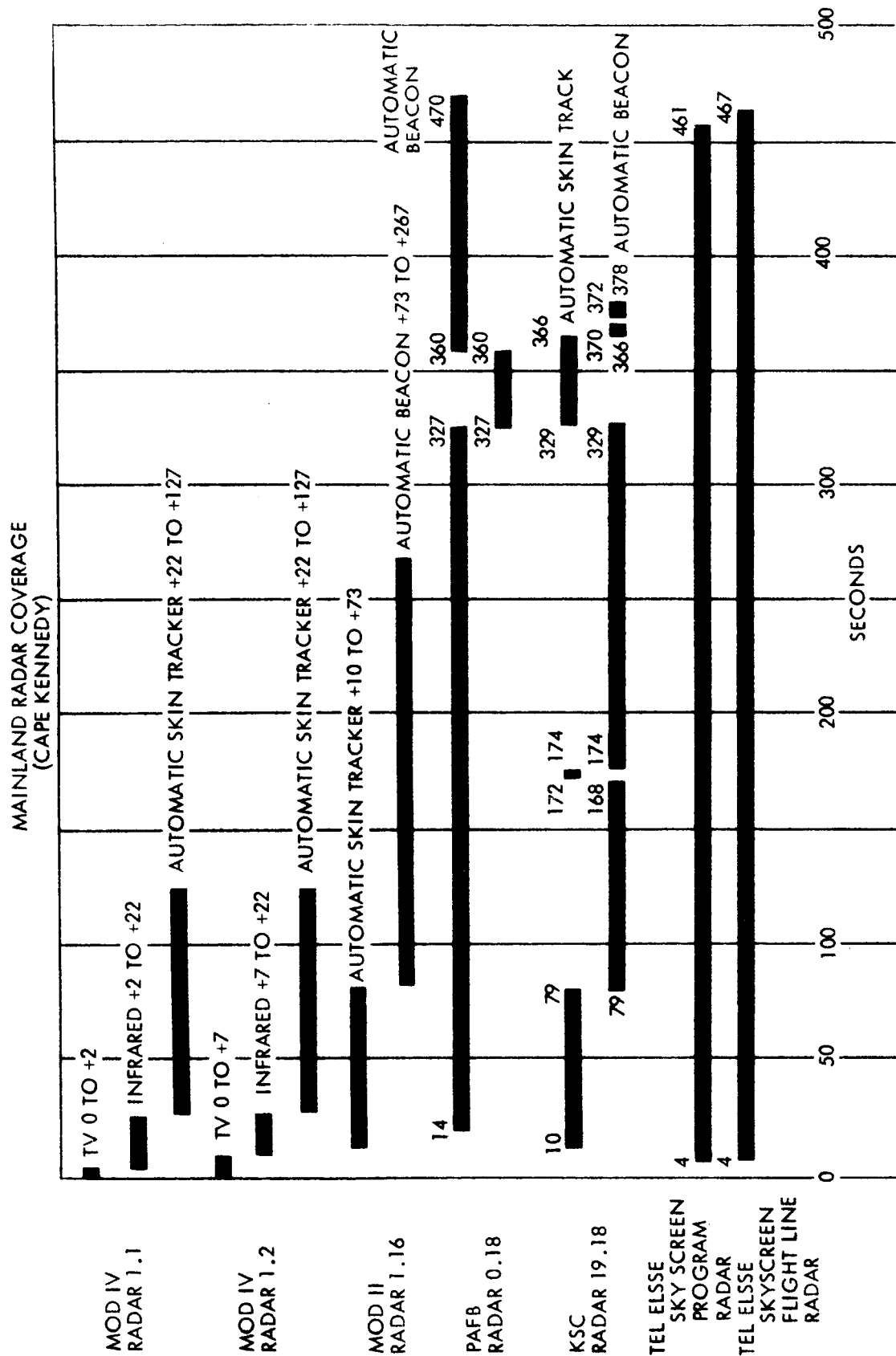


Figure 3.1-3: Tracking Coverage

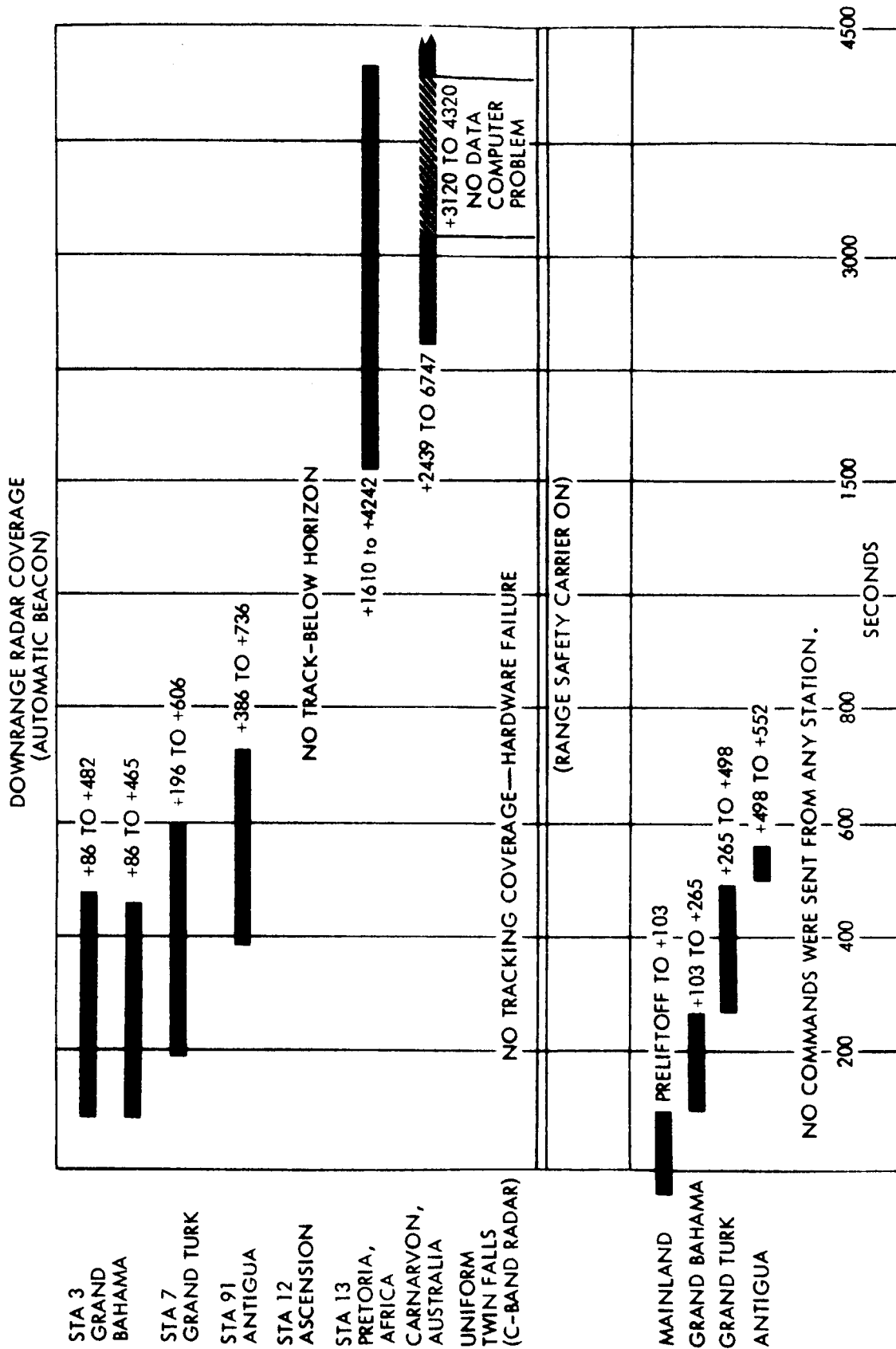


Figure 3.1-3: Tracking Coverage (Cont'd)

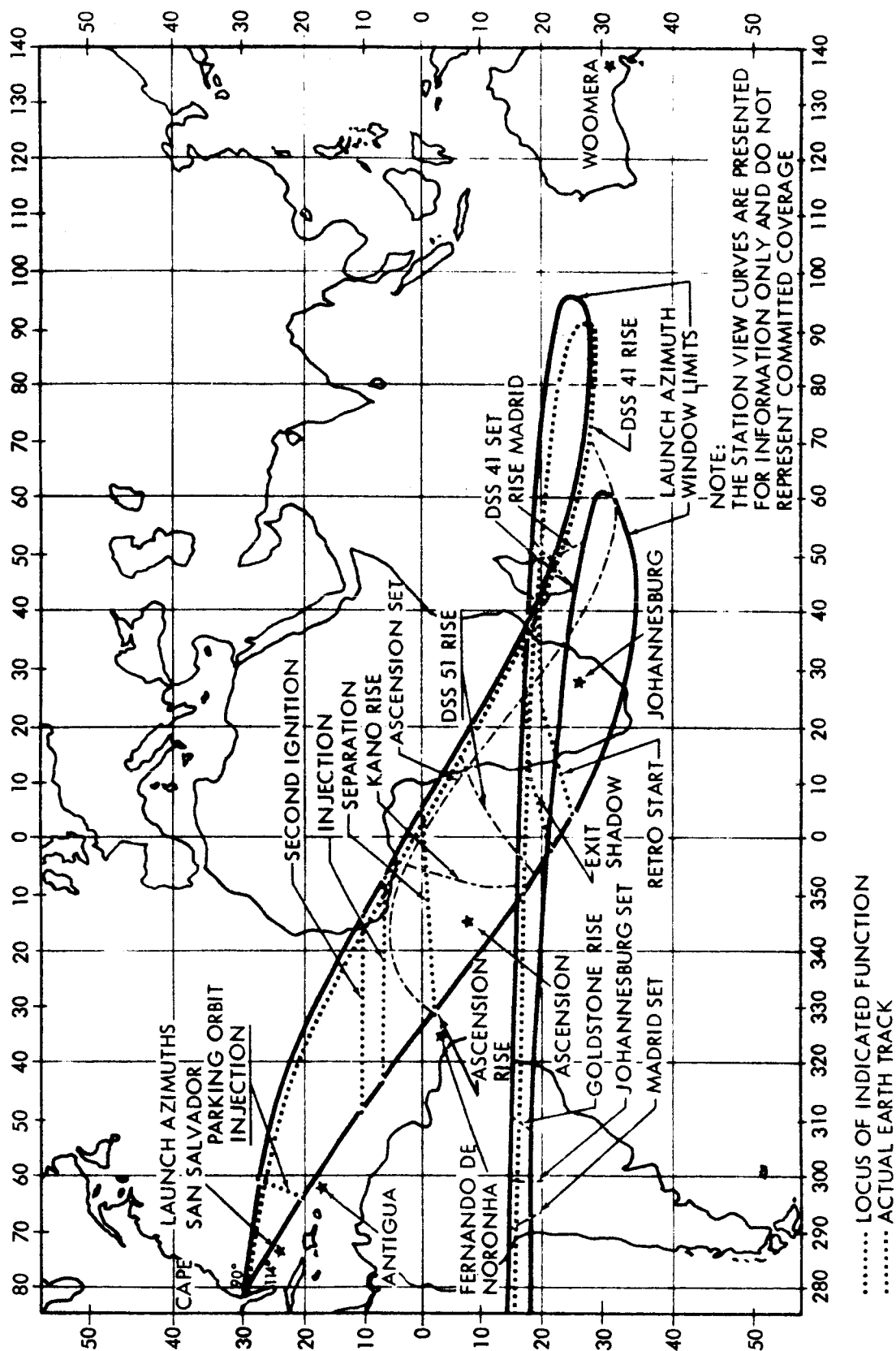


Figure 3.1-4: Earth Track for Nov. 6-7, 1966

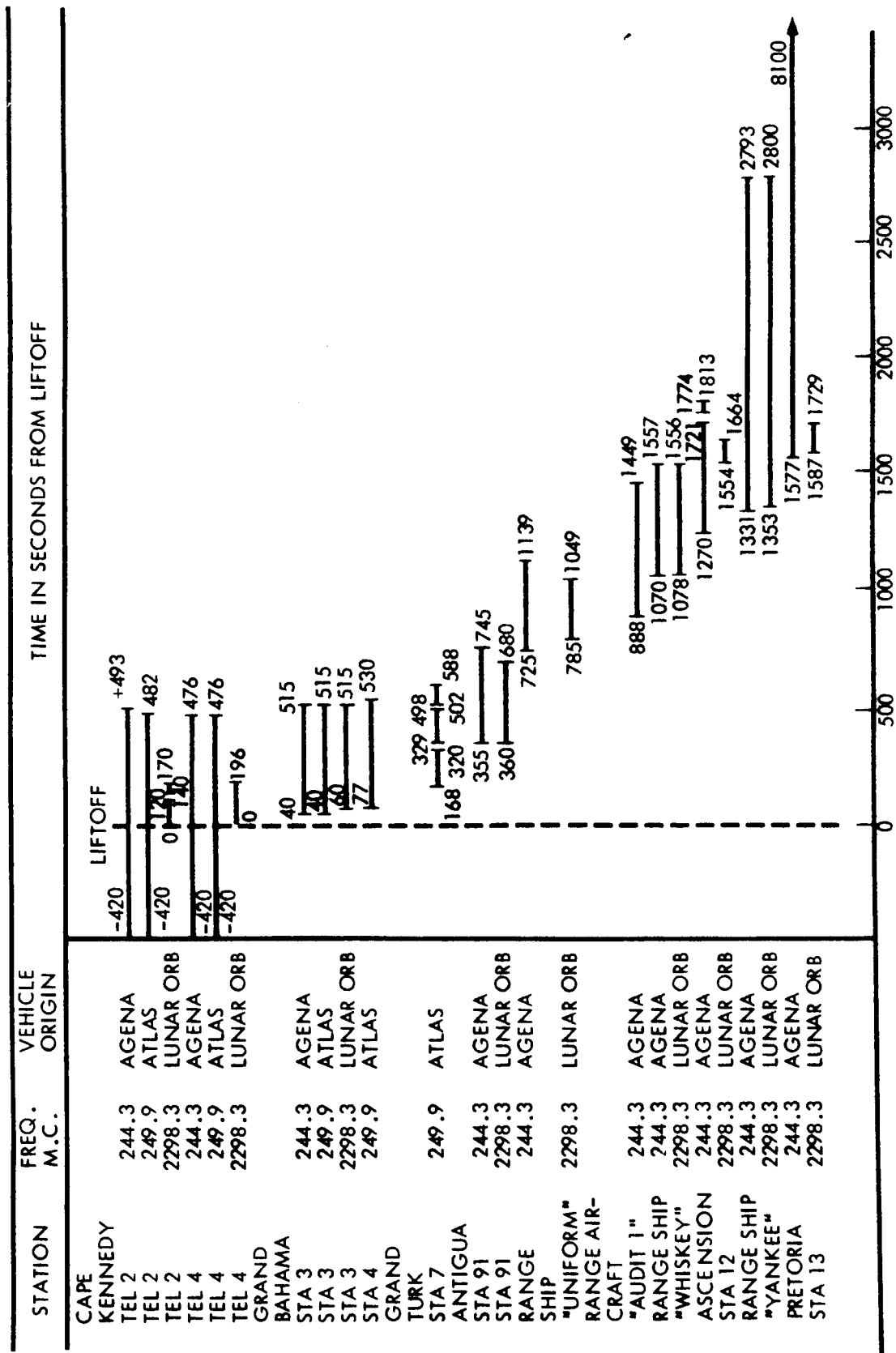


Figure 3.1-5: Telemetry Coverage

3.1.3 LAUNCH VEHICLE PERFORMANCE

The first stage of the launch vehicle was an SLV-3 (Atlas) S/N 5802. All SLV-3 flight objectives were satisfied. This was the tenth SLV-3 vehicle to be launched from the ETR and the second vehicle in support of the Lunar Orbiter program.

A satisfactory ascent trajectory was attained. The performance of all Atlas systems was satisfactory. Atlas-Agena separation was properly accomplished, and good telemetry data was obtained for Atlas systems analysis.

Atlas-Agena separation was initiated by the autopilot programmer backup signal at SECO plus 27.5 seconds rather than the normal guidance discrete due to a longer than expected vernier phase. The guidance discrete was transmitted 0.26 second after the autopilot backup signal. Detrimental effects were not observed as a result of the autopilot initiation of separation.

The second stage of the launch vehicle was an Agena-D, S/N 6631. The Agena performance was satisfactory throughout the flight. Engine burn durations were longer than expected for both first and second burn; however, this is explained by the lower than expected engine thrust. All available data indicated that the vehicle flight trajectory was satisfactory and the velocity errors were well within acceptable limits.

Significant ascent trajectory events and times in seconds relative to initial vehicle (2-inch) motion are covered in Table 3.1-7.

Table 3.1-7: Ascent Trajectory Event Times

Event	Times (+ Sec)	
	Nominal	Actual
Liftoff (2-inch motion)		2321:00:195GMT
BECD Discrete	129.0	127.993
Booster Flight Lock-in Dropout		128.108
Booster Jettison Conax Valve Command		131.104
Start Agena Secondary Timer Discrete		269.739
SECO Discrete	287.2	290.683
SECO Relay		290.690
Start Agena Primary Timer	290.6	292.766
VECO Discrete	307.5	313.997
VECO Relay		314.002
Jettison Shroud	309.5	316.500
Initiate Separation Discrete	311.5	318.204 *
Agena First-Burn Ignition (90% Pc)	364.9	367.0
Agena First-Burn Cutoff	516.8	522.0
Agena Second-Burn Ignition (90% Pc)	1196.9	1199.1
Agena Second-Burn Cutoff	1283.6	1287.0
S/C Agena Separation		1452.4

* Event initiated by autopilot programmer backup signal at SECO plus 27.5 seconds.

The configuration of the Atlas-Agena launch vehicle for Mission II was identical to the Lunar Orbiter Mission I launch vehicle. Details of the Atlas-Agena configuration are presented in Mission I report (Boeing Document D2-100727-1, Volume I) and in the Lunar Orbiter B Launch Report (Lockheed Document LMSC-274110). The general space vehicle system configuration is shown in Figures 3.1-6, 3.1-7, and 3.1-8.

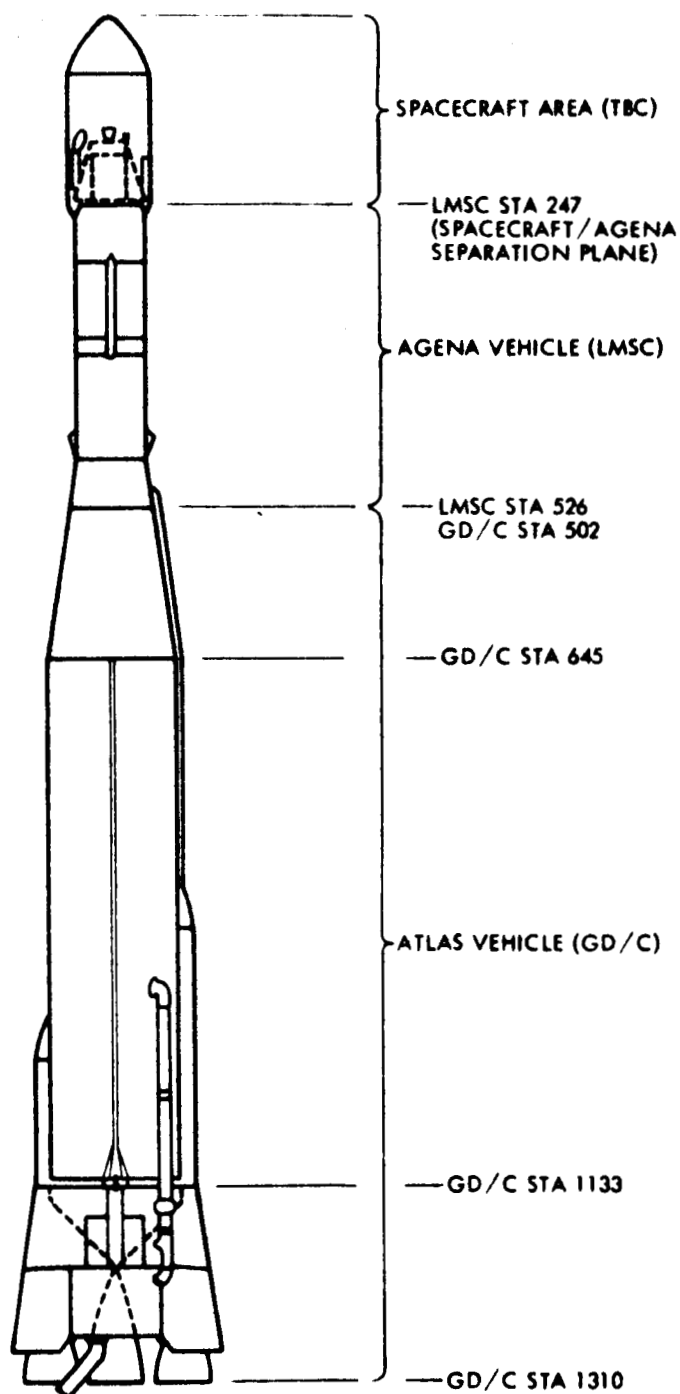


Figure 3.1-6: Lunar Orbiter Space Vehicle

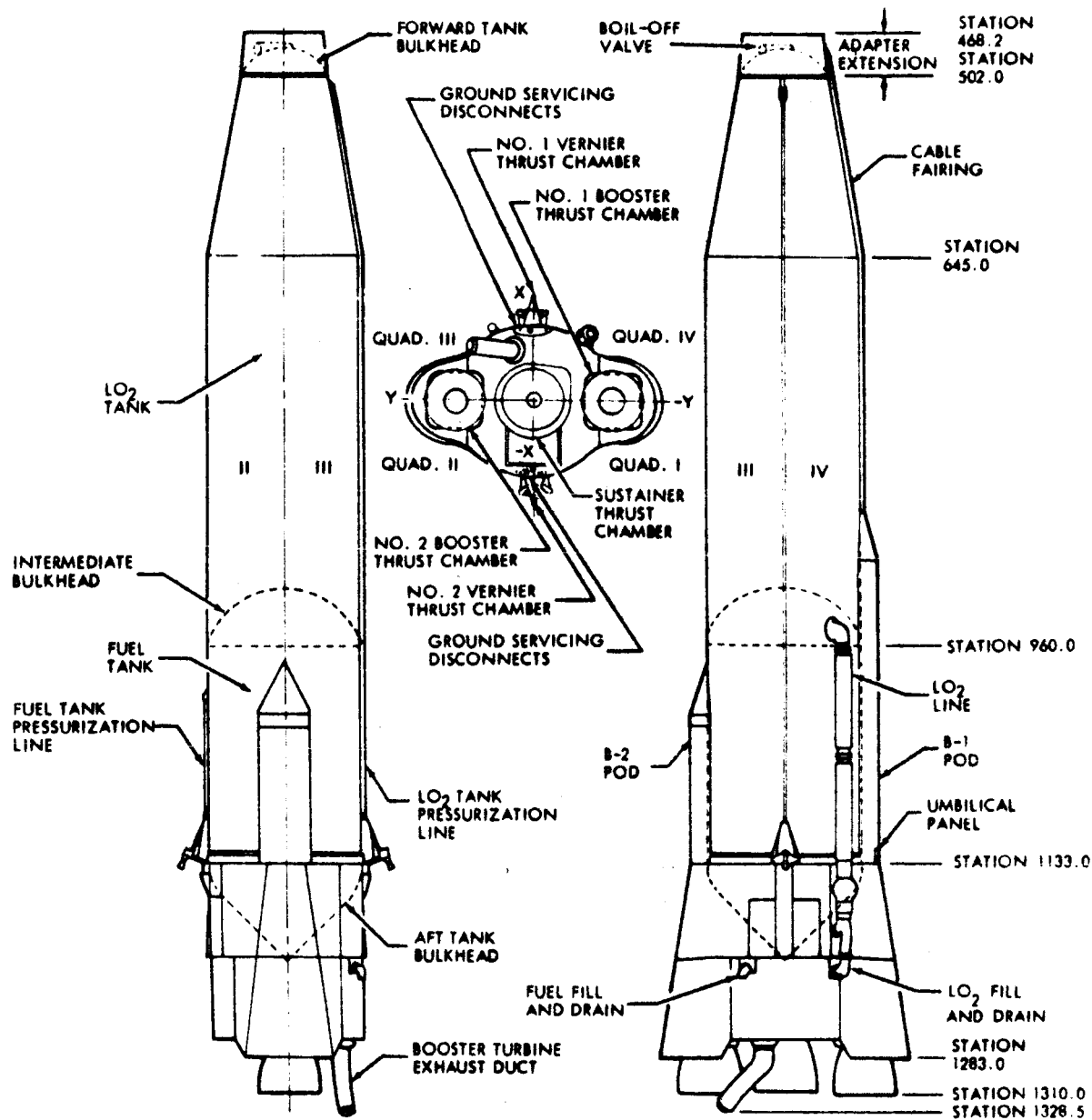


Figure 3.1-7: SLV Configuration

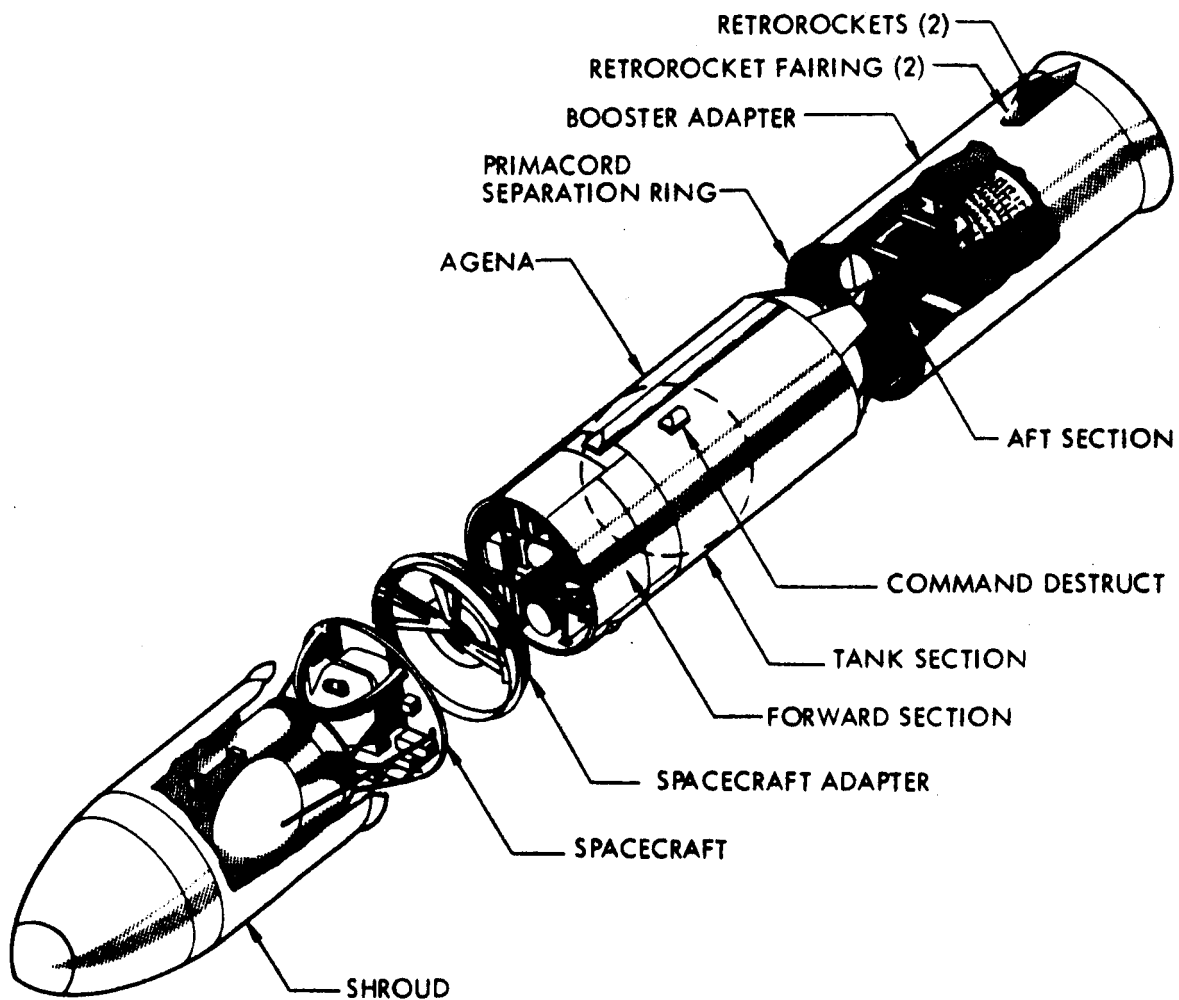


Figure 3.1-8: Lunar Orbiter-Agena Basic Configuration

3.1.3.1 Atlas Performance

The Atlas launch vehicle, S/N 5802, had three primary objectives and one secondary objective in support of Lunar Orbiter Mission II. The primary goals were: (1) to place the upper stage into the proper coast ellipse, (2) to initiate or relay commands properly for separation of the upper-stage vehicle and start the Agena primary timer; and (3) to relay commands to the ATLAS/AGENA interface to jettison the shroud and start the secondary timer commands of the launch vehicle.

The secondary objective was determination of the Atlas performance by using telemetry data.

All objectives were achieved successfully.

3.1.3.2 Agena Performance

The second-stage Agena vehicle, S/N 6631, had two primary objectives and one secondary objective in support of Lunar Orbiter Mission II. The primary goals were (1) to inject the spacecraft into a lunar-coincident transfer (cislunar) trajectory within prescribed orbit dispersions and (2) perform Agena attitude and retromaneuvers following Agena-spacecraft separation to ensure that the Agena would not, to the specified probabilities, intercept the spacecraft, pass within 20 degrees of the center of Canopus seeker field of view, or impact the Moon. The secondary aim of the Agena vehicle was to provide tracking and telemetry data for evaluation of Agena performance.

All objectives were satisfied. The Agena engine performance was less than predicted, but was within the 3-sigma allowable limits. A detailed technical description of the flight parameters is contained in Document LMSC-274110, Lunar Orbiter B Launch Report, prepared by the Space Systems Division of Lockheed Missiles and Space Company.

3.2 FLIGHT OPERATIONS

The primary objective of Mission II was to obtain topographic information of specific lunar areas to assess their suitability for use as Apollo and Survey landing sites. Other objectives were:

- Improve the knowledge of the lunar topography in areas outside the Apollo area of interest.
- Improve the definition of the lunar gravitational field.
- Provide measurements of micrometeoroid flux and radiation levels in the lunar environment.

To satisfy the mission objectives, thirty sites were selected for photography. Thirteen potential Apollo sites distributed within the area of interest ($\pm 5^\circ$ latitude and $\pm 45^\circ$ longitude) on the lunar surface were designated as primary sites (IIP-1, IIP-2, etc.). Seventeen additional sites were designated as secondary sites (IIS-1, IIS-2, etc.). The location of photo sites is specified in Table 3.2-1 together with pertinent operational comments.

Table 3.2-1: Photographic Site Locations

Primary Sites

Site	Latitude	Longitude	Comments
IIP-1	4° 10' N	36° 55' E	
-2	2° 45' N	34° 00' E	
-3	4° 20' N	21° 20' E	
-4	4° 45' N	15° 45' E	
-5	2° 36' N	24° 48' E	Ranger 8 impact point
-6	0° 45' N	24° 10' E	
-7	2° 10' N	2° 00' W	
-8	0° 05' N	1° 00' W	
-9	1° 00' N	13° 00' W	
-10	3° 28' N	27° 10' W	
-11	0° 05' S	19° 55' W	
-12	2° 25' N	34° 40' W	
-13	1° 30' N	42° 20' W	

Secondary Sites

IIS-1	4° 10' N	36° 55' E	To be taken as soon as possible after primary photography of P-1 without intervening maneuvers.
IIS-2	3° 36' N	36° 25' E	Converging stereo at point halfway between Orbits 52 and 53 (4 frames each) with three-axis maneuvers and V/H on.
IIS-3	9° 5' N	174° 50' E	Farside. Vertical centered on point 20 degrees before PM terminator. Roll maneuver only. V/H off.

Table 3.2-1: Photographic Site Locations (Cont'd)			
Site	Latitude	Longitude	Comments
IIS-4	5° N	174° E	Farside. Oblique northerly with southern edge of wide-angle frame centered on point 20 degrees before PM terminator with horizon just included at northern edge of frame. V/H off. Roll maneuver only.
IIS-5	20° S	158° E	Farside. Oblique southerly with northern edge of wide-angle frame centered on point 20 degrees before PM terminator with horizon just included at southern edge of frame. V/H off. Roll maneuver only.
IIS-6	4° 15' N	4° 30' E	Oblique from point of closest approach. V/H on. Three-axis maneuver.
IIS-7	0° 05' N	1° 00' W	Oblique southerly from point of closest approach. V/H off. Three-axis maneuver.
IIS-8	0° 30' N	12° 50' E	Vertical. V/H on. Three-axis maneuver.
IIS-9	2° 20' N	0° 30' E	Vertical. V/H on. Three-axis maneuver.
IIS-10.2	3° 20' N	11° 00' W	Westerly oblique. Phase angle = 4 degrees with camera axis above Sunline relative to site. V/H off. Three-axis maneuver.
IIS-11	4° 40' N	27° 04' W	Vertical. V/H on. Three-axis maneuver.
IIS-12	8° 00' N	20° 00' W	Northerly oblique. V/H off. Three-axis maneuver.
IIS-13	3° 20' N	43° 50' W	Vertical. V/H on. Three-axis maneuver.
IIS-14	9° 16' N	100° 17' E	Farside. Vertical centered on point 20 degrees before PM terminator. Roll maneuver only. V/H off.
IIS-15	11° 00' N	53° 00' W	Northerly oblique. V/H on. Three-axis maneuver.
IIS-16	2° 40' N	54° 30' W	Vertical. V/H on. Three-axis maneuver.
IIS-17	7° 25' N	59° 00' W	Northerly oblique. V/H on. Three-axis maneuver.

3.2.1 FLIGHT PLAN

3.2.1.1 Introduction

The flight plan prepared to satisfy the aforementioned Mission II objectives was published in Boeing Document D2-100149, Volume 3 (P-8A) Flight Operations Plan, Lunar Orbiter, dated October 21, 1966.

This mission employed a nominal trajectory with liftoff on November 7, GMT during the launch period from November 6 through November 11, 1966.

A nominal 90-hour cislunar trajectory was planned, with midcourse correction scheduled at 28 hours and 70 hours after injection into the cislunar trajectory. A plane change of 6.15 degrees was scheduled at injection into the initial lunar orbit.

Approximately 8 days waiting time was possible from initial orbit injection until photography of the first of the 30 photo sites in the final orbit phase. Following photography there was a requirement for readout of 216 frames of film, which dictated a mission duration of 36.7 days.

3.2.1.2 Preparation

The preparation of this flight plan became a time-critical item due to late changes in the mission specification. Major changes, involving relocation of all primary targets, were received as late as 10 days before deployment of operations personnel for premission training exercises. To effect release of the operational plan before training started, it was necessary to proceed with operational planning before mission design was complete and to postpone an operational review of the plan until after its release. There were, however, relatively few changes to the published plan. The most significant was the insertion of additional information to better define command loading requirements by specifying the photo sites covered by each major command sequence. Also, the FPAC director requested transfer into final orbit earlier than planned to permit more time to prepare for photography of the first site.

3.2.1.3 Mission I/Mission II Comparisons

The Mission II plan was similar to that prepared for Mission I in that they were both intended for a distributed target mission designed to satisfy the same general objectives. Significant differences in the Mission II plan as compared to that for Mission I were as follows:

- There was no requirement for photography in initial lunar orbits. Consequently, the Mission II activities, particularly the command activities associated with photography and subsequent film movement, were considerably reduced in that phase of the mission.
- Spacecraft and operational crew activity in the photo phase of Mission II was greater due to the requirement to photograph three additional primary sites and 17 secondary sites. Secondary sites were not included in the plan for Mission I, although some were identified and photographed during the mission.
- In the majority of cases, the Mission II plan called for photography of each primary site with multiple eight-frame sequences taken on successive orbits; whereas single 16-frame sequences were employed for Mission I.
- The Mission II plan provided greater film budgeting flexibility by maintaining four frames in the camera storage looper at all times. This was designed primarily to facilitate inflight adjustment to the timing of photography without disruption of subsequent film budget planning.
- A simplified bar chart output of the sequence of events computer program (SEAL) was used to satisfy the event sequence requirements in the Mission II plan. The Mission I plan also included detailed event lists.

- Overlapping DSS tracking coverage was reduced considerably in the Mission II plan. However, two-station coverage was available during velocity maneuvers, and for three-way doppler, and time correlation activities.

3.2.1.4 Significant Events Summary

Table 3.2-2 contains a summary of the most significant activities reflected in the Mission II flight plan and the times of these activities. It should be noted that orbits are numbered sequentially throughout the mission, with Orbit 1 commencing at the first apolune passage after lunar injection. This was the numbering system used during the mission, whereas the initial release of the flight plan showed orbits numbered sequentially commencing with Orbit 1 in both the initial and final orbit phases of the mission.

Table 3.2-2: Significant Events Summary			
Time		Orbit	Event
Planned *	Actual		
311:00:26	310:23:21:00.2		Liftoff
311:00:30	310:23:23:08.4		Atlas Booster Engine Cutoff (BECO)
311:00:34	310:23:27:07.2		Agena first burn ignition
311:00:42	310:23:40:59.1		Agena second burn ignition
311:00:44	310:23:41:12.0		Cislunar injection
311:00:47	310:23:46		Spacecraft separation-start
			Deployment
	310:23:48:49		DSS-51 one-way rf lock
	310:23:51:53		DSS-51 two-way rf lock
	311:00:12:15		DSS-41 one-way rf lock
	311:00:30:00		DSS-41 two-way rf lock
			Sun acquired prior to data retrieval at DSS-41
311:02:00	311:01:15		Start gyro drift rate test no. 1
	311:06:50		Completed first star map and antenna map
311:07:00	311:06:48		Start Canopus acquisition (Roll 360°)
	311:08:21		Canopus acquired.
311:10:10	311:08:34	4	Start gyro drift rate test no. 2
311:11:20	311:10:34		Bleed propellant lines
	311:16:13		Pitched spacecraft off Sun for first time.
			Thermal relief maneuver.
	311:23:56		First gyro wheel current transient observed.
	312:12:12		Lost Canopus lock when propellant squibs fired. First midcourse correction delayed.
	312:15:50		Canopus reacquired
312:04:20	312:19:19		Start first midcourse maneuver.
	312:19:30		Ignition, 1st midcourse, ΔV : +21.1 mps, engine burn time: 18.1 sec.
	312:21:29		Pitched off Sun for thermal relief.
313:22:20			Second midcourse maneuver (not needed)
	314:02:05		Second Canopus loss
314:21:21	314:20:26:37.8		Ignition, lunar orbit injection, ΔV : 829.7 mps, engine burn time: 611.6 sec.
	314:20:55		Third Canopus loss, due to lunar reflection.
	315:10:00		Started test to evaluate performance of star tracker when exposed to reflections from Moon. Conclusion: Operate star tracker only during sun occultation.

Table 3.2-2: Significant Event Summary (Continued)

Time		Orbit	Event
Planned *	Actual		
315:17:24	315:22:34 316:15:13:52 317:13:40	(5) 12 18	Fourth Canopus loss Readout Goldstone test pattern Demonstrated automatic Canopus reacquisition by stored program commands. Telemetry indicated occultation time storage.
	317:21:12	20	Pitched off Sun for thermal relief (36 hours).
	318:18:45	26	First of several cycles of increased limit cycle rates, possibly due to system electrical noise.
	319:12:46	31	First micrometeoroid hit. Pressure leakage from sensor detected by gyros.
321:18:54	319:22:58:24.5	(46) 33	Ignition, orbit transfer. ΔV : 28.1 mps, engine burn time 17.4 sec.
322:13:56	322:15:24:16	(51) 52	Photograph Site II P-1
322:14:00	322:15:24:16	(51)	Photograph Site II S-1
322:15:50	322:17:18:00	(52) 53	Start first priority readout (Site II P-1)
322:17:26	322:18:53:59	52	Photograph Site IIS-2a
322:20:54	322:22:23:12	53	Photograph Site IIS-2b
323:01:24	323:02:54:25	54	Photograph Site IIS-3
323:04:52	323:06:22:53	55	Photograph Site IIS-4
323:07:20	323:08:49:42	56	Photograph Site IIP-2
323:14:16	323:15:44:21	58	Photograph Site IIP-3a
323:17:44	323:19:13:25	59	Photograph Site IIP-3b
323:21:12	323:22:40:59	60	Photograph Site IIP-4
324:00:40	324:02:12:35	61	Photograph Site IIP-5
324:08:40	324:10:12:17	63	Photograph Site IIS-5
324:14:36	324:16:08:48	65	Photograph Site IIP-6a
324:18:08	324:19:37:54	66	Photograph Site IIP-6b
325:01:00	325:02:30:45	68	Photograph Site IIS-6
325:07:56	325:09:27:36	70	Photograph Site IIS-7
325:14:58	325:16:29:25	72	Photograph Site IIS-8
325:21:52	325:23:24:10	74	Photograph Site IIS-9
326:01:18	326:02:52:35	75	Photograph Site IIP-7a
326:04:50	326:06:21:36	76	Photograph Site IIP-7b
326:11:46	326:13:17:09	78	Photograph Site IIS-10
326:15:14	326:16:49:08	79	Photograph Site IIP-8a
326:18:46	326:20:18:11	80	Photograph Site IIP-8b
326:22:14	326:23:14:13	81	Photograph Site IIP-8c
327:05:04	327:03:09:14	83	Photograph Site IIS-11
327:08:38	327:10:11:15	84	Photograph Site IIP-9
327:12:02	327:13:36:26	85	Photograph Site IIP-10a
327:15:32	327:17:05:30	86	Photograph Site IIP-10b
327:22:30	328:00:05:41	88	Photograph Site IIS-12
328:01:58	328:07:03:49	89	Photograph Site IIP-11a
328:05:30	328:10:32:53	90	Photograph Site IIP-11b
328:08:54	328:14:58:00	91	Photograph Site IIP-12a
328:12:22	328:17:27:06	92	Photograph Site IIP-12b
328:19:18	329:00:22:55	94	Photograph Site IIS-13
329:03:18	329:04:58:04	96	Photograph Site IIS-14
329:05:46	329:07:21:13	97	Photograph Site IIP-13a

Table 3.2-2: Significant Event Summary (Continued)			
Time		Orbit	Event
Planned*	Actual		
329:09:12	329:10:50:17	98	Photograph Site IIP-13b
329:12:40	329:14:16:08	99	Photograph Site IIS-15
329:19:36	329:17:45:15	101	Photograph Site IIS-16
329:23:06	329:21:12:53	102	Photograph Site IIS-17
330:03:44	330:08:58	(103) 105	Cut Bimat
330:06:28	330:15:06	(104) 107	Start Final Readout
	341:01:16	179	TWTA failed to turn on, terminating readout.
347:17:00		224	Mission complete.

* Per Nominal P8A Mission, D2-100149 Vol III (P8A:)

3.2.2 FLIGHT CONDUCT

3.2.2.1 Spacecraft Control

Paragraphs 3.2.2.1.1 and 3.2.2.1.2 describe, respectively, the command programming and photography controls established to meet the requirements of the flight plan (reference Paragraph 3.2.1). These paragraphs include descriptions of personnel activities as well as recommendations for future missions. Special attention should be given to the fact that Mission II control was significantly more effective than Mission I control. This was due primarily to the addition of off-line command programmers and to the successful efforts of the flight operations teams to follow the mission plan as closely as possible. Where deviations to the plan were required, they were documented in operations directives and revision instructions to the mission plan.

3.2.2.1.1 COMMAND PROGRAMMING

Summary

As of 22:00 GMT on December 8, a total of 3,571 commands had been prepared and transmitted to the Lunar Orbiter II spacecraft in flight and executed without incident. Approximately 50 extra commands that were transmitted as backup commands were not executed.

Despite the more complex schedule of photo activity of this mission compared to that of Lunar Orbiter I, command preparation activity proceeded smoothly and on schedule. This was due to adherence to premission planning, better scheduling of core maps, doubling the number of command programmers, and strict adherence to SPAC procedures.

Premission Activity

The most complex portions of Mission II were analyzed from the standpoint of flight programmer considerations. This resulted in a definition of the functions to be included in each core map and a schedule of core map loading, to be used also by FPAC and mission control personnel to plan their activities.

Countdown commands and Mode 2 commands for Mission II had been prepared and sent to the appropriate stations during the final readout phase of Lunar Orbiter I.

Launch plan commands were sent to Cape Kennedy (DSS-71) during Mission II training.

Mission Activity

Command preparation activity was divided into two parts: off-line planning and on-line command preparation. During the peak activity periods of the mission, there were one off-line and one on-line command programmer on each team.

Using the film budget and core map schedule of the mission plan, the off-line programmer planned the layout of each core map and defined the contents of each command sequence. He prepared a planning map and an event flow chart for use by the on-line programmer in preparing commands. The chart was used as an aid in tracing command sequences through the flight programmer. He also prepared a detailed spacecraft event sequence with the GMT of major events to be reviewed by SPAC analysts, mission control, and the mission advisors for their confirmation of the planned sequence.

Off-line planning for each map started approximately 14 to 16 hours before the scheduled transmission of the map and ended by the time of the preliminary command conference 7 hours before transmission. Occasionally it was necessary to schedule the transmission of portions of a map during different transmission windows because there was not room in the core for all the commands at once.

Deviations from the mission plan were incorporated only by means of revision instructions to the film budget due to tracking data, or upon receipt of an operations directive from the SFOF. Strict adherence to this procedure stabilized command preparation activity throughout the entire mission.

Using the plans of the off-line programmer, the on-line programmer prepared the commands to be transmitted to the spacecraft. Data for this activity (camera or engine-on time, maneuver magnitudes, camera mode, etc.) was given to the on-line programmer in a command preparation directive following the preliminary command conference. Improved forms for these directives, correcting deficiencies of those used in Mission I, were quite satisfactory. The directives were issued in accordance with standard SPAC procedures. These forms were the only ones accepted by the on-line programmer in making command generation computer program (COGL) runs. Any changes in command information required a revised directive.

COGL activity was completed and Mode 1 commands were on the way to the DSS by the time of the final command conference (approximately 2 hours before transmission). Generally, minor changes, such as camera-on time or maneuver angles, were requested by FPAC at this conference. These changes were readily incorporated using Mode 3 commands, which were subsequently verified in a COGL simulation.

Recommendations

Manpower, forms, procedures, and schedules for command preparation activities were entirely adequate. No changes are recommended for subsequent missions.

3.2.2.1.2 PHOTOGRAPHY CONTROL

Photography control, which covers exposure control, shutter speed determination, oblique photography planning, camera on-time determination, photo sequence, and film management will be found in Volume II of this document.

3.2.2.2 Flight Path Control

From launch through completion of photographic readout, maintaining control of the spacecraft trajectory (or flight path) is the responsibility of Flight Path Analysis and Command (FPAC). Responsibility for control of the mission from prelaunch checkout through about launch plus 6 hours belongs to the DSN FPAC. After the spacecraft has been acquired and is supplying good tracking data to the SFOF (about launch plus 6 hours), the DSN FPAC team is relieved by the project FPAC team. At this point the project FPAC team assumes the responsibility for flight path control for the remainder of the mission. Within both teams the tracking data analysis function is carried out by a JPL analyst. A description of the two FPAC teams is contained in Boeing Document D2-100727-3, Lunar Orbiter 1 Final Report, Mission Operational Performance.

Flight path control by the FPAC team entails execution of the following functions.

- Tracking Data Analysis - - (1) Monitoring and passing judgment on the quality of the incoming radar tracking data (doppler and range). This raw tracking data is the sole link between the spacecraft and FPAC, and is the basis for determination of the current position and velocity of the vehicle. (2) The preparation of tracking predicts to support the DSS in spacecraft tracking.
- Orbit Determination - - The process of finding a trajectory that "best fits the tracking data." This included the tasks of editing the raw tracking data into a form acceptable to the orbit determination computer program (ODP), and subsequent operation of this program to obtain that trajectory which best fits the data - usually a lengthy task that consumes large blocks of computer time.
- Flight Path Control - - When the orbit determination process yields a trajectory, the flight path control function is initiated to determine the need for a corrective maneuver or the design of a planned maneuver. Thus, this function is principally one of guidance, control, and prediction.

FPAC executes these functions to design maneuvers that will best achieve the objectives of the nominal flight plan. This nominal flight plan is furnished to FPAC by the mission design group and provides the criteria, ground rules, and constraints that must be observed in any maneuver design. The computer programs, or FPAC software system, used for maneuver designs are identical to that used during Mission 1, with the exception of some internal modifications to individual programs. A description of the FPAC software system is contained in Boeing Document D2-100727-3, Lunar Orbiter 1 Final Report, Mission Operational Performance.

From a trajectory point of view, the mission can be subdivided into the following phases:

Countdown, Launch, and Acquisition Phase - - Covers the period from FPAC entry into the countdown through DSN acquisition of the spacecraft and subsequent handover from DSN FPAC team to project FPAC team.

Injection thru Midcourse - - From the completion of the 2nd Agena burn through the completion of the midcourse maneuver. This phase overlaps the acquisition portion of the previous phase.

- Midcourse through Deboost - - From end of midcourse burn through completion of the deboost maneuver.
- Initial Ellipse - - From end of deboost burn through the transfer maneuver.
- Photo Ellipse - - From end of transfer burn through completion of photo readout.

Table 3.2-3 lists the principal FPAC events and their times of occurrence (GMT) within these phases. The orbit determination and flight path control functions executed in these phases will be discussed in the following subsections.

Table 3.2-3: Trajectory Sequence Of Events

Launch and Acquisition

Nov. 6, 12:00 -- FPAC begins prelaunch checkout of software system
 Nov. 6, 23:21 -- Launch
 Nov. 6, 23:27 -- Agena first burn complete. Start 677-sec. coast
 Nov. 6, 23:42 -- Agena second burn complete. Cislunar injection
 Nov. 6, 23:52 -- First DSS51 two-way doppler data
 Nov. 7, 03:00 -- DSN FPAC hands over control to project FPAC

Injection through Midcourse

Nov. 7, 06:40 -- Calculated 10 m/sec midcourse for execution at cislunar injection plus 15 hours, 19 m/sec at plus 40 hours
 Nov. 7, 09:00 -- Selected M/C maneuver time of November 8, 12:56
 Nov. 8, 12:50 -- Rescheduled M/C maneuver to Nov. 8, 19:30, because of loss of roll reference.
 Nov. 8, 13:00 -- Calculated 21.1 m/sec midcourse for execution at cislunar injection plus 41 1/2 hours
 Nov. 8, 19:30 -- Start midcourse burn

Midcourse through Deboost

Nov. 9, 02:35 -- Determined 2nd midcourse not required
 Nov. 9, 23:06 -- Completed design of deboost maneuver
 Nov. 10, 20:26 -- Start deboost burn

Initial Ellipse

Nov. 11, 01:55 -- Confirmed expected post-deboost state
 Nov. 15, 09:45 -- Completed design of transfer maneuver
 Nov. 15, 22:58 -- Start transfer burn

Photo Ellipse

Nov. 16, 05:45 -- Confirmed expected post-transfer state
 Nov. 18, 15:25 -- Start of photography
 Nov. 25, 21:13 -- End of photography
 Dec. 6, 23:44 -- Completion of photo readout

3.2.2.2.1 COUNTDOWN, LAUNCH, AND ACQUISITION PHASE

Project FPAC entered the countdown procedure at launch minus 5 hours on 6 November 1966. Check cases of the project FPAC user programs were run on both computer strings. These were completed at T-4 hours on the project (X) string and at T-3 hours on the DSN (Y) string. No problems were encountered on either string.

Frequency reports from ETR (DSS-71), were received on schedule and frequency parameters were supplied to the real-time computer system (RTCS) for DSIF predicts. All liftoff predicts program (PRDL) cases were run as required. The actual liftoff time PRDL case was cancelled since liftoff occurred at the expected time.

Launch occurred on Nov. 6, 23:21:00.195 (GMT) at a launch azimuth of 92.9 degrees. Table 3.2-4 lists the major powered flight events ("mark" times) from liftoff through completion of Agena retro.

The project FPAC orbit determination group was scheduled to begin an orbit determination based on Johannesburg DSS-51 tracking data. However, due to the systems problem, the DSS-51 data was not available to the FPAC team until launch plus 1 hour and 30 minutes.

Woomera DSS-41 acquired the spacecraft as scheduled. Due to a communications outage at launch plus 1 hour and 9 minutes, only 9.5 minutes of three-way doppler and angle data were available to project FPAC for an early orbit determination. These data were the first available and were processed by the ODP to obtain the first project OD solution, 1102.

The early orbit determination results obtained by project FPAC, DSN FPAC, and the RTCS at AFETR, all projected to lunar encounter, are shown in Figure 3.2-1.

Table 3.2-4: Powered Flight Trajectory Events

Mark	Event	Actual Time (GMT)
0	Liftoff	Nov. 6, 23:21:00.195
1	Atlas Booster Engine Cutoff (BECO)	23:23:08.4
2	Atlas Booster Engine Jettison	23:23:11.5
3	Start Agena Secondary Timer	23:25:29.9
4	Atlas Sustainer Engine Cutoff (SECO)	23:25:50.9
5	Start Agena Primary Timer	23:25:53.1
6	Atlas Vernier Engine Cutoff (VECO)	23:26:14.3
7	Shroud Separation	23:26:16.8
8	Atlas-Agena Separation	23:26:18.4
9	Agena First Ignition	23:27:07.13
10	Agena First Shutdown (Parking Orbit Injection)	23:29:42.44
11	Agena Second Ignition	23:40:59.2
12	Agena Second Shutdown (Cislunar Injection)	23:42:27.2
13	Agena-Spacecraft Separation	23:45:12.0
14	Begin Agena Yaw	23:45:14.96
15	End Agena Yaw	23:46:14.96
16	Agena Retro	23:55:11.8

Three and one half hours after liftoff, spacecraft acquisition was verified. FPAC control was then handed over to the project by the DSN.

DSIF stations used for tracking during Mission II were:

Station	Station Identification
Goldstone (Pioneer)	11
Goldstone (Echo)	12
Woomera	41
Johannesburg	51
Madrid	61

DSS-12, -41, and -61 were the prime Lunar Orbiter tracking stations.

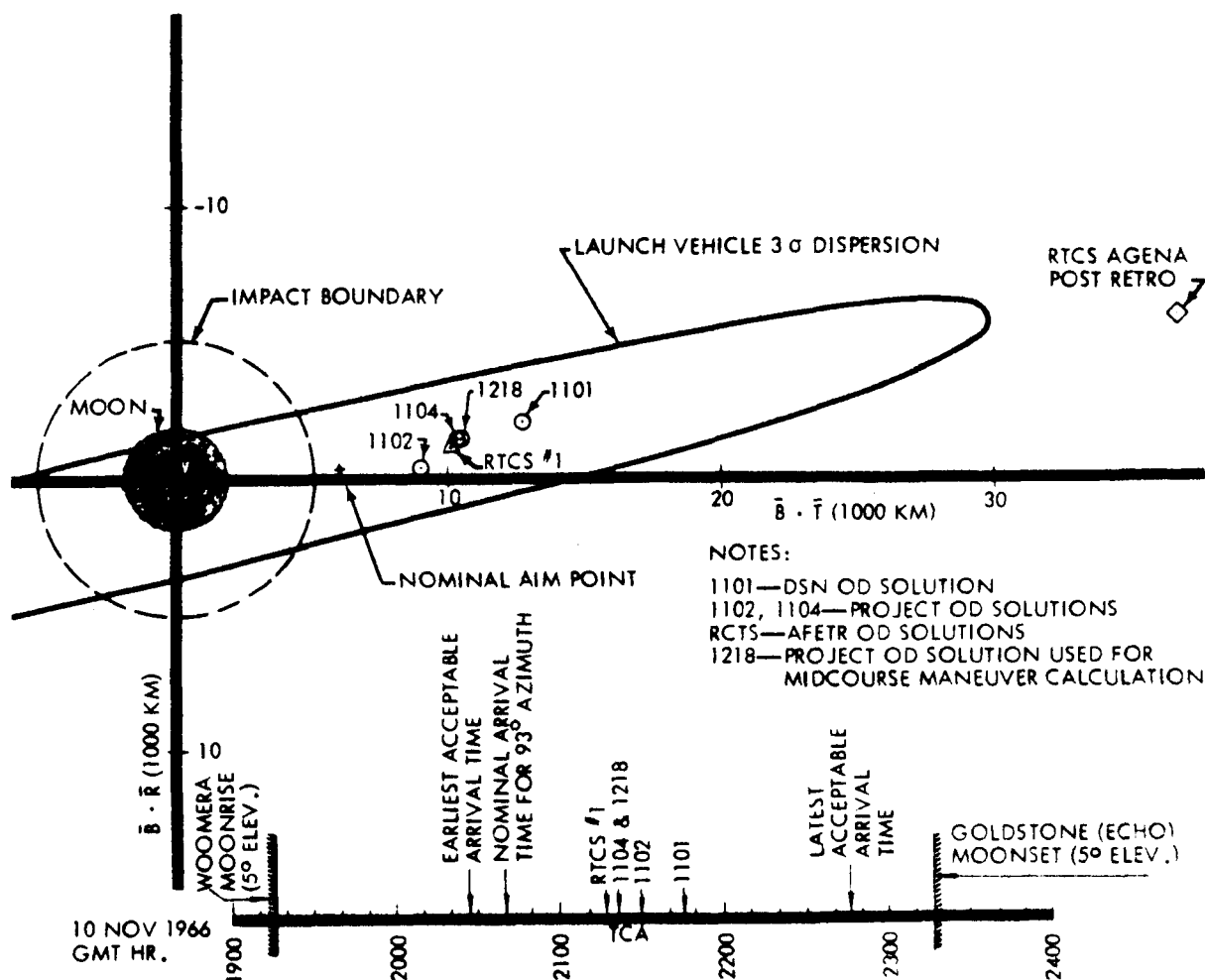


Figure 3.2-1: Early Orbit Determination Results

3.2.2.2.2 INJECTION THROUGH MIDCOURSE

Events during the injection through midcourse phase of the mission followed the pre-mission plan with the exception of a requirement to redesign the midcourse maneuver to accommodate a delay in execution. Other than this anomaly all aspects of flight path control were as expected.

Orbit Determination

Table 3.2-5 shows the chronological sequence of the lunar encounter parameters obtained from the eight project orbit determinations performed before midcourse. Final design of the midcourse maneuver was based on OD 1218. OD 1218 was based on 28 hours of two-way-lock doppler data from DSS-41, -12, -51, and -61. The fit of the doppler data to the orbit solution was excellent.

Table 3.2-5: Pre-Midcourse Orbit Determination Encounter Parameter Summary

Orbit Solution	B-T (km)	B-R (km)	Time of closest approach (GMT)
1102*	8,993.4	- 478.8	Nov. 10, 21:29:59.039
1104* *	10,418.2	-1,473.1	21:21:07.327
1206	10,426.0	-1,473.7	21:21:06.725
1208	10,425.1	-1,473.9	21:21:06.572
1310	10,427.7	-1,474.7	21:21:04.925
1112	10,427.2	-1,477.5	21:21:07.496
1114	Used to evaluate encounter statistics		
XX16	This number was skipped		
1218	10,428.1	-1,476.6	21:21:07.731
1320	10,430.5	-1,475.3	21:21:06.119
Nominal Aimpoint	6,120	- 410	20:39:30.6

* This very early solution was based on only 9 minutes of DSS-41 tracking.

* * This early solution was based on 1 hour of DSIF tracking; subsequent solutions used longer tracking arcs.

(Appendix B contains supporting data for the orbit determination work).

In Mission I the orbit determination estimates of the uncertainty in the lunar encounter parameters considered only the contributions of doppler random noise. During this mission, uncertainties contributed by the gravitational constants of the Earth and Moon and the tracking station locations were also included. Using accepted numbers for the above uncertainties, the more realistic estimate of lunar encounter uncertainties based on OD 1112 for Mission II are contrasted below with those obtained using the obsolete Mission I procedure.

	Mission I Procedure	Mission II Procedure
Elements	OD 1112	OD 1114
Approach Hyperbola Perilune Altitude	0.66	25.2
σ Uncertainty (km)		
Time of Closest Approach	1.3	6.0
σ Uncertainty (sec)		

Midcourse Design and Execution

Within 2 hours after cislunar injection, projected lunar encounter parameters (see Figure 3.2-1) indicated that the second Agena burn had resulted in a trajectory well within the midcourse capability of the spacecraft. It was also apparent that although a midcourse maneuver would be required, midcourse execution time would not be critical and an early midcourse would not be necessary.

The criteria used in designing the midcourse maneuver were:

- 1) Delay maneuver as long as practicable to minimize the effect of midcourse execution errors on lunar encounter conditions;
- 2) Perform the first midcourse maneuver at least 50 hours before orbit injection to allow time for a second midcourse;
- 3) Minimize ΔV required for lunar orbit injection (deboost), transfer, and midcourse with a maneuver at selected midcourse time.

A study of midcourse execution time was made using OD 1206, which was based on 3.3 hours of tracking and which became available 6 hours after lunar injection, correcting both the time of flight to the nominal encounter time (November 10, 20:39: GMT), and the miss parameters (B·T and B·R) were corrected to those computed in the midcourse targeting program. Figure 3.2-2 shows the results of this study. The midcourse maneuver could be delayed to the limit, i.e., 40 hours after cislunar injection, without the slightest danger of exceeding the ΔV budget for the maneuver 93 m/sec.

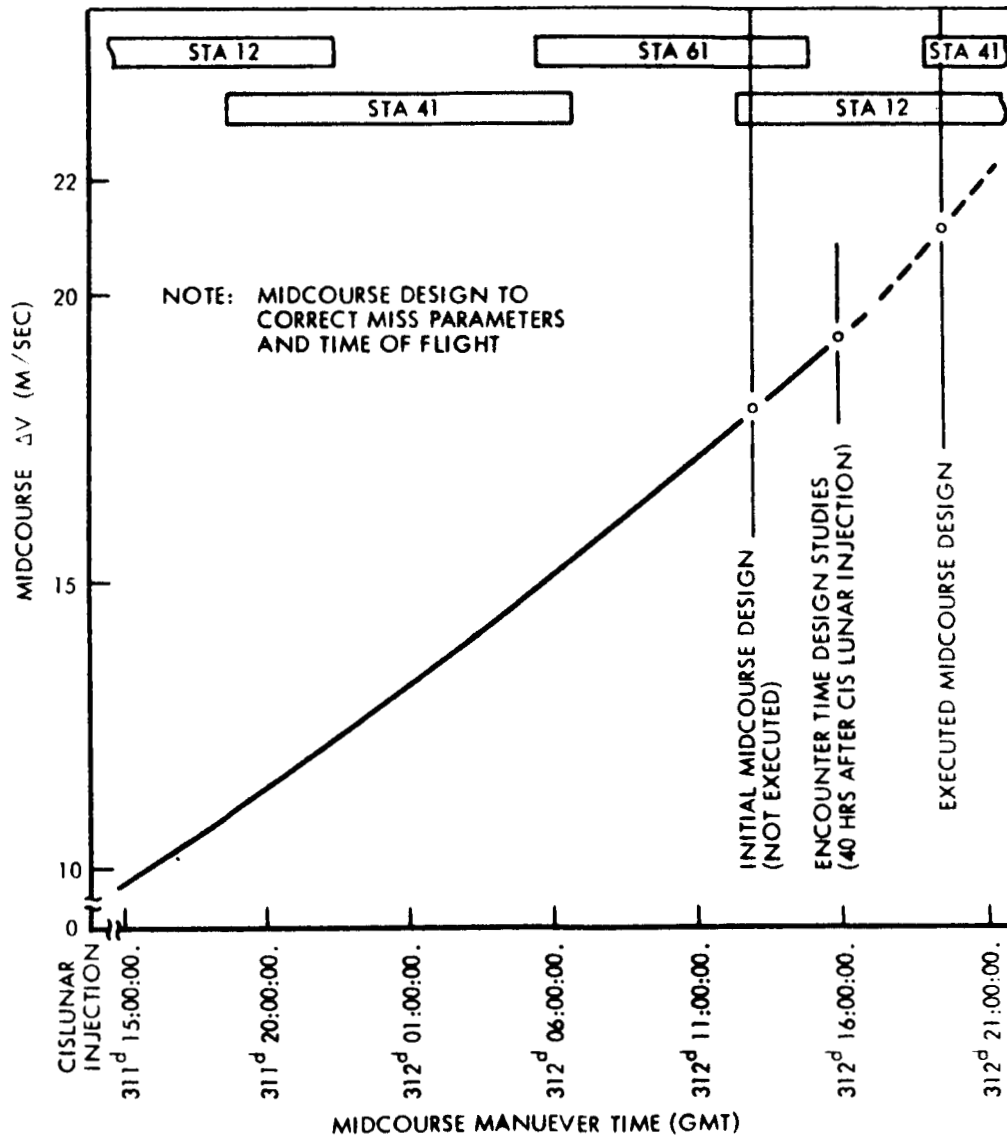


Figure 3.2-2: Effect of Midcourse Time on ΔV Required

Optimization of deboost, transfer, and midcourse ΔV is done automatically by the FPAC software programs for a given midcourse execution time and specified lunar encounter time. By varying the encounter time for a selected midcourse execution time, it is possible to minimize the total ΔV for midcourse, deboost, and transfer. The results of this analysis are shown in Figure 3.2-3 for a midcourse executed at approximately 40 hours after cislunar injection. The minimum total ΔV in this case happens also to correct the encounter time to within 2 minutes of nominal. On the basis of the data contained in Figures 3.2-2 and 3.2-3 it was decided to correct both the miss parameters and encounter time with a first midcourse maneuver executed about 40 hours after cislunar injection.

It is desirable to perform the midcourse maneuver while the spacecraft is in a two-station view period. Accordingly, engine ignition was scheduled for approximately 37 hours after cislunar injection (30 minutes after DSS-12 rise) so that both DSS-12 and -61 would view

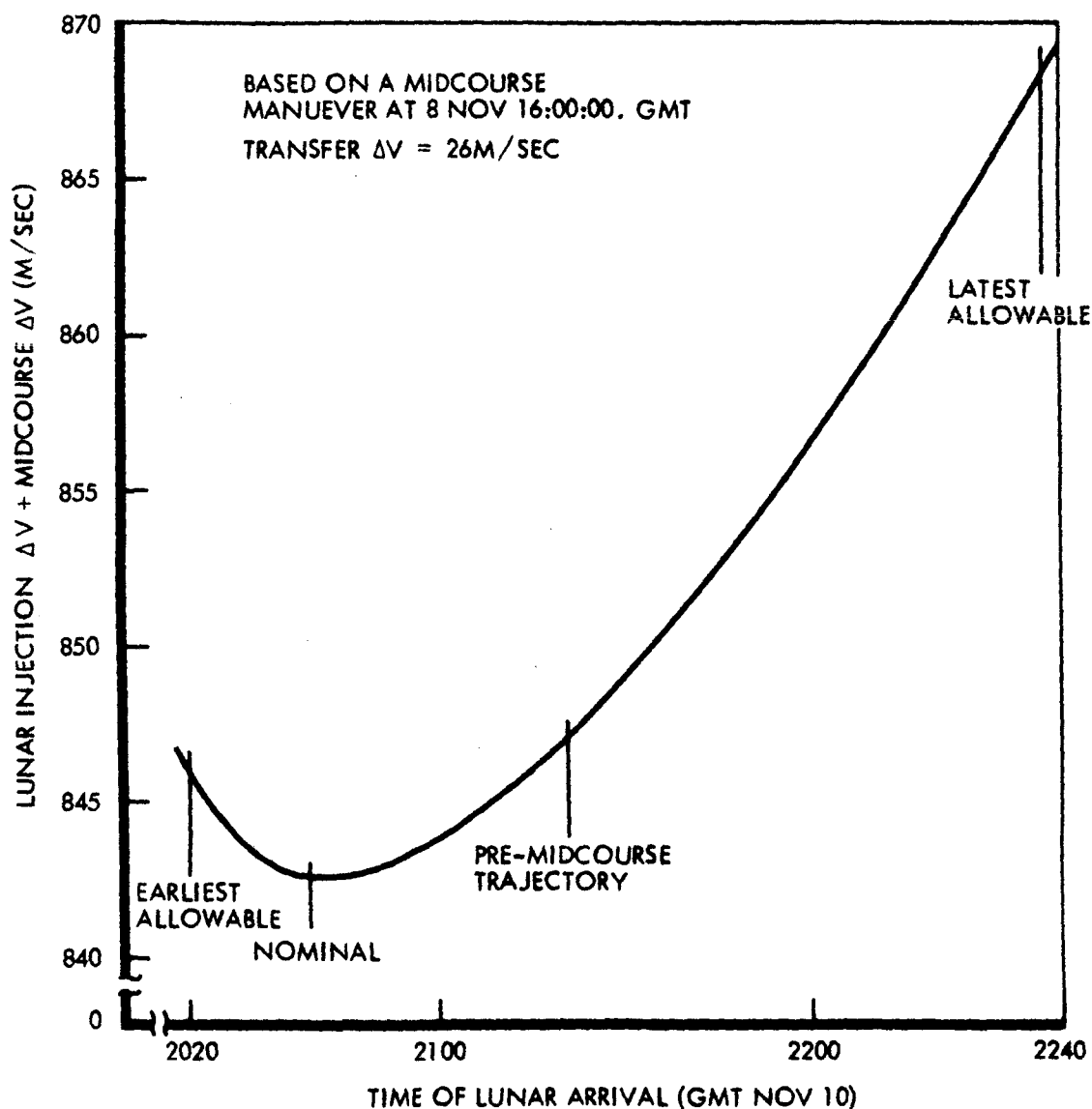


Figure 3.2-3: Effect of Time of Flight on Total ΔV Requirements

the engine burn. The impulsive deboost design program was used to confirm that the midcourse design would allow injection into a nominal initial ellipse. A discrepancy in solutions resulted and was traced to an error in the injection program. Both the midcourse and injection design programs use a reference target in lunar orbit (perilune longitude and latitude at a specified time). By replacing the reference target in the photo ellipse originally used with a target early in the initial ellipse, the magnitude of the discrepancy was minimized and satisfactory agreement was obtained between the midcourse and injection design programs.

The midcourse maneuver was aborted when Canopus was lost from the star tracker field of view after the propellant squib valves were fired but before initiation of the attitude maneuver. The midcourse maneuver was rescheduled for the next two-station view period at approximately 43.5 hours after cislunar injection. This time was 30 minutes after DSS-41 rise during overlap with DSS-12. The ignition time of November 8, 19:30:00.0 (GMT), necessarily exceeded the 40-hour limit for first midcourse execution; had a need for a second midcourse ensued, the available time for tracking, orbit determination, and design would have been short. The latest time for a second midcourse is 25 hours prior to lunar injection to allow sufficient time for orbit determination and lunar injection design. A backup first midcourse maneuver for November 8, 23:30:00 (GMT), was also designed but was not needed. The midcourse maneuver was executed November 8 at 19:30:00 and consisted of the following attitude maneuver and engine burn specified by FPAC.

Sun line roll = 41.90 deg.

Canopus for roll reference

Pitch = 30.16 deg.

$\Delta V = 21.15$ m/sec.

This attitude maneuver was selected from 12 possible two-axis maneuvers on the basis of: (1) viewing DSS line of sight vector not passing through any antenna null regions; (2) minimizing total maneuver rotation; and (3) maintaining Sun lock as long as possible. OD 1218 was used for the midcourse final design. Midcourse targeting resulted in the following set of encounter parameters. The preflight nominals and pre-midcourse values are also given. These data are presented graphically in Figure 3.2-4.

	Nominal (Preflight design)	Pre-Midcourse (actual)	Post-Midcourse (encounter design)
B·T (km)	6120	10,425.9	6,010.1
B·R (km)	-410	-1,474.5	-390.5
TCA (GMT)	Nov. 10, 20:39	Nov. 10, 21:21:07.3	Nov. 10, 20:39:00
V_{∞} (km/sec)	0.95666	0.95305	0.9623

Figure 3.2-5 shows the Earth-Moon-spacecraft geometry at the time of the midcourse maneuver and the direction of the desired velocity change. Engine ignition occurred at November 8, 19:30:00 (GMT), and the engine burned for 18.1 seconds. The resulting doppler shift was 315 cps. The doppler data observed during the burn indicated a nominal burn as shown in Figure 3.2-6.

3.2.2.2.3 MIDCOURSE THROUGH DEBOOST

Orbit Determination

The first orbit determination after the midcourse maneuver (OD 2100) was not started until 5 hours after that maneuver because the trajectory curvature was so small in this region that meaningful determinations of spacecraft position could not be made earlier.

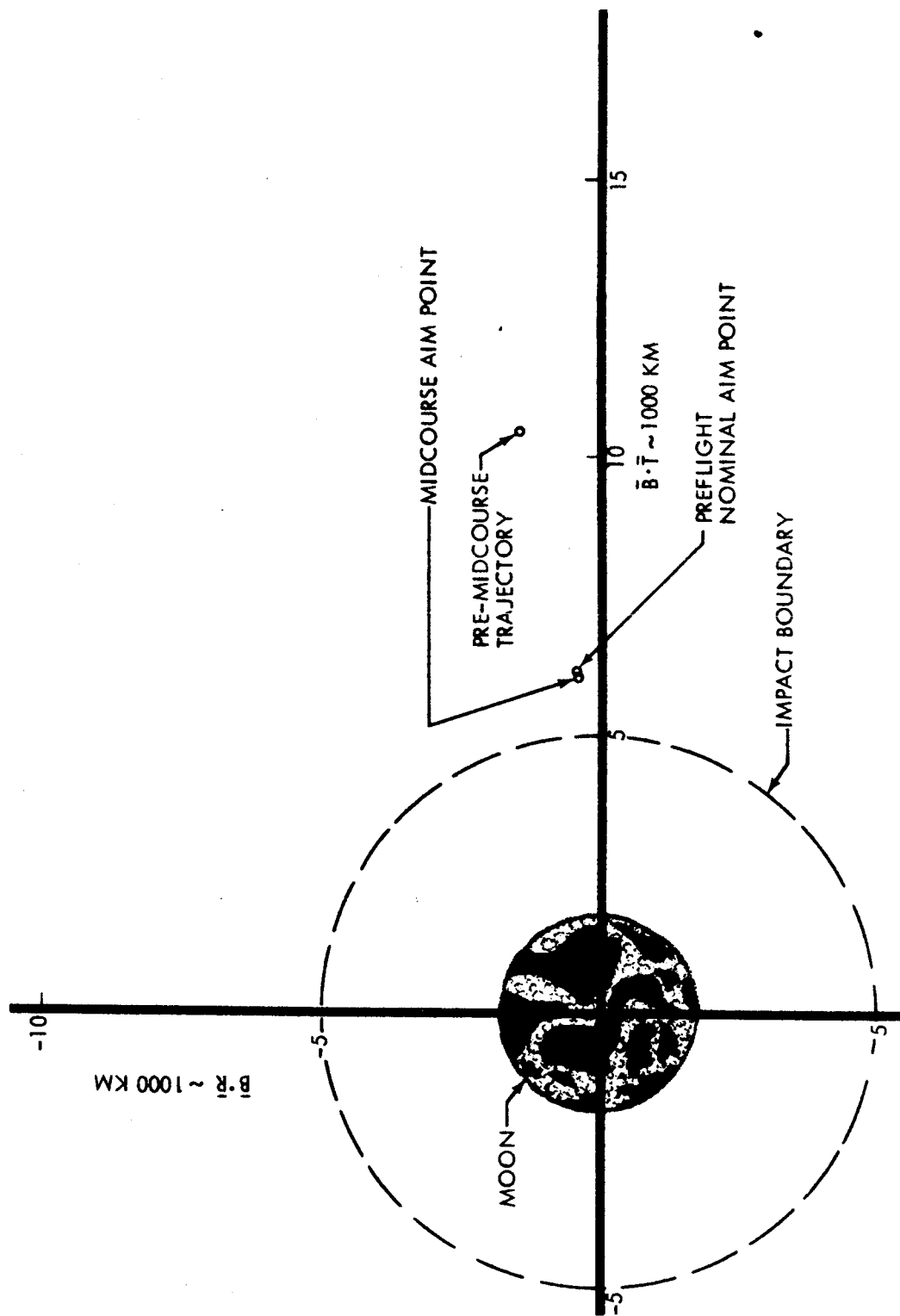


Figure 3.2-4: Pre-Midcourse Encounter Parameter Summary

PROJECTION IN
EARTH'S EQUATOR
MIDCOURSE TIME NOV 8, 19:30:00. (GMT)

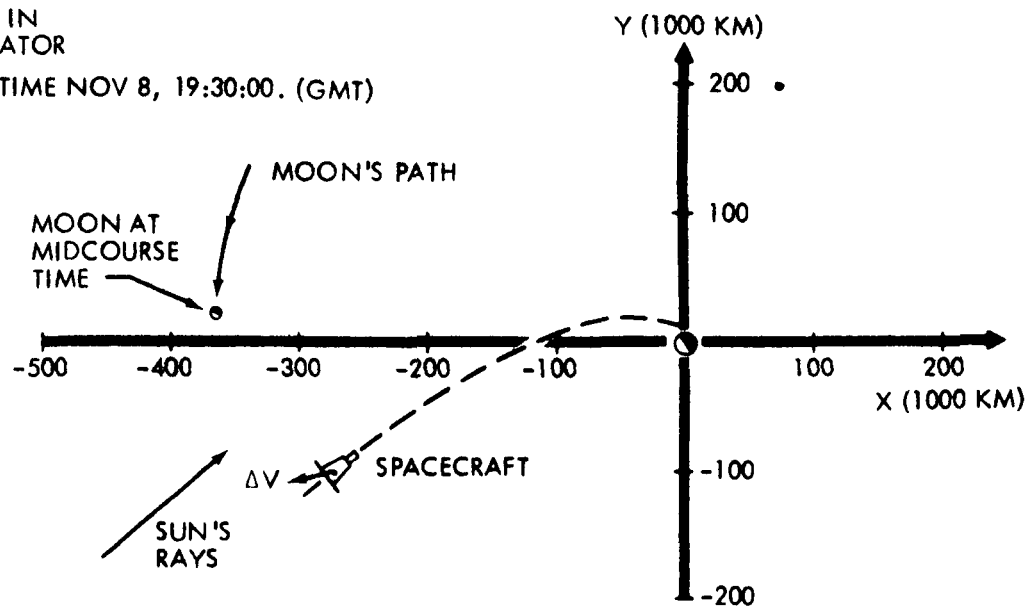


Figure 3.2-5: Midcourse Geometry

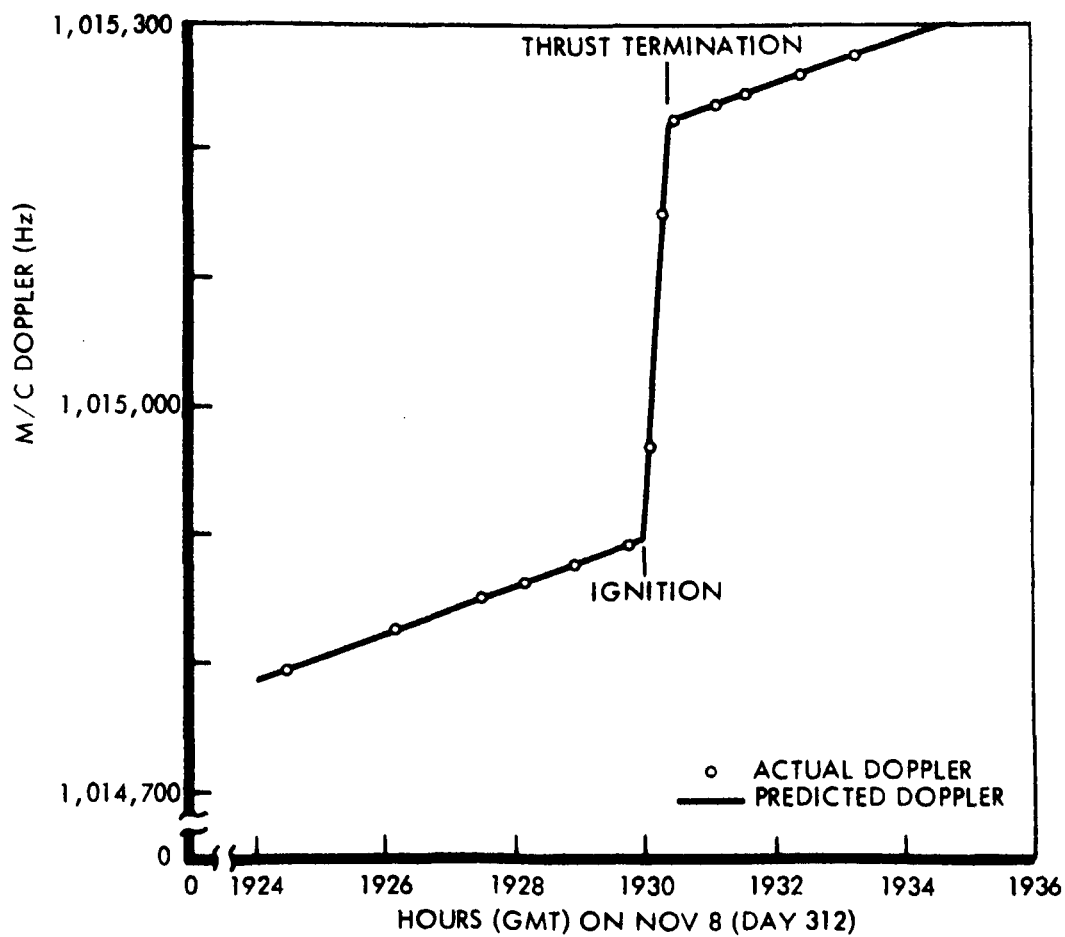


Figure 3.2-6: Midcourse Doppler Shift

Mission 1 experience indicated that this starting time was premature with doppler data alone, but some 36 ranging points were available which would help the determination. The determination was successful. It predicted encounter perilune altitude and closest approach time within 8 km and 12 sec of the best estimates subsequently achieved with 25 hours of tracking. Table 3.2-6 shows the early orbit determination prediction, the best estimate of the actual encounter conditions, and the midcourse-designed encounter conditions.

Table 3.2-6: Encounter Conditions

Elements	Midcourse Designed	1st OD (OD 2100)	Best Estimate (OD 2112)
Perilune Altitude (km)	2724.7	2724.0	2732.0
Time of Closest Approach (GMT) (314 ^d 20 ^h 39 ^m XX ^s)	0.0	24.4	12.5
$\bar{B} \cdot \bar{T}$ (km)	6010.1	6032.0	6043.6
$\bar{B} \cdot \bar{R}$ (km)	-390.5	-393.0	-373.3
\bar{B} (km)	6022.8	6055.0	6055.1

Ranging data were used in about 50% of the determinations made during this mission phase; when used with long periods of doppler tracking data, minor inconsistencies in the determinations were noted. These were attributed primarily to the necessity for a very large calibration correction which was applied to the raw range data.

The orbit determination used for the deboost maneuver calculation was OD 2112. This determination used 21.5 hours of two-way lock doppler data from DSS-41, -12, and -61. The first data point used in the determination was 2.5 hours after the midcourse maneuver because a 36-degree-pitch maneuver occurred 2 hours after midcourse. Since large pitch and yaw maneuvers disturb the trajectory (uncoupled gas jet thrusts), it was felt that a more accurate estimate of spacecraft position and velocity could be obtained by moving the starting point of the determination past this maneuver. The estimate of the encounter parameters obtained from this determination is shown in Table 3.2-6. The predicted uncertainties in the lunar encounter conditions obtained from this determination (using the new procedure described in the previous mission phase writeup) were:

1 σ Uncertainties

Perilune Altitude	0.95 km
Time of Closest Approach	5.1 sec
$\bar{B} \cdot \bar{T}$	1.1 km
$\bar{B} \cdot \bar{R}$	6.6 km
\bar{B}	6.7 km

More information about this determination is shown in Appendix B.

Appendix B also contains summaries of all the orbit determination performed during this phase.

After the orbit determination for the deboost maneuver was completed, several more determinations were done to verify the prediction of lunar encounter time (time of closest approach). Estimates of this quantity improve as the spacecraft approaches the Moon because the gravitational field of the Moon causes the trajectory curvature to increase and thus provide better geometrical conditions for a determination.

Deboost Design and Execution

A discrepancy was found to exist between the post-midcourse encounter parameters generated by the midcourse program and the encounter parameters obtained by forwarding the designed post-midcourse state to time of closest approach (TCA) with an integrating trajectory program. The reason for this difference was not determined until after the mission when an error in the trajectory integration portion of the midcourse program was located. The effect of this error on flight path control was that although the optimum targeting parameters ($B \cdot T$, $B \cdot R$, TCA) were computed, the associated midcourse ΔV to satisfy these targeting parameters was slightly in error. This resulted in an actual post-midcourse trajectory with encounter parameters slightly different than designed. A comparison of the designed post-midcourse encounter parameters, the actual post-midcourse encounter parameters, and the corrected encounter parameters for the designed post-midcourse state is as follows:

	Designed Post M/C Encounter Parameters	OD 2112 Actual Post M/C Encounter Parameters	Corrected Encounter Parameters Based on Forwarding the Designed Post M/C State
$B \cdot T$ (km)	6,010.1	6,043.6	6,033.4
$B \cdot R$ (km)	-390.5	-390.5	-381.5
TCA (GMT) Nov. 10, 20:39:00.		Nov. 10, 20:39:12.9	
V_{∞} (km/sec)	0.9623	0.95781	0.9574

Thus the designed midcourse maneuver resulted in a trajectory having built-in errors that had to be corrected with the deboost maneuver.

OD 2112, based on 21.5 hours of tracking data, was used to design the deboost maneuver. Deboost design was later verified using OD 2114 based on 31.5 hours of tracking data.

The design philosophy for the deboost maneuver was to guide the spacecraft from its approach hyperbola into an ellipse such that the ellipse inclination and apolune attitude were at their nominal values. An attempt was also made to hold the remaining ellipse parameters, ascending node longitude (Ω), argument of perilune (ω), and perilune altitude (h_p) as close to nominal as possible. Goudas No. 2 lunar harmonics were used in extending the trajectory to a reference target in the initial ellipse.

Different orbit injection solutions were obtained by FPAC operations and the Seattle back-up group because of their different software programs. The operational software attempted to maintain constant Ω and ω , with h_p as the adjusting parameter, whereas the Seattle software kept Ω and h_p constant with ω as the independent variable. Because perilune altitude was more important than argument of perilune, and the Seattle solution had a value of Ω closer to the nominal value, it was decided to target to the Seattle solution, resulting in the following initial ellipse design.

	Design	Nominal
Apolune Altitude h_a (km)	1850.0	1850.0
Orbit Inclination i (deg)	11.94	11.95
Ascending Node Longitude Ω (deg)	341.8	340.8
Argument of Perilune ω (deg)	162.1	156.8
Perilune Altitude h_p (km)	202.2	200.0

The finite burn program was run to refine the solution and to generate the required attitude maneuvers. Engine ignition was designed to occur at November 10, 20:26:37.3 (GMT). The required maneuver was:

Roll	(deg)	-8.96
Pitch	(deg)	-101.38
ΔV	(m/sec)	829.7

The attitude maneuver was selected from the twelve possible two-axis maneuvers on the basis of (1) DSS vector not passing through any antenna null regions, and (2) minimum total rotation angle.

Verification of the lunar injection solution was obtained by forwarding predicted post-injection conditions, designing a transfer maneuver, and then running the photo prediction program. The predicted value of lighting angle over the reference target in the photo ellipse (2° W longitude, 2.37° N latitude) was identical to the nominal value of 70.5 degrees.

A series of flyby maneuvers was also designed for use in the event of engine failure. These maneuvers consisted of an initial three-axis maneuver to point the camera axis along the local vertical, then five consecutive pitch maneuvers, and finally a three-axis maneuver to point the camera toward Earth. Nine photo frames were planned for the flyby mode.

The deboost attitude maneuver was performed 14 minutes before engine ignition. Actual start of engine burn occurred on November 10, 20:26:37.3, and the burn lasted for 611.6 seconds, producing a doppler shift of 1,970 cps. Doppler data observed during the burn confirmed nominal execution of the maneuver. See Figure 3.2-7.

The geometry at maneuver time is shown in Figure 3.2-8. At November 10, 19:10:10 (GMT) (76 minutes before ignition) Station 41 rose to begin the two-station view period with Station 12. View of the spacecraft from DSS-12 and -41 was occulted by the Moon 34 minutes after thrust termination.

3.2.2.2.4 INITIAL ELLIPSE

Orbit Determination

Immediately following the monitoring of the doppler shift during the deboost maneuver, incoming tracking data was logged and edited in preparation for a quick determination of the elements of the first orbit. The objective was to ensure that the stations would promptly reacquire the spacecraft when it emerged from behind the Moon. It was necessary to determine the new orbit, calculate a set of station doppler predicts based on this determination, and send these predicts to the station within minutes after deboost. A "quick look" orbit determination (4200) was completed at deboost + 35 minutes using about 15 minutes of two-station view--this orbit was not regarded as definitive but, coupled with the nominal deboost doppler shift, gave an indication that the deboost was near nominal. A more definitive orbit determination was achieved at deboost + 54 minutes and station predicts were computed by the DSN and sent to the stations before spacecraft emergence. A comparison of the designed post-deboost orbital elements, the best estimate of these elements (OD 4206), and the first orbit determination results (4102) are shown in the following table:

Orbital Elements	Deboost Design	First OD Results (OD 4102)	Best Estimate (OD 4206)
h_p	202.1	192.5	196.3
h_a	1850.	1850.9	1871.3
i	11.94	11.75	11.97
Ω	341.8	347.01	341.7
ω	162.1	157.16	161.6

No difficulties were encountered in the initial orbit determination and it was not necessary to employ backup procedures.

Orbit determination activities during the 5 days from deboost to transfer consisted of routine updating of the spacecraft state and support of the orbit transfer maneuver design. Lunar gravitational harmonics were not evaluated in Mission II as they were during this phase in Mission I. Plots of the orbital elements determined during this phase are shown in Figures 3.2-9 through 3.2-12. The orbit determination reports detailing the solutions are presented in Appendix B.

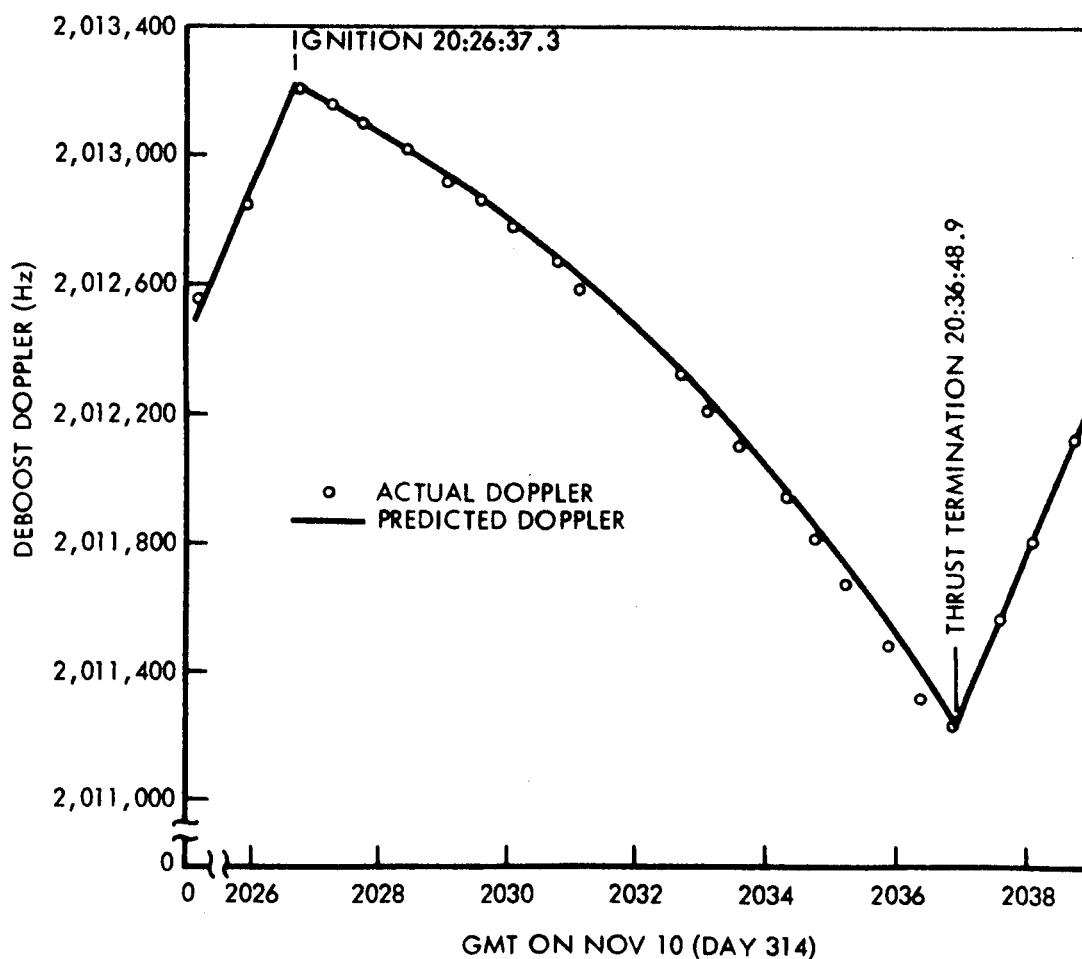


Figure 3.2-7: Deboost Doppler Shift

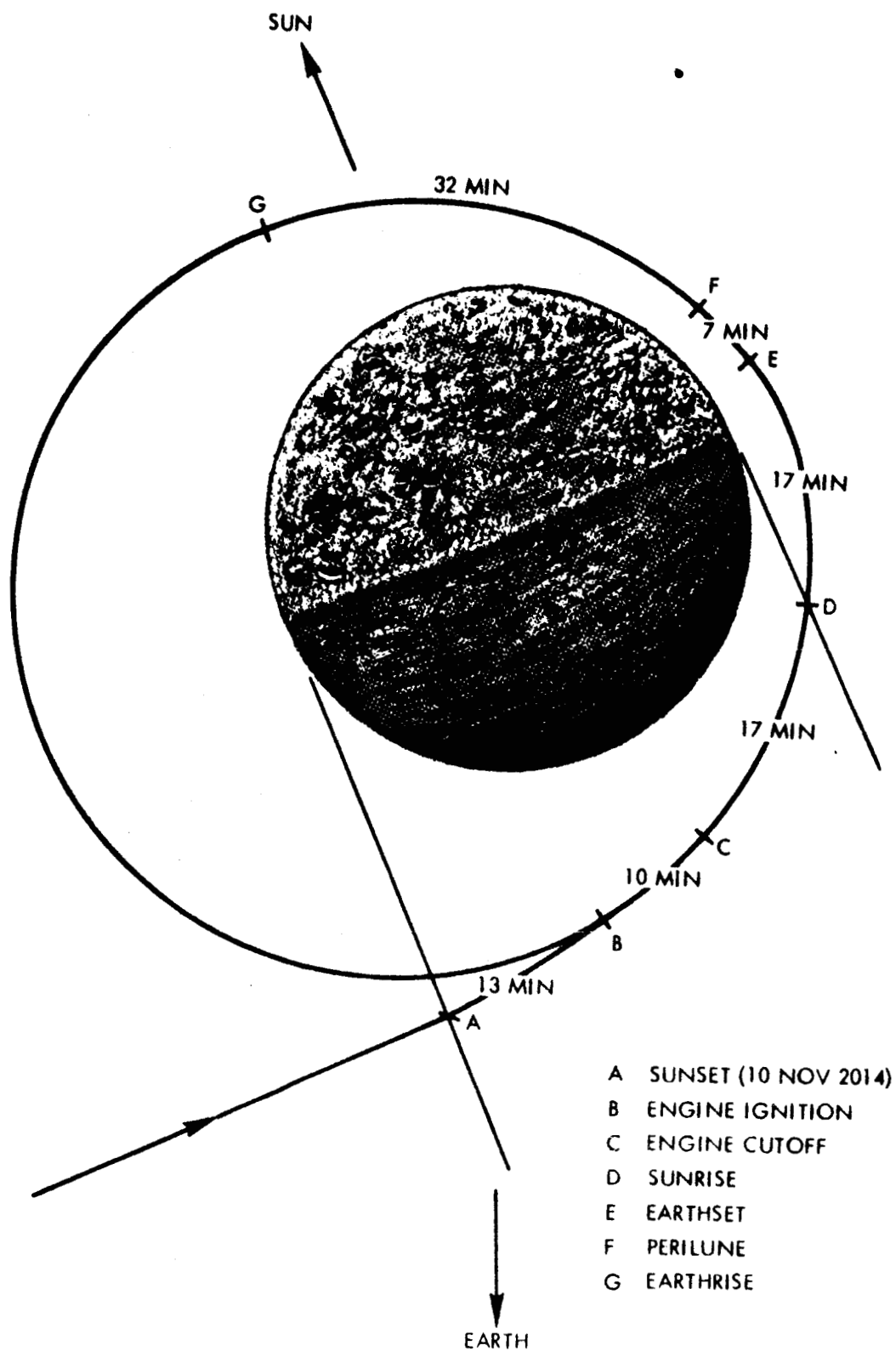


Figure 3.2-8: Geometry at Deboost

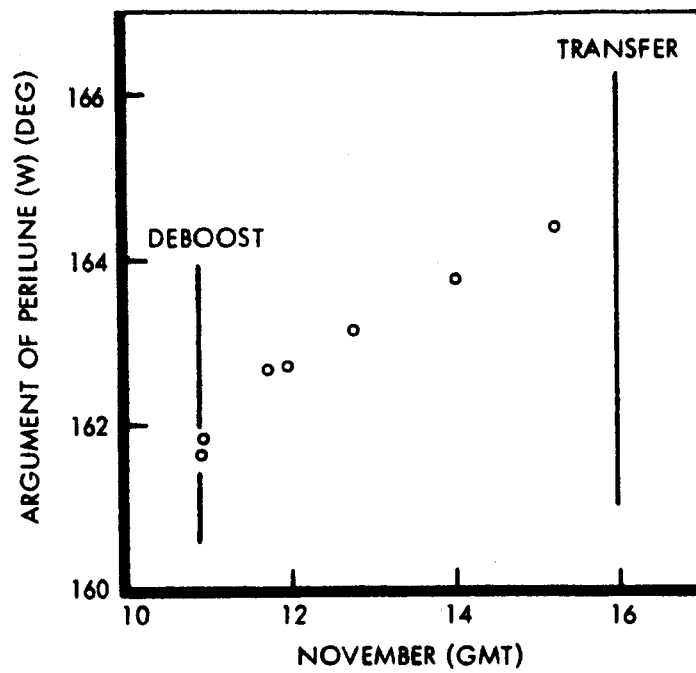


Figure 3.2-9: Initial-Ellipse Argument of Perilune History

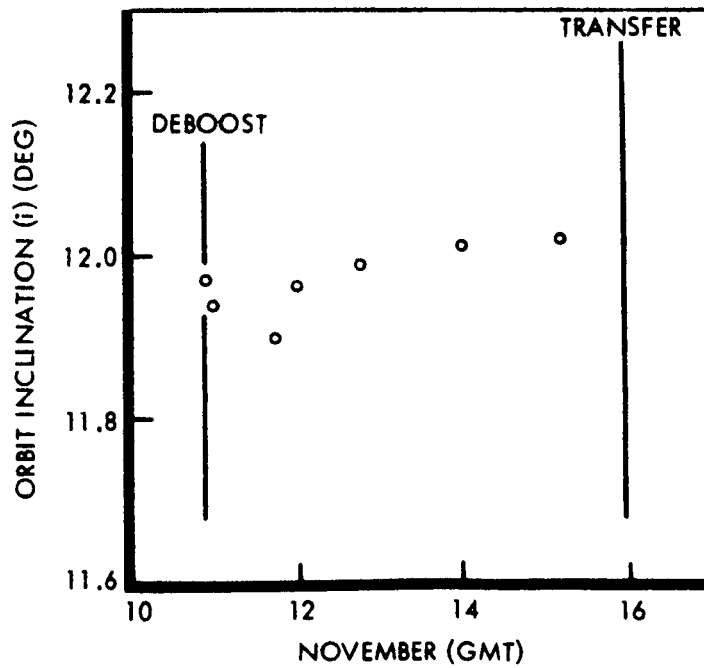


Figure 3.2-10: Initial-Ellipse Orbit Inclination History

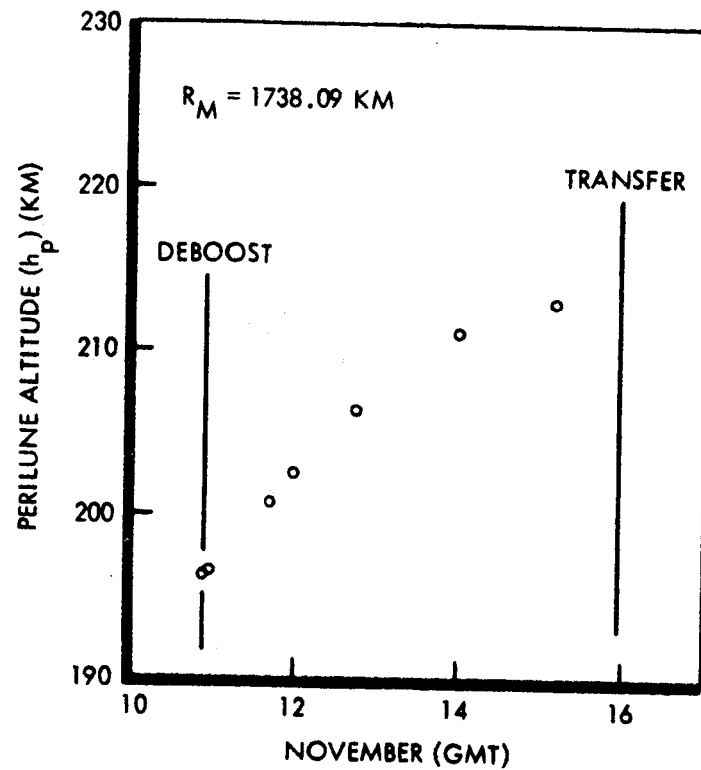


Figure 3.2-11: Initial-Ellipse Perilune Altitude History

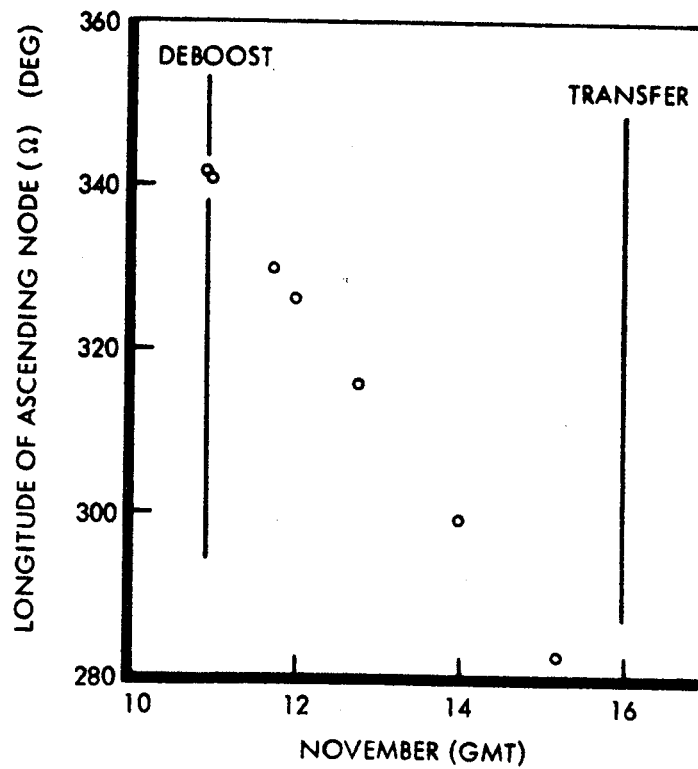
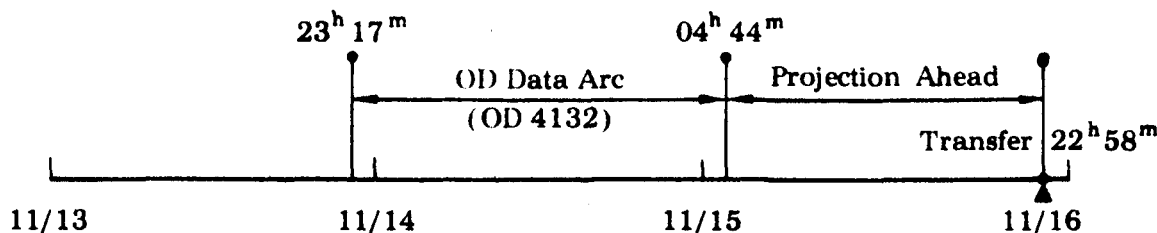


Figure 3.2-12: Initial-Ellipse Longitude of Ascending Node History

The scatter in the estimated values of orbit elements for this mission was considerably reduced as compared to Mission I. This is attributed to improved orbit determination procedures developed from experience in Mission I, and to improved estimates of the lunar gravitational field obtained from Langley Research Center.

The orbit determination used for the transfer calculation (OD 4132) used 29.5 hours of two-way-lock doppler tracking data from DSS-12, -41, and -61. The placement of the data relative to the transfer time is shown in the following figure:



This determination put the transfer calculations on a very firm basis because the projection to transfer was shorter than the data arc used. This situation provides an ideal orbit determination basis for performing a maneuver calculation. Further details of this determination are given in Appendix B.

Several hours before the transfer maneuver, a set of engine-burn doppler predicts was computed. This computation used the latest orbit determination results and the predicted nominal orbit conditions after the engine burn. These predicted doppler data were plotted in the region of the burn. The actual doppler shift data were plotted on the same curve during the maneuver from the incoming raw TTY data. The resulting curve (Figure 3.2-13) showed that the expected doppler shift was obtained, giving a quick indication that the maneuver was nominal.

Special analyses using ranging data not previously available contributed significantly to experimental verification of theoretical corrections to the lunar ephemeris proposed by Eckert of IBM. This work was performed by W. L. Sjogren of JPL.

Transfer Design and Execution

The primary task of the flight path control group during the initial ellipse phase of Mission II was the design of an appropriate transfer maneuver. The transfer from initial to photo ellipse was executed on November 15, 1966, at 22:58:24.53 GMT and resulted in a photo ellipse almost identical to the designed ellipse. This event concluded approximately 5 days in the initial ellipse and initiated the principal phase of the mission: photograph 13 potential Apollo landing sites.

The design of the transfer maneuver was based on the following ground rules:

- Minimum perillune altitude of 45.3 km;
- Minimum photo sidelap of 5%;
- Illumination angles between 50 and 80 degrees at primary targets;
- Transfer at least 24 hours prior to first photo;
- A minimum of 30 minutes between end of Earth occultation and start of engine burn.

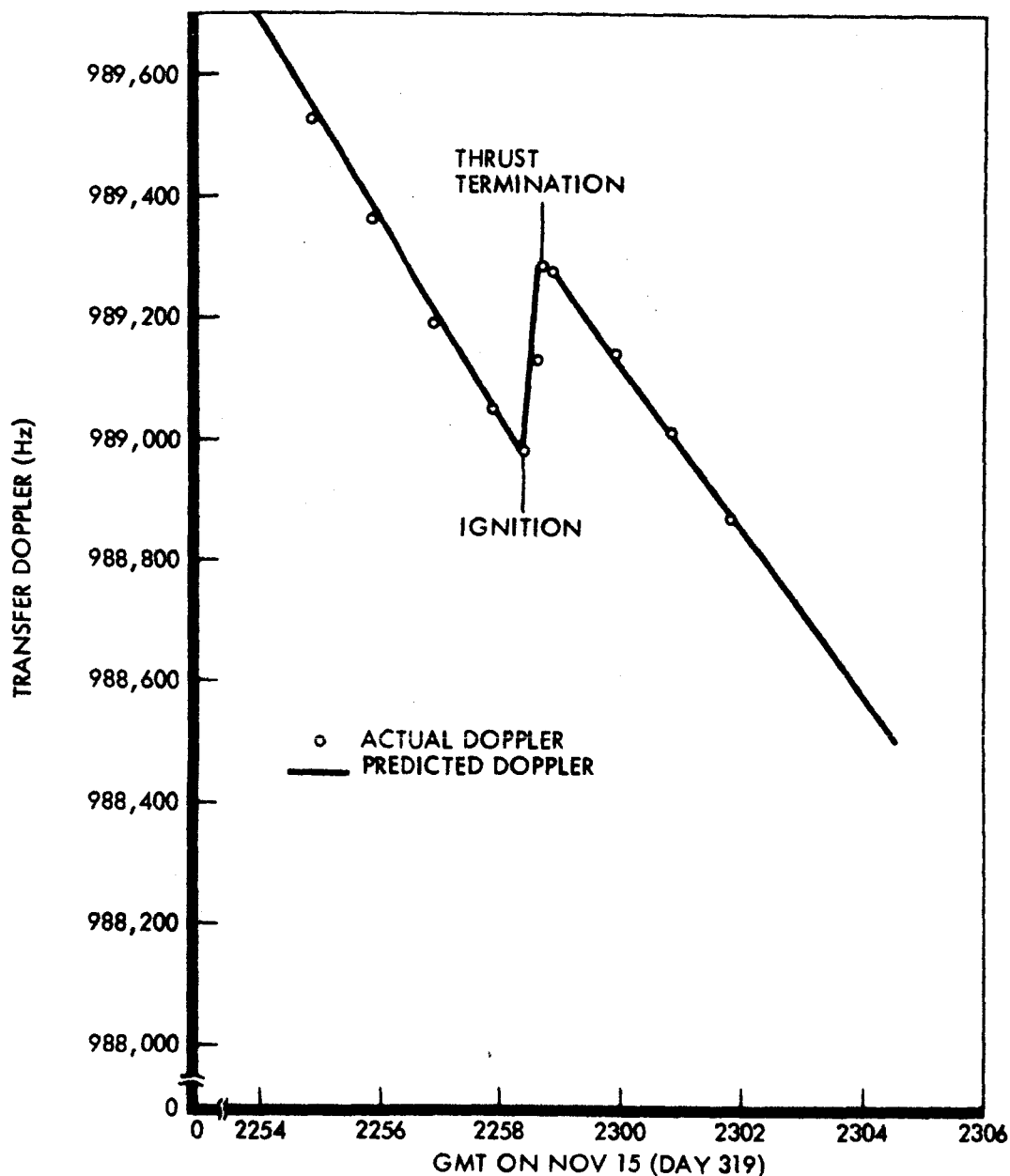


Figure 3.2-13: Transfer Doppler Shift

A set of lunar harmonic coefficients evaluated by NASA-Langley from Mission 1 data, designated LRC 9/4/66 harmonics, was used during the transfer design. The maneuver design was based on a state vector from orbit determination solution 4132.

Orbit 33 of the initial ellipse was selected for transfer, allowing between 18 and 19 orbits from transfer to first photo.

As a precaution, a backup maneuver was also designed. This maneuver was to be executed only in the event that the prime transfer maneuver could not be performed. The backup maneuver would have been executed two orbits later than the prime transfer, and was designed using OD solution 4132.

The transfer maneuver was designed by targeting to the three parameters: (1) perilune radius (R_p); (2) latitude of perilune (μ); (3) orbit inclination (i). The desired value for the perilune radius, 1783.4 km, was composed of the following components: 1738 km nominal lunar radius, 3.8 km local elevation at the anticipated lowest perilune, 3.6 km control errors and Moon model uncertainty, and 38 km minimum altitude to satisfy V/H sensor constraints. The sum of these components is the minimum allowable perilune radius for the design of the photo ellipse. The desired value of perilune latitude on Orbit 76, about halfway through the photo sites, was 2.37 degrees north. This value minimized the photo altitude, centered the perilune trace among the photo sites, and satisfied lighting angle constraints. The nominal premission design value of 11.95 degrees for orbit inclination ensured that the 5% minimum photo sidelap constraint would be met.

The minimum ΔV maneuver was 28.1 m/sec at a true anomaly of 170.0 degrees. The time of this transfer maneuver met the 30-minute minimum tracking time constraint, and the required ΔV was well below the budgeted 166 m/sec.

The attitude maneuver angles required to perform this transfer were:

Sun line	roll	33.01 degrees
	pitch	23.47 degrees

Selection of this attitude maneuver sequence was based on maintaining Sun lock as long as possible and compliance with antenna constraints with a minimum of angular rotation.

The orbital geometry at the time of transfer is shown in Figure 3.2-14. The predicted conic elements at perilune of Orbit 76 are given below with the desired nominal values from premission design:

Element	Pretransfer Prediction	Preflight Nominal	
Apolune radius (km)	3596.1	3588.0	
Perilune radius (km)	1783.4	1783.4	
Inclination (deg)	11.95	11.95	} Selenographic * of date coordinates
Argument of Perilune (deg)	168.5	168.5	
Longitude of ascending node (deg)	188.5	189.3	

The predicted conic elements before and after the impulsive transfer maneuver are given below to indicate the change in each caused by the maneuver. All elements are given for November 15, 22:58:24.53 GMT.

Element	Pretransfer	Posttransfer	
R_a (km)	3582.5	3590.3	
R_p (km)	1951.3	1788.3	
i (deg)	12.03	11.91	} Selenographic * of date coordinates
ω (deg)	164.9	163.3	
Ω (deg)	272.5	272.8	

* Selenographic of date coordinates are Moon-fixed coordinates inertially fixed at some epoch—for this data the epoch is at perilune.

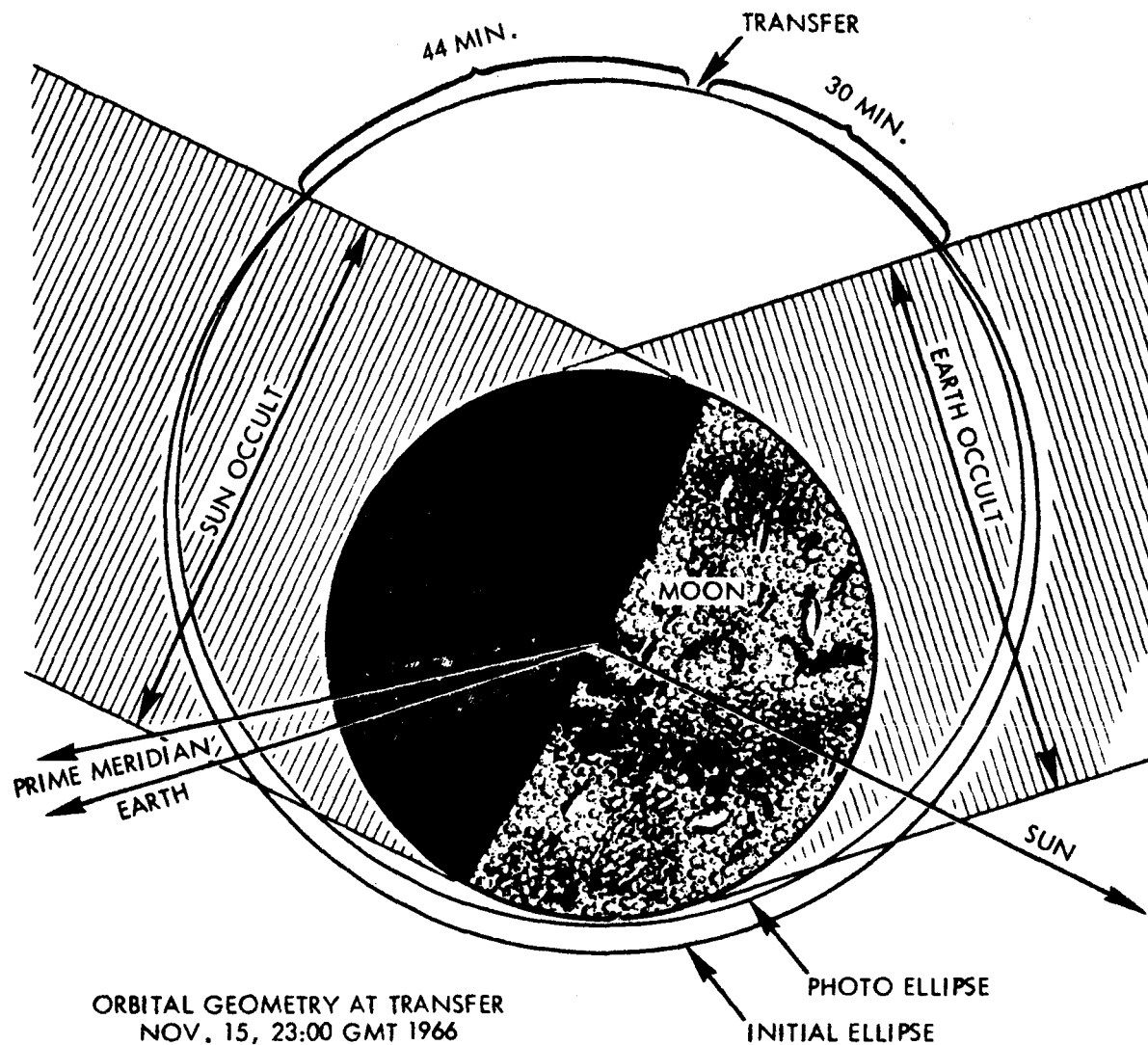


Figure 3.2-14: Orbital Geometry at Transfer

Prior to acceptance of this final design of the transfer maneuver two alternative sets of search parameters were investigated: R_p , ω , i ; a , R_p , Ω . In each case, some conic element was allowed to deviate to satisfy the search parameters. No other set of search parameters gave results as satisfactory as the set used in the final design, R_p , μ , i .

The predicted results of the transfer design are shown graphically in the following figures. Figure 3.2-15 shows the perilune altitude (referred to the nominal lunar radius of 1738.09 km) as a function of longitude of descending node in the area of photo activity. Figure 3.2-16 is a plot of the primary photo orbit traces and includes the targeted perilune trace. Figure 3.2-17 indicates the spacecraft altitude above the nominal lunar radius at photo time for each of the primary targets, as well as the Sun angle at nadir for each primary photo event.

NOTE:
ALTITUDE BASED ON $R_{\text{MOON}} = 1738.09 \text{ KM}$

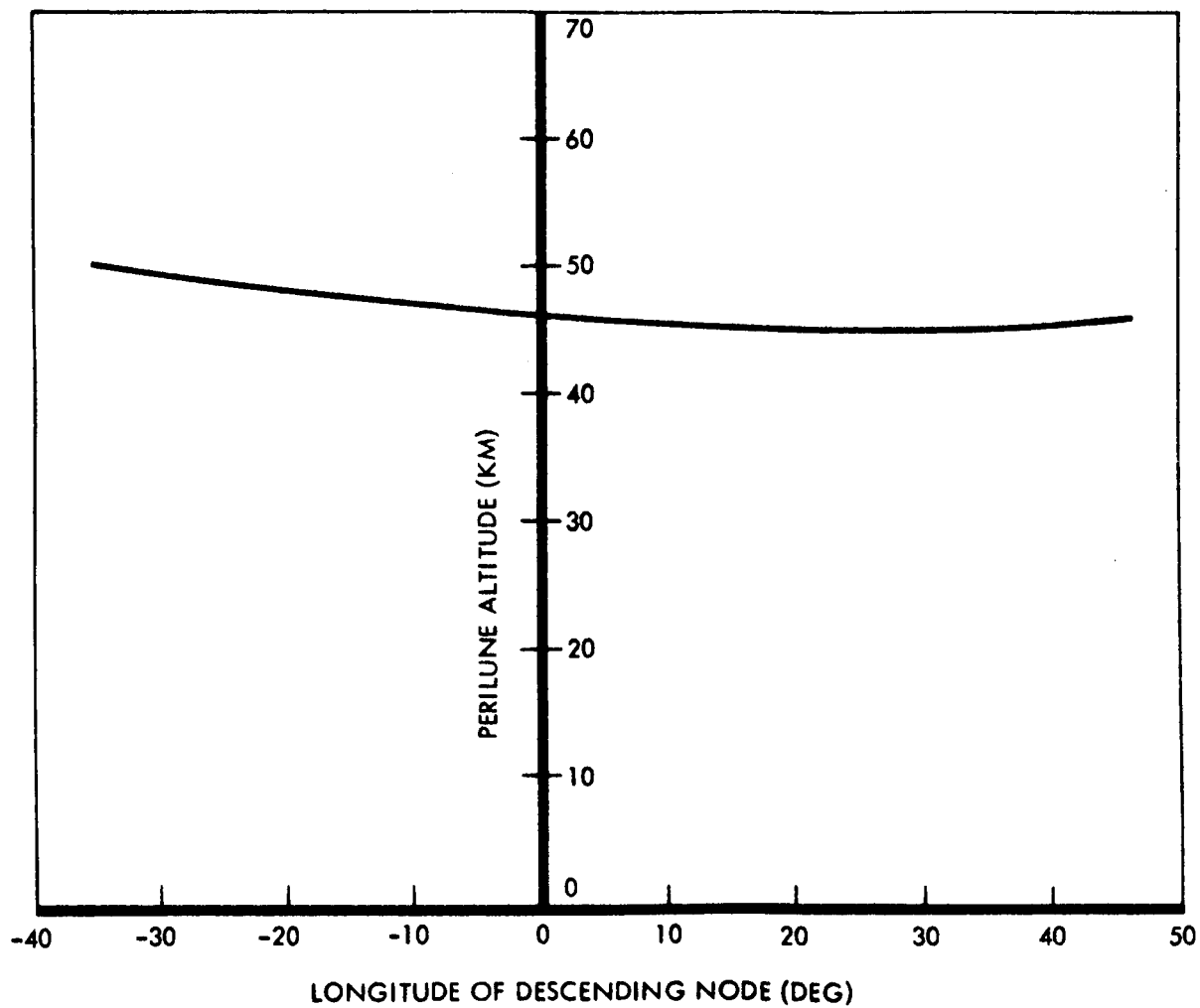


Figure 3.2-15: Perilune Altitude vs Longitude of Descending Node —Photo Ellipse Prediction at Transfer

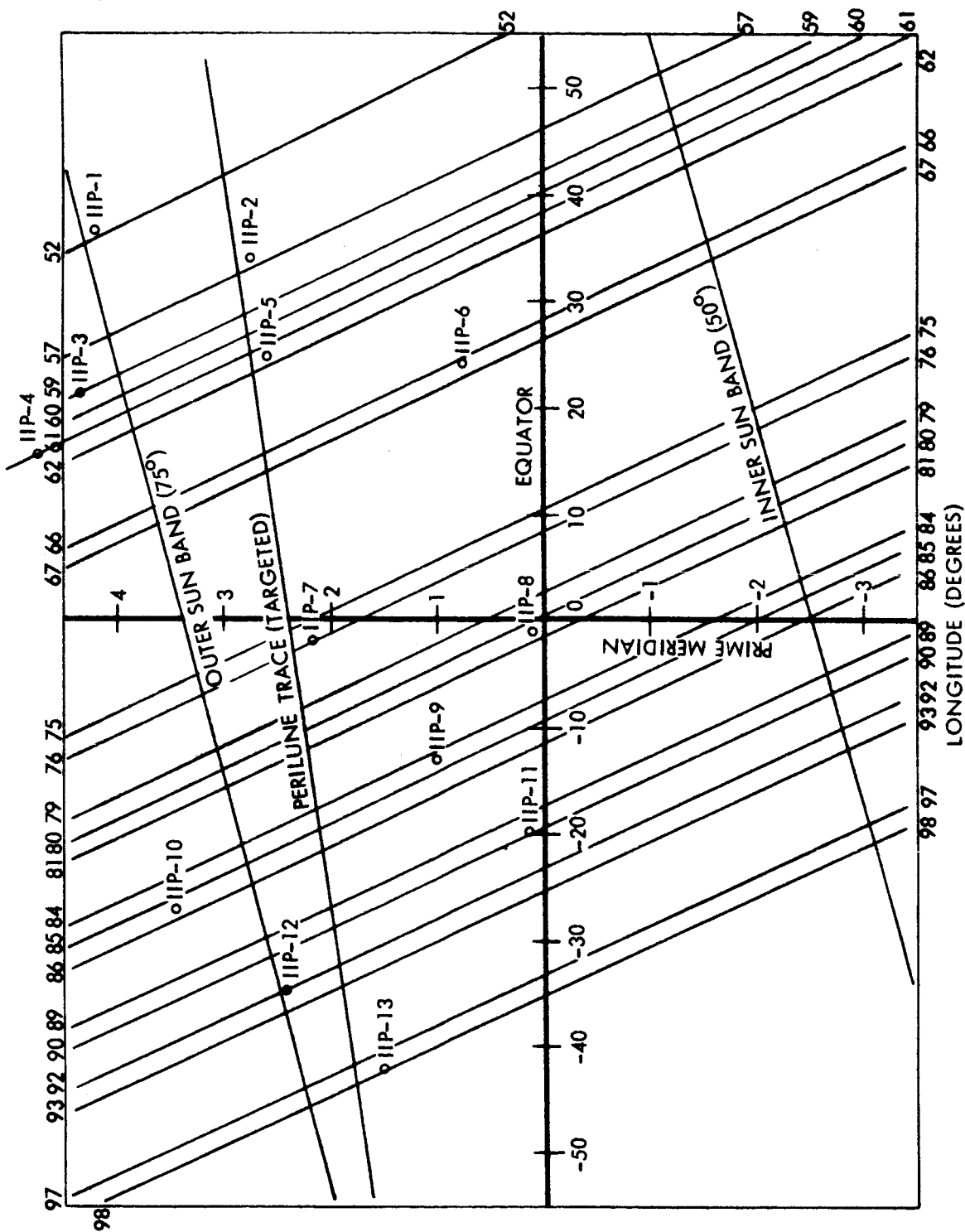


Figure 3.2-16: Photo Orbit Traces for Primary Targets

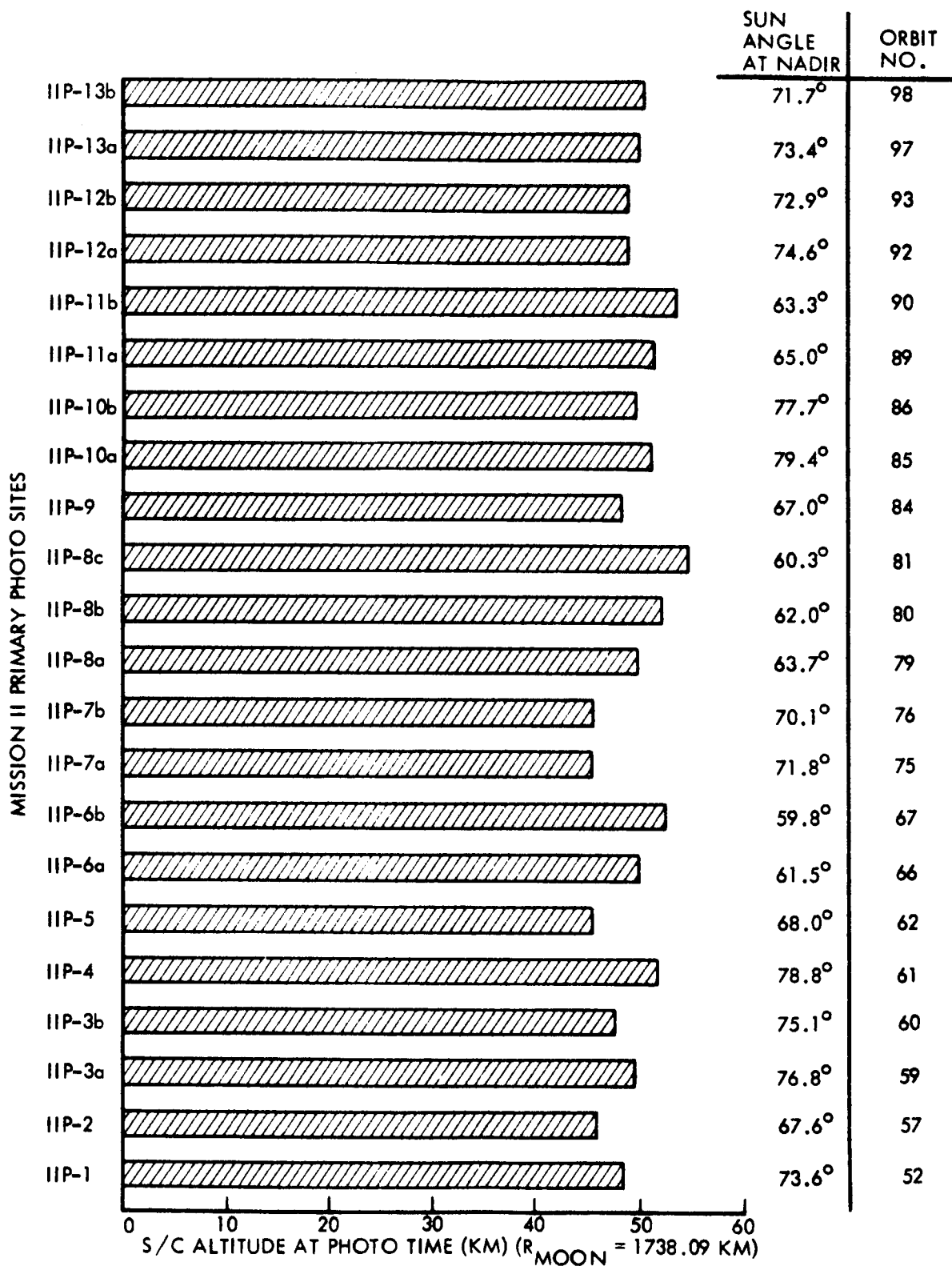


Figure 3.2-17: Predicted Primary Photo Altitudes based on Transfer Design LRC 9-4-66 Harmonics.

3.2.2.2.5 PHOTO ELLIPSE

The photo ellipse phase of Mission II extended from the end of the transfer burn through the completion of the photo readout.

The principal FPAC tasks in this phase included:

- A high-quality orbit determination prior to each primary photo event, which was the basis for the design of camera pointing maneuvers.
- Design of secondary site photo maneuvers on a noninterference basis with primary photo activity.
- Trajectory predictions including Sun rise and set times and Earth occultation periods.

Orbit Determination

Immediately after monitoring the transfer maneuver doppler shift, tracking data was logged and edited in preparation for the first orbit determination after the burn. This calculation was started at T + 45 (Transfer + 45 minutes) and by T + 75 minutes the calculation was complete and the results reported. Although not definitive, this calculation-together with the excellent agreement observed between the predicted and actual doppler shift during the burn--strongly indicated that a nominal maneuver had occurred. The following table shows the designed posttransfer conditions, the first estimate of these conditions obtained at T + 75 minutes (OD 5302), and a more definitive estimate (OD 5106) obtained at T + 7 hours.

Elements	Designed Post-transfer Conditions	First Estimate (OD 5302)	Best Estimate (OD 5106)
h_p (km)	50.2	50.5	49.7
h_a (km)	1858.2	1852.5	1852.6
i (deg)	11.91	11.99	11.89
Ω (deg)	272.8	272.6	273.3
ω (deg)	163.3	163.5	162.83

No difficulties were encountered in the initial orbit determination and no backup orbit determination procedures were necessary. Plots of orbital elements obtained during this phase are shown in Figures 3.2-18 through 3.2-22.

This mission phase was the most active of all. A total of 23 orbit determinations were made before Bimat cut and 17 of these were used to directly support command conferences. Table 3.2-7 shows the orbit determination runs used to support command conferences for each photo event. Details of each of these orbit determinations may be found in Appendix B. Typically, the preliminary command conference was held 10 hours before a photo maneuver and the final command conference 7 hours before a maneuver. Consequently, it was necessary to predict spacecraft position and velocity for the maneuver calculations as much as 16 to 18 hours before maneuver execution. To minimize the unavoidable prediction errors it was standard orbit determination procedure to estimate the present position and velocity of the spacecraft using a tracking data arc spanning more time than the trajectory prediction arc out to the maneuver time. This standard procedure in practice reduced to using a shorter tracking arc than desired to support the preliminary command conference and then increasing the amount of data used for the determination to support the final command conference. Usually an update of the camera-on time was required at the final conference as a result of the newer orbit determination. Appendix

B includes a tabulation of the maneuver angle and camera-on time changes associated with updated orbit determinations. A summary of the data arc lengths and prediction intervals for each photo site may also be found in Appendix B.

Table 3.2-7: Orbit Determinations used for Photo Site Command Conferences

Photo Site No.	Orbit Determination Number	
	PCC*	FCC* *
P-1	5214	5316
S-1	5214	5316
S-2a, S-2b	5316	5316
S-3	5316	5316
S-4	5316	5316
P-2	5220	5220
P-3a	5220	5322
P-3b	5220	5322
P-4	5220	5322
P-5	5322	5328
S-5	5322	5322
P-6a	5328	5132
P-6b	5328	5132
S-6, S-7	5132	5132
S-8, S-9	5236	5236
P-7a, P-7b	5138	5138
P-8a	5240	5342
P-8b	5240	5342
S-10.2	5240	5342
P-8c	5342	5144
S-11	5342	5144
P-9	5144	5246
P-10a	5144	5246
P-10b	5144	5246
S-12	5150	5252
P-11a	5150	5252
P-11b	5150	5252
P-12a	5252	5354
P-12b	5252	5354
S-13	5354	5354
S-14	5354	5354
P-13a	5258	5260
P-13b	5258	5260
S-15	5260	5260
S-16	5260	5260
S-17	5260	5260

* PCC-Preliminary Command Conference

** FCC-Final Command Conference

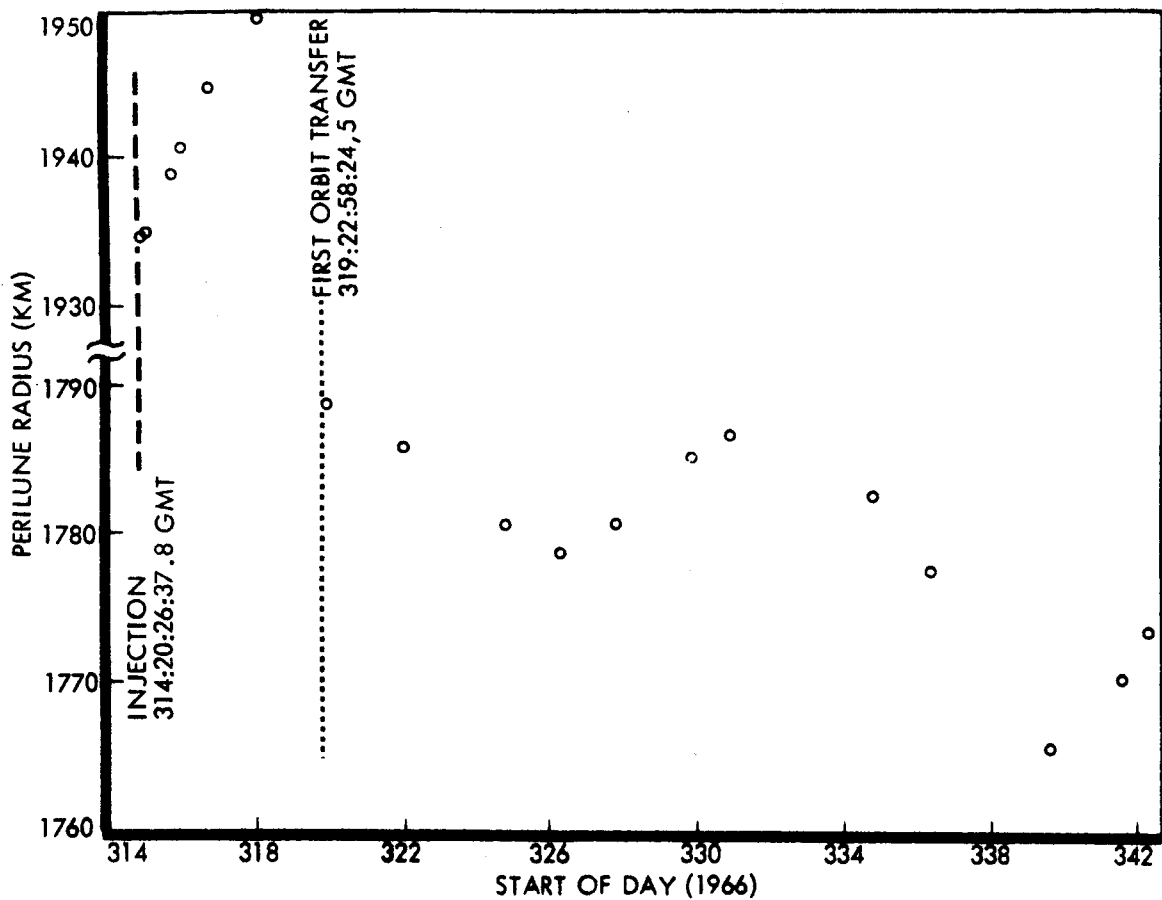


Figure 3.2-18: Photo Ellipse—Perilune Radius History

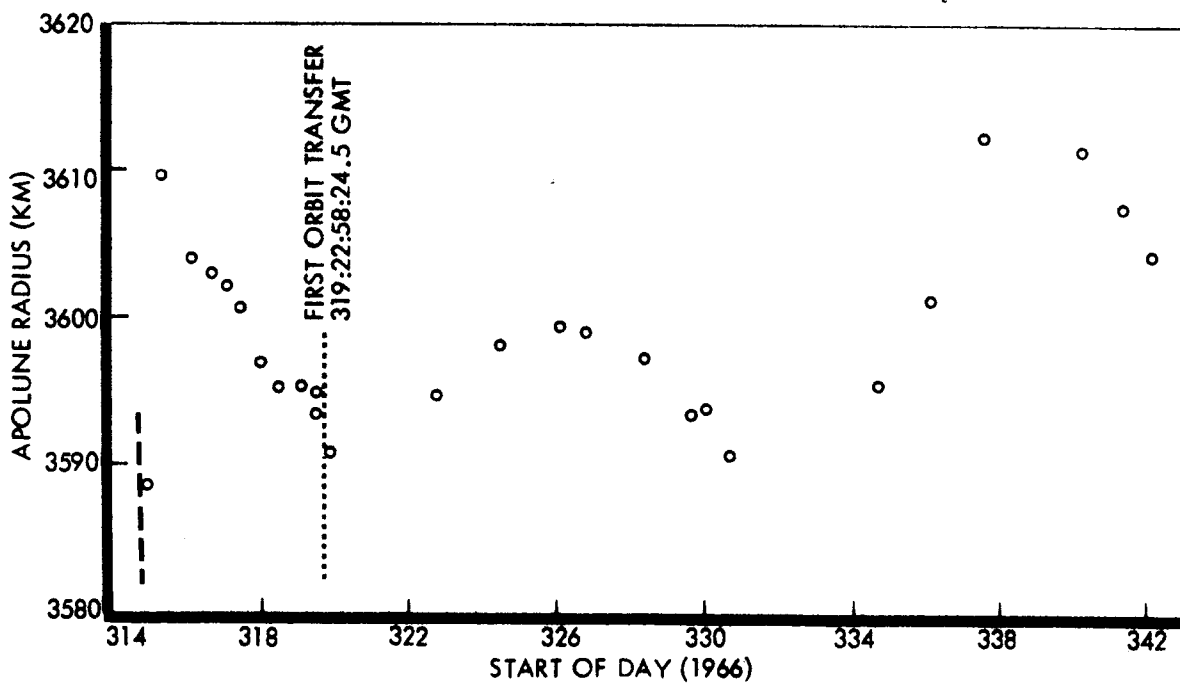


Figure 3.2-19: Photo Ellipse—Apolune Radius History

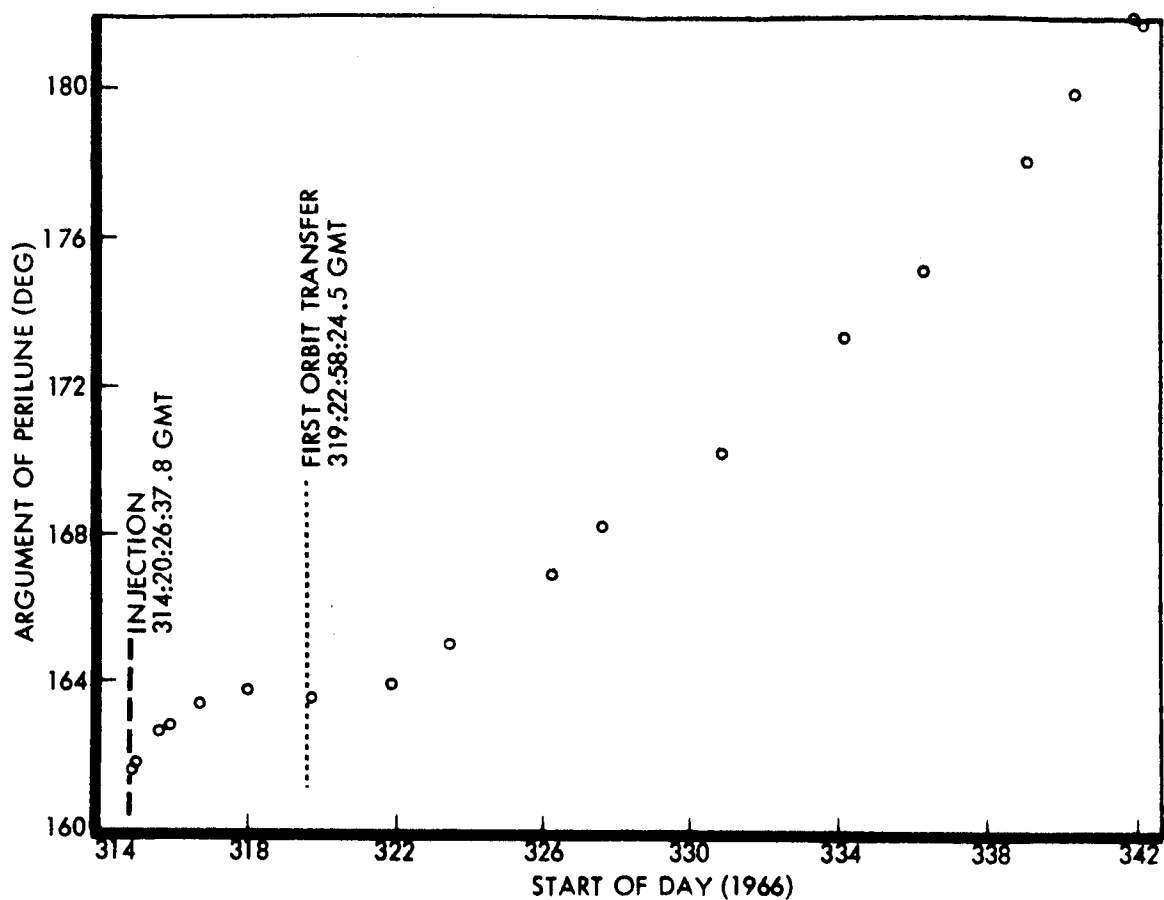


Figure 3.2-20: Photo Ellipse—Argument of Perilune History

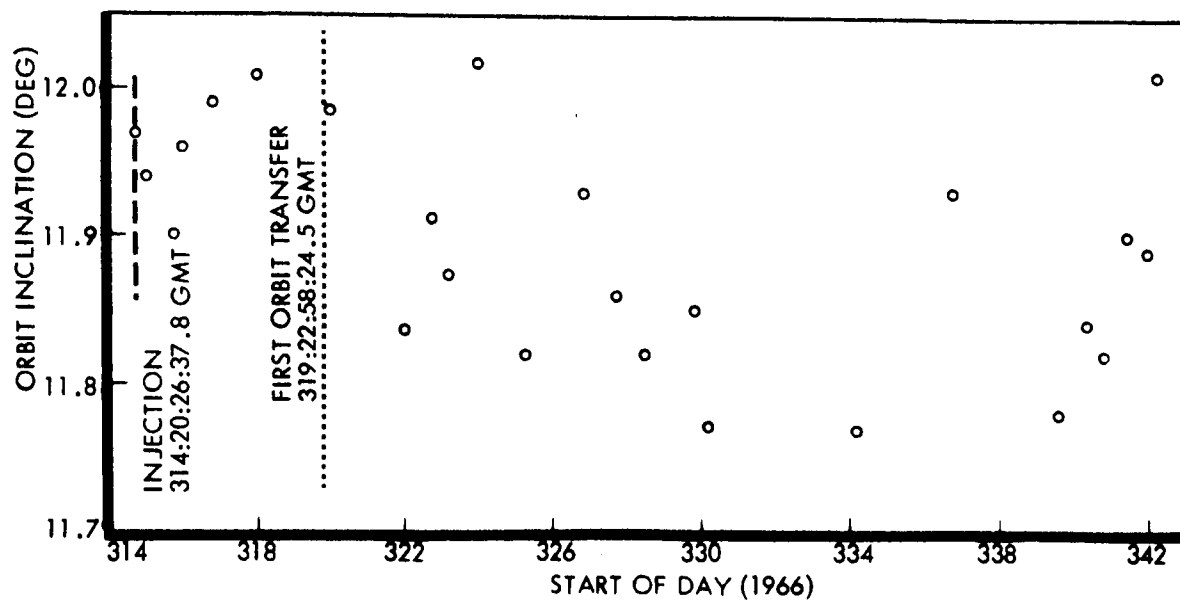


Figure 3.2-21: Photo Ellipse—Orbit Inclination History

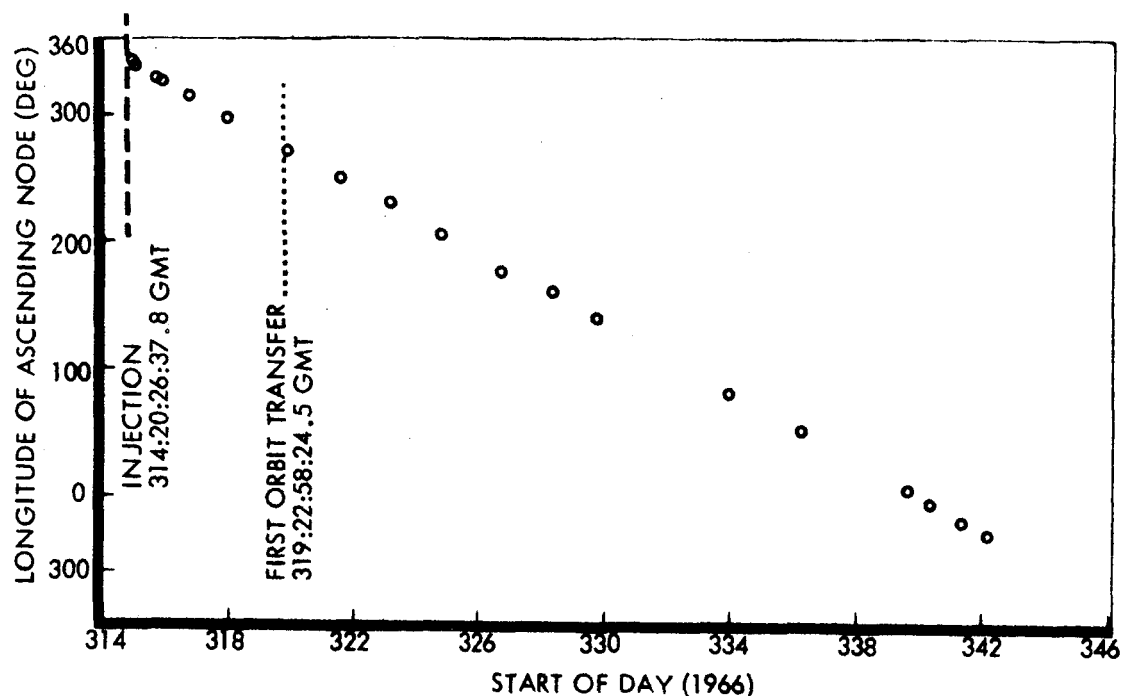


Figure 3.2-22: Photo Ellipse — Longitude of Ascending Node History

A new DSIF procedure allowed tracking data to be obtained during photo readout. Although this data was 2 to 10 times more noisy and had more frequent blunder points caused by photo readout interference, it was nevertheless usable data. Because this data was available, tracking restrictions on readout were eliminated. Interruptions every ninth orbit for tracking purposes, as in Mission I, were not required. The presence of the blunder points required that the tracking data be processed carefully; this increased the computation time by about 20%.

Sunset times obtained from SPAC were processed during this phase in an attempt to verify along track spacecraft position estimates. These data did not enter into the estimation process but rather were used as independent data to check sunset times derived from orbit estimates. The high level of activity precluded comprehensive checking but sunsets that were checked agreed well with the predicted values. An effort will be made to use these sunset times to a greater extent in the future.

Instability of the orbit determination solutions became a problem after the perilune altitude passed its minimum value and began to increase. Solutions comparable to the initial ellipse solutions became increasingly difficult to attain and divergence occurred in several cases. These divergent situations were remedied in most instances by using different data samples, changing the location of the epoch of the solution, or estimating different parameters. The consensus was (and is) that these difficulties were associated with inadequacy of the particular set of lunar harmonics coefficients used during the mission.

Photo Design

In Mission II, all photo activity occurred during the second ellipse. There were 184 frames exposed for primary photo sites and 27 frames exposed for secondary sites.

Volume II of this document contains a detailed listing of photo information, including actual camera-on times and spacecraft attitude maneuvers. A summary of the frames exposed is given in Table 3.2-8.

Table 3.2-8: Frame Numbers Versus Photo Sites

Frame Numbers	Photo Site
5 through 20	IIP-1
21 through 24	IIS-1
25 through 28	IIS-2a
29 through 32	IIS-2b
33	IIS-3
34	IIS-4
35 through 42	IIP-2
43 through 50	IIP-3a
51 through 58	IIP-3b
59 through 66	IIP-4
67 through 74	IIP-5
75	IIS-5
76 through 83	IIP-6a
84 through 91	IIP-6b
92	IIS-6
93	IIS-7
94	IIS-8
95	IIS-9
96 through 103	IIP-7a
104 through 111	IIP-7b
112	IIS-10.2
113 through 120	IIP-8a
121 through 128	IIP-8b
129 through 136	IIP-8c
137	IIS-11
138 through 145	IIP-9
146 through 153	IIP-10a
154 through 161	IIP-10b
162	IIS-12
163 through 170	IIP-11a
171 through 178	IIP-11b
179 through 186	IIP-12a
187 through 194	IIP-12b
195	IIS-13
196	IIS-14
197 through 204	IIP-13a
205 through 212	IIP-13b
213	IIS-15
214	IIS-16
215	IIS-17

The lunar harmonics designated LRC 9/4/66 were used in the design of all camera pointing attitude maneuvers and camera-on times.

To minimize timing error in the camera-on times, the state vectors were forwarded to within a few minutes of the expected camera-on times for the primary photo events using an integrating trajectory program. Thus, the mean element trajectory program was used over only a short span of time.

Table 3.2-9 compares the orbit numbers predicted as a part of the transfer design for the primary photo events and the actual orbits in which the photo events occurred.

Table 3.2-9: Site Versus Orbit Number

Site No.	Predicted Orbit No.	Actual Orbit No.
IIP-1	52	52
IIP-2	57	57
IIP-3a	59	59
IIP-3b	60	60
IIP-4	61	61
IIP-5	62	62
IIP-6a	66	66
IIP-6b	67	67
IIP-7a	75	76
IIP-7b	76	77
IIP-8a	79	80
IIP-8b	80	81
IIP-8c	81	82
IIP-9	84	85
IIP-10a	85	86
IIP-10b	86	87
IIP-11a	89	91
IIP-11b	90	92
IIP-12a	92	93
IIP-12b	93	94
IIP-13a	97	98
IIP-13b	98	99

Following Site IIP-6, it became necessary to delay photo events one or two orbits to achieve the desired and predicted coverage of the remaining sites.

The lunar harmonic model designated LRC 9/4/66 used for the predictions did not accurately describe the long-term changes in the node longitude. As time passed, the predicted and actual orbit traces diverged gradually until it was necessary to take subsequent photos on a later orbit to maintain coverage.

Many of the secondary sites were also changed to different orbits to prevent interference with primary photography or to obtain desired coverage if interference was not involved.

Figure 3.2-23 shows the spacecraft altitude (based on a mean lunar radius of 1738.09 km) at photo time for each primary photo event. Also given are sunlight incidence angle and orbit number. These data were extracted from the individual enroute photo maneuver designs. Figure 3.2-24 shows perilune altitude (above the mean lunar radius) as a function of descending node longitude as predicted earlier during transfer maneuver design predictions as well as from photo maneuver designs. The difference between the two predictions shows that the LRC 9/4/66 Moon model does not represent perilune perturbations adequately.

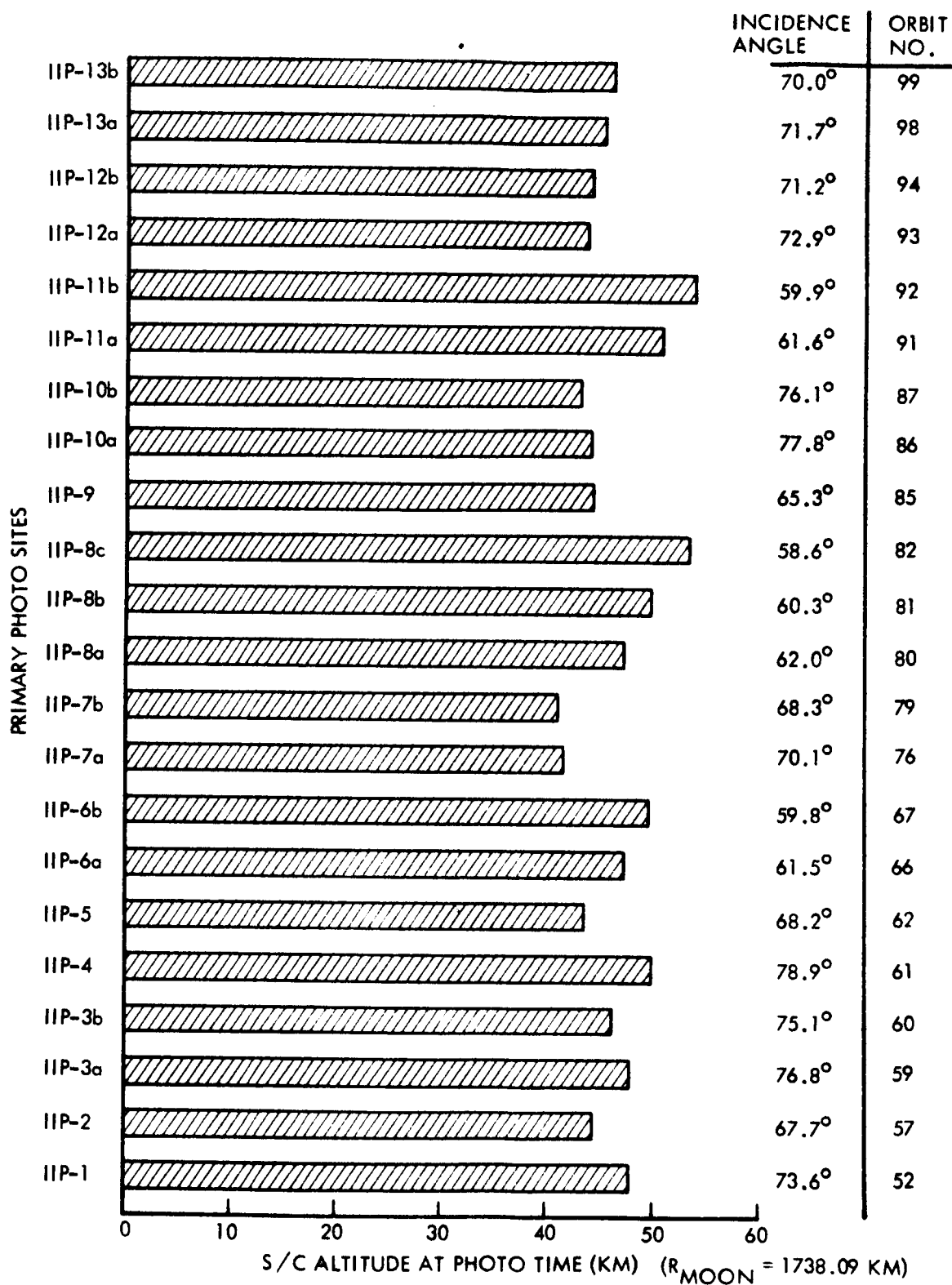


Figure 3.2-23: Predicted Primary Photo Altitudes (Based on Real-Time Eval Runs LRC 9-4-66 Harmonics)

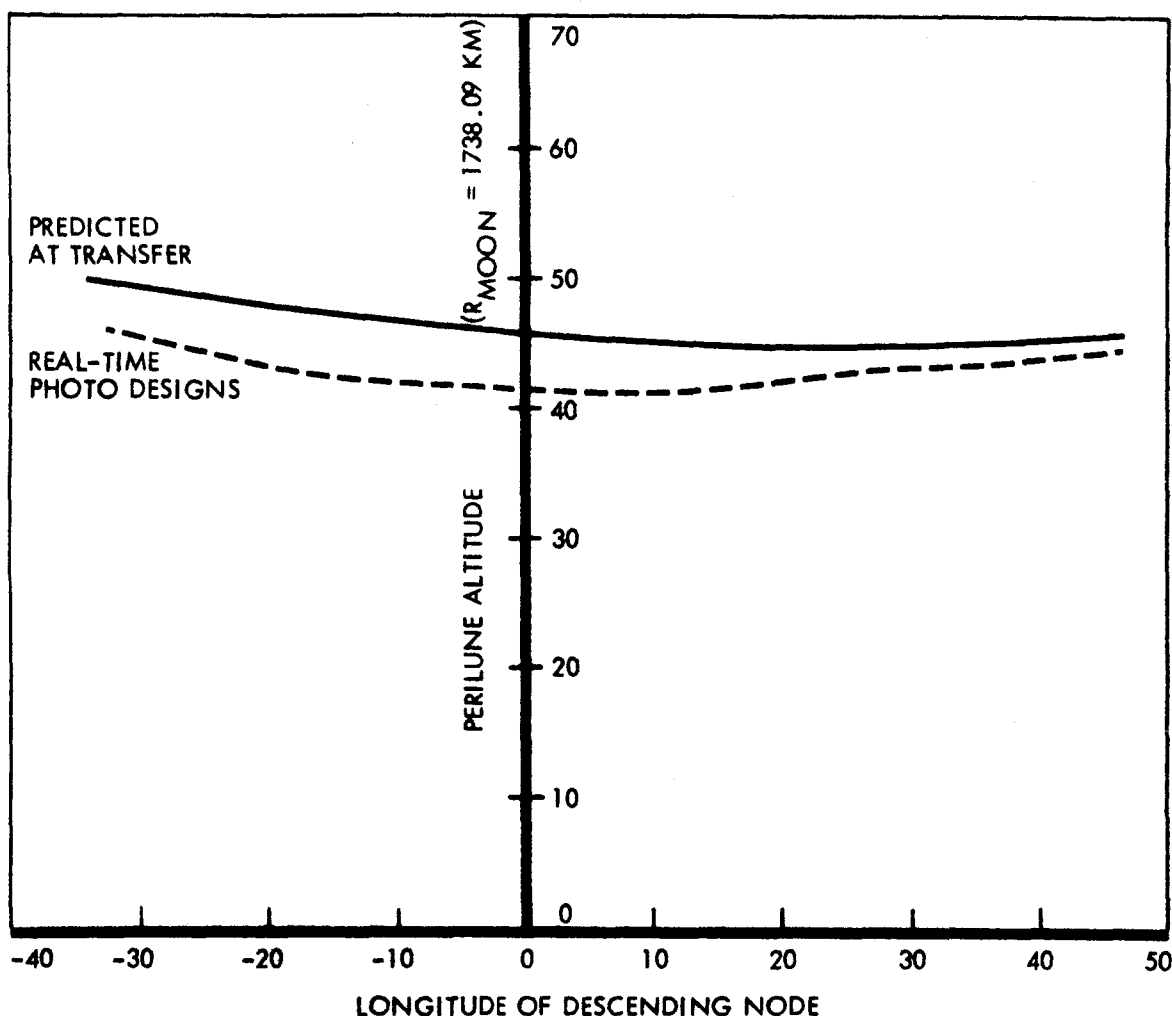


Figure 3.2-24: Predicted vs Actual Perilune Altitudes

3.2.3 SPACECRAFT PERFORMANCE SUMMARY

Launch Phase

Liftoff and injection into cislunar trajectory by the launch vehicle were within nominal limits. No problems were encountered.

Cislunar Phase

DSS-51 (Johannesburg) acquired one-way rf lock 28 minutes after launch, acquired two-way rf lock 2 minutes later, and tracked the spacecraft for approximately 11 hours. DSS-41 (Woomera) acquired three-way lock 51 minutes after launch and a normal hand-over (DSS-51 to DSS-41) occurred 69 minutes after launch.

Sun acquisition was not recorded, having been accomplished prior to DSS-41 acquisition. A star map maneuver was initiated 7 hours, 27 minutes after launch. At the end of the 360 degree roll maneuver, it was determined that the spacecraft had originally been oriented to Canopus.

The midcourse maneuver was accomplished successfully 44.15 hours after launch. The maneuver had been scheduled to occur approximately 7 hours before, and was rescheduled due to loss of Canopus reference when the fuel and oxidizer squibs were fired. Time delay in reacquiring Canopus caused rescheduling of the maneuver. The spacecraft remained pitched off the sunline after the midcourse maneuver. Periodic pitch and yaw maneuvers were required to counteract drifts in spacecraft orientation.

Orbital Phase

Lunar orbit injection was performed 93 hours after launch, placing the spacecraft in a nominal orbit with apolune of 1864.8 km, perilune of 202.4 km, inclination of 11.96 degrees, and period of 218.2 minutes.

During the initial orbit phase, Goldstone film was read out to all three prime DSS's to verify the coordination procedures between the SPAC photo data analyst and the DSS video engineers, and to verify system operational readiness.

Transfer to final orbit took place during Orbit 33, 215.5 hours after launch. The orbit met all requirements established for Mission II. For procedural simplicity, orbits were numbered sequentially through both initial and final orbits rather than as they were in Mission I.

First photos were taken during Orbit 52. During the film advance, frames taken during Orbit 51, the shutter actuation telemetry channel, PB04, indicated 23 counts for 11 actuations. PB04 continued to give erratic counts during the remainder of the mission. Actual shutter operations, however, proved to follow the commands precisely, and no double exposures were found during readout.

Site photography progressed normally. The last primary site, P-13b, was photographed during Orbit 99. The last photograph was of Site S-17 during Orbit 102. Bimat was cut during Orbit 105, and, after two false starts due to mislocation of film, final readout started in Orbit 107.

Readout progressed at a rapid rate, averaging 2.8 frames per orbit until Orbit 179, when the TWTA failed to turn on. There were approximately eight frames remaining to be read out, data from 2.4 frames of these eight however, had been obtained during priority readout in Orbits 53 through 57. During final readout, TWTA helix current was above tolerance at turn-on, decreasing to proper level after 7 to 10 minutes of operation. The TWTA power output did not appear to be affected by the change in helix current, and a change in appearance of the GRE film could not be found up to the time when readout was terminated.

During final readout, the spacecraft remained pitched off the sunline to maintain lower temperatures, thus allowing the maximum possible readout time per orbit.

At the end of the photo mission, the spacecraft had recorded three micrometeoroid strikes: on DM04 at GMT 319:12:45; on DM05 at GMT 329:17:23; and on DM13 at GMT 338:02:05.

The radiation dosage measurement system (RDMS) had recorded 1.75 rads on scintillation counter 1 (cassette) and 1.0 rads on counter 2 (looper). At these levels, the film was not degraded.

The Canopus star tracker was operated continuously through the cislunar phase of the mission until orbit injection. During the orbital phase of the mission, the tracker was operated intermittently to update the celestial reference. Continuous operation was impractical due to the tendency to track other bright objects (glint). Each time the tracker was turned on, the attitude control thrusters fired in a transient mode. The resultant motion was small, and the spacecraft did not go outside the dead-zone cycle limits.

During Orbits 97, 127, 131, 150, 176, 180, and 181 the stored "readout drive off" command failed to turn the readout electronics off, requiring transmission of real-time commands to turn off the electronics. Note that Orbits 180 and 181 were after TWTA failure. The film was being rewound during these orbits.

None of the above anomalies, except the TWTA failure, had a significant effect on operation of the spacecraft, nor were any mission objectives lost. Although it was disappointing to lose 5.6 frames of photos, it should be recognized that the number of frames read out was greater than the 194 frames established in the photo system specification and much more than satisfied the area coverage requirements of the original work statement.

Following is a discussion and performance analysis of the spacecraft subsystems. Figure 3.2-25 is a block diagram showing relationships between the subsystems. Table 3.2-10 shows the times of key events during the mission. Complete sequence of events will be found in Appendix B in Volume VI of this document. A brief summary of the spacecraft subsystems is included in Volume I of this document. Further description of these subsystems is given in Boeing Document D2-100727-3, Lunar Orbiter I Final Report -- Mission Operational Performance.

Table 3.2-10: Key Events

GMT				Event
Day	Hour	Min.	Sec.	
310	23	21	00.195	Liftoff
	23	42	27.2	Cislunar Injection
	23	46	12.0	S/C-Agena separation
	23	47		Antenna and solar panel deployment
	23	48	49	DSS-51 one-way rf lock
	23	51	53	DSS-51 two-way rf lock
311	00	12	15	DSS-41 one-way rf lock
	00	30	00	DSS-41 two-way rf lock
				Sun presence (exact time unknown)
	08	21	27	Canopus acquisition
	10	34		Bleed propellant lines
312	19	30	00.0	Ignition, midcourse maneuver, $\Delta V + 21.1$ mps Engine burn time: 18.06 sec.
314	20	26	37.3	Ignition, lunar orbit injection $\Delta V = 829.7$ meters per second, engine burn time: 611.6 sec.
319	12	45	40	Recorded first micrometeoroid hit
319	22	58	24.5	Ignition, orbit transfer maneuver; $\Delta V = 28.1$ meters per second; engine burn time: 17.42 sec.
322	15	24	16	First photographic exposure, Site II P-1 (Orbit 52)
322	17	18	00	Start first priority readout (Orbit 53) of actual Moon photo (high-res. Frame 6, second exposure, Site II P-1).
329	21	12	53	Last photographic exposure--Site II S-17 (Orbit 102)
330	08	58	00	Bimat cut (Orbit 105)
330	15	04	00	Start final readout, after advancing film from "cut Bimat" position (Orbit 107).
341	01	16	00	TWTA failed to turn on, terminating readout (Orbit 179).

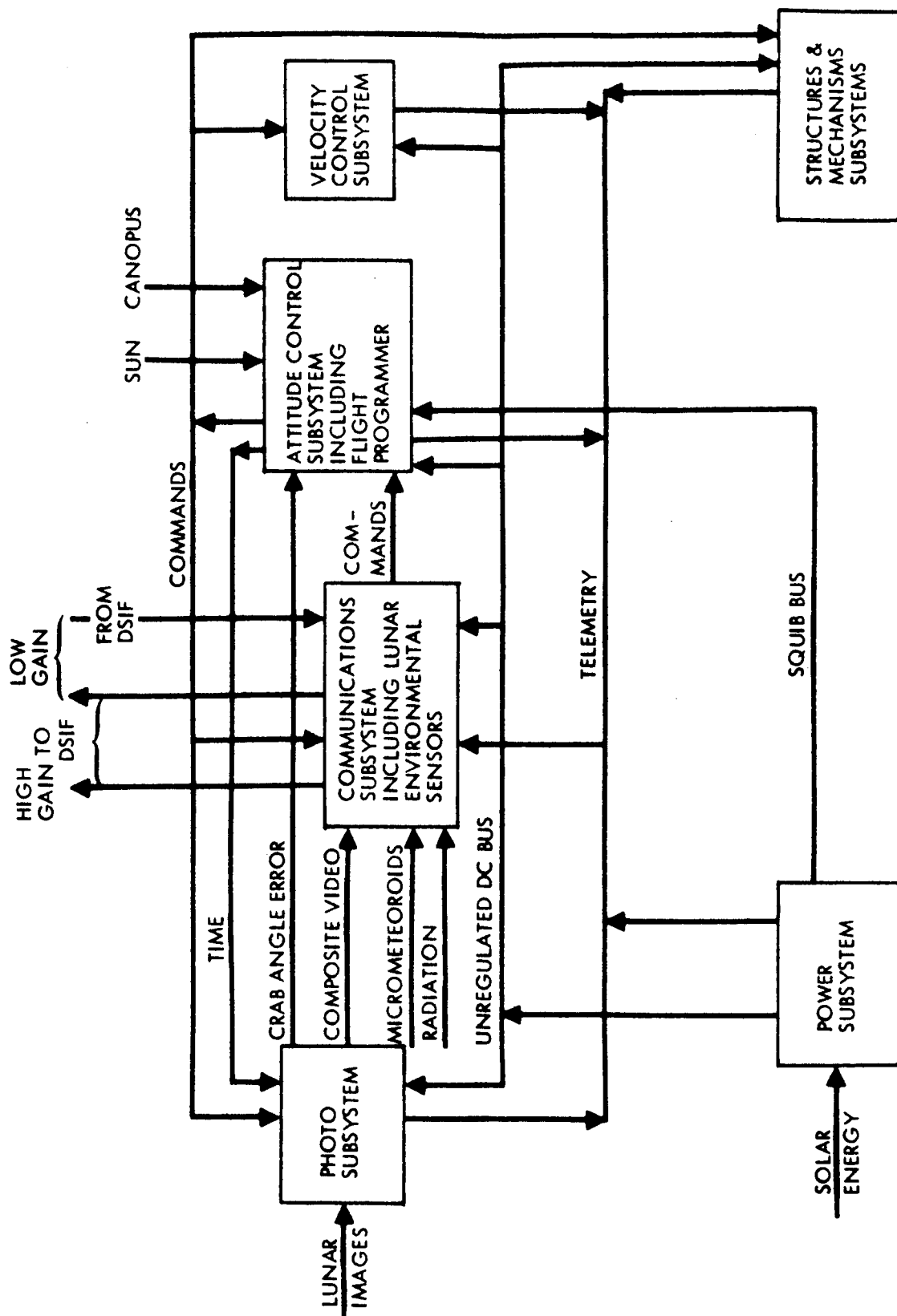


Figure 3.2-25: Spacecraft Block Diagram

3.2.3.1 Photographic Subsystem

The operation of the photographic subsystem (PS) throughout Mission II was satisfactory. The temperature and humidity profiles followed predicted trends from the spacecraft temperature behavior. Photography and processing proceeded as planned. Priority readout verified proper photographic operation.

The spacecraft was launched into the Earth shadow resulting in a cooling period until the spacecraft entered the sunlight. The spacecraft then began to get warmer but the camera window temperature (measurement PT03) continued to drop until the measurement reached its lower saturation level (39.1°F). After the measurement remained saturated for approximately 2.5 hours, the camera thermal door was commanded to open and close to verify that the door was completely closed. After an additional 2 hours, the camera window temperature increased sufficiently to rise above the measurement saturation level. The window temperature continued to increase and had reached 45.6°F when the spacecraft was turned 36 degrees "off-Sun." The window temperature increased for an additional 1 hour after the spacecraft was pitched "off-Sun" and reached 49.3°F, where it remained for 1 hour before starting to decrease. Twelve and one-half hours later, the temperature had decreased to 42.8°F, at which time the spacecraft was turned back "on-Sun." Again the window temperature continued to decrease and reached saturation (39.1°F) 1.5 hours later. It remained saturated for 2.5 hours, even though the spacecraft was "on-Sun." This indicates that the camera thermal door was closed prior to the door open and close operation and that the temperatures observed were due to the lagging thermal characteristics of the camera window.

The PS was kept in the solar eclipse mode with heaters inhibited throughout translunar cruise. At injection, the heater inhibit was released and the PS heaters were allowed to operate. A day before the first photo pass, the normal sequence of "solar eclipse on/off" commands was programmed to thermal stabilize the photo subsystem.

The readout of the Goldstone test film was conducted in Orbits 12 and 14 with all three stations recording. This verified capability for the readout operations. Photography started during Orbit 52 on November 18, and proceeded normally through Orbit 102 on November 25. The nominal photo mission plan was followed, except for a shift of Site S-10 to a location with more favorable illumination by NASA direction, the V/H sensor was not turned on for the oblique Sites S-16 and S-17. Observation of reassembled photographs and analysis of average density data indicated that exposures were generally satisfactory, within the limits imposed by the transmission spread between the two lenses.

The PS temperatures followed the warming trend of the spacecraft temperatures during the photographic/priority readout mission phase. The priority readouts were shortened from 43 minutes to 27 minutes after Orbit 82, which stopped this warming trend in the PS short of the 75°F Bimat storage temperature limit.

Spacecraft film processing was conducted as in the nominal mission plan, except where altered by operations directive. Fifty-three processing periods, which were required to meet the mission specification, generated 53 stoplines with associated degradation of about 0.5 inch of film. Approximately 25% of the spacecraft film was processed with Bimat that was partially dried out. Bimat cut and clear were completed normally in Orbit 105.

Final readout was conducted to minimize the readout period. The only constraints observed were TWTA temperature and Sun and Earth occultations. The thermal history of the PS indicated that readouts longer than 86 minutes (two frames) could be performed. The average final readout was 2.8 frames per orbit. The PS heaters were inhibited throughout final readout and all temperatures followed expected profiles.

"SOFT FOCUS"

During priority readout, a complete medium-resolution frame was generally read out along with portions of the two adjacent high-resolution frames. The video engineers began reporting "soft focus" in the second high-resolution frame scanned during the readout.

The change in focus was rather abrupt when going from the medium-resolution frame to the high, which suggests a problem in the telephoto camera. However, it was felt that a change in the photo video chain (PVC) focus during readout could also be responsible and this could be easily checked. Therefore, during readout sequences 917 and 023, the readout was stopped and the focus pattern noted and photographed. No change in the focus pattern was detected. As a further check during sequence 025, the PVC was optimized at the beginning of readout. It was found that the PVC was at optimum focus setting and no change was made.

From this it was concluded that the problem was not in the PVC. Not enough of the reconstructed pictures have been inspected at the time of this writing to fully analyze this condition. Only extensive analysis of the pictures can establish the importance of the effect, and its relation to system specifications.

PB-04 SHUTTER COUNTER ANOMALY

The shutter count telemetry of the photo subsystem provides data on the number of 610-mm focal-plane shutter operations. The signal, SLT, that starts the 610-mm shutter action also triggers a five-stage binary counter. Throughout Mission II the shutter counter behaved erratically. The five modes of counter operation during the mission were:

- 1) Correct counting;
- 2) Double counting;
- 3) Half counting;
- 4) No counting;
- 5) Indeterminate counting.

Shutter count data for each photo sequence of Mission II is included in Table 3.2-11.

Table 3.2-11: Shutter Count PB-04 Data

Orbit	Site	Correct PB-04 Counts	Actual PB-04 Counts
51	Film Advance	8	17
		1	2
		1	2
		1	2
52	P-1	16	32
	S-1	4	8
53	S-2a	4	8
54	S-2b	4	8
55	S-3	1	2
56	S-4	1	2
57	P-2	8	16
59	P-3a	8	16
60	P-3b	8	4
61	P-4	8	0
62	P-5	8	8
64	S-5	1	1

Table 3.2-11: Shutter Count PB - 04 Data (Continued)			
Orbit	Site	Correct PB - 04 Counts	Actual PB - 04 Counts
66	P-6a	8	3
67	P-6b	8	0
69	S-6	1	0
71	S-7	1	1
73	S-8	1	1
75	S-9	1	0
76	P-7a	8	0
77	P-7b	8	0
79	S-10.2	1	0
80	P-8a	8	0
81	P-8b	8	0
82	P-8c	8	16
83	S-11	1	2
85	P-9	8	16
86	P-10a	8	16
87	P-10b	8	16
89	S-12	1	2
91	P-11a	8	8
92	P-11b	8	8
93	P-12a	8	8
94	P-12b	8	8
96	S-13	1	1
97	S-14	1	1
98	P-13a	8	8
99	P-13b	8	8
100	S-15	1	1
101	S-16	1	1
102	S-17	1	1
103	Film Advance	16	16
104	Film Advance	4	4

In the following sections, the film handling system, V/H sensor, and photo-video performance are discussed. Certain departures from ideal performance are discussed, but except for processing defects and the shutter count problem, they are not true anomalies and did not result in significant data loss. These points are included as part of the operational history of Mission II. For complete discussion of the photographs taken on Mission II, refer to Volume II of this document.

FILM HANDLING SYSTEM

Camera Film Advance

The absolute accuracy, $\pm 5\%$, of the camera loop content telemetry limits the ability to determine if the film advance was within specification (11.69 ± 0.12 inches per advance). However, the film advance per photo frame as calculated from telemetry was, in all cases, nominal ± 1 telemetry bit. Also, film advance length determined from frame readout time verified nominal advance. Some frames had time codes overlapping the first framelet of a subframe. This condition falls within normal film advance tolerances.

Film Advance Through Processor During Processing

The average processing rate during Mission II was 2.408 inches per minute, as determined from telemetry. This rate is well within the specified 2.4 ± 0.1 inches per minute

rate. The rates calculated during processing sequences varied from 2.31 to 2.57 inches per minute. Telemetry accuracy influenced the apparent processing rates for short processing sequences, resulting in the above wide range of calculated rates.

PROCESS ANOMALY

In addition to the Bimat processing defects inherent in the operational employment of the system (dryout, stoplines, etc.), several frames with significant data loss were reported by the video engineers. The affected areas were in Frames 101, 102, 103, 104, and 119. The observed patterns were attributed to air inclusions in the Bimat. The impact on the mission cannot be determined without film analysis of all affected frames.

80-MM-LENS TRANSMISSION

As discussed previously, the high 80-mm-lens transmission relative to the 610-mm lens caused a number of overexposed wide-angle frames. Average density measurements and data received from Eastman Kodak Company indicated about a one-stop difference between the two lenses.

V/H SENSOR PERFORMANCE

The V/H ratio, as indicated by the PR01 telemetry channel, was plotted against time for each prime-site photo sequence. These plots will be found in Volume VI, Appendix E. A smooth curve was drawn through all the data points to allow interpolation for the actual photo times. In many cases, an extrapolation to the last frame time was required. The time used was GMT corrected to actual spacecraft time at which the ratio was sampled. The correction was -4.4 seconds relative to the GMT tag of the telemetry frame and includes transmission time and the time position of PR01 within the frame.

The predicted V/H ratios for each photo site are also shown in the plots and were taken from the postmission EVAL analysis. The V/H operation was within the nominal accuracy of the system (1 to 2 milliradians per second). The only exception is Site IIP-5, but in this case the spacecraft was rolled to a point target and the V/H EVAL prediction was no longer valid.

The telemetry values of V/H varied from the EVAL prediction from +0.4% to -4%. The average deviation for Mission II was -2.38% as compared to -8% average deviation for Mission I. This shows appreciable improvement in the predictions for the later mission.

3.2.3.2 Power Subsystem

Power subsystem performance throughout Mission II was exemplary. Solar array current was higher than in Mission I, primarily due to an increase in solar constant compared to Mission I. This had the effect of masking the expected degradation of the array. Due to the absence of a shunt regulator fault in Mission II, the electrical loads were lighter than in Mission I. Consequently, batteries did not discharge to the extent experienced in Mission I, and battery temperatures were lower.

POWER SUBSYSTEM PERFORMANCE

Solar Array

Due to the elliptical path of the Earth about the Sun and the time of year, the solar array on Lunar Orbiter II was operated under solar intensities significantly higher than those of Mission I. The solar intensity in Earth space at launch for Mission I was 1.945 Langleys/min., and had increased to 2.034 Langleys/min. at Mission II launch. This 4.6% increase in solar intensity corresponds very well with the increase in maximum array power from 389 watts for Mission I to 407 watts for Mission II. The solar panel tem-

perature extremes seem to have reacted to the more intense solar environment, as shown in the following tabulation.

<u>Panel Temperature</u>	<u>Mission I</u>	<u>Mission II</u>
Minimum (°F)	-190	-173
Maximum (°F)	210	214

As solar intensity continued to increase through Mission II, it tended to compensate for degradation of array performance. Although the measurement tolerance of array current exceeds the magnitude of apparent degradation, it appears that array degradation did not exceed 2% through Orbit 200. Figure 3.2-26 shows array output plotted against temperature for Orbits 3 and 90.

It is interesting from an operational standpoint to note that the array provided a convenient tool to verify spacecraft attitude in pitch and yaw. At a given array voltage and temperature, the array current is very nearly an exact cosine function of the angle between the Sun vector and a line normal to the panels. As this angle is the vector sum of the pitch and yaw angles, and as the shunt regulator holds array voltage constant, calculations and predictions of attitude in pitch and yaw could be corroborated with a reading of array current taken with proper consideration of array temperature.

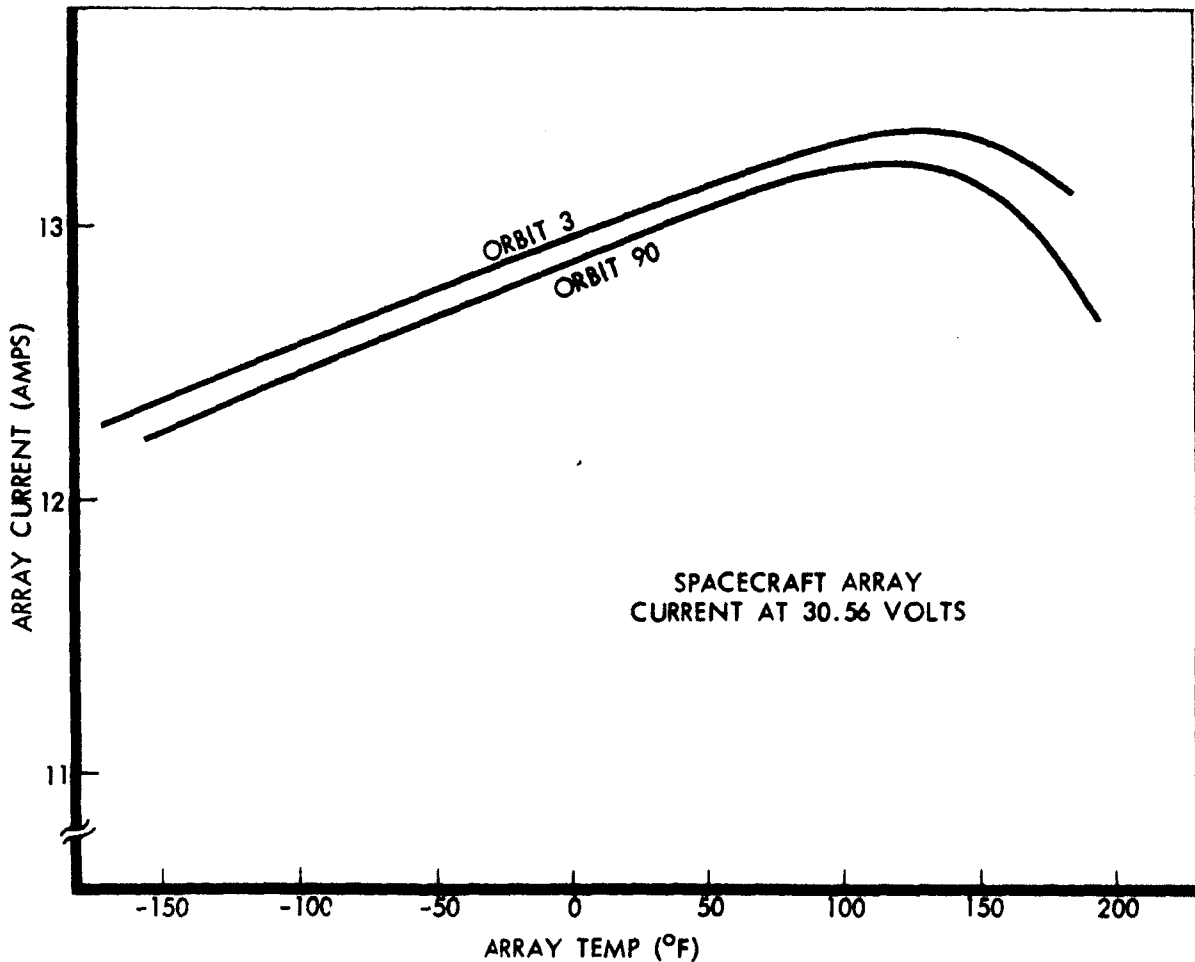


Figure 3.2-26: Array Output vs Temperature

Battery

In general, Mission II imposed a lighter load on the battery than Mission I. The spacecraft equipment mounting deck temperatures were on the order of 5°F cooler and nighttime loads were lighter by the amount of the shunt regulator fault of Mission I. Thus, as would be expected, end-of-discharge voltage remained higher, and depth of discharge was not as great. As shown in Figure 3.2-27 the end-of-discharge voltage is estimated to be 24.25 volts at the end of the photographic mission. Although sunrise was still not visible at the end of the mission, this value could be extrapolated with a fair degree of accuracy. Figure 3.2-27 provides a profile of the discharge depth through the mission. It is noted that calculations of discharge depth scatter more widely during the part of the mission in which part or all of the Sun occultation period occurs during Earth occultation. During this time, sunrise and/or sunset as well as battery current are predicted. Assuming an actual battery capacity of 13 ampere-hours, the depth of discharge varied between 24.5 and 28% for most of the mission.

Prior to inhibiting the photo heaters in Orbit 110, the depth of discharge was a strong function of spacecraft temperature. As the spacecraft temperature increased between Orbits 35 and 75, the heater thermostats called for less heat with an attendant reduction in discharge.

The battery overcharge ratio is the ratio of ampere-hour input to output and provides an index of battery and charge controller operation associated with energy balance. A ratio of 1.35 has been recommended as reasonable for battery temperatures of 90 to

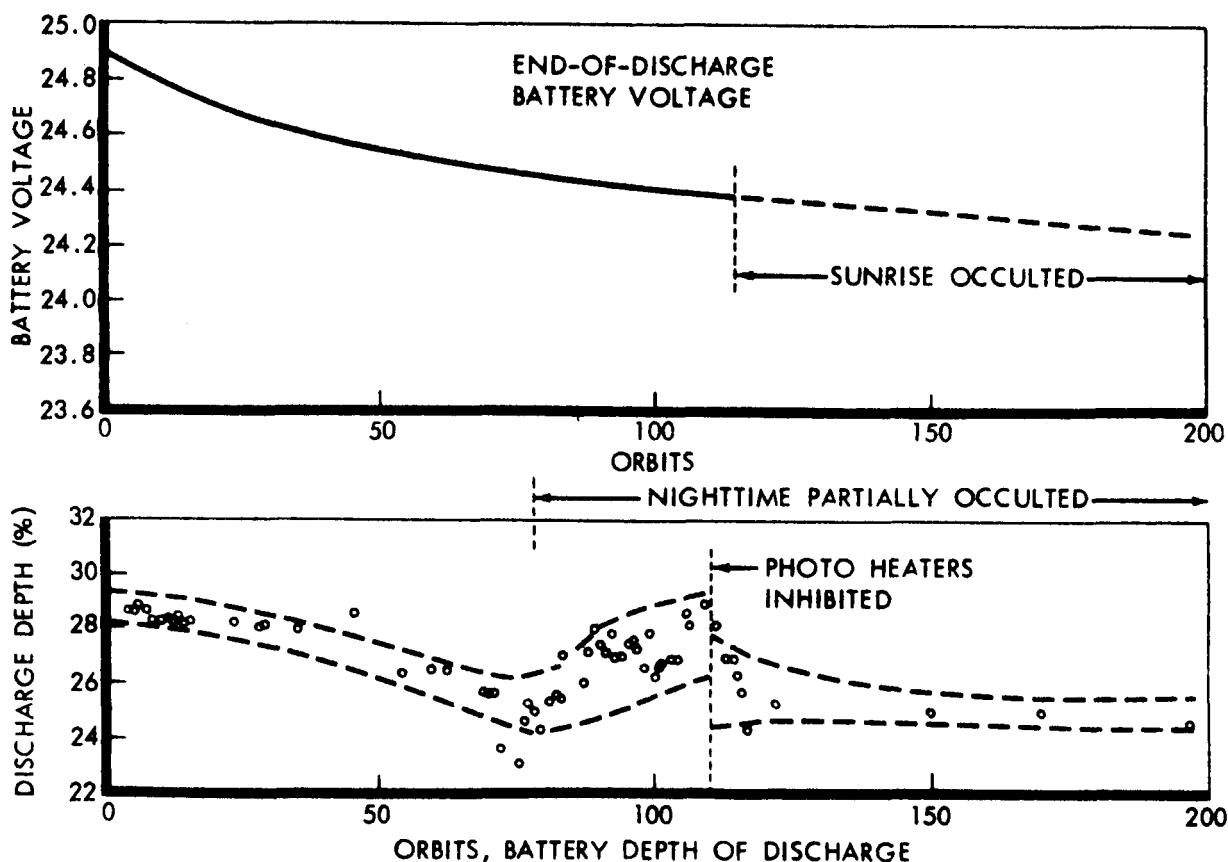


Figure 3.2-27: Battery Characteristics

95°F. During Mission II, overcharge ratios ran from 1.50 to 2.0 with the average around 1.65. This indicates a large energy surplus that was dissipated from the battery as heat.

Battery temperatures remained quite moderate throughout the mission. The trickle charge mode of operation was never initiated because temperatures did not reach 125°F during daytime operation. The mission maximum (occurring at night) was 128°F with orbital maximums generally running 85 to 90°F and orbital minimums varying from 50 to 65°F.

Charge Controller

The charge controller constant-current mode of operation maintains the charge rate of 2.85 amps as long as battery temperature and voltage sensors indicate that this is a safe rate. When the voltage-temperature combination indicates that the charge rate should be limited, the charge controller goes into its constant-voltage mode of operation. It typically takes from 80 to 90 minutes after sunrise to reach this point. The constant-voltage charge rate is then determined by battery temperature. A cooler battery accepts charge at a lower rate. As it heats, the rate increases.

The significant difference in charge controller operation between Missions I and II was the greater suppression of charge rate imposed by the constant-voltage mode of operation in Mission II. Within 15 to 18 minutes after going into this mode, the charge decreased to the order of 1.5 to 1.8 amps. This is compared with suppressed rates of 2.2 to 2.5 amps during Mission I. The reason for the different levels was the cooler temperatures at which the Mission II battery operated.

Shunt Regulator

This unit—with its associated dissipative elements—worked flawlessly in Mission II. By dissipating as much as 263 watts at times, the bus voltage was limited to exactly 30.56 volts, from which it never deviated during sunlight hours.

Spacecraft Loads

The electrical load imposed upon the power subsystem by other subsystems varied throughout the mission from a minimum of 3.37 amps (base load with photo heaters inhibited) to 8.23 amps during engine burns. The night-time load averaged near 4 amps. The readout load was typically 6.68 amps. Because a significant portion of the total load is imposed by thermostatically controlled heaters, the total at any given time is a function of spacecraft temperature. Table 3.2-12 presents a tabulation of values representing typical ranges of load current encountered in different modes of operation. The night-time load currents are also a function of the bus voltage, which decreases as the battery discharges. The constant-resistance loads draw less current as the night progresses, and the constant-power loads draw more. The losses within the power subsystem itself are approximately 0.28 amp.

Electrical Power Management Program

The computer program HUBL was devised primarily to maintain an accounting of the spacecraft battery state of charge. This is accomplished in the status mode of operation by integrating battery current for each data frame interval. The energy input during charging is modified by a calculated rate of efficiency. To maintain continuity of battery status calculations through periods of Earth occultation, values of battery current and temperature calculated by the predict mode of operation are used.

A sufficient backlog of data and experience is available from Mission II to devise a system for approximating battery data during Earthset without having to resort to the time-

Table 3.2-12: Typical Current by Mode

SPACECRAFT LOAD										S/C MODE	EE07 (AMPS)			
											MIN.	NOM.	MAX.	
S/C BASE LOAD	"INHIBIT HTRS" ON	"SOLAR ECLIPSE" ON	"SOLAR ECLIPSE" OFF	"INHIB. HTRS" OFF	CANOPUS TRACKER	PROPELLANT HTRS.	TWTA	R/O ELECT	R/O DRIVE	PROCESSOR				
DAYTIME														
X	X									CRUISE **	3.37	3.49	3.74	
		X								**	0	0.51	0.63	
			X							**	0	1.40	2.20	
				X								0.12		
X		X								CRUISE	3.37	4.00	4.38	
X			X							DAYTIME STANDBY	3.37	4.89	5.95	
					X							1.85		
X		X			X						5.22	5.85	6.23	
X			X		X						5.22	6.74	7.80	
						X						1.60		
X			X			X				TWTA ON	4.97	6.49	7.45	
X	X					X				TWTA ON	4.97	5.09	5.35	
X	X					X	X			R/O ELECT, ON	5.38	6.50	6.76	
X	X					X	X	X		READOUT	6.62	6.74	7.00	
X									X	PROCESS	4.68	5.35		
NIGHTTIME														
X	X									CRUISE ***	3.52	3.56	3.88	
X		X								STANDBY NIGHTTIME	3.91	3.96	4.14	
				X								0.15		
X		X		X						ACQUIRE CANOPUS	4.05	4.11	4.29	
					X						1.36	1.50	1.55	
X		X			X						5.27	5.46	5.69	

*HEATERS INHIBITED ** FUNCTION S/C TEMP. ***FUNCTION OF BUS VOLTAGE

consuming predict mode. During Mission 11, sequential status runs using averaged predictions of charge-discharge rates were tried. Modifications to HUBL to select the correct battery current constant automatically are in work.

Launch to Sun Acquisition

From the first use of internal power during prelaunch to Sun acquisition, the batteries discharged approximately 4.2 amp-hours, giving a depth of discharge of 32.3%. Within 35 minutes after Sun acquisition, the full charge rate had begun to taper with the constant-voltage mode of operation and was 0.73 amp within another 30 minutes. The array deployment sequence was not acquired on telemetry, but the array was deployed and supplying 13.27 amps at 30.56 volts by 55 minutes and 50 seconds after liftoff.

Cislunar Through Orbit Injection

The first 16 hours of cislunar flight were flown with the Sun acquired, during which time the array temperature stabilized at 91°F, the battery at 95°F. As the battery heated, the charge current increased to about 1 amp, where it stabilized. Spacecraft loads were minimal (about 110 watts) and the shunt regulator had to dissipate 253 watts or more.

Subsequently, the spacecraft was pitched approximately 36 degrees off the Sun and all temperatures readjusted. The array cooled to 65°F and the battery to 85°F, which reduced the charge rate to about 0.8 amp, and the power dissipated by the shunt regulator was reduced to about 170 watts. Solar misalignment was later increased to 40 degrees.

The Sun was again acquired 31 hours into the cislunar phase of the mission, and array temperature for the first time attained its optimum 100 to 107°F temperature. Array output peaked at 13.33 amps (407.4 watts).

The total load during engine burn was 8.1 amps at the midcourse maneuver. Array power was still sufficient to maintain the bus voltage at 30.56 volts with 63 watts surplus being dissipated in the shunt regulator.

After the midcourse maneuver, when the spacecraft was again pitched 36 degrees off the Sun, battery and array temperature settled back into the 70 to 80°F range with a corresponding adjustment of electrical parameters.

Prior to orbit injection, the "heater inhibit" was removed. From this time until it was re-applied after completion of the photo orbits (Orbit 110), the spacecraft load current reflected the variable cycling period of the photo heaters.

The battery was discharging at rates from 4.12 amps to over 8.23 amps from the time the spacecraft went into the shadow of the Moon until the time that Sun was reacquired in the first orbit. Energy discharge was 3.58 amp-hours for a discharge depth of 27.5%. During the 11-minute engine burn, battery voltage dropped from 24.32 to 23.68 volts. The charge controller had restored the battery voltage to 29.28 volts 84 minutes after sunrise and had gone into the constant-voltage mode of operation.

Initial Orbits Through Orbit Transfer

Typical orbital array performance is illustrated by Figure 3.2-28, showing array temperature and current during the initial high orbits (1 to 33). Typical battery performance is illustrated by Figure 3.2-29, showing battery current, voltage, and temperature for Orbits 8 and 9. For this battery charge-discharge cycle, depth of discharge was 27.5% and overcharge ratio was 1.74.

Tank deck heaters were turned on periodically during Sun presence; under these conditions, the total spacecraft load was almost 6 amps. With the Sun acquired as it was for

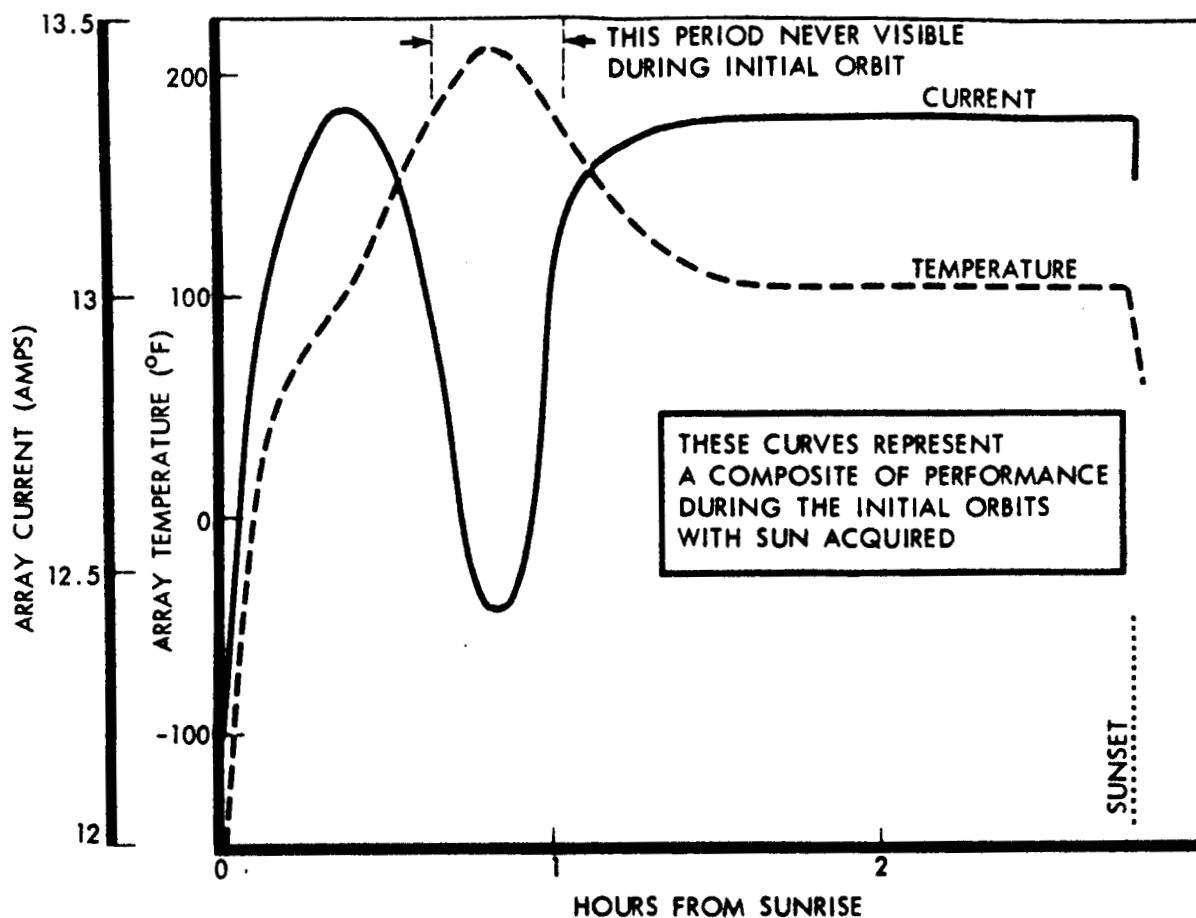


Figure 3.2-28: Array Characteristics During Initial (High) Orbit

the first 20 orbits, there were still 5 to 5.5 amps of surplus current. Readout capability was tested during this phase; maximum total load was 6.62 amps.

Maximum orbital battery temperature had been slowly increasing to 94°F in Orbit 16, at which time the spacecraft was pitched off Sun 36 degrees for one orbit. This had a temporary cooling effect that helped for three or four orbits, after which the previous maximum temperatures were attained. In Orbit 20, the spacecraft was pitched off the Sun 32 degrees and left there. Maximum battery temperatures typically were 78 to 80°F.

The orbit transfer maneuver had no significant impact on the power subsystem.

Photo Orbits

The low orbit, although approximately 8.7 minutes shorter than the high orbit with night periods approximately 1 minute longer, had no significant effect on energy balance. As the mission progressed, Earth occultation blacked out a period of telemetry that first concealed sunset in Orbit 79. Sunrise and all night-time operation was first concealed in Orbit 116. Sunset again reappeared in Orbit 119, but sunrise (and end-of-discharge voltage) was not visible throughout the remainder of the photographic mission. During this period, calculations of discharge depth and battery voltage were based on predictions and extrapolations.

Battery operation during the readout orbits is illustrated by Figure 3.2-30, which shows voltage, current, and temperature during Orbits 108 and 109 selected as typical.

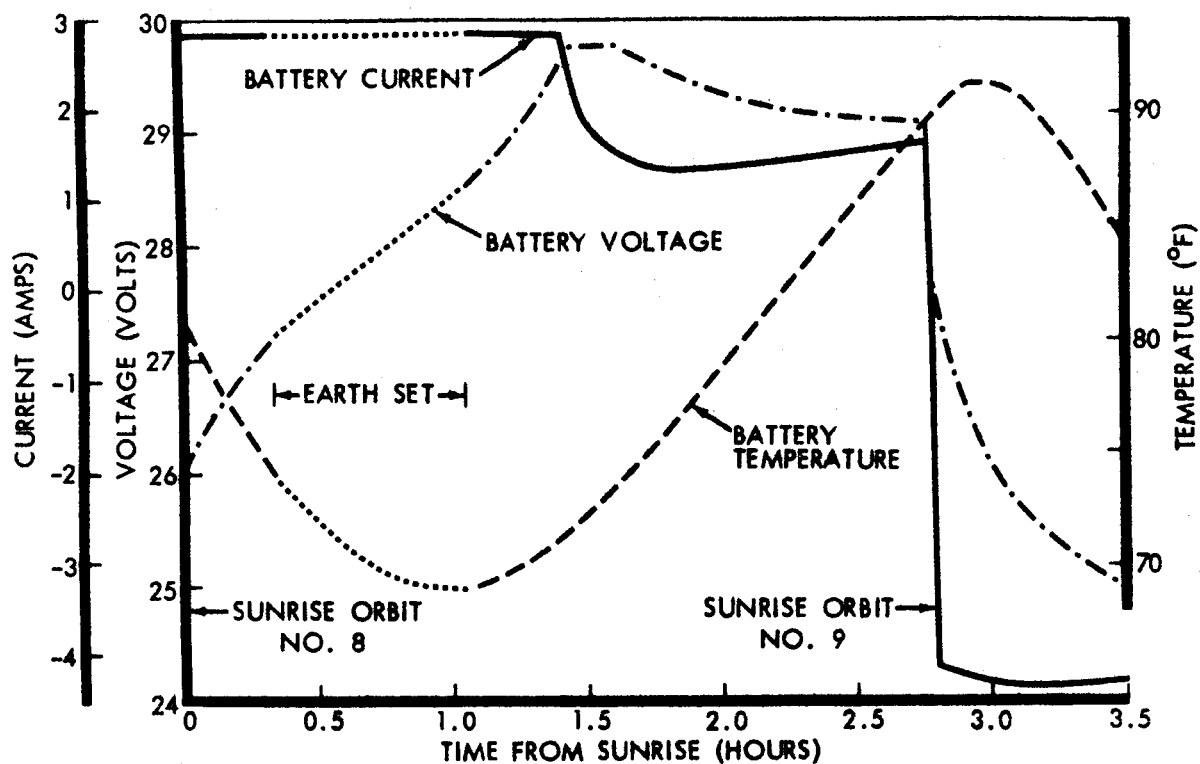


Figure 3.2-29: Battery Characteristics Orbit 8-9

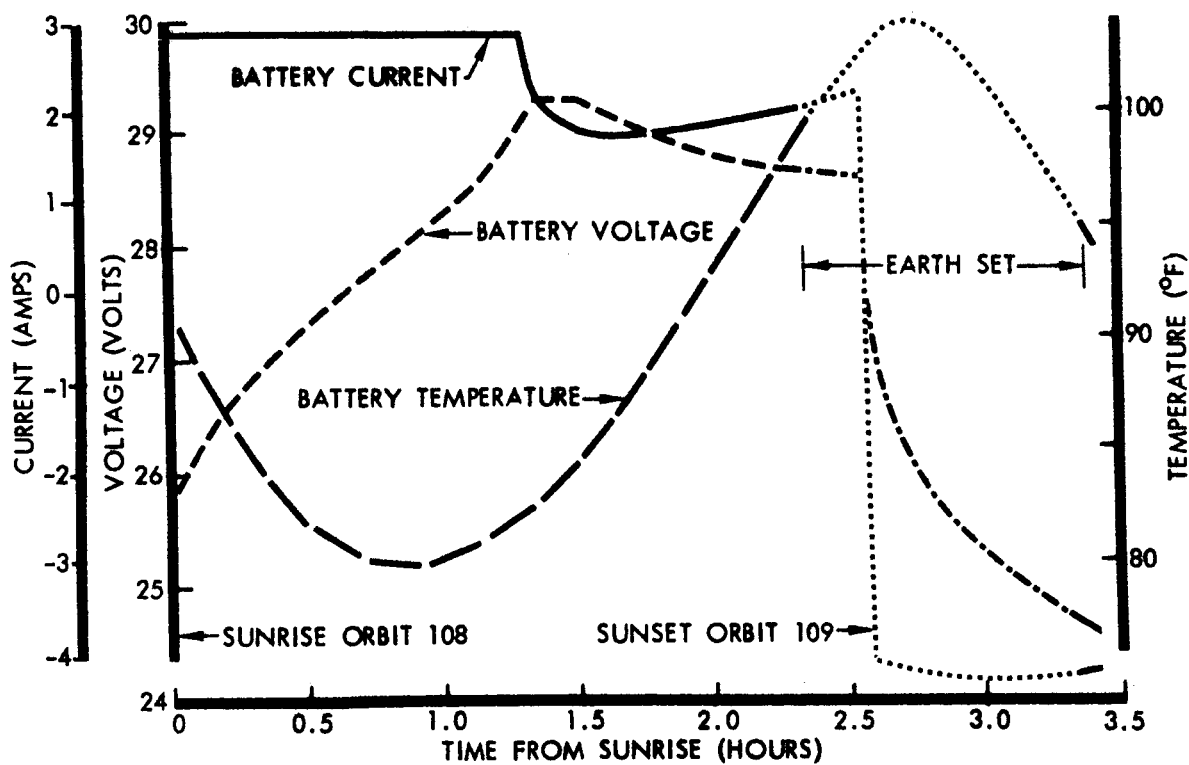


Figure 3.2-30: Battery Characteristics Orbit 108-109

The electrical loads supported by the power subsystem during each phase of the photo orbits and each mode of operation are tabulated in Table 3.2-12. For each mode of operation that includes thermostatically controlled heaters, the total spacecraft load will vary between the minimum and maximum values shown, with the nominal value being associated with average spacecraft temperature conditions. The total load during camera operation is taken as an extension of the processing mode.

Spacecraft attitude during the normal photo orbits (through Orbit 178) varied from 5 or 10 degrees off Sun for photography to 38 degrees off Sun for cooling purposes during readout. The solar array misorientation associated with these maneuvers had no effect on the power subsystem operation beyond reducing the current drawn by the shunt regulator to maintain bus voltage at 30.56 volts.

After the traveling-wave-tube-amplifier problem in Orbit 179, the spacecraft was pitched over 50 degrees off the Sun for maximum cooling. Bus voltage then dropped to the level of battery voltage for approximately 1 minute while supporting a 5.05-amp load.

3.2.3.3 Communications Subsystem

Communications subsystem performance was satisfactory throughout the mission up to the time that the traveling-wave-tube amplifier (TWTA) would not turn on. This occurred within 12 hours of the planned end of the mission. There were no errors in any of the verified command words executed by the flight programmer. Transponder performance was satisfactory. Telemetry data showed that rf output power varied inversely with the transponder temperature as expected.

Both high- and low-gain antennas performed successfully and were properly deployed when the spacecraft was initially acquired by Woomera DDS-41.

Some increases in the TWTA helix current were noted at turn-on beginning in Orbit 74 and continuing through priority readout. Beginning with the final readout, an additional increase in helix current was noted at each turn-on. Although these turn-on indications were not normal, the TWTA output was normal until the unit failed to turn on.

LAUNCH TO ACQUISITION

The communications subsystem functioned nominally from the time of liftoff. Telemetry data received via the Agena Interface provided real-time data at the SFOF from liftoff to 24 minutes after launch with only 3 minutes of bad data. When data loss occurred, the communications subsystem was functioning normally in Modulation Mode 3 (performance telemetry). Real-time data at the SFOF was not again available until well after cislunar injection.

CISLUNAR TO INJECTION

Cislunar injection occurred 21.5 minutes after launch and immediately prior to the first S-band acquisition by the DSN. Acquisition reports received from the DSN show that DSS-72 (Ascension) acquired the spacecraft 21.6 minutes after launch at a signal strength of -135.1 dbm. (This acquisition occurred approximately 10 seconds after the Agena second burn terminated and 4.3 minutes prior to the start of the spacecraft antenna deployment.) Other acquisition reports show that, almost simultaneously with the initiation of Sun acquisition, at 27.6 minutes after launch, DSS-51 (Johannesburg) acquired the spacecraft two-way at a signal strength of approximately -111 dbm and remained in contact for about 11 hours. (It is noted that DSS-51 acquired the spacecraft prior to the stored program switchover to Mode 4.)

At 51.3 minutes after launch, DSS-41 (Woomera) acquired the spacecraft three-way with DSS-51 and it is again noted that DSS-41 acquired while the spacecraft was transmitting in Mode 3. No signal strength level at the time of DSS-41 acquisition was reported; however, just after the spacecraft switched to Mode 4 at 54.1 minutes after launch, the signal strength was -108 dbm. This signal level is within 3 db of the value predicted for initial acquisition.

Real-time data from three-way station 41 became available again at the SFOF 61 minutes after liftoff. The communications subsystem measurements indicated that the spacecraft signal strength (AGC) was within allowable limits. The static phase error (SPE), however, was high (+6 to +9 degrees) but well within the phase lock capabilities of the spacecraft transponder. The high SPE was due to frequency offset of the DSS-51 transmitter.

The signal strength variations of both the ground receiver and the spacecraft did not exceed 8.0 db during the 360-degree roll of the first star map. This variation was most likely due to nulls in the low-gain-antenna radiation pattern. The occurrence of station handover (DSS-51 to DSS-41) was of particular interest during the roll maneuver. Immediately after handover, the spacecraft SPE changed to less than 0.5 degree, well within the command limits of plus or minus 3.5 degrees.

Ninety-nine minutes after liftoff, DSS-41 commanded Mode 4 "off." The decrease in ground signal strength resulting from the change to normal Mode 3 was 5.5 db; this value is approximately the maximum value that can be obtained from the best-case tolerances of the communications subsystem.

Two high-gain antenna maps were obtained during 360-degree-roll maneuver star mapping operations. The antenna maps show that the spacecraft roll position determined by the attitude control subsystem and by antenna boresight agree within 2 degrees.

FIRST ELLIPSE TO FINAL READOUT-LINK PERFORMANCE

Telemetry Link

Downlink telemetry operation throughout the mission was excellent with normal signal level margins of from 1 to 3 db above the nominal link design during the orbital phase of the mission. Early in the mission it was discovered that the Modes 1 and 3 30-kc oscillator in the modulation selector was operating approximately 110 Hz above nominal center frequency. This created a slight problem in connection with "locking up" the ground demodulators until the tuning range of the demodulators was checked and re-adjusted as required.

Command Link

No problems were encountered with the uplink operation throughout the mission. DSS transmitter power levels during lunar orbit were normally held at 1 or 2 kw and signal level margins at the spacecraft were normally from 3.5 to 7.5 db above the nominal design. The spacecraft AGC measurement (CE08) closely followed DSS transmitter power changes as well as carrier suppressions caused by command or ranging modulation. For constant transmitter power levels the spacecraft AGC measurement indicated a 2.5- to 4.5-db variation each orbit due to transponder temperature changes.

Video Link

The performance of the video link was very satisfactory throughout the mission up to the time the TWTA would not turn on. High gain antenna pointing errors were mini-

mal, evidenced by the signal level readings taken at the DSS stations during readout. These readings varied from -90.0 to -98.5 dbm, which corresponds to video margins of 7.5 db above and 1.0 db below the nominal link design. The signal levels for most of the mission were from -92 to -95 dbm, which yield video margins of 5.5 to 2.5 db over the nominal link design. During the mission, no readout was degraded by low signal levels from the spacecraft.

COMPONENT PERFORMANCE

Transponder

The performance of the transponder was very satisfactory throughout Mission II. The transponder output power was 100 to 150 mw lower than that obtained from the Mission I transponder; however, it was well above the specification limit of 400 mw until the latter portion of the mission, when it went as low as 379 mw when transponder temperatures of 100°F were reached.

The telemetered transponder output power indication, CE10, varied inversely with temperature with typical values of 466 mw at 65°F and 422 mw at 90°F. The minimum output power is of greatest concern, and is best illustrated by Figure 3.2-31, which is a plot of minimum transponder power and maximum transponder temperature for each orbit of the mission beginning at lunar injection. Contrary to Mission I indications, the transponder output power seemed to be dependent only on temperature and did not exhibit "step function" changes observed in Mission I. Figure 3.2-31 does, however, indicate that transponder output power appeared to degrade as the mission progressed. For example, in Orbit 34/35 at a temperature of 85°F, CE10 indicated 438.5 mw as opposed to 425 mw in Orbit 134/135 (same temperature). This degradation appears to have started sometime around Orbit 45; however, it is possible that this phenomenon is due to misleading data caused by the thermal inertia of the transponder.

Early in the mission it was noted that the ranging code transmitted from the spacecraft was reversed in phase with respect to the code being transmitted to the spacecraft. Because DSN personnel had not been properly instructed, this situation created problems in the DSN ranging equipment and, as a result, completely accurate range data could not be obtained. It was an unnecessary problem because the reversal was known before launch and should have been accommodated by operation of a switch prior to any ranging operations.

The signal level indicated by the transponder automatic gain control (AGC), CE08, reflected the effect of increasing range during cislunar flight, as well as changes in ground transmitter power levels. In most cases, CE08 tracked the reported changes in ground transmitter power within 1 db. Command modulation on the uplink was clearly evident on CE08: one tone causing a decrease of about 2 db, and two tones causing a decrease of 3 to 4 db. Ranging modulation caused the uplink carrier power (CE08) to decrease by approximately 8.5 db as expected. CE08 was also found to vary with transponder temperature. During a typical orbital temperature cycle of approximately 21 degrees, changes of 2.5 to 4.5 db were noted for CE08.

During the latter part of the mission it was noted that the sensitivity of the transponder AGC measurement appeared to be slowly increasing, i.e., a particular DSS transmitter power and transponder temperature at the end of the mission produced an AGC value 2 to 3 db higher than comparable transmitter powers and transponder temperatures at lunar injection. This fact is substantiated by the plots of Figure 3.2-32, which show data values taken at Earthrise throughout the orbital phase of the mission. Figure 3.2-32 also shows CE08 normalized to a constant DSS transmitter power of 2 kw. From this normalized plot it is evident that at approximately Orbit 120 CE08 begins to slope upward, i.e., increase in sensitivity. In Orbits 45 and 150 (equal transponder temperatures of 65°F), the difference in the CE08 indication is approximately 3 db, -90

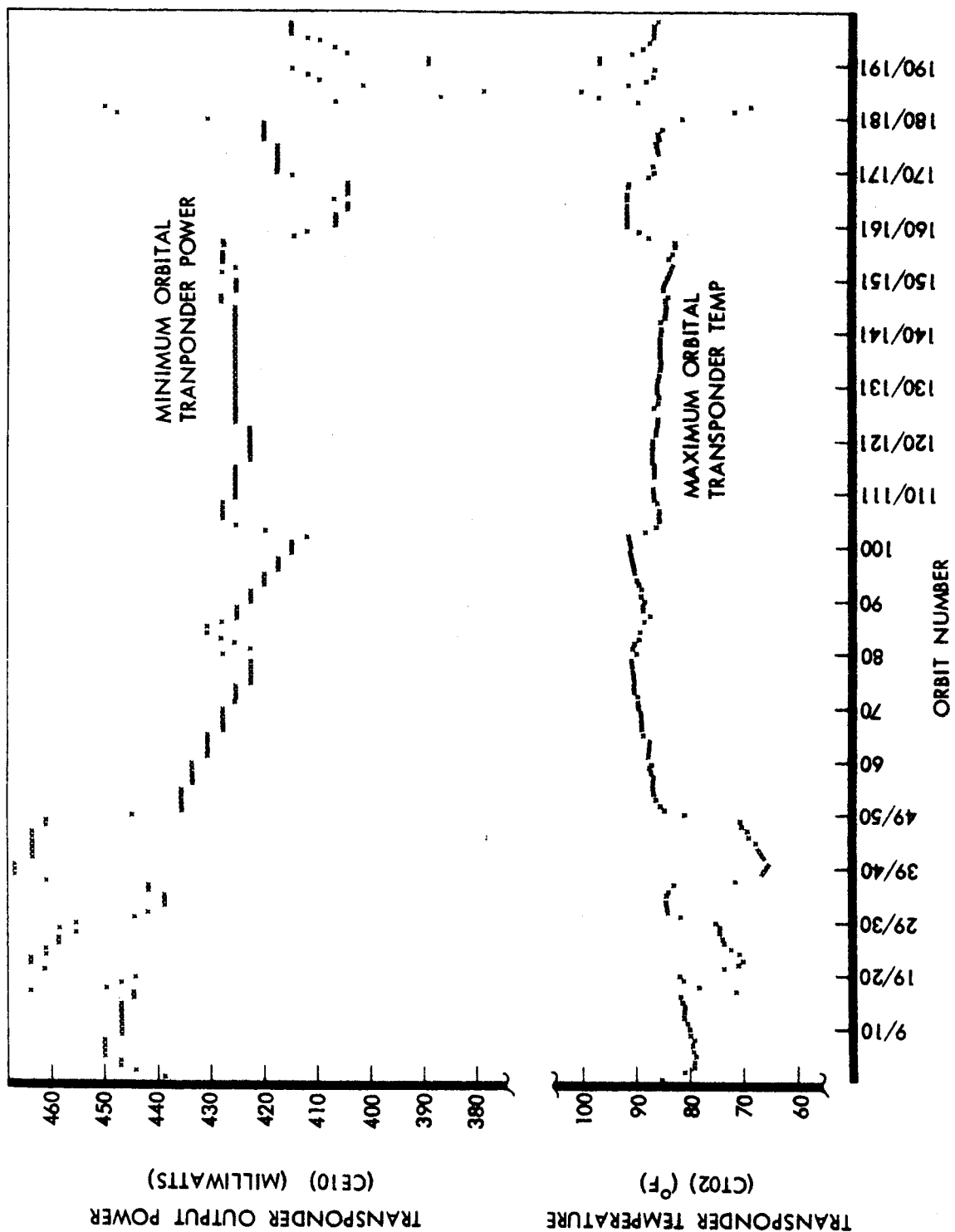


Figure 3.2-31: Transponder Output Power and Temperature Variations During Lunar Orbit

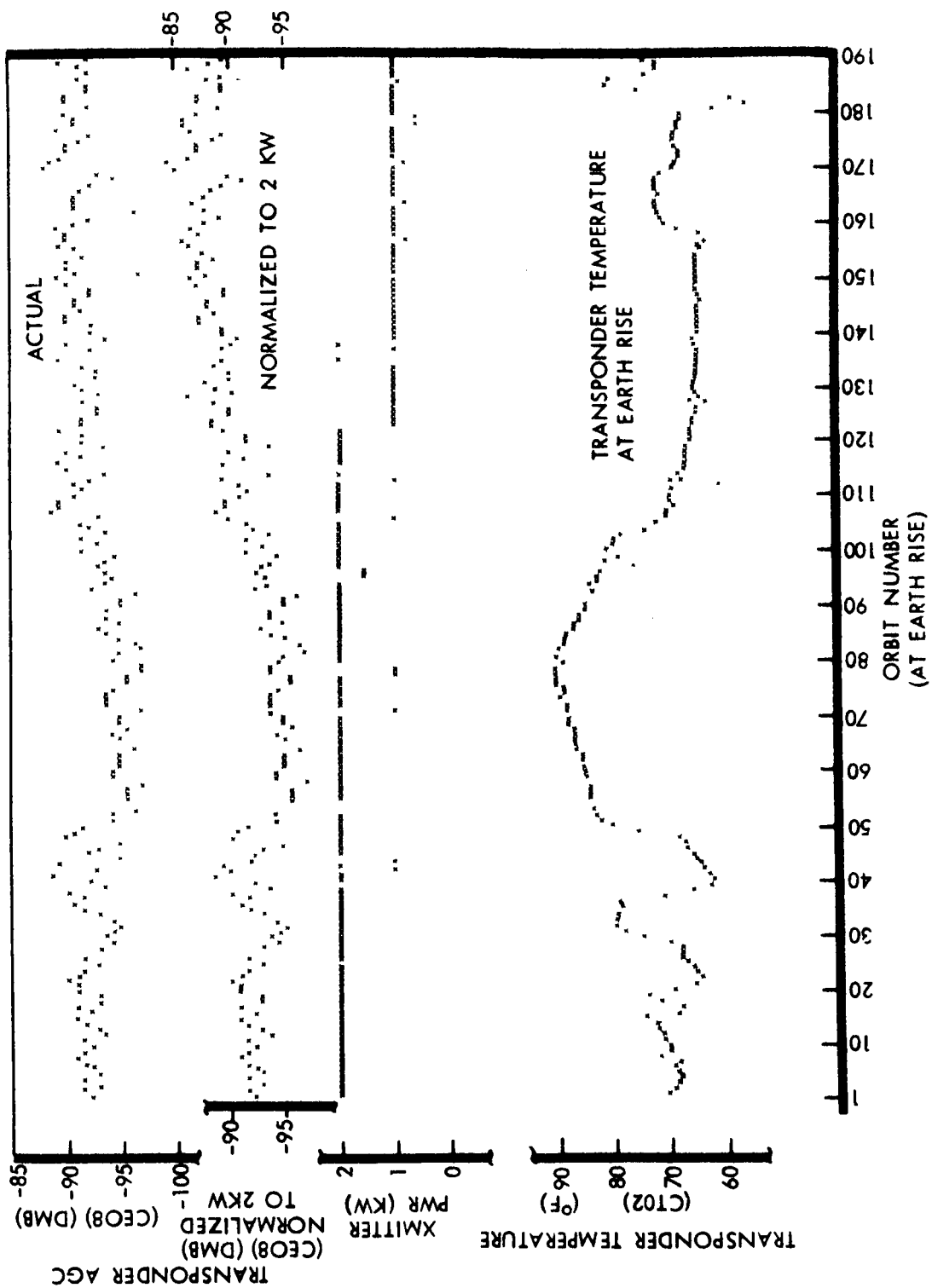


Figure 3.2-32: Transponder Data

Multiplexer Encoder

The multiplexer encoder functioned perfectly throughout the mission. All telemetry channels performed properly, indicating that all channel gates were operating; EE01 signal conditioner zero reference and EE08 precision power supply voltage were constant at 0 mv and 20.00 vdc, respectively, indicating correct coding of analog channels; CC01 spacecraft identification, CC03 command verification word, CC06 external-internal clock, and the telemetry frame marker were correct from start to finish, indicating correct programming in the multiplexer encoder. Occasional samples of these measurements indicated a switch to internal clock. Closer examination revealed that the error occurred generally in an area near a bad data frame and that the programmer did not enter the halt mode (indicating no clock switch occurred). It is concluded that if any faults occurred they were transient in effect, that their occurrence was not progressive, and that performance of the multiplexer encoder did not affect the operation of the mission.

Command Decoder

The command decoder performed precisely as planned throughout the mission. There were no errors in any of the verified words that were executed into the flight programmer. Threshold command operation was approximately -123 dbm carrier signal at the spacecraft, which was within 2 db of the prelaunch value.

Modulation Selector

Except for the frequency of the Mode 1 telemetry subcarrier oscillator, the modulation selector operation was satisfactory. The Mode 1 subcarrier oscillator operated approximately 110 Hz high throughout the mission and was high prior to liftoff. A failure report has been written with a recommendation to measure subcarrier oscillator frequency before launch.

Signal Conditioner

Operation of the unit was satisfactory. The additional unit installed for measurements ST09 through ST12 appears to have performed satisfactorily. CE09, signal conditioner voltage measurement, varied from 4.60 to 4.68 volts throughout the mission, which is within the $\pm 1\%$ stated in the measurement list.

High- and Low-Gain Antennas

Both the high- and low-gain antennas performed successfully during all of Mission II. Verification of successful deployment was obtained from telemetry measurements CC04 and CC05. These are discrete channels that indicate 0 when the antenna is stowed and 1 when the antenna has deployed. CC04 (low gain) and CC05 (high gain) indicated dbm in the former versus -87 dbm in the latter orbit. As a result of this apparent increase in sensitivity, the DSS stations were required to decrease their transmitter power levels as much as 5 db (from 2 kw) at times to comply with the command transmission limit of -90 dbm for spacecraft AGC.

The transponder static phase error (SPE), CE06, displayed a sinusoid-like cycle variation during each orbit of the mission, with the average total excursions being equal to about 4.75 degrees. This variation was due to doppler shift in the spacecraft received frequency. The amplitude was generally centered about 0-degree SPE with equal positive and negative excursions. Immediately following lunar injection, the SPE went further negative than positive due to inaccuracy in the initial doppler predicts. On occasion, the SPE exceeded the command transmission limit of -3.4 degrees. This made it necessary for the DSSs to change transmitter frequency to decrease the SPE. No problems were experienced after good orbit determination and doppler predicts were established.

0 at launch; both indicated 1 after acquisition by Woomera. The gains of both antennas were nominal. Based on DSS-received signal strengths and the communications system link analysis, the gain of the directional antenna was approximately 24.5 db and the omnidirectional antenna exhibited a normal pattern.

The high-gain antenna responded properly to all rotation commands. The antenna rotated through a full 360 degrees during the course of the mission in addition to several 30-degree rotations to compensate for "pitching" off the Sun. In all of these rotations the encoder that telemetered the rotation angle (CD01) functioned perfectly.

Traveling-Wave-Tube Amplifier

During the mission, the TWTA was successfully commanded on and off for 129 cycles with total operating time of 198.2 hours. This does not include three on-off cycles during the two countdowns, but does include two cycles during cislunar flight for high-gain antenna mapping and two during the initial ellipse for reading out the Goldstone test-film. Priority photo readout began after the initial photography on Orbit 53 and continued during each orbit through Orbit 104. Average TWTA operating time during priority readout was 39.4 minutes per orbit. After Bimat cut, final readout was initiated on Orbit 106 and continued until the TWTA failed to come on when commanded during Orbit 179. Average operating time during final readout was 135.1 minutes per orbit.

A detailed study of telemetry data which reflected TWTA conditions was made. Histories of EMD temperature, TWTA collector temperature and current, helix current and voltage, and rf power output were studied in an attempt to establish a relationship between these functions and the TWTA failure. While these studies showed that helix current was high and experienced step functions not occurring in a normally operating TWTA, no relationship between the abnormal helix current and the TWTA failure could be established.

After extensive ground testing in an attempt to duplicate the failure conditions of the spacecraft, it was determined that shorting of the TWTA helix power supply came very close to explaining the failure. Many conditions could cause such a short, but the three most promising appear to be:

- 1) High-voltage breakdown (corona) between Terminal #5 of the high-voltage transformer and case;
- 2) High-voltage breakdown due to deterioration of insulation material by corona;
- 3) Failure of the filter capacitor in the high-voltage supply.

The most likely cause of the failure is considered to be Item 3. Until more information is available, the TWTA anomaly must be considered as random. For further discussion of this anomaly, see Appendix D in Volume VI of this document.

3.2.3.4 Attitude Control Subsystem

The Lunar Orbiter II attitude control subsystem met all mission objectives. All problems encountered were solved by changes in operational procedures, while meeting all performance requirements. Nitrogen consumption was held to 5.5 pounds for the photographic mission. The spacecraft was flown off the sunline for about half the mission to reduce degradation of the EMD thermal paint. Use of the Canopus star tracker was restricted to sunset periods (except during cislunar flight) because of a tendency to track other bright objects. This phenomenon has been tentatively identified as "glint" caused by reflection of sunlight from a variety of surfaces, including the Moon.

The flight programmer responded correctly to every command received from the command decoder during the mission. One-thousand two-hundred eighty-nine real-time commands and 2282 stored program commands were received. Repetitive execution of stored program commands accounts for an estimated total of 12,000 commands executed by the programmer. Total programmer clock drift was 1.21 seconds. The programmer breadboard was used at SFOF to follow the mission sequence of commands and maintain a check of flight programmer operations during spacecraft occultation periods.

Throughout the mission the attitude control subsystem maintained stable operation for both reaction control and thrust vector control. Control modes included: conventional limit cycle (CLC) in pitch and yaw using Sun sensors to hold closed-loop Sun lock, and in roll using Canopus tracker roll error to hold closed-loop Canopus lock; inertial hold (IH) using pitch, yaw, and roll gyros in rate integrate mode for position reference; and constant rate mode (CR) using pitch, yaw, and roll gyros in rate mode for maneuvers.

ATTITUDE CONTROL SUBSYSTEM PERFORMANCE

During Mission II, the attitude control subsystem performed its many tasks within design specification. Two-hundred eighty-four single-axis maneuvers were performed during the photographic portion of the mission. Maneuver accuracy of the attitude system was -0.05 , -0.02 , and $+0.11\%$ for roll, pitch, and yaw respectively, which is within the design tolerance. Attitude maneuver rates for all axes were within the design limits of 0.5 ± 0.05 degree per second for maneuvers in narrow deadband. Maneuver rates in the wide deadzone ranged from 0.039 to 0.058 degree per second.

Spacecraft orientation with respect to the Sun and Canopus was maintained within ± 0.2 and ± 2.0 degrees, depending on the deadband commanded. Deadband accuracies were within telemetry resolution for narrow and wide deadzones except when operating with the yaw fine Sun sensors in narrow deadband, which produced a plus bias of approximately 0.05 degree above the normal telemetry resolution.

Attitude control was maintained with the spacecraft pitched from 26 to 38 degrees away from the Sun for approximately 56% of the mission. The "pitched-off" attitude was required to reduce spacecraft temperatures and delay thermal paint degradation. Drifts in the inertial reference were within design limits.

Stable control of the spacecraft attitude was maintained throughout three velocity control engine burns for a total of 647 seconds. Spacecraft pointing accuracy and burn termination were performed within the design tolerances as far as could be determined from the telemetry resolution. Operational methods used to control spacecraft attitudes are presented below.

Cislunar Coast

The cislunar portion of the mission required a $+ 36$ -degree pitch off-Sun maneuver to reduce temperatures and delay thermal paint degradation. Canopus was not being tracked automatically during the first pitch maneuver resulting in a roll error at the termination of the maneuver. A -9.0 -degree roll maneuver was performed less than an hour later to place Canopus on the negative side of the ± 4.1 -degree tracker field of view. The spacecraft then drifted in the plus direction ($+$ gyro drift), allowing observation for a roll gyro drift test. Canopus was later acquired while still in the field of view and the spacecraft maneuvered back to the Sun. The second pitch maneuver did not cause a roll error, since the spacecraft was automatically tracking Canopus within the deadband tolerance of the attitude control subsystem. Subsequent pitch maneuvers for thermal relief were made while locked on Canopus, thereby simplifying the control technique.

Spacecraft Velocity-Change (ΔV) Maneuvers

The midcourse correction, lunar orbit injection, and orbit transfer maneuvers were performed based on a normal Sun reference while in an automatic control mode. The roll axis was updated "open loop" based on ground calculations. This technique required a roll update maneuver from 2 to 6 hours prior to the velocity correction. The roll axis would then drift through zero error at the time the roll maneuver for the velocity correction was initiated. The required attitude control accuracy of ± 0.2 degree with respect to the Sun and Canopus was thereby ensured.

Photo Maneuvers

Accurate pitch and yaw photo maneuvers were possible during this phase of the mission because the spacecraft was locked on the Sun in 0.2-degree deadband. The roll axis reference was updated by turning on the tracker for 3 minutes and acquiring Canopus during Sun occultation. Automatic roll updating was more efficient and contained less chance for error than manual updating; however, the roll axis inertial reference drifted away from an ideal Canopus reference at the start of the photo roll maneuver. The roll error for each photo was calculated based on a drift rate of $+ 0.5$ degree per hour and the location of the roll axis in the deadzone at the start of each roll maneuver. These errors, as well as the pitch and yaw errors during the actual photo sequence, are tabulated in Table 3.2-13. All pitch and yaw errors were within ± 0.2 degree. The maximum roll error for a primary photo site was $+ 0.261$ degree. Maximum roll error for a secondary photo site was $+ 0.357$ degree. The majority of photo sites had roll errors that were less than 0.2 degree. The figure also includes attitude rate information for the shutter-open period for each photo site. These rates were much less than the 0.01 degree per second design rate requirement.

In general, each photo site required a three-axis maneuver, usually a roll, yaw, pitch sequence. There were 34 three-axis maneuvers, one two-axis maneuver, and four single-axis maneuvers for photos during the mission.

The crab angle sensor was not used as an attitude reference at any time. No conclusions have been reached concerning the accuracy of the crab angle sensor or its proper operation.

Readout

Off-Sun operation was required throughout readout to satisfy thermal requirements and retard thermal paint degradation. A plus-26-degree pitch maneuver was performed while locked on Canopus at the beginning of readout. This maneuver was chosen as an optimum for both attitude control and communications within the power and thermal constraints. The plus maneuver allowed continuation of automatic updating of the roll axis by acquiring Canopus during sunset. It was only necessary to monitor the yaw axis to keep Canopus within the tracker field of view in yaw and at the same time satisfy antenna pointing constraints. The pitch axis drift rate was $+0.03$ degree per hour and required very little attention.

Roll and yaw data were readily available during readout since the spacecraft position error did not exceed sensor telemetry saturation limits. The pitch axis, however, reached a Sun sensor telemetry saturation level at ± 26.0 degrees. Pitch angles as high as 38 degrees were encountered during readout. It was therefore necessary to calibrate solar panel array current versus total angles off the Sun to determine pitch attitude. Knowing the total angle off-Sun and the yaw angle, the pitch angle could be determined. This procedure proved to be accurate within ± 0.3 degree over a period of several days.

Table 3.2-13: Attitude Data For Photo Sites

Photo Site	Number of Frames	Initial Roll Error (deg)	Max. Rate During Photo			Attitude Error During Photo			Crab Angle Variation (deg)
			Roll (deg/sec)	Pitch (deg/sec)	Yaw (deg/sec)	Roll (deg)	Pitch (deg)	Yaw (deg)	
P1 & S1	16 & 4	+0.19	+0.00239	+0.0026	-0.0024	-0.17 to -0.067	-0.02 to 0.15	0.11 to 0.7	-0.05 to 0.18
S-2a	1	-0.08	0	+0.00403	-0.0039	0.145	0.142 to 0.10	0.09 to 0.065	-0.032 to 0.20
S-2b	4	+0.064	+0.00213	-0.00391	-0.00196	-0.16 to -0.14	0.06 to -0.02	0.16 to 0.13	-0.30 to 0
P-2	8	-0.11	-0.00217	+0.0030	-0.00467	-0.085 to -0.09	0.14 to 0.145	0.045 to 0.04	0.15 to 0.20
P-3a	8	+0.08	-0.00204	+0.00382	-0.00226	-0.12 to -0.09	-0.05 to +0.03	+0.14 to 0.12	-0.18 to -0.15
P-3b	8	+0.261	+0.00304	+0.00208	-0.0020	-0.15 to -0.10	+0.02 to 0.05	0.07 to 0.05	-0.05 to +0.10
P-4	8	+0.207	+0.00117	+0.00304	-0.00652	-0.16 to -0.15	0.02 to 0.07	0.08 to 0.075	0
P-5	8	-0.241	-0.00209	-0.00221	-0.00179	-0.12 to -0.14	-0.08 to -0.12	0.14 to 0.085	-0.13 to 0.20
P-6a	8	-0.130	+0.00167	0	-0.00067	-0.08 to -0.06	0.155	0.06 to 0.045	0.10 to 0.15
P-6b	8	+0.040	+0.00291	0	-0.00305	-0.13 to -0.11	0.14	+0.01 to -0.04	-0.12
S-6	1	-0.15	+0.00226	+0.00087	+0.00104	+0.16	+0.15	-0.05	-0.12
S-7	1	-0.211	0	+0.00107	-0.0010	-0.14	-0.09	+0.14	0.208
S-8	1	-0.041	+0.00127	0	-0.0067	-0.16 to 0.14	0.05	0.16 to 0.15	0.07 to 0.05
S-9	1	+0.070	-0.0010	+0.000167	+0.0020	-0.07	0.15	0.16	0.025
P-7a	8	-0.112	-0.0023	+0.00267	-0.0028	-0.14 to -0.17	0.06 to 0.10	0.03 to 0	-0.05 to +0.05
P-7b	8	+0.080	+0.00252	0	-0.00305	-0.14 to 0.12	0.15	0.04 to 0	0.10 to 0.15
S-10.2	1	-0.16	+0.00087	+0.0023	-0.00113	-0.12	-0.10	0.065	-0.075
P-8a	8	-0.15	+0.0030	0	-0.0010	-0.17 to -0.12	0.10	0.12 to 0.14	-0.15 to +0.15
P-8b	8	-0.13	+0.0010	-0.0020	+0.0019	-0.14 to -0.11	0.06 to 0.02	0.06 to 0.08	-0.20 to -0.10
P-8c	8	-0.070	+0.00113	-0.00233	-0.00117	-0.14 to -0.10	0.16 to 0.11	0.16 to 0.14	-0.07 to -0.10
S-11	1	+0.060	-0.0010	+0.00368	+0.00433	-0.17 to -0.15	-0.14 to -0.10	0.14 to 0.16	-0.17 to -0.3
P-9	8	+0.20	-0.0022	+0.0010	-0.0009	-0.06 to -0.01	0.14 to 0.15	0.12 to 0.09	-0.07 to +0.20
P-10a	8	-0.071	+0.0006	+0.00213	-0.00033	-0.13 to 0.12	0 to 0.05	0.10 to 0.09	0 to -0.20
P-10b	8	+0.023	0	0	-0.00087	-0.14	+0.15	0.04 to 0.02	-0.25 to -0.05
S-12	1	-0.057	+0.0020	-0.0010	+0.00043	-0.05	+0.05	-0.17	0.208
P-11a	8	+0.020	+0.00078	-0.0019	-0.00193	-0.16	-0.06 to -0.12	0.14 to 0.10	-0.20 to -0.05
P-11b	8	-0.010	-0.00118	-0.0019	-0.0008	-0.16 to -0.14	0.11 to 0.08	0.13 to 0.12	-0.05 to 0
P-12a	8	-0.140	+0.0016	+0.00173	+0.00487	-0.14 to -0.11	0.14 to 0.16	-0.04 to +0.06	-0.15 to -0.10
P-12b	8	-0.057	+0.00133	+0.0030	-0.0017	-0.14 to -0.12	-0.02 to +0.08	0.10 to 0.08	-0.10 to 0.10
S-13	1	-0.357	-0.00113	+0.00195	-0.0020	-0.17	-0.10	0.14	-0.40
S-14	1	-0.33	0	+0.0010	-0.00152	+0.06	---	---	0.208
P-13a	8	-0.079	+0.00073	+0.0023	-0.00117	-0.11 to -0.09	0.07 to 0.12	0.07 to 0.05	0.05 to 0.20
P-13b	8	+0.136	-0.00077	+0.00317	-0.0013	-0.15 to -0.16	0.09 to 0.15	0.10 to 0.08	-0.07 to 0
S-15	1	-0.109	0	+0.0009	+0.0037	-0.14	-0.08	-0.16	0.208
S-16	1	-0.078	-0.0008	+0.00207	-0.0017	-0.14	-0.05	+0.04	-0.35
S-17	1	-0.03	0	+0.00217	+0.0024	+0.18	+0.04	-0.17	0.208

NOTE: No attitude data are available for photo Sites S-3, S-4, and S-5 due to the photography sequence occurring during telemetry data occultation interval (earthset).

COMPONENT PERFORMANCE

Canopus Star Tracker

The Canopus tracker was first turned on at 311:06:09:44, approximately 6 hours into cislunar flight. The tracker acquired and tracked Canopus, indicating the spacecraft was oriented toward Canopus at that time. This was verified by making a 360-degree star map and a high-gain-antenna received signal strength map. The roll error from Canopus was then used in a closed-loop mode until the midcourse maneuver.

The first star map matched the a priori map fairly well except for the appearance of a broad (approximately 50-degree) object that had a peak map signal strength of about 4 volts. At this time, the Earth had a clock angle of 130 degrees and a cone angle of 140 degrees. It was surmised that the Earth, which was 30 degrees out of the field of view in cone angle, was being reflected off the low-gain antenna boom and into the tracker. The apparent lag in cone angle of the peak signal strength is consistent with the location of the low-gain antenna.

The propellant squib valves were fired just prior to midcourse at 312:12:11:14. Immediately thereafter, Canopus track was lost and the attitude control system went into inertial hold in roll. This resulted in a delay of the midcourse maneuver while a second star map was made. It has subsequently shown that loss of Canopus was not caused by electromagnetic interference and may have been caused by dust shaken from the spacecraft.

The second star map matched the a priori map fairly well but glint from the Earth was again evident. In this case, however, the maximum signal due to Earth glint was down to 1.1 volts due to the greater Earth range. After the second map, the Canopus tracker continued to track Canopus but it was not used in a closed-loop mode to control the system. Instead, open-loop roll update commands were transmitted to the vehicle as required to maintain Canopus in the field of view and to zero the roll error in preparation for midcourse, deboost, and transfer maneuvers.

The deboost maneuver occurred during sunset. Immediately after sunrise, Canopus was lost due to reflections of moonlight from the low-gain antenna. A subsequent experiment established that Canopus could not be tracked reliably through the lighted portion of the lunar orbit and that continued exposure to moonlight would degrade the Canopus tracker map signal voltage. As a result, it was determined that the tracker should only be operated during sunset.

After transfer during photography and readout, the method of roll control adopted was:

- 1) Turn tracker on after sunset;
- 2) Acquire Canopus in closed-loop mode to update roll attitude;
- 3) Turn tracker off before sunrise.

The method worked well with reasonable nitrogen consumption rates and minimum operational problems.

As of Saturday, December 3, 1966, the tracker had completed 165 on-off cycles and 139 hours of "on" time.

Sun Sensors

The Sun sensors performed as expected for Mission II, providing a celestial reference for a variety of non-nominal situations.

Initial Sun acquisition took place automatically within the required 60 minutes from launch. As soon as telemetry data was available during initial Sun acquisition (60 minutes after launch), it was observed that the Sun had already been acquired in pitch and yaw. Exact time of acquisition could not be determined. Reacquisition of the Sun after Sun occultation or attitude maneuvers was performed approximately 120 times; 99 of these acquisitions were done in the narrow deadband and 21 were done in the wide deadband. Every acquisition went as expected.

The Sun sensor readings while occulted from the Sun are presented below:

Sun Sensor Output During Sun Occultation

Mode	Pitch	Yaw
Fine	Observed T. M. +0.051 deg	+0.061 deg
	Ground Test +0.002 to +0.100 deg	-0.034 to +0.061 deg
Coarse	Observed T. M. +0.24 deg	+0.41 to 0.69 deg
	Ground Test -0.053 to +0.537 deg	+0.126 to +0.690 deg

*NOTE: Resolution of telemetry for coarse eye is 0.3 degree.

These values are close to those observed during ground testing, and are useful in ascertaining null shift in sensor position readings when viewing the Sun.

The capability for switching between fine, coarse and fine, and coarse only Sun sensors proved invaluable for "off-Sun" operation. There were only six pitch off-Sun maneuvers; however, 56% of the time was spent off-Sun. The ability to stay off-Sun using the coarse Sun sensors greatly reduced nitrogen consumption. Yaw Sun sensor degradation due to the large pitch attitude was higher than expected. At a pitch angle of 30 degrees, yaw was observed to be degraded approximately 0.77 for Mission II as compared to 0.75 for Mission I. The predicted degradation for this case is $\cos 30$ degrees, or 0.866. Moonlight on the coarse Sun sensors caused shifts in error output for various portions of the orbit. There was no effect on the mission.

Closed-Loop Electronics

The closed-loop electronics (CLE) performed flawlessly throughout the mission. The (CLE) successfully selected, on command from the programmer, the inertial reference unit, Sun sensors, and Canopus star tracker, closing the loop between sensor outputs and reaction control thrusters. The crab angle sensor modes were not used in conjunction with the attitude control system.

The minus-pitch Sun sensor limiter had a very "hard" limit at 26 degrees, while the plus-pitch Sun sensor limiter had a very "soft" limit that allowed readings to be taken at angles as large as 29 degrees. This difference did not affect operation of the attitude control system.

The minimum-impulse circuit or "one shot" appeared to be operating between 11 and 14 milliseconds throughout the mission. A value of 11 milliseconds is nominal. Single-pulse operation occurred approximately 70, 50, and 20% of the time for the roll, pitch, and yaw axes, respectively.

Reaction Control Subsystem

The reaction control subsystem thrusters performed satisfactorily during the mission.

The number of thruster operations for the photographic mission was estimated by reviewing vehicle telemetry data for the mission, and are tabulated below.

<u>Thruster Operations</u>				
<u>Mode</u>	<u>Roll</u>	<u>Pitch</u>	<u>Yaw</u>	<u>Total</u>
Limit Cycle	3,840	4,800	5,280	13,920
Maneuvers	<u>514</u>	<u>420</u>	<u>406</u>	<u>1,340</u>
Total	4,354	5,220	5,686	15,260

The individual thruster performance was evaluated for as many of the spacecraft maneuvers as possible. Actual, predict, and specification values for each axis are tabulated below.

<u>Thruster Performance</u>			
<u>Axis</u>	<u>Actual Thrust (Lb)</u>	<u>Predicted (Lb)</u>	<u>Spec. Values (Lb)</u>
Roll	0.069 \pm 0.001	0.066 \pm 0.002	0.051 to 0.070
Yaw	0.064 \pm 0.002	0.058 \pm 0.003	0.045 to 0.062
Pitch	No Data	0.057 \pm 0.003	0.045 to 0.062

The observed thrust appeared to be higher than the predicted values for roll and yaw. there were no pitch maneuvers that allowed a pitch thrust determination. The pitch thrust was probably 0.064 pound also. Roll thrust was within tolerance of specification value and the yaw thrust was on the high side of the tolerance. These slightly high thrust values in no way degraded the mission. Also, maneuver accuracy was not degraded in any way and nitrogen consumption was not increased perceptibly.

Slight cross-coupling was observed during maneuvers and limit cycle; however, in view of the data observed it is impossible to estimate the magnitude of the cross coupling or even to determine if it is caused by thruster misalignment or gyro cross-coupling.

Thruster Vector Control

Control of spacecraft attitude during the three engine burns was performed perfectly by the thrust vector control subsystem. Residual rates after each burn were lower than predicted maximums for stable limit cycle operations. The maximum residual rates for all the burns were less than 0.07 degree per second.

During propellant bleed, the actuators moved away from center rather than recentering because the pitch and yaw axes were in inertial hold rather than the rate mode. At first midcourse the spacecraft recovered from these offsets without difficulty. At the propellant bleed event, the forward loop gain of the TVC subsystem was proved to be nominal.

Travel of the center of gravity from nominal was minimal during Mission 11. Maximum excursion of the actuators for all the burns were: pitch +0.1 to -0.2 degree and yaw +0.3 to +0.08 degree.

IRU Performance Summary

The inertial reference unit performed satisfactorily throughout the mission, accumulating approximately 746 hours of "on" time from launch to the end of photo readout. The

gyro rate integrate mode drift rates were within the design tolerance (± 0.5 degree per hour) throughout the regular mission in all three axes. The range of the pitch drift rate was positive 0.2 degree per hour to zero. The roll and yaw axes drifts were measured at approximately 0.2 degree per hour and $+0.3$ respectively to peak values of 0.45 degree per hour. Mission drift rates were all positive while ground test drift rates were all negative.

Spacecraft maneuver error was less than 0.11" for all three axes. This indicates that the rate mode error for all the gyros was within the design specification of 0.1".

No long-term changes were observed in any of the gyro wheel currents. The wheel currents remained within the range of $\pm 5\%$ of their respective nominal values throughout the mission with one exception. The roll gyro wheel current randomly jumped from 3 to 9% above the nominal value and then decreased exponentially to the original value. This transient condition is attributed to positional changes of the rotating element due to minute oil film thickness changes. No degradation of gyro life is expected since this phenomena has been shown not to have a detrimental effect on gyro life in tests on similar units by the vendor. All long- or short-term gyro temperature effects were within the limits of test experience.

No direct method of evaluating accelerometer performance is available. The tracking data uncertainty in velocity determination is on the order of ± 0.1 meter per second. Data analysis did not indicate accelerometer error greater than this value.

Nitrogen Consumption

Nitrogen consumption for the attitude control system for Mission II is presented in Figure 3.2-33. Mission I usage and a prediction for Mission II, based on actual Mission I events, are also presented for comparison.

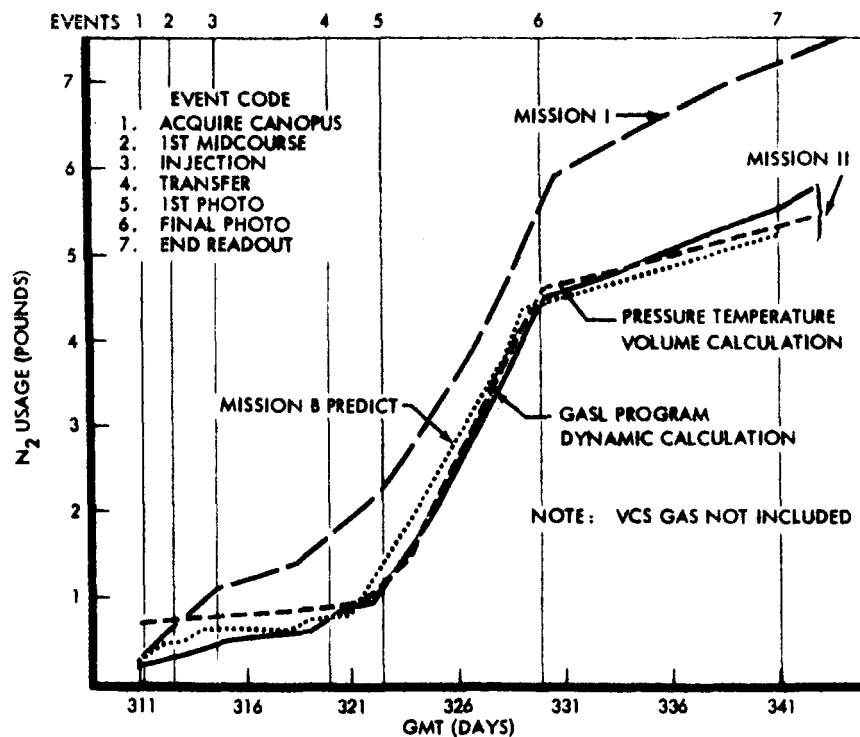


Figure 3.2-33: Attitude Control Subsystem Nitrogen Usage

It will be noted that nitrogen usage for Mission II is substantially less than that of Mission I, even though Mission II had 34 three-axis photo maneuvers as compared to 12 for Mission I. The reasons for Mission II low nitrogen usage as compared to Mission I are:

- 1.) There was much less trouble with the star tracker in locating Canopus.
- 2.) The operational methods used to fly off the Sun were revised to eliminate a large number of pitch maneuvers.
- 3.) A substantial number of maneuvers and celestial reacquisitions were performed in the wide deadband.
- 4.) No leakage problems occurred in the VCS system as in Mission I.
- 5.) Lower gyro drift rates minimized the number of update maneuvers.

At Day 342, the amount of "unaccounted-for" nitrogen since launch was approximately 0.2 pound. This is 0.006 pound per day of unaccounted-for nitrogen, which indicates a very small leakage.

As in Mission I, occasional multiple pulsing of the thrusters was observed during limit cycle. This again did not cause additional nitrogen consumption, however, due to the presence of disturbance torques.

A slight disturbance, which occurred in one to three axes whenever the star tracker was turned on during Mission II, caused the additional use of a small amount of nitrogen. However, it is estimated that this occurrence consumed only about 0.004 pound per day. The total nitrogen used for Mission II through GMT 342:08 follows:

Attitude control system	5.50 pound
Velocity control system	<u>3.14 pound</u>
	8.64 pound
Initial N ₂ at launch	15.15 pound
Nitrogen available for extended mission	6.51 pound

The maneuvers performed on Mission II from launch through GMT 342:00:00 are given below.

<u>Purpose of Maneuver</u>	<u>Maneuvers</u>			<u>Totals</u>	<u>Planned Totals</u>
	<u>Roll</u>	<u>Pitch</u>	<u>Yaw</u>		
Star map	3	0	0	3	3
Attitude update	14	3	13	30	25
Thermal pitch-off maneuver	0	9	0	9	6
Velocity change	6	6	0	12	12
Photo maneuver	80	66	70	216	216
Other	<u>8</u>	<u>6</u>	<u>0</u>	<u>14</u>	<u>4</u>
Total	111	90	83	284	266

Number of Total Done In:

Narrow deadband	98	82	78	258
Wide deadband	13	8	5	26

Celestial Reacquisitions

	<u>Narrow Deadband</u>	<u>Wide Deadband</u>	<u>Total</u>
Canopus acquisition	139	7	146
Sun acquisition	99	21	120

FLIGHT PROGRAMMER AND SWITCHING ASSEMBLY PERFORMANCE

The programmer clock error was - 1.21 seconds at the end of Mission II. From clock start (launch minus 3 minutes) until November 25, the error rate was - 1.85 milliseconds per hour. From November 25 to December 7 (end mission) the drift rate changed slowly from - 1.85 milliseconds to - 0.77 millisecond per hour, for a mission average of -1.60 milliseconds per hour. This drift rate is 47% of the rate allowed by the design specification.

The following commands were not exercised during Mission II

- 1.) Terminate (TER);
- 2.) Slow four-picture sequence (AE, AF, AH);
- 3.) Slow eight-picture sequence (AE, AF, AH);
- 4.) Slow sixteen-picture sequence (AE, AF, AH);
- 5.) Switch yaw control ON (VHO);
- 6.) Switch yaw control OFF (VHO*);
- 7.) RF OFF (CF);
- 8.) Radiation dosage measurement OFF (CL);
- 9.) Power mode select OFF (PMS*);
- 10.) Accelerometer OFF (ACO*).

Interlocking command functions are those performed by the programmer in response to other spacecraft subsystem (excepting the command decoder) stimuli. For example, in response to a Sun occultation signal from the power subsystem, the spacecraft clock value at occultation is stored in the programmer memory. Several interlocked command functions were not exercised:

- 1.) Acquire canopus plus;
- 2.) Acquire Sun yaw;
- 3.) Acquire Sun pitch;
- 4.) Clock switchover.

Items (2) and (3) were commanded during initial Sun acquisition; however, the spacecraft did not maneuver since the Sun had already been acquired.

PROGRAMMER AND SWITCHING ASSEMBLY ENVIRONMENT

Temperature Range

The flight programmer was subjected to a maximum temperature of 112°F and a minimum temperature of +51°F during Mission II. All flight programmers have been functionally tested (functional analysis test) over the environmental temperature range of + 85 to + 40°F. One flight programmer has been tested over the temperature environment of + 100 through + 32°F (qualification test). It should be noted that the flight programmer of Mission II operated at a temperature about the maximum qualification value. In addition, the Mission II maximum temperature was higher than that of Mission I by 5°F.

The switching assembly was subjected to +68°F maximum and +43°F minimum temperatures during Mission II. The temperature environments of the tests conducted on the switching assemblies were identical to those of the flight programmer.

Supply Voltage Range

The maximum bus voltage in the spacecraft was 30.56 volts and the minimum voltage was 23.6 volts (extrapolated). The flight programmer and switching assembly were tested and proven over the voltage range of +21 to +31 volts.

SWITCHING ASSEMBLY OPERATION

All commands interfaced by the switching assembly were performed correctly. During Mission II all switching assembly commands were exercised.

FLIGHT PROGRAMMER BREADBOARD

As in Mission I, the programmer breadboard "followed" the mission in real time from launch countdown through the end of photo readout. As each command sequence was sent to the appropriate DSS, a papertape was being punched in the MSA #2 area. When the command sequence was transmitted to the spacecraft, the tape was inserted into the programmer breadboard. During Earth occultation, operation of the flight programmer was followed at the SFOF by observing breadboard performance.

Countdown commands and Mode 2 commands sent to the DSN before the mission were punched on paper tape as they were being sent and were then checked on the programmer breadboard.

"Map loading," "ranging on," and "ranging off" real-time commands were followed with a SPA005 real-time command as in Mission I. This prevented zeroes from being stored in any memory location other than location 005 when a subsequent "ranging on" or "off" RTC might increment the stored program address (memory location 004). "RF on" and "rf off" RTC's could have caused the same anomaly, but were not used after launch.

Mission II was flown with an infinite jump in memory location 006 when repetitive Sun occultation time storages were not anticipated.

FLIGHT OPERATION EVALUATION

Hardware

The functional capabilities of the flight programmer provided the control required to fly

the spacecraft during Mission II. However, the following changes--suggested by the programmer analyst group after Mission I--would complement the existing design capability.

- 1) Design the compare time (COT) instruction so that it would increment its time value address after a comparison had occurred instead of at the initiation of the COT command. This would allow real-time exit from a COT, performance of a subprogram, and re-entry to the COT command without restorage of the COT time value address.
- 2) Design a stored program maneuver command whose maneuver-type-and-value address did not increment after each execution. This would allow an unlimited number of stored program maneuvers to be performed from one command storage.
- 3) Design a command to allow a jump loop to be performed a programmed number of times. At present, the termination of such a loop must be executed by a real-time command transmission.

Software

The spacecraft time/Greenwich mean time correlation (TIML) program was run throughout Mission II. Output of the TIML program indicated a negative clock drift. The following changes, incorporated as a result of Mission I experience, increased the usefulness of the TIML program.

- 1) For Mission I, the sum of the equipment and transmission time delays was rounded off to the nearest tenth of a second. As the spacecraft orbited the Moon, the variable transmission delay introduced excessive errors in the subsequent spacecraft clock predict outputs of the TIML program. The TIML program now carries out the total delay value to the nearest hundredth second. This substantially decreased the errors in the clock predicts.
- 2) The calculations required to convert spacecraft clock time recorded on the film to GMT values were performed manually during Mission I. An additional capability was added to the TIML program to calculate the GMT value corresponding to a recorded time.

Problem Areas

During Mission II, there were several problems with equipment in or related to the attitude control system, or in other subsystems, which resulted in non-nominal operation of the attitude control system. Summarized below are the problems and their effects on the mission.

Thermal Problem

Again on Mission II, spacecraft overheating was encountered resulting in operating the spacecraft in a "pitch off-Sun" attitude for approximately 56% of the mission. There were 25 pitch off maneuvers and updates of the inertial reference required as compared to 151 maneuvers during Mission I. The large reduction of required maneuvers resulted from the use of improved procedures developed during Mission I. Nitrogen consumption was further reduced for these thermal maneuvers by performing a large number of them in wide deadband.

Canopus Star Tracker Glint Problems

During the mission, Canopus track was lost four times, caused by "glint" into the star tracker. The first loss of track resulted in aborting the first attempted midcourse maneuver. After this loss, the spacecraft was kept in inertial hold in roll while in the Sun to prevent the loss of Canopus. The tracker was used only to update the roll inertial reference. Recovery of tracker lock on Canopus could be obtained by switching the tracker off, then back on, provided that Canopus was still in the field of view of the tracker. As a result of this problem, the spacecraft did not acquire Canopus in the closed-loop mode, except in the shadow of the Moon.

Canopus Tracker Intensity Degradation

With the spacecraft in lunar orbit, the Canopus tracker could not be operated in the Sun without degradation of the star map voltage. A test was performed in which the tracker was operated for longer and longer periods in the Sun. As a result, the star map voltage was degraded from 3.0 volts to 2.4 volts by the reflected light from the illuminated limb of the Moon. To prevent further degradation, the tracker was operated only in the dark, which required turning the tracker on, then off each orbit. From the results of this test, it is evident that the tracker could not track Canopus near the illuminated limb of the Moon without degradation to the star map voltage.

Tracker Turn-On Disturbance

During Mission II, it was noticed that a transient spacecraft rotation occurred, usually in all three axes, whenever the Canopus tracker was turned on. The magnitudes were random, varying between 0 and 0.04 degree per second. Since the transient was measured by all gyros, it was assumed that reaction control jets were actually firing as a result of the programmer signal to turn on the tracker. This transient occurred throughout the mission; it was estimated that this random jet firing used 0.125 pound of nitrogen during the mission.

Spacecraft Oscillations

On several occasions throughout Mission II the spacecraft limit cycle rates increased five to ten times the normal limit cycle rates for several cycles. After several cycles, the oscillation damped to normal levels. The oscillations occurred mostly in the yaw axis; however, there were instances in which all three axes were simultaneously in this mode. Rate changes as high as 0.011 degree per second at a switching line have been noted. These higher limit cycle rates could be caused by sticky jets, or random noise in the closed-loop electronics.

3.2.3.5 Velocity Control Subsystem

Operation and performance of the Velocity Control Subsystem (VCS) was excellent throughout the mission. Three propulsive maneuvers were conducted in support of the primary mission, and one maneuver was conducted for experimental purposes in the extended phase of Mission II. These were: 21.1-mps midcourse maneuver, 829.7-mps injection maneuver, 28.1-mps transfer maneuver, and a 100-mps inclination change maneuver.

Prelaunch propellant and nitrogen servicing operations were accomplished without difficulty. There were 276.99 pounds of propellant loaded, as were 15.15 pounds of nitrogen. The spacecraft launch weight was 855.22 pounds. Based on these weight data, the nominal velocity increment capability of the VCS was determined to be 1017 meters per second with a 3-sigma tolerance of ± 43 mps.

Flight data performance analyses (see Table 3.2-14) indicate that the rocket engine delivered an average thrust of 101 pounds during the midcourse and orbit injection maneuvers.

Table 3.2-14: Velocity Control Subsystem Maneuver Performance - Mission II

	Velocity Change (mps)	Burn Time (sec)	Thrust (lb)	Specific Impulse (lb-sec/lb)
Midcourse				
Predict	21.1	18.4±0.6	100	276
Actual	21.1	18.1	100.5±0.5	276.5±0.5
Injection				
Predict	829.7	617.7±10	100	276
Actual	829.7	611.6	101	276
Transfer				
Predict	28.09	17.5±0.9	101.5	276
Actual	28.1	17.4	102.25	276
Inclination Change				
Predict	100.0	62±2.5	98.7	276
Actual	100.0	61.3	100.1	276

Delivered thrust was 102.25 pounds during the orbit transfer maneuver; this higher value was caused by large ullage volumes and the time required for tank pressures to decay from the regulator lockup value. Average delivered thrust was determined to be 100.1 pounds during the inclination change maneuver, which was conducted subsequent to completion of photo readout; this value is slightly lower than orbit transfer because the nitrogen supply shutoff squib had been actuated and the maneuver was conducted in a "blow-down" mode; tank pressures were not maintained by the introduction of nitrogen from the supply tank and pressures decayed approximately 16 psi. The engine specific impulse was determined to be approximately 276 seconds during all four maneuvers. A total velocity change of 978.9 mps had been imparted to the spacecraft with a total engine operating time of 708.4 seconds.

System temperatures were generally in the region of 40 to 80°F throughout the flight--a satisfactory operating regime. Propellant tank heaters were activated on 25 occasions to ensure that the propellant temperature remained above 40°F. Total heater-on time was 1545 minutes.

Nitrogen and propellant isolation squib valves were actuated without incident as far as the VCS was concerned; however, the Canopus reference was lost within one frame following propellant squib actuation. Prior to actuating the propellant squib valves, the propellant line bleed event was accomplished.

Gimbal actuators performed according to expectations. During maneuvers, the pitch actuator varied between +0.1 and -0.2 degree, while the yaw actuator was generally +0.1 to +0.3 degree. No actuator movement was observed as a result of launch-induced environmental conditions. Rather than remaining in the null position, the actuators deflected during the bleed event because the inertial reference unit was in "inertial hold," whereas it should have been in the "rate" mode. The amount of deflection was not sufficient to cause concern.

Table 3.2-15 Propellant and Nitrogen Servicing Summary - VCS

	Fuel	Oxidizer	Nitrogen
On-board, lb	94.586	182.41	15.15
Ullage volume, cu in.	64.97	119.2	--
Pressure, psig	45	50	3675
Temperature, °F	61	60	73

After completion of VCS servicing as shown in Table 3.2-15, the complete flight-configuration spacecraft was weighted and balanced; launch weight was determined to be 855.22 pounds. Calculations were performed to ascertain the velocity increment capability of the spacecraft based on the aforementioned weights and the rocket engine performance as determined from ground tests. The "Delta V" capability was found to be 1017 ± 43 meters per second (the tolerance is 3 sigma).

OPERATIONAL READINESS TEST

An operational readiness test (ORT-1) was conducted on November 3, (Day 307), prior to scheduled launch, for verification of spacecraft readiness, countdown completeness, and SPAC/ETR integration. At power turn-on (16:07 GMT), all VCS pressures and temperatures were normal. During the VCS test, which was initiated at 19:16:44 GMT, the pitch and yaw actuators were deflected to -0.864 and +0.267 degree, respectively, and then re-centered. Maximum engine valve temperature was 73.1°F. All events proceeded normally through the simulated liftoff, at which time the test was terminated.

LAUNCH AND GENERAL MISSION EVENTS

The launch countdown was initiated on November 6, (Day 310) with power turn-on occurring at 15:36 GMT; all VCS parameters were normal. The VCS countdown test was successfully conducted at 18:02 GMT, resulting in actuator motions essentially identical to that observed during the ORT-1, and a maximum engine valve temperature of 74°F. Vehicle liftoff occurred at 23:21:00.195 GMT. Real-time telemetry loss occurred as expected until acquisition of the spacecraft by DSS-41; the spacecraft separated from the Agena at 23:46 GMT.

Upon acquisition by DSS-41 at 00:16 GMT (Day 311), it was verified that the propellant tanks had been pressurized to a nominal value of 192 psia. The gradually increasing thermal environment slowly increased the pressure levels to 193 and 197 psia, fuel and oxidizer, respectively.

The next significant VCS event concerned bleeding the propellant lines between the engine and the then-closed propellant squib valves. The bleed event occurred at 10:33 GMT on November 7; the engine valves were open for 30 seconds, thereby increasing valve temperature by 11.4°F as expected. It was noted that the pitch and yaw gimbal actuators had deflected to +0.364 and +0.267 degree respectively rather than remaining in a neutral position. It was then discovered that the attitude control subsystem (ACS) was in the inertial hold mode for pitch and yaw axes, whereas it should have been in the rate mode for those axes. The sequence was not repeated because the deflections were small and would not produce any deleterious effects. Procedures will be amplified on subsequent missions to ensure that the proper ACS mode is in effect at the time of conducting the bleed event. It is possible that the actuators could be deflected to their limits of motion, draw excessive current, and be damaged if the ACS is not in the rate mode.

Preparation for a 17.9-mps midcourse maneuver commenced at 12:11 GMT on November 8, (Day 312) with actuation of the propellant isolation squib valves. Positive confirmation of valve actuation was received when propellant tank pressures decayed 2 psi

(ullage volume increase as propellant filled the downstream lines); it was also observed that the presence of fuel caused a decay in valve temperature of 0.9°F. At approximately 12:13 GMT, however, loss of the Canopus attitude reference was observed. As Canopus was not rapidly reacquired, the midcourse maneuver was aborted and rescheduled for a later time.

The midcourse maneuver for trajectory adjustment was then reprogrammed for an engine ignition at 19:30:00 GMT and a velocity change magnitude of 21.1 mps. The maneuver was conducted without incident and the required velocity was achieved with an engine operating time of 18.1 seconds.

The orbit injection maneuver was programmed for engine ignition to occur at 20:26:37.3 GMT on November 10, (Day 314); the desired velocity change was 829.7 mps. The maneuver was completely successful, the desired orbital elements being achieved within the capabilities of tracking data resolution. Engine operating time was determined to be 611.6 seconds; engine valve temperature was 70 to 71°F during engine operation, and reached a maximum value of 108.8°F approximately 1.5 hours following the maneuver.

The maneuver to transfer from the initial orbit to the photographic orbit was performed with engine ignition occurring at 22:58:25.4 GMT on November 15, (Day 319). The desired velocity change of 28.1 mps was achieved with an engine operating time of 17.4 seconds. Tracking data indicated that the desired perilune altitude was achieved with an error on the order of 0.3 km. This maneuver completed the propulsive maneuvers required to fulfill the primary requirements of Mission II.

After completion of photographic readout, an orbital inclination change maneuver was proposed to elevate the orbital inclination to a region that encompasses higher order gravitational model coefficients. The maneuver would thus provide tracking and engineering data in direct support of Mission C, which was being planned to be flown at an inclination of approximately 21 degrees. With suitable allowances for future maneuvers, the maneuver was planned to impart a velocity change of 100 mps in a manner such as to increase the inclination to a value of 17.5 degrees. Engine ignition occurred at 20:36:28.7 GMT on December 8, (Day 342); the desired velocity and inclination change were obtained with an engine operating time of 61.3 seconds. At 13:44 GMT, prior to this maneuver, the nitrogen shutoff squib valve was actuated closed; hence, the maneuver was conducted in a blowdown mode.

SUBSYSTEM TIME-HISTORY DATA

Before presenting VCS data time histories during the mission, it is pertinent to briefly mention the data resolution characteristics. The spacecraft telemetry system converts transducer analog signals to an equivalent number of "data counts"; thus, the telemetry resolution is dependent upon how finely the transducer calibration can be subdivided. This is indicated in Table 3.2-16.

Table 3.2-16: Velocity Control Subsystem Telemetry Resolution

Nitrogen Supply Pressure, AP01	16 psi/count
Fuel Tank Pressure, AP02	1 psi/count
Oxidizer Tank Pressure, AP03	1 psi/count
Nitrogen Tank Temperature, AT01	0.6°F/count
Engine Valve Temperature, AT03	0.9°F/count
Pitch Actuator Position, AD01	0.02 deg/count
Yaw Actuator Position, AD02	0.02 deg/count

The above will explain some of the apparently "random" fluctuations in the following data presentations.

Figure 3.2-34 presents the quantity of nitrogen gas remaining in the storage vessel at discrete times throughout the primary phase of the mission. The gas weight data are calculated on the basis of the storage tank's known volume, pressure, temperature, and compressibility factor. The data points are plotted at 6-hour increments and actually represent a 6-hour average centered about the plotted time. For reference, a nominal mission budget and a significant mission event code is included in the plot. The actual consumption rates are worthy of special mention: note, for instance, the extremely small usage during the period between orbit injection and transfer. This results from two factors: (1) operation of the ACS in wide deadzone, and (2) small gyro drift rates, thereby requiring only 13 maneuvers for attitude update and thermal control. Consumption during site photography is observed to be greater than budgeted. This follows from the fact that the nominal mission budget is predicated on photographing 11 sites, whereas, during Mission II there were 29 sites photographed. Nitrogen consumption during this period is calculated to be 0.44 pound per day. Low consumption is again apparent during final readout; i.e., 0.06 to 0.07 pound per day. Even though the ACS was in the narrow dead-zone mode, gyro drift rates were low and only 12 maneuvers were required for attitude update.

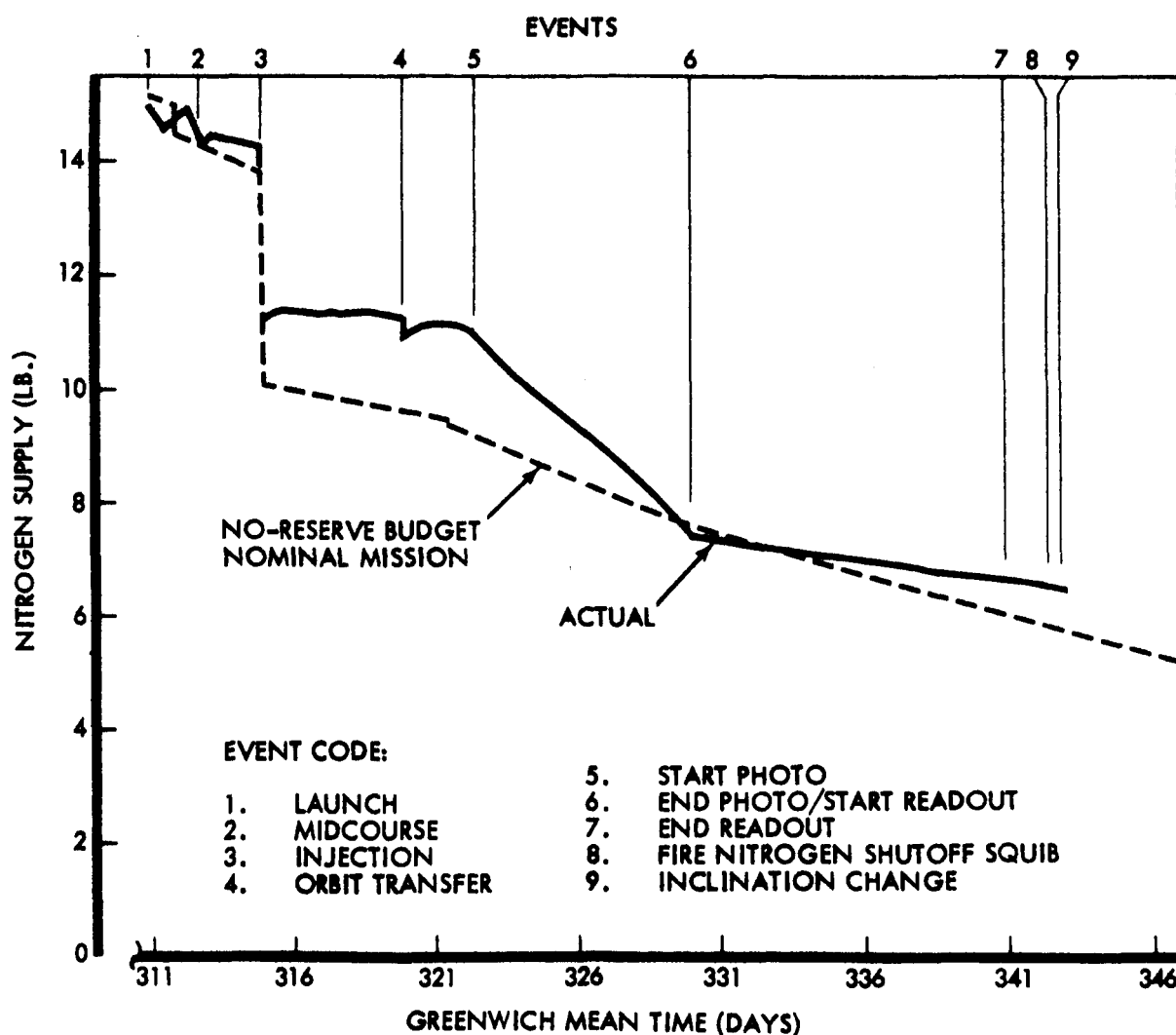


Figure 3.2-34: Velocity Control Subsystem Available Nitrogen History

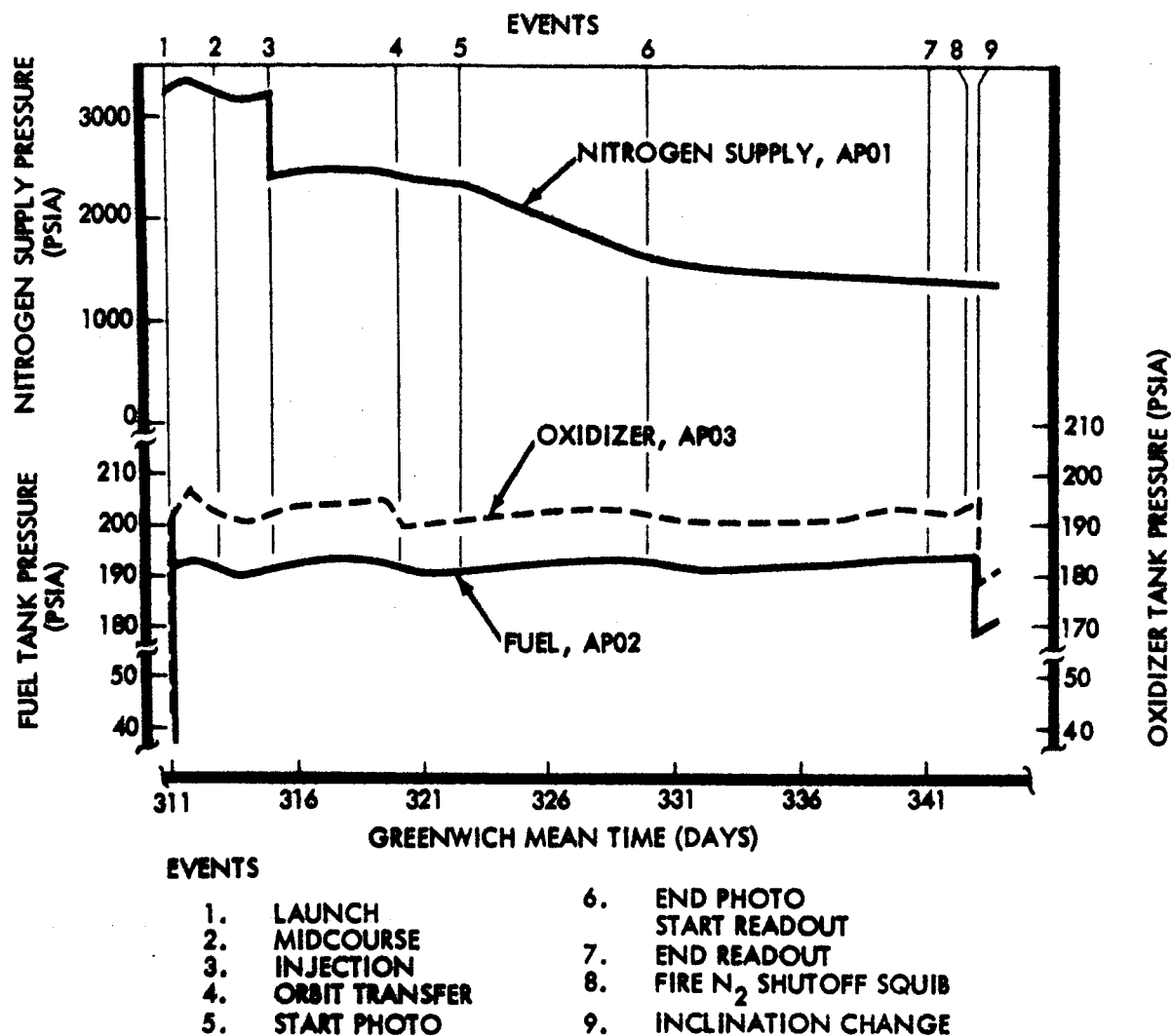
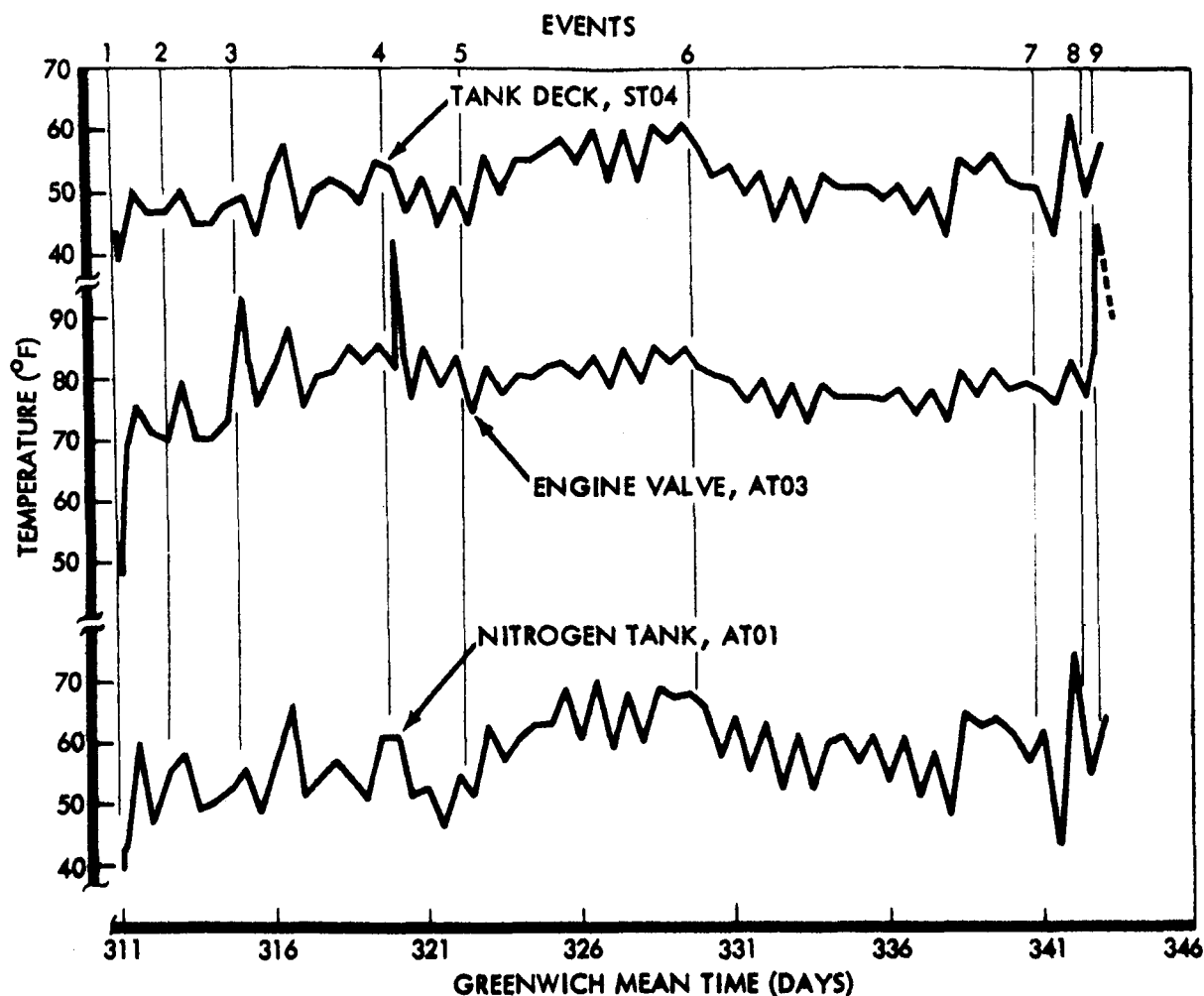


Figure 3.2-35: Velocity Control Subsystem Pressure-Time Histories

Figure 3.2-35 shows the variations in subsystem pressures during the flight. The fluctuations in propellant tank pressures are essentially the result of whether the spacecraft was locked on the Sun, or pitched off 30 to 35 degrees for thermal control. As an example, Sun lock was maintained throughout site photography (Day 322 to Day 330) and pressures gradually increased as did local temperatures (Figure 3.2-36). The spacecraft was then pitched off during readout, and the pressure decay is due solely to the decreasing thermal effects. The marked decay at Day 343 is the result of conducting the inclination change maneuver with the propellant pressurization system isolated from the nitrogen supply. The pressure profiles throughout the mission are nominal.

Figure 3.2-36 plots subsystem temperature-time histories in a similar manner (though at only 12 hour increments). Local temperature values were generally in the region of 40 to 80°F during the flight, varying somewhat when the spacecraft was pitched on and off the Sunline. Propellant tank heaters were used during the initial orbital phase of the mission to keep propellant tank deck temperature (ST04) above a value of 40°F. The heaters were activated on 25 occasions for a total on time of 1545 minutes, an average value of 62 minutes per cycle. All temperatures remained well within acceptable limits.



EVENTS:

1. LAUNCH
2. MIDCOURSE
3. INJECTION
4. ORBIT TRANSFER
5. START PHOTO

6. END PHOTO
START READOUT
7. END READOUT
8. FIRE N₂ SHUTOFF SQUIB
9. INCLINATION CHANGE

Figure 3.2-36: Velocity Control Subsystem Temperature-Time Histories

MANEUVER PERFORMANCE

During the primary photographic mission of Lunar Orbiter II, the velocity control subsystem provided three propulsive maneuvers for alteration of the spacecraft's trajectory or orbital elements. These maneuvers consisted of a midcourse, orbit injection, and orbit transfer; 878.9 mps were expended of an on-board velocity increment capability of 1017±43 mps. A fourth maneuver was conducted at the start of the extended-mission phase to alter the orbital inclination angle. This maneuver raised the total velocity expenditure to 978.9 mps. A summary of the subsystem performance for the four maneuvers is presented in Table 3.2-14. The orbit injection maneuver (which is the most representative) indicates that the system had a delivered performance of 101 pounds of thrust at a

specific impulse of 276 seconds. For comparison, the engine on Lunar Orbiter 11 demonstrated the following performance characteristics during the acceptance test.

	5-Second Test Data	70-Second Test Data
Thrust	100.5	100.2
Specific Impulse	281.3	279.3
Mixture Ratio	1.982	1.980

The engine acceptance test data are normalized to a standard propellant temperature of 70°F. An average value of propellant temperature (ST04) during flight, and specifically for the injection maneuver, was on the order of 51°F. Adjusting the acceptance test performance for actual temperatures indicates an anticipated flight specific impulse value of 276.3 pound-second/pound. The agreement between predicted and actual performance is well within the capability to "trim" the system and evaluate flight telemetry results.

Actual performance data are calculated results, since there is no measurement of engine chamber pressure or propellant flow rates. Knowing spacecraft weight (from "bookkeeping" operations on nitrogen and propellant expenditures) and determining engine operating time and spacecraft acceleration from telemetry data, the analytical approach is to assume values of specific impulse and calculate a thrust value that will match the acceleration profile. Iterations are performed to converge calculated and actual accelerations, thereby determining average values of thrust level and specific impulse. These values that are reflected in Table 3.2-14. It is also possible to infer an average operating mixture ratio; this is accomplished by adjusting flight conditions with the proper influence coefficients, then comparing with acceptance test data. From the orbit injection maneuver, the estimated operating mixture ratio was found to be 2.005.

A cursory analysis of DSIF tracking data during propulsive maneuvers has been conducted by trajectory determination personnel to evaluate the velocity maneuver accuracy. Spacecraft telemetry data does not verify the accuracy of a velocity maneuver--only that the flight programmer has properly counted a specific number of accelerometer pulses. Tracking data is required to ascertain the actual velocity change magnitude. The tracking data uncertainty in velocity determination is on the order of ± 0.1 mps. Preliminary data analysis did not indicate any greater errors.

Figures 3.2-37 and 3.2-38 present VCS telemetry data obtained during the orbit injection maneuver; Figure 3.2-37 shows pressure and temperature data, and Figure 3.2-38 plots dynamic data in the form of gimbal actuator positions and accelerometer output. These data and their trends are nominal and as expected.

The orbital inclination change maneuver that was performed at the start of the extended mission was conducted in somewhat of a nonstandard manner. Prior to the maneuver, the nitrogen supply shutoff squib valve was actuated, thereby sealing off the propellant pressurization system from any further nitrogen supply that would be required for the maintenance of nominal pressure levels. This was done to provide the maximum amount of nitrogen for extended-mission ACS usage. Under a blowdown mode of operation, it was predicted that propellant pressures would decay approximately 16 psi. At engine ignition, fuel and oxidizer pressures were 195.1 and 195.2 psia, respectively; at engine cutoff, these values had decayed to 176.7 and 177.0 psia. The blowdown process results in a decrease in ullage gas temperature; hence, it is to be expected that pressure levels will "rebound" slightly as the temperatures stabilize. One hour following the maneuver, fuel and oxidizer pressures were 178.8 and 179.0 psia, respectively.

Engine valve temperature during and following each maneuver was normal. A brief summation of maximum valve temperature (AT03), resulting from thermal soak-back, is presented in Table 3.2-17.

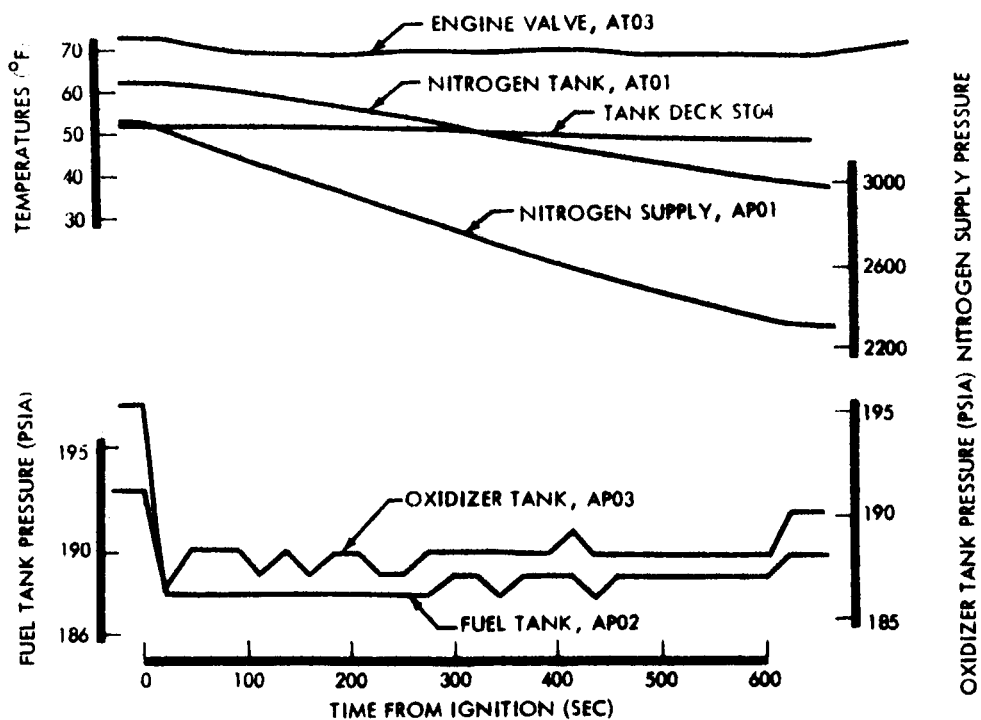


Figure 3.2-37: Velocity Control Subsystem—Orbit Injection Maneuver—System Pressures and Temperatures

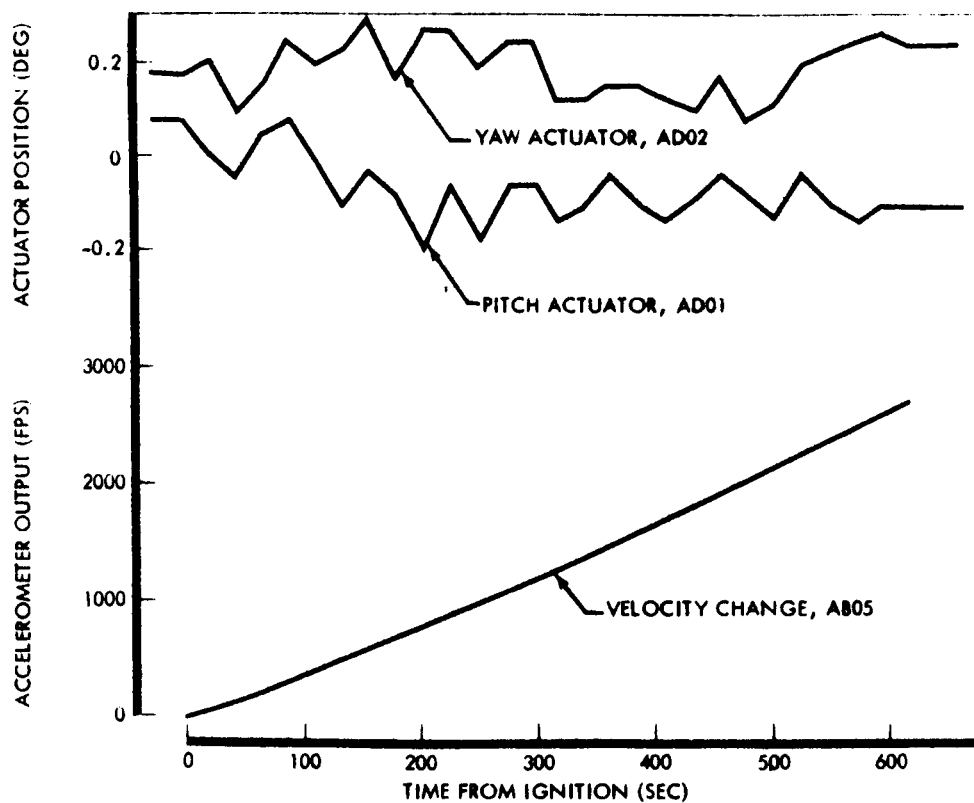


Figure 3.2-38: Velocity Control Subsystem—Orbit Injection Maneuver—System Dynamics

Table 3.2-17: Engine Valve Temperature Maximum Soak-Back	
Midcourse	95.5°F
Orbit injection	108.8°F
Orbit transfer	102.0°F
Inclination change	104.7°F

The maximum value generally occurred approximately 90 minutes after maneuver completion.

The gimbal actuator motions presented in Figure 3.2-38 are considered to be typical. The average deflection trend during the maneuver reflects the motion of the spacecraft's center of gravity. Table 3.2-18 summarizes actuator position before and after each maneuver.

Table 3.2-18: Gimbal Actuator Position				
	Pitch (degree)		Yaw (degree)	
	Pre-	Post-	Pre-	Post-
Launch	0.006	0.006	0.079	0.055
Midcourse	0.364	0.095	0.243	0.197
Injection	0.073	-0.106	0.173	0.243
Transfer	-0.084	-0.017	0.290	0.079
Inclination Change	-0.039	0.006	0.079	0.173

The slight discrepancies between the conclusion of one maneuver and the beginning of the next are reflections of the data resolution characteristics as shown in Table 3.2-16. The deflections indicated between launch and midcourse are the result of conducting the bleed event while in inertial hold as discussed previously.

COMPUTER PROGRAM PERFORMANCE

TRBL

A program change to TRBL was made after Mission I to determine the rotation angle (CD01) and corrective boresight maneuvers for the high-gain antenna where the spacecraft was being flown "off the Sun." The program change was accomplished by the optimal inclusion of one additional chain link. Previously TRBL was only used by the attitude control subsystem group; however, during Mission II it was also shared by the communications subsystem group.

The program change consisted of essentially the same logic used in the "rewritten" CORL program from Mission I. This consisted of taking the vehicle attitude, i.e., roll, pitch, and yaw, and transforming the INTL/LIFL trajectory data in accordance with the attitude that the vehicle had assumed. The antenna rotation angle and corrective maneuvers were then computed from the transformed trajectory data.

The program ran successfully during the entire mission and no changes are planned prior to Mission III.

SGNL

The SGNL program operated successfully throughout Mission II. The calculations performed by the program fell well within the limits allowed. The program output consists of

two parts: predicted signal-to-noise ratios and antenna rotation angles (CD01). Some examples of predicted versus actual signal-to-noise ratios follow:

CISLUNAR CRUISE

GMT 312:01:08

MODE 1 DSS-41

Predicted SNR	Actual SNR	Tolerance
31.8 db	32.6 db	+9.9 db - 8.1

LUNAR ORBIT

GMT 315:07:00

MODE 1 DSS-41

Predicted SNR	Actual SNR	Tolerance
26.6 db	27.0 db	+9.9 db - 8.1

LUNAR ORBIT

GMT 316:15:00

MODE 2 DSS-12

Predicted SNR	Actual SNR	Tolerance
17.2 db	17.1 db	+3.8 db - 1.9

CD01

Predict	359 degrees
Actual	358 degrees

The 1-degree difference between the predicted and actual value of CD01 could result in a variation of not more than 1 db in the signal-to-noise ratio. That is, if CD01 had been 359 degrees (the predicted value) instead of 358 degrees, the actual SNR may have been as high as 18.1 db. During the mission, it was found that 1-degree changes from the predicted antenna pointing did not result in significant signal level changes.

The predicted antenna rotation angles (CD01) resulted in DSS-received signal levels that ranged from -92 to -96 dgm. This range of signal levels was as expected with the vehicle locked to the Sun-Canopus reference.

Since SGNI is operating satisfactorily, no changes are planned for Mission III.

3.2.3.6 Structures and Mechanisms Subsystem

The spacecraft structures performed as planned by producing a stable, rigid platform for

the spacecraft equipment and for extension of the antennas and solar panels, which performed as programmed during the boost and acquisition phase of the flight.

The camera thermal door performed as intended. As indicated in Section 3.2.3.1, "Photographic Subsystem," incomplete closure of the camera door after launch was suspected, but analysis of flight data indicated proper door operation.

The ordnance devices for deployment of the antennas and solar panels and to actuate the fuel and oxidizer valves all operated as scheduled.

Canopus track was lost after firing the propellant squib valve in preparation for the mid-course maneuver. This resulted in rescheduling of the midcourse maneuver as outlined in Section 3.2.3.4, "Attitude Control Subsystem."

THERMAL CONTROL

No significant thermal anomalies occurred except the EMD thermal coating degradation similar to that experienced with Lunar Orbiter I. Degradation of the thermal coating caused no impairment of the spacecraft mission objectives because its effect was offset by pitching the spacecraft off the Sun line, thus maintaining temperatures at the desired level.

Thermal Coating Degradation

With the spacecraft EMD normal to the Sun vector, high temperatures developed. This was due to degradation of the thermal coating from ultraviolet radiation and low-energy protons.

The extent of degradation that occurred during Mission II was larger than anticipated from laboratory tests of coating samples. This experience was similar to that of Mission I. Figure 3.2-39 shows thermal coating absorptance data for Lunar Orbiter I and II compared to data from samples tested at Hughes Aircraft Corporation. The solar absorptivity was calculated using data from telemetry measurements ST01 and ST03. See Figure 3.2-39.

Because of the excessive thermal coating degradation experienced during Mission I, a new coating was applied to Lunar Orbiter II, which laboratory tests indicated would give superior performance. The new coating was an overcoat of S-13G material developed by Illinois Institute of Technology Research Institute on the original coating of B-1056, as used on Lunar Orbiter I. The actual performance was superior to that achieved in Mission I, though not as good as expected.

Table 3.2-19 compares the thermal coating properties of the two spacecraft at Orbits 20, 71, and 186. The data show an increase in absorptivity throughout Mission II. The rate of degradation was initially lower in Mission II, but increased to a higher rate at Orbit 186.

Although the degradation rates are not a major problem during a 30-day mission, they will impose a limitation during a 1-year extended-life mission. As the EMD is positioned farther from the Sun vector, the incident solar energy is correspondingly reduced on the solar panels, limiting the amount of electrical energy available for operating the spacecraft subsystems.

Paint Sample Performance

Four paint sample coupons were attached to the exterior and located near the outer periphery of the EMD on the + Z axis. These thermal coating samples included one silver second surface mirror, B-1056; B-1056 with an overcoat of S-13G; and B-1056 with an overcoat of B-1059. Figure 3.2-40 shows the peak temperature of the coupons as they

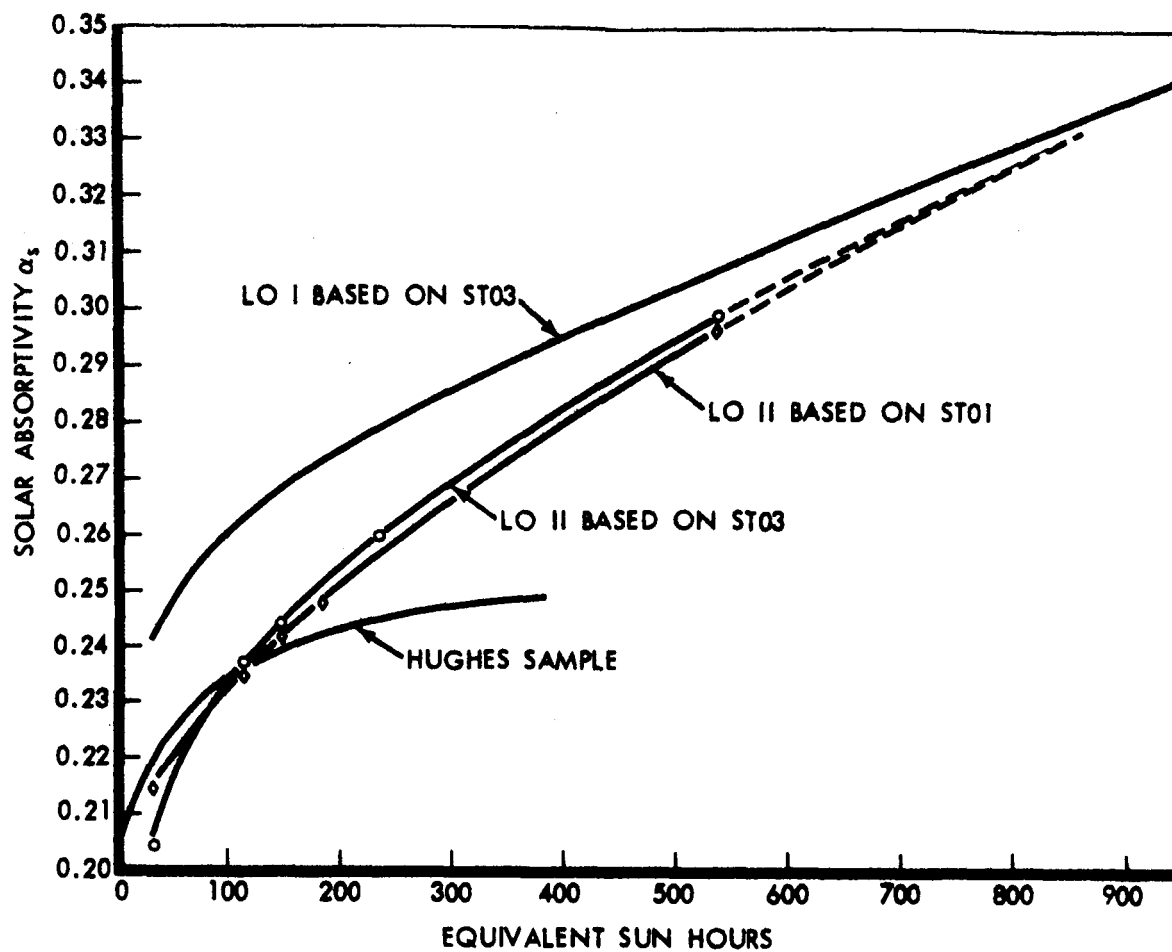


Figure 3.2-39: Thermal Coating Absorptivity Degradation from Solar Radiation

occurred each orbit through Orbit 73, at which time the peak temperature occurred during Earth occultation. Telemetry data from thermistors ST01 and ST03 are shown for comparison.

The mirror coupon ran considerably below the paint coupons but was not shown on the chart.

The telemetry coupon temperature data received from the spacecraft was higher than expected, based on laboratory sample coupon tests and inflight coating radiation characteristics determined from EMD thermistors ST01 and ST03. Hence, it may be assumed that the coupon samples were gaining additional energy from one or more of the following sources:

- Conduction from the EMD structure;
- Reflected solar radiation from the EMD;
- Thermal radiation from Solar Arrays 2 and 3;
- The B-1056 surface surrounding each of the test coupons. The coupon mount will degrade more rapidly than any of the test coupons. The resulting higher temperatures may well be the source of the energy.

Thermal energy generated by electrical current in the thermistor, approximately 1/10,000 watt, does not appear to be significant.

Since the coupon temperature data is known to be in error, calculation of coupon α values is not possible at this time. Further analysis will be required to determine the magnitude of the correction factor required to transform the coupon sample temperature data to coupon sample radiation characteristics.

Table 3.2-19: Thermal Coating Properties (Selected Orbits)

	ORBIT 20		Hughes Tested Sample
	L.O. II	L.O. I	
Solar Absorptivity (α_s)	0.245	0.275	0.242
Solar Absorptivity $\frac{d\alpha_s}{dt}$ Rate of Degradation	0.0208/100 hrs.	0.0263/100 hrs.	0.012/100 hrs.
	ORBIT 71		Hughes Tested Sample
	L.O. II	L.O. I	
Solar Absorptivity (α_s)	0.262	0.281	0.248
Solar Absorptivity $\frac{d\alpha_s}{dt}$ Rate of Degradation	0.014/100 hrs.	0.01/100 hrs.	0.004/100 hrs.
	ORBIT 186		Hughes Tested Sample
	L.O. II	L.O. I	
Solar Absorptivity (α_s)	0.298	0.307	No Data
Solar Absorptivity $\frac{d\alpha_s}{dt}$ Rate of Degradation	0.011/100 hrs.	0.0087/100 hrs.	No Data

Thermal Effect of Micrometeoroid Impacts

Thermal effects of the three micrometeoroid impacts were not detected. The major possible thermal effects of such activity are an increase in EMD thermal coating degradation, and damage to the thermal barrier. Degradation of the thermal coating was continuous and uniform, with no abrupt changes in rate as would be caused by a micrometeoroid shower. Thermal barrier damage was insignificant, based on no significant change in X-axis temperature gradient.

One temperature telemetry sequence observed on channel ST04 located on the tank deck may indicate that a micrometeoroid penetrated the spacecraft. Approximately 30 seconds after sunrise in Orbit 39, ST04 temperature increased for approximately 4 minutes, and then decreased to its normal value. This is shown graphically in Figure 3.2-41. A possible explanation for this curve is a micrometeoroid impact near ST04 thermistor, with kinetic energy converted to thermal energy.

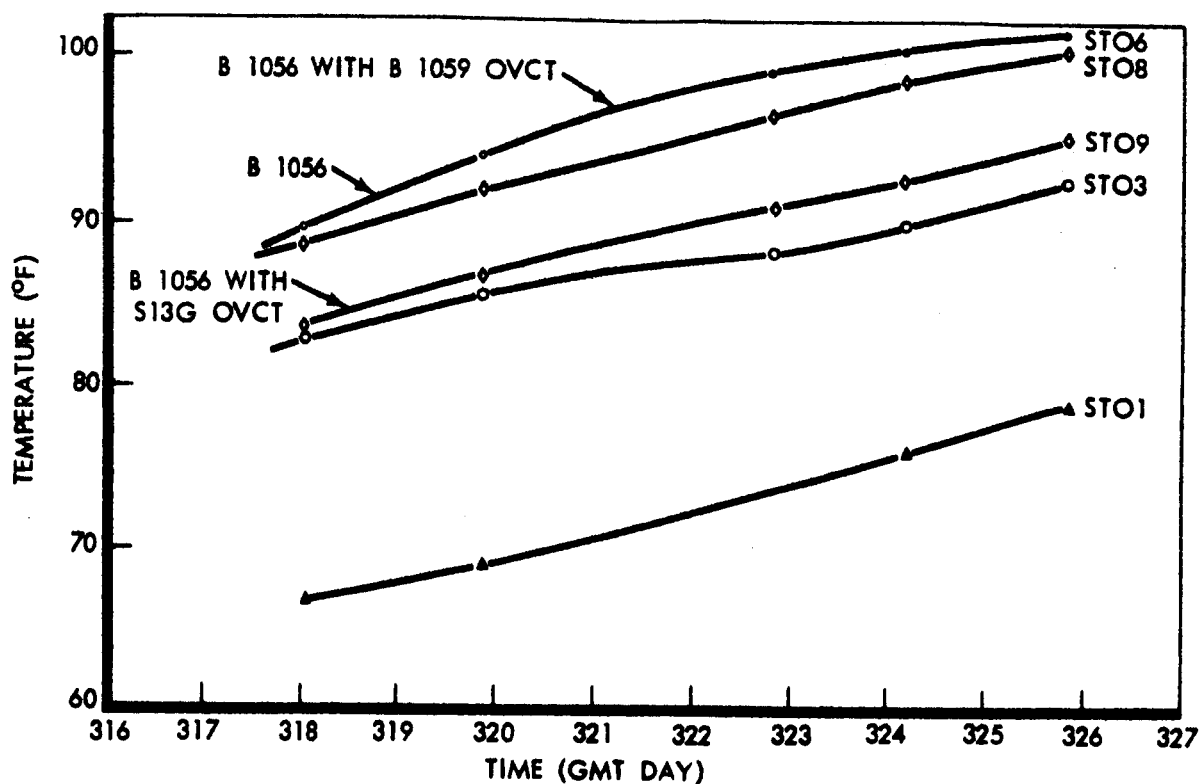


Figure 3.2-40: Thermal Coating Coupon Performance

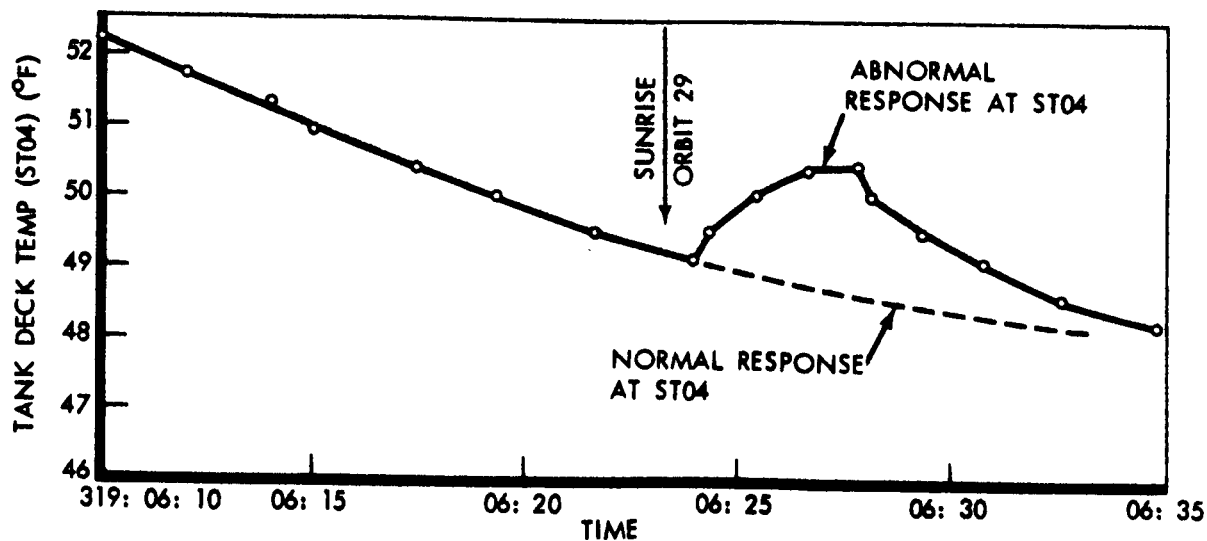


Figure 3.2-41: ST04 Thermistor Anomaly in Orbit 29

Thermal Design Changes

Changes in thermal design between Lunar Orbiters I and II include the different EMD thermal coating, and addition of a nonreflective coating on the low-gain-antenna boom. Addition of the four thermal coating samples to the EMD had little effect on thermal performance of the spacecraft, as only about 16 square inches of EMD were covered.

The difference in the thermal coating of the EMD was the addition of a 3 ± 1.5 mil thick S-13G overcoat to the basic 8 to 10 mil B-1056 coating. The low-gain antenna boom of Lunar Orbiter II was painted black to reduce light reflection to the star tracker. There was no detectable effect on spacecraft temperatures.

The data in Table 3.2-20 show peak temperatures for selected telemetry channels during Mission II.

Locations of the telemetry sensors shown on the chart are indicated on Figure 3.2-42.

VIBRATION DATA

The flight vibration peak responses associated with Mission II were less than the test peak response envelope. Comparison between flight and test data is shown in Appendix F, Volume VI of this document.

Table 3.2-20: Orbital Peak Temperatures

Orbit	ST01	ST02	ST03	ST04	CT01	CT02	PT06	PT07	PT08	ET02	Angle Off Sun	Comments
Orbit Injection	65.4	88.6	84.6	53.9		89.7	61.3	58.7	60.4	111.8		
1	63.5	84.1	81.9	51.7		85.0	61.0	59.6	61.2	105.1	6	Start Initial Orbits
2	62.1	78.8	79.9	50.8		81.0	59.5	59.0	60.7	95.7	On-Sun	Tank Heaters On 86 min.
3	61.6	76.8	79.4	57.1		79.4	59.1	58.7	60.9	92.2		
4	62.1	76.8	79.4	53.0		79.4	59.5	58.7	60.9	91.9		
5	62.1	76.3	79.4	56.6		79.0	59.5	59.0	61.2	91.2		Tank Heaters On
6	62.6	76.8	79.9	53.0		79.4	59.8	59.3	61.2	91.2		
7	62.6	76.8	80.4	52.1		79.4	60.1	59.3	61.5	90.9		
8	63.1	76.8	80.4	57.5		79.4	60.1	59.6	61.7	91.2		Tank Heaters On 70 min.
9	63.5	77.3	80.4	53.9		79.8	60.7	59.9	62.0	91.2		
10	63.5	77.3	80.9	52.6		79.8	60.7	59.9	62.0	91.2		Tank Heaters On 101 min.
11	64.0	77.8	80.9	58.5		80.2	61.0	60.2	62.5	91.5		TWTA On 42 min.
12	81.3	78.3	81.9	54.8	165.3	81.0	67.1	64.1	64.5	92.2		
13	64.9	78.8	81.9	53.9		81.0	63.3	62.4	64.2	92.6		TWTA On 37 min.
14	80.7	78.8	82.5	53.0	163.1	81.0	78.4	65.8	65.9	92.6		
15	65.4	79.3	82.5	53.0		81.4	64.0	63.1	64.8	92.6		Tank Heaters On 131 min.
16	65.9	79.8	82.5	59.8		81.8	63.3	62.1	64.2	93.9		
17	53.7	66.6	70.6	54.4		71.2	56.7	58.1	60.7	79.8	38	Tank Heaters On 66 min.
18	64.5	76.3	80.4	57.5		78.2	60.7	59.6	61.7	88.8		
19	65.9	79.3	81.9	54.8		81.0	62.0	60.8	62.8	93.3		
20	66.4	80.3	82.5	54.4		81.8	62.6	61.5	63.4	94.6	32	Tank Heaters On 24 min.
21	56.5	68.5	72.5	53.9		72.9	57.9	59.0	60.9	82.8		Tank Heaters On 120 min.
22	56.0	66.6	72.0	59.4		70.8	56.7	57.5	59.9	79.0	32	
23	56.5	66.2	72.0	57.1		70.0	56.5	56.9	59.1	79.4		
24	57.0	67.1	72.5	58.5		70.8	56.7	57.2	59.1	79.4		Tank Heaters On 75 min.
25	58.4	69.0	73.9	58.9		72.0	57.3	57.5	59.6	81.7		Tank Heaters On 75 min.
26	58.8	70.4	74.9	58.0		73.3	57.9	58.1	60.1	83.5		Tank Heaters On 48 min.
27	59.8	71.4	75.9	59.4		74.1	58.5	58.7	60.7	84.9		
28	60.2	71.9	76.4	54.4		74.5	59.1	59.0	60.9	85.6		
29	59.8	72.3	76.4	58.5		74.5	59.5	59.3	60.9	85.6		
30	61.2	72.8	77.3	58.9		75.3	59.8	59.6	61.5	86.3		Possible Micrometeoroid Hit at ST04 Recorded
31	67.8	80.9	83.5	55.7		81.8	63.3	71.8	63.4	95.7	On-Sun	Micrometeoroid Hit

Table 3.2-20: Orbital Peak Temperatures (Continued)

Orbit	ST01	ST02	ST03	ST04	CT01	CT02	PT06	PT07	PT08	ET02	Angle Off Sun	Comments
32	68.8	83.5	85.1	55.7		83.8	64.6	63.1	64.8	99.1		Deboost to Final Orbit
33	69.2	84.6	85.7	55.7		84.6	65.7	63.7	65.4	99.5		
34	69.2	84.1	85.1	55.7		84.6	65.7	64.1	65.4	98.8		
35	69.2	83.0	85.1	55.7		84.2	65.3	63.7	65.4	96.0		
36	69.2	83.0	85.1	55.7		83.8	65.3	63.7	65.4	95.0	36	
37	69.2	82.5	85.1	55.3		83.4	65.3	63.7	65.4	95.0		
38	54.2	67.1	71.5	51.7		71.6	57.9	59.3	61.5	79.4		
39	51.4	62.5	68.7	51.7		67.0	55.3	56.6	58.6	73.0		
40	51.9	61.6	69.6	52.1		66.2	59.1	58.4	58.6	71.6	36	Tank Heaters On 30 min. Tank & Photo Day Heaters On 40 Min.
41	51.4	61.1	69.2	52.1		65.4	60.4	59.3	59.6	70.6		
42	51.9	61.6	70.1	52.1		66.2	60.7	59.9	59.4	74.7		
43	52.8	62.9	71.1	52.6		67.0	61.3	60.2	59.6	74.4		Tank Heaters On 40 Min.
44	54.7	63.9	71.1	53.0		67.4	62.0	60.8	60.1	74.4	30	Tank Heaters On 43 Min.
45	54.7	64.8	71.5	53.0		67.9	62.0	60.8	60.4	75.7		Tank Heater On 38 Min. Solar Eclipse On Between Sunset & Sunrise Each Orbit
46	55.6	65.7	73.4	53.5		69.1	68.2	66.1	64.5	77.4		
47	56.5	66.2	73.9	54.4		69.1	68.9	67.9	65.6	77.8		
48	57.9	67.6	74.9	50.8		70.4	68.9	67.9	65.6	79.4		
49	57.9	68.1	74.9	49.9		70.8	68.5	67.9	65.9	80.5	On-Sun	TWTA On 35 min. TWTA On 37 min. TWTA On 30 min.
50	69.7	80.9	85.1	52.1		80.6	69.7	67.6	67.4	93.9		
51	71.2	85.2	87.3	53.9		84.6	70.0	67.9	68.3	99.5		
52	72.2	86.3	87.9	54.8		85.8	69.7	68.7	69.6	94.1		
53	87.3	86.3	88.5	55.3	169.9	86.2	74.4	71.7	71.4	100.2		
54	88.5	86.8	89.1	56.2	171.1	86.6	74.8	71.7	71.4	100.5		
55	88.5	86.8	89.1	56.6	171.1	87.0	74.8	71.3	70.8	100.5		
56	86.7	86.8	89.1	56.6	168.7	87.0	74.0	70.9	71.1	100.5	30	TWTA On 26 min.
57	87.3	86.8	89.1	57.1	168.7	87.0	74.0	70.9	71.1	100.2		TWTA On 29 min.
58	86.7	86.8	89.1	57.1	167.5	87.0	74.0	71.3	71.1	100.5		TWTA On 25 min.
59	75.1	87.4	89.6	57.5	158.1	87.4	72.4	70.6	71.1	101.2		TWTA On 33 min.
60	75.1	88.0	89.6	57.5	162.1	87.0	72.4	70.6	71.1	101.6		TWTA On 31 min.
61	75.6	88.6	89.6	57.5	163.1	87.8	72.4	70.9	71.4	101.6		TWTA On 37 min.
62	76.1	88.6	90.2	58.0	164.1	88.6	72.8	70.9	71.4	102.0		TWTA On 38 min.
63	76.1	88.6	90.2	58.0	167.6	87.4	72.8	70.9	71.4	102.0		TWTA On 36 min.
64	76.6	89.1	90.2	58.5	168.7	87.8	73.6	71.3	71.8	102.7		TWTA On 48 min.
65	76.6	89.1	90.8	58.5	169.9	88.6	73.6	71.3	72.1	102.7		TWTA On 46 min.
66	77.1	89.7	90.8	58.9	168.7	88.6	74.0	71.7	72.1	103.0		TWTA On 42 min.
67	77.1	89.7	90.8	58.9	167.6	89.0	73.6	71.7	72.1	103.7		TWTA On 40 min.
68	77.6	90.3	90.8	58.9	171.2	89.0	74.0	71.7	72.1	104.1		TWTA On 48 min.
69	78.2	90.3	91.4	59.4	172.5	89.3	74.4	72.1	72.4	104.1		TWTA On 50 min.
70	78.2	90.9	91.4	59.4	173.8	89.3	74.4	72.1	72.7	104.8		TWTA On 54 min.
71	78.7	90.9	91.4	59.4	173.8	89.3	75.2	72.5	73.1	105.1		TWTA On 49 min.
72	78.7	91.5	92.0	59.8	173.8	89.7	75.2	72.9	73.1	105.1		TWTA On 49 min.
73	79.2	91.5	92.0	59.8	173.8	90.1	75.7	73.3	73.7	105.1		TWTA On 49 min.
74	79.2	91.5	92.0	59.8	175.1	90.1	76.1	73.3	73.7	105.1		TWTA On 50 min.
75	79.7	91.5	92.0	60.3	176.5	90.1	76.1	73.7	73.7	105.5		TWTA On 49 min.
76	80.2	92.1	92.6	60.3	176.5	90.5	77.0	74.6	74.4	105.8		TWTA On 54 min.
77	80.2	92.1	92.6	60.3	176.5	90.5	77.4	74.6	74.7	106.2		TWTA On 52 min.
78 *	76.1	86.3	87.9	60.3	177.9	90.9	77.2	75.0	75.1	106.5		TWTA On 51 min.
79 *	75.6	85.2	87.3	60.3	177.9	90.9	77.9	75.4	75.4	106.9		TWTA On 51 min.
80 *	48.6	68.1	66.4	58.5	176.5	85.4	67.4	73.3	75.4	106.2		TWTA On 50 min.
81 *	67.3	77.8	79.9	60.3	176.5	90.5	74.8	75.8	76.1	107.6	30	TWTA On 50 min.
82 *	62.6	75.3	76.4	60.3	171.2	90.1	73.2	75.8	76.1	108.0		TWTA On 29 min.
83 *	60.7	74.3	74.9	60.3	172.5	89.3	72.0	74.6	75.1	107.6		TWTA On 37 min.
84 *	57.9	72.8	73.0	59.8	173.8	89.0	70.0	73.7	74.7	107.6		TWTA On 37 min.
85 *	55.6	71.9	71.1	59.8	172.5	88.6	69.3	73.7	75.1	107.6		TWTA On 34 min.
86 *	55.1	71.9	71.1	59.8	172.5	88.2	69.3	73.7	74.7	108.0		TWTA On 39 min.
87 *	50.9	69.9	68.2	59.4	177.9	87.0	67.4	72.9	74.7	108.0		TWTA On 51 min.
88 *	49.6	69.0	66.9	59.4	173.8	86.6	66.7	72.5	74.7	108.0		TWTA On 32 min.

Table 3.2-20: Orbital Peak Temperatures (Continued)

Orbit	ST01	ST02	ST03	ST04	CT01	CT02	PT06	PT07	PT08	ET02	Angle Off Sun	Comments
89 *	48.6	69.0	66.4	59.4	173.8	86.2	66.7	72.5	74.7	108.0		TWTA On 32 min.
90 *	45.4	67.6	64.6	58.9	175.1	85.0	65.7	72.1	74.7	107.2		TWTA On 36 min.
91 *	45.4	67.6	64.6	59.4	173.8	85.0	65.7	72.1	75.1	107.2		TWTA On 35 min.
92 *	44.0	67.1	63.7	58.9	175.1	84.6	65.3	72.1	75.1	106.9		TWTA On 34 min.
93 *	42.6	66.6	62.7	58.9	175.1	84.2	65.0	72.1	75.4	106.9		TWTA On 35 min.
94 *	39.3	65.3	60.9	58.5	175.1	82.6	63.6	71.3	75.1	106.2		TWTA On 34 min.
95 *	39.8	65.3	60.9	58.5	176.5	83.0	63.6	71.3	75.1	106.5		TWTA On 34 min.
96 *	37.5	64.3	59.6	58.0	176.5	81.8	62.6	70.6	74.7	105.8		TWTA On 34 min.
97 *	26.8	59.3	52.9	55.7	171.2	75.7	58.2	67.6	73.1	100.5		TWTA On 32 min.
98 *	36.0	63.9	59.1	58.0	175.1	81.4	62.0	70.2	74.4	105.5		TWTA On 33 min.
99 *	31.2	61.6	56.0	53.5	173.8	78.6	60.1	69.0	73.7	103.0		TWTA On 33 min.
100 *	34.6	63.4	58.2	58.0	176.8	80.6	61.7	69.8	74.4	105.1		TWTA On 33 min.
101	No Data											
102 *	93.9	94.0	91.5	62.1	177.8	91.3	79.2	75.4	75.1	102		TWTA On 32 min.
103 *	95.2	94.0	95.1	62.1	177.8	91.7	79.7	75.4	75.1	102.7		TWTA On 36 min.
104 *	95.2	94.0	95.1	62.1	173.7	88.2	79.7	75.4	75.1	100.2		TWTA On 41 min.
105 *	86.7	86.8	87.9	56.6	171.1	86.2	74.8	72.5	72.4	97.8		TWTA On 37 min.
106 *	70.7	85.7	86.8	55.3	—	85.4	70.4	69.4	70.2	97.1		No Readout
Orbit	ST01	ST02	ST03	ST04	CT01	CT02	PT06	PT07	PT08	ET03	Angle Off Sun	Comments
107	92.6	85.7	87.3		179.3	85.0	76.5	71.7		92.9	28	First R/O
108	92.0	86.3	87.9		179.3	85.4	79.4	74.2		93.9		TWTA on 119 Min.
109	92.6	86.8	87.9		180.8	85.8	80.7	75.8		95.7		TWTA on 104 Min.
110	93.9	88.0	88.5		180.8	86.6	81.6	76.7		97.1		TWTA on 127 Min.
111	93.9	88.0	88.5		180.8	86.6	82.1	77.2		97.4	28	TWTA on 128 Min.
112	93.9	88.6	88.5		180.8	86.6	82.1	77.2		98.8		TWTA on 135 Min.
113	93.9	88.8	88.5		180.8	86.6	82.1	77.2		99.1		TWTA on 136 Min.
114	93.3	88.6	88.5		180.8	87.0	82.6	77.6		99.8	31	TWTA on 137 Min.
115	93.3	88.6	88.5		180.8	86.6	82.1	77.6		99.8		TWTA on 138 Min.
116	92.6	88.6	87.9		180.8	86.6	82.6	77.2		100.2*		TWTA on 139 Min.
117	93.9	89.1	87.9		180.8	87.0	82.6	77.6		101.2*		TWTA on 141 Min.
118	93.9	89.1	87.9		180.8	87.0	82.1	77.2		101.6*		TWTA on 142 Min.
119		Data			Bad							TWTA on 140 Min.
120	93.3	89.1	87.9		108.8	87.0	82.6	77.6		102.7		TWTA on 142 Min.
121	93.3	89.1	87.9		180.8	87.0	82.6	77.6		103.0		TWTA on 142 Min.
122	92.6	88.6	87.9		180.8	86.2	82.1	77.6		103.0		TWTA on 142 Min.
123	92.6	88.0	87.3		179.3	85.8	82.1	77.6		102.7*		TWTA on 136 Min.
124	92.0	88.0	87.3		180.8	85.8	82.1	77.2		102.0*		TWTA on 139 Min.
125	91.4	87.4	87.3		179.3	85.0	81.6	76.7		101.6*		TWTA on 139 Min.
126	92.6	88.0	87.3		180.8	85.4	80.7	76.7		102.7*		TWTA on 140 Min.
127	92.6	88.0	87.3		179.3	85.4	81.6	77.2		103.7*		TWTA on 141 Min.
128	92.6	86.3	87.3		180.8	85.0	83.6	79.0		97.8*		TWTA on 141 Min.
129		Data			Bad							TWTA on 140 Min.
130		Data			Bad							TWTA on 138 Min.
131	91.4	88.0	86.8		179.3	85.4	80.7	76.3		103.0		TWTA on 141 Min.
132	92.0	88.0	86.8		180.8	85.4	80.7	76.3		103.0		TWTA on 141 Min.
133	91.4	87.4	86.8		179.3	85.0	80.2	75.8		102.7		TWTA on 140 Min.
134		Data			Bad							TWTA on 141 Min.
135	91.5	87.5	86.3		179.3	85.1	79.3	75.0		102.4	33.0	TWTA on 136 Min.
136	91.5	86.9	85.7		179.3	85.1	79.8	75.0		103.8	33.3°	Battery Up
137	91.5	88.0	86.3		179.3	85.1	78.8	74.6		103.8		TWTA on 129 Min.
138	91.5	87.5	85.7		177.9	85.5	79.3	74.6		104.1	33.4°	Battery Up
139	91.4	88.0	86.2		179.3	85.4	79.2	75.0		104.1		TWTA on 129 Min.
140	91.4	88.0	86.2		179.3	85.4	79.2	75.0		103.7	34.7°	TWTA on 140 Min.
141	90.8	88.0	85.7		179.3	85.0	79.7	75.0		103.4		TWTA on 128 Min.
142	90.2	87.4	85.7		177.8	85.0	79.2	74.6		103.4		TWTA on 139 Min.
143	90.2	87.4	85.7		177.8	85.0	78.8	74.6		103.0		TWTA on 137 Min.
144	89.7	86.9	85.7		177.9	84.7	78.8	74.6		102.7		TWTA on 131 Min.
145	89.1	86.9	85.2		176.5	84.3	78.4	74.2		102.0		TWTA on 137 Min.

Table 3.2-20: Orbital Peak Temperatures (Continued)

Orbit	ST01	ST02	ST03	ST04	CT01	CT02	PT06	PT07	PT08	ET03	Angle Off Sun	Comments
146	89.1	86.3	85.2		176.5	84.3	78.4	73.8		101.6	36.3°	TWTA on 136 Min.
147	90.2	86.8	85.1		177.8	84.2	78.3	73.7		102.7	36.4°	TWTA on 135 Min.
148	90.2	86.8	85.1		177.8	84.2	78.3	73.7		103.4	36.4°	TWTA on 135 Min.
149	90.2	87.4	85.1		177.8	84.6	78.3	72.4		103.7	36.4°	TWTA on 133 Min.
150	89.6	87.4	85.1		177.8	84.8	77.9	73.3		103.7	36.5°	TWTA on 128 Min.
151	89.0	86.8	84.6		176.4	83.8	77.9	73.3		103.7	36.7°	TWTA on 132 Min.
152	89.0	86.8	84.6		177.8	83.8	77.0	72.9		103.0	37.0	TWTA on 134 Min.
153	89.0	86.8	84.6		176.4	83.4	77.4	72.9		103.0	37.3	TWTA on 133 Min.
154	88.5	86.3	84.6		176.4	83.4	77.4	72.9		102.0	37.7	TWTA on 131 Min.
155	87.9	85.7	84.6		176.4	83.8	77.4	72.5		101.6	37.9	TWTA on 130 Min.
156	87.3	85.7	84.0		175.0	83.0	76.5	72.1		101.2	38.2	TWTA on 131 Min.
157	87.3	85.2	84.0		175.0	82.6	76.1	71.7		100.9	38.5	TWTA on 130 Min.
158	86.7	84.1	83.5		173.7	82.2	75.2	71.3		99.1	38.8	TWTA on 129 Min.
159	95.8	91.5	90.2		183.8	87.4	80.2	74.6		105.8	29.2	TWTA on 125 Min.
160	98.5	95.3	91.4		185.5	89.3	82.6	76.3		112.2	28.1	TWTA on 133 Min.
161	99.9	95.9	92.6		188.8	91.3	84.2	78.1		113.9	28.0	TWTA on 131 Min.
162	99.9	96.6	92.6		187.1	91.7	84.7	79.4		113.6	28.3	TWTA on 133 Min.
163	99.9	96.6	93.2		187.1	91.7	85.7	79.9		113.2	28.3	TWTA on 131 Min.
164	99.9	96.6	93.2		187.1	91.3	85.7	80.4		113.2	28.7	TWTA on 132 Min.
165	99.2	96.6	93.2		187.1	91.7	85.7	80.4		112.5	29.1	TWTA on 130 Min.
166	99.2	95.9	93.2		187.1	90.5	85.7	80.9		112.2	29.2	TWTA on 131 Min.
167	99.2	95.9	93.2		187.1	90.9	85.7	80.9		112.2	29.6	TWTA on 130 Min.
168	99.2	95.3	92.6		188.8	90.9	85.7	80.4		111.8	29.9	TWTA on 128 Min.
169	97.8	95.3	92.6		185.5	90.9	85.2	80.4		111.8	30.0	TWTA on 128 Min.
170	91.4	90.3	87.9		180.8	87.4	81.6	77.6		107.2	36.7	TWTA on 125 Min.
171	92.6	89.7	87.9		180.8	86.6	80.7	76.7		105.8	35.8	TWTA on 127 Min.
172	92.0	89.7	87.3		180.8	86.2	80.7	76.3		106.2	36.0	TWTA on 97 Min.
173	90.8	89.7	86.8		179.3	85.8	77.9	73.7		105.8	36.3	TWTA on 126 Min.
174	90.8	89.1	86.8		179.3	85.8	79.2	74.2		108.7	36.4	TWTA on 126 Min.
175	91.4	89.1	86.8		180.8	85.8	79.2	74.6		105.7	37.0	TWTA on 127 Min.
176	90.8	89.1	86.8		179.3	85.8	78.8	74.2		108.7	37.4	TWTA on 125 Min.
177	90.2	88.0	86.2		179.3	85.0	78.8	74.2		105.1	38.0	TWTA on 125 Min.
178	89.6	88.6	86.2		176.4	85.0	78.3	73.7		108.0	38.0	
179	89.0	88.0	85.7		177.8	85.0	77.9	71.8		104.1	36.7	
180	68.8	88.0	84.6			85.0	66.7	65.4		108.0		TWTA Failed

* Maximum value occurred during earthset. Maximum recorded reading shown

3.2.4 DATA SYSTEM PERFORMANCE

The Lunar Orbiter ground data system consists of the components and data flow described in Figures 3.2-43, 3.2-44, and 3.2-45. The entire system performance was satisfactory, with only a few minor problems that are noted below.

3.2.4.1 Ground Equipment at DSS-12, -41, and -61

3.2.4.1.1 DSS ANTENNA PROBLEMS

Primarily due to overheating problems in the Masers, it was necessary at all sites to use the Paramp in lieu of the Maser for varying durations of time. It is of interest to note that at one time DSS-11 successfully tracked and commanded the spacecraft while the DSS-12 Maser was being repaired. Telemetry and commands were transmitted by microwave link between DSS-11 and DSS-12 with no noted degradation.

Intermittent failures of the antenna pointing system at DSS-41 and DSS-61 resulted in short loss of lock on several occasions prior to resolution of the malfunction.

3.2.4.1.2 GROUND RECONSTRUCTION EQUIPMENT (GRE) PROBLEMS

Although the GRE equipment generally performed within specifications during Mission II, the following problems were noted at the DSS sites.

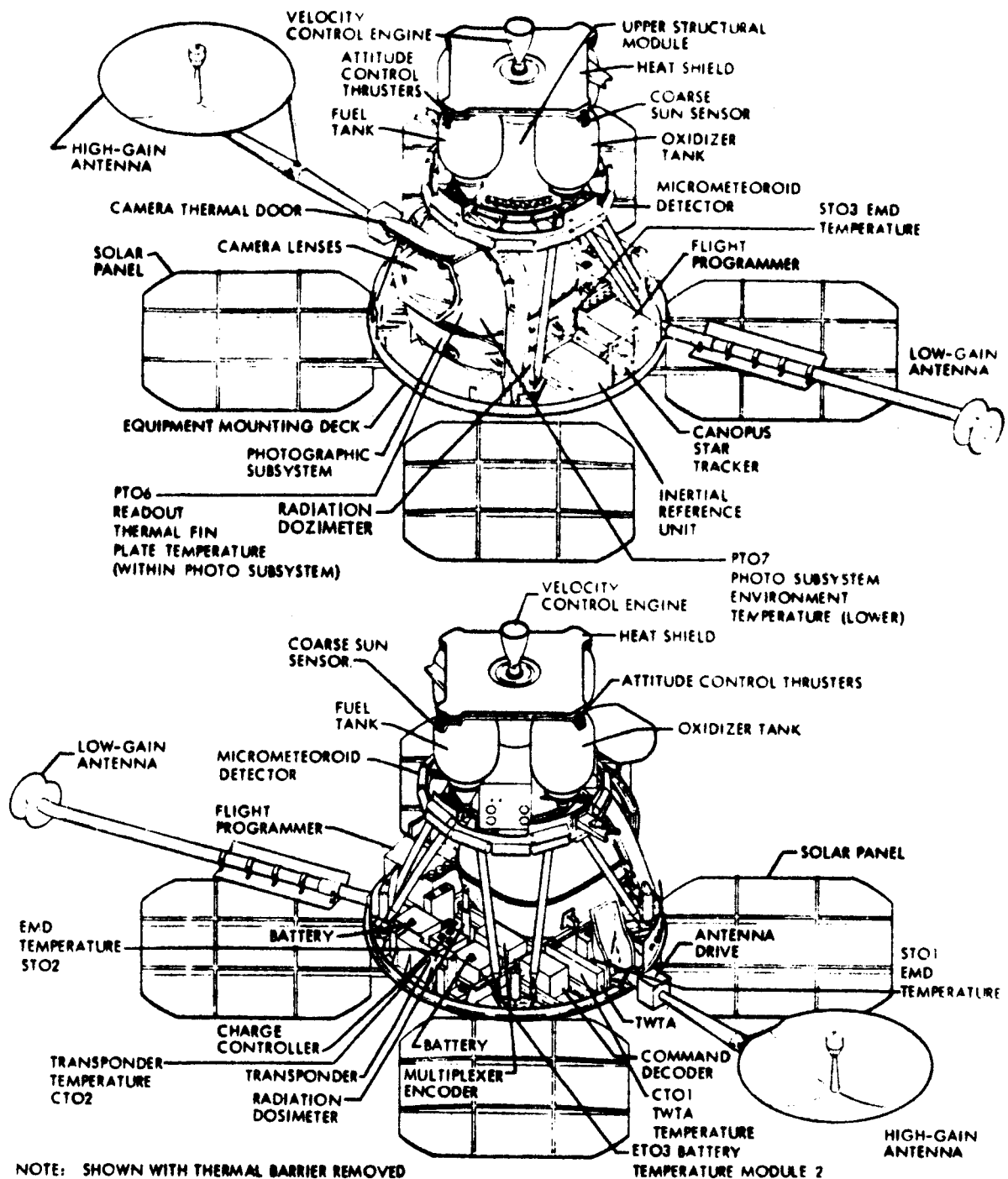


Figure 3.2-42: Selected Telemetry Measurement Locations

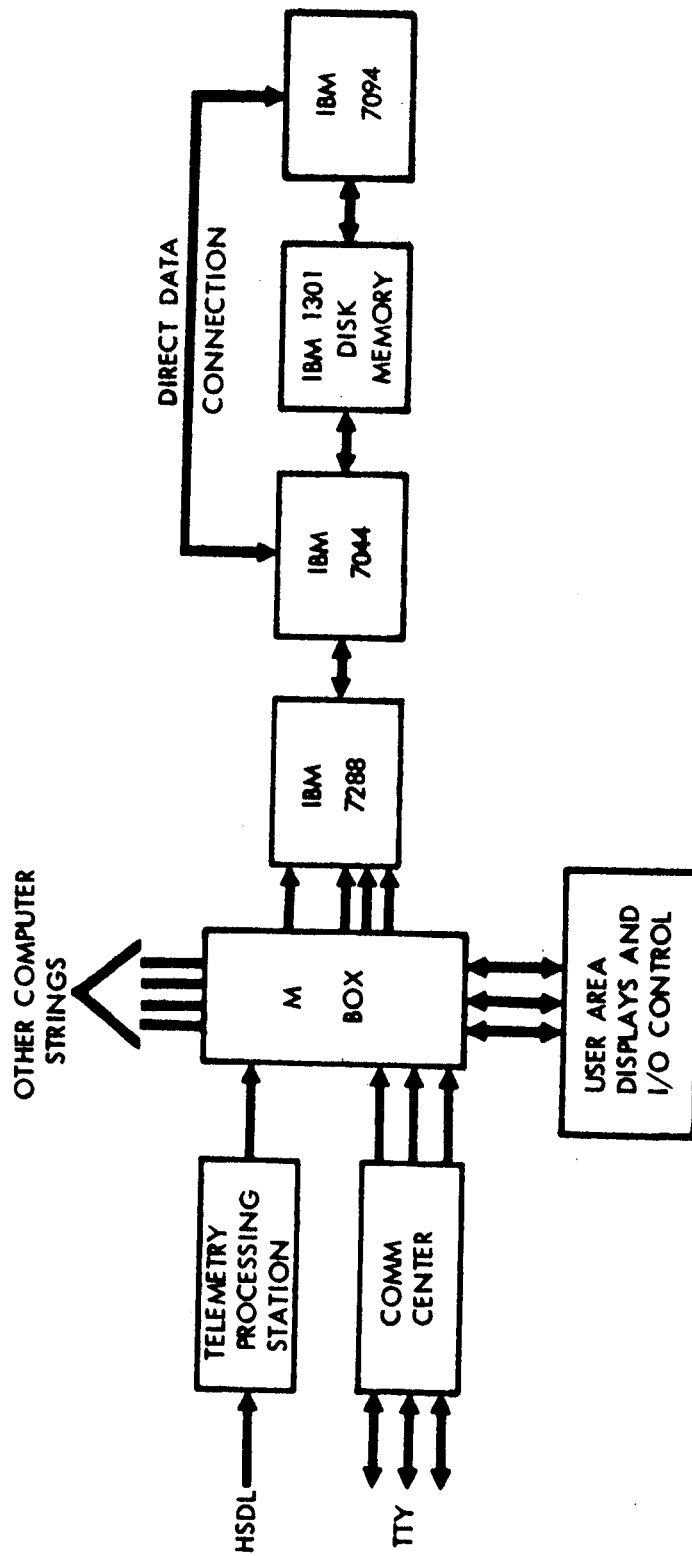


Figure 3.2-43: SFOF Data Processing (Typical Computer String)

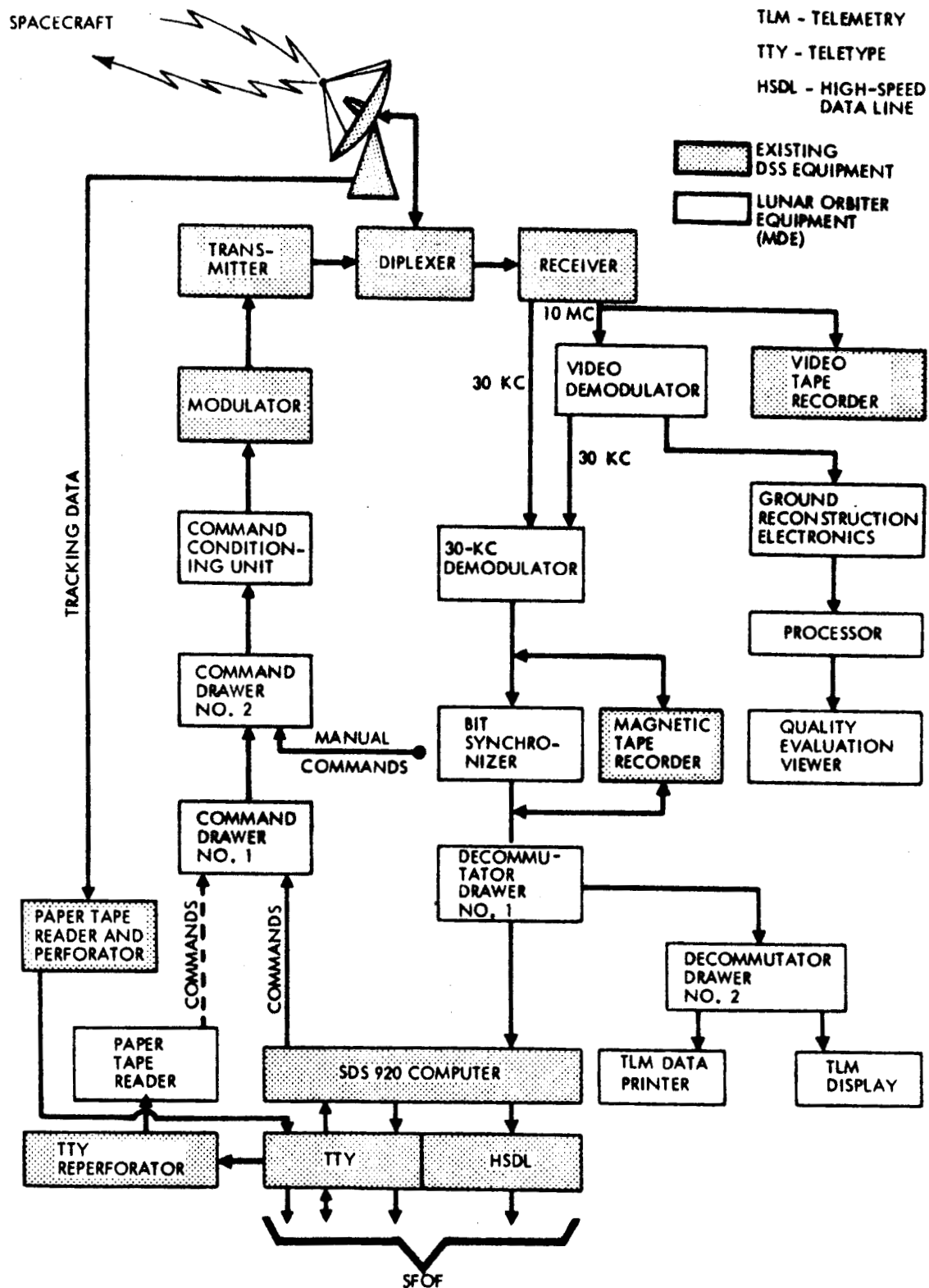


Figure 3.2-44: Deep Space Station Data Flow Operation

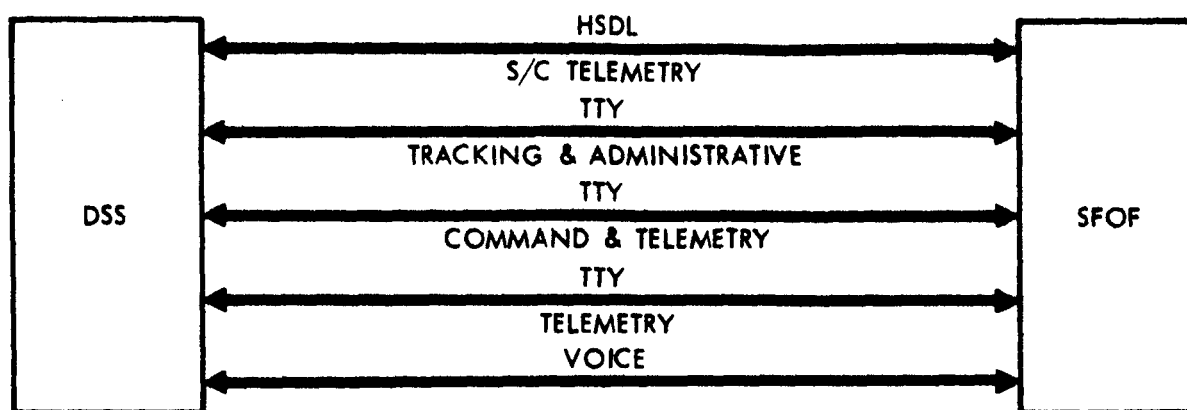


Figure 3.2-45: DSS-SFOF Ground Communications

Kine Tube Problems

- Excessive Flare - Minimized by using locally fabricated masks over the scan line.
- Phosphor Streaking - Increased from slight to moderate during the mission.
- Density Variations Across Film - Occurred primarily at the center and at the ends of the scan line. The variations at the center of the scan line were greatly reduced by a GRE circuitry change that improved sweep linearity. The variations generally increased as the mission progressed.
- Scan Line Location - Difficulty was encountered selecting a scan line due to phosphor irregularities.

Scan Line Control Problems

- Centering - It was often difficult to maintain a constant scan line length and to keep the line centered.
- Focus - Uniformity of focus across the scan line was a problem. It was also noted that the symmetry control generally had to be set almost to the extreme CCW position at DSS-61.

3.2.4.1.3 PROCESSING AND FILM EVALUATION PROBLEMS

Generally, the processing went very well at all sites. The task of maintaining constant solution temperatures, developer replenishment rate and specific gravity, and transport speed was handled quite easily by the processing technicians. The densitometer and sensitometer worked satisfactorily throughout the mission. The quality evaluation viewer also performed well even though a few minor mechanical problems were noted with this equipment. The processing problems were as follows.

- Filter Changes - The present methods for changing filters are awkward. The use of shutoff valves in the supply lines would facilitate this task.
- Temperature Control - Although it was possible to keep the solution temperatures within limits, DSS-61 found it more and more difficult to maintain good temperature control toward the end of the missions.

- Water Streaking - This problem was particularly severe at DSS-61. It is believed that it is caused by silt, precipitates, and high mineral content in the local water supply. The water problems were aggravated during periods of heavy or extended rains.

3.2.4.2 Ground Communication System

Ground communication between the Deep Space Stations (DSS) consists of one high-speed data line (HSDL), three full duplex teletype (TTY) lines, and one voice line. The communications lines for the overseas sites, Madrid and Woomera, are routed through relay stations and the Goddard Space Flight Center. Communications lines from Goldstone are connected directly to the SFOF.

The HSDL is the primary source for spacecraft performance telemetry data. Two full duplex TTY lines serve as a backup for spacecraft telemetry data and for the transmission of command data to a DSS and the response from the DSS. The third line is used for tracking and administrative data. The HSDL can carry 100% of the spacecraft performance telemetry data; a single TTY line can carry 39%; and two TTY lines can carry 87%. Since a configuration of one or two TTY lines cannot carry all the spacecraft performance data, the TTY lines carry only priority data. There is one two-TTY configuration and twelve one-TTY configurations that may be used, depending on the mission phase, to transmit telemetry data to the SFOF.

The normal configuration for telemetry data consists of the HSDL and two TTY lines. Both sources of data are entered into the computer and written on magnetic tape (as is the tracking and administrative data on the third TTY line). Either source of telemetry data may be selected for processing by the computer. The processed data is written on the master data table for user program access and may also be displayed on 100-wpm teleprinters and/or SC-3070 high-speed bulk printers and MILGO/DYMEC plotters. The data stream from the HSDL is usually processed unless the line is down; then one of the TTY data configurations is processed.

3.2.4.2.1 DSS-12 GROUND COMMUNICATIONS

Ground communication between DSS-12 and the SFOF was excellent. The HSDL was reported down on only three occasions for a total of 21 minutes during the entire mission. All TTY lines were operating normally during these times; therefore, virtually no data were lost from DSS-12 due to ground communications. There were no reports of any of the TTY lines being down.

3.2.4.2.2 DSS-41 GROUND COMMUNICATIONS

Ground communication between DSS-41 and the SFOF was good. The HSDL was reported down on 16 occasions for a total of 225 minutes. The average down time was 14 minutes. On six occasions the HSDL was down for 20 minutes or more. In all cases when the HSDL was down, two TTY lines were in operation and served effectively as a backup. The three TTY lines were reported down on 21 occasions for a total of 300 minutes, or an average of 14 minutes each. All three TTY lines were down for 19 minutes on only one occasion. Fifteen minutes of high-speed T/M data were retransmitted from the FR-1400; 90 minutes of tracking data were retransmitted. Only a negligible amount of data were lost due to ground communications problems. No data were lost at critical times.

3.2.4.2.3 DSS-61 GROUND COMMUNICATIONS

Ground communication between DSS-61 and the SFOF was good. The HSDL was reported down 13 times for a total of 238 minutes. The down time averaged 18 minutes.

On four occasions the down time exceeded 20 minutes and once was down for 90 minutes. Four times all TTY and HSDL were down, and approximately 30 minutes of data were lost. The TTY lines provided adequate backup during all other HSDL outages. The three TTY lines were reported down 39 times, averaging 8 minutes each for a total of 317 minutes. The data losses did not happen during critical times.

3.2.4.3 SFOF

The SFOF data systems equipment consists of the central computing complex, the telemetry processing station (TPS), input-output (I/O) devices, and internal communications. The entire systems performed very well, losing only an insignificant amount of the data that was received at the SFOF.

3.2.4.3.1 CENTRAL COMPUTING COMPLEX

All three computer strings were used to support Mission II. All the strings performed acceptably. The only chronic hardware problem involved the W string, which failed to reproduce the common environment regions correctly from disk when switching computer strings. The computer strings were used as follows.

<u>Computer String</u>	<u>Total Hours</u>	<u>Dual Mode 2</u>
X	514	149
Y	377	131
W	96	32

The total amount of Mode 2 time used was 987 hours.

Dual Mode 2 was used during all critical mission phases. Only a normal amount of random supporting equipment failures was experienced. These were corrected as they occurred.

3.2.4.3.2 GRE AND PHOTO PROCESSOR

The photo data system was installed at the SFOF just prior to Mission II. No problems were encountered during the installation of the equipment, but the following problems were encountered during initial checkout of the system.

- Excessive noise in the microwave link between the mission dependent equipment (MDE) at Goldstone and the interface equipment at the SFOF. Reworking the grounding system of the link eliminated most of the noise.
- DC offset of the incoming video. A clamping circuit was added to the interface equipment to clamp the incoming video to ground, thus eliminating the problem.
- Loss of sync during transitions of the video signal from black to white level. The gains of the transmission system were lowered between the MDE at Goldstone and the interface equipment at the SFOF, and the gain of the final Video amplifier was raised before presentation to the GRE. The sync pulse being transmitted then remained at a constant value. The response of the sync detection circuit was slowed to a rate which was close to that of the incoming video, enabling the sync detection circuit of the interface equipment to hold sync during large transitions of the signal.

During photo readout, no major problems occurred and no readout time was lost. Two masks were used on the GRE. Black electrician tape was placed on the kine tube to compensate for halo effect. A second mask was designed to compensate for space-

craft PS signature. The mask was placed about 3 inches from the kine tube and consisted of strips of material having a density of approximately 0.35. The mask was not in focus and so did not leave stripes on the film, but did have a smoothing effect on the transition between the masked and unmasked area. The mask appeared to work well on spacecraft signals that were of a high level, but became noticeable when the incoming video was of a density less than about 0.8. At the lower densities, the mask over-compensated for the PS signature.

The following minor problems occurred with the processor.

- Long heat-up time - Plumbing for the processor was not complete in time for Mission II, so the mission was completed with tempered deionized water. Due to the limited temperature capability of the tempered water, heat-up time of the processor was more than twice the normal rate.
- Chemical circulating pump failure - Several failures of the circulating pumps occurred; one was a motor failure, and one a cracked pump housing. Pump seals were replaced several times, but the pumps continued to leak. A large pan was placed under the processor to catch the escaping liquid.

3.2.4.4 Software

The software system for Mission II contained changes from the Mission I software. The system was demonstrated successfully prior to the Mission II training exercises. Two relatively minor problems were discovered in the demonstration and were corrected after launch during a noncritical part of the mission. The software system generally worked exceptionally well. There were no serious software failures, although a chronic data communication problem does exist in the 7044 software.

3.2.4.4.1 SYSTEM SOFTWARE

The SFOF mission-independent software system performed satisfactorily throughout Mission II, with one exception. This was the chronic occurrence of internal restarts on the 7044's caused by Comm Error 01 (the 7044 has sent an incorrect response indicating that the sense lines are down and it is not known whether it is incoming or outgoing sense line failure) and Comm Error 03 (the 7044 has sent an unacceptable sense line code indication that the 7044 to 7094 sense lines are down). No significant amounts of spacecraft data were lost due to the comm errors. However, in most cases, both the 7094 and 7044 must be restarted. Each restart requires about 2 minutes.

3.2.4.4.2 FPAC SOFTWARE SYSTEM PERFORMANCE

Many changes were made to the FPAC software system between Missions I and II. Most of these were the result of the first operational use of the system (Mission I) indicating various shortcomings and some computational inaccuracies. Each program change accomplished preceding Mission II and its performance during the mission will be discussed. Also, a description of the program changes that are necessary for Mission III is included.

Methods of data communication were added to the orbit determination program (ODP) to minimize data handling by operations personnel. The capability, which involves using the OD to store specified state vectors and matrices into general input program (GENI) where they can be assessed by the other FPAC programs, was used extensively during Mission II. Only minor modifications will be required for future missions. These involve better control of data storage in GENI and also minor corrections to printout variables.

The capability of computing camera pointing commands for photos on the farside of the Moon was added to the software system and used for a variety of secondary sites during Mission II. The addition of SPACEL (Space Link) as the trajectory program for EVAL (photo evaluation) made the postflight analysis of photos more rapid and accurate. This was also quite helpful in the design of a variety of secondary sites.

A single programming error that was made evident in Mission I (start-of-burn time) for the deboost maneuver computed by GCIL (guidance for injection) was corrected for Mission II and operated successfully.

During the course of Mission II it was discovered that the two targeting programs PMG (post-midcourse guidance) and PIG (preinjection guidance) require different conventions for input argument of perilune. Since this could be the cause of much confusion, a program change has been accomplished to correct this for future missions.

A thorough check on the midcourse maneuver indicated an error present in both MCIL and GCML (midcourse command programs) involving the computations of the midcourse maneuver. Although the effect was small, a correction has been made.

During the design of the Mission II transfer maneuver, it was found that a description of the orbit prior to and following the maneuver would be of great assistance. A change request was made to add this capability to the software system.

The programs requiring changes caused only minor losses of time in that work-around procedures had to be developed. Generally, the entire FPAC software system performed without any serious problems during Mission II.

3.2.4.4.3 SPAC SOFTWARE SYSTEM PERFORMANCE

The SPAC software consists of the IBM 7094 computer programs that monitor the telemetry from, and predict the status of, the spacecraft subsystems. It also consists of a program that prepares and simulates command sequences to be transmitted to the spacecraft computer and a program that coordinates mission planning. Minor changes to several of the programs between missions resulted in added flexibility and reliability. These included changing the primary form of output to accelerate distribution, reducing the complexity of input to some of the programs to facilitate preparation, and introducing new capability to several of the programs to increase flexibility.

Table 3.2-21 is a tabulation of all SPAC computer programs executions. Unsuccessful executions are divided into three groups. Input errors include mispunched input cards and incorrect messages and option switches entered from the input console. System errors consist of system hardware and software failure. SPAC software errors include all SPAC software failures. The only SPAC software failure that occurred was diagnosed and compensated for in real-time during the mission and has been modified for use in support of Mission C.

3.2.5 LUNAR ENVIRONMENTAL DATA

3.2.5.1 Radiation Data

During Mission II, the radiation dosimetry measurement system functioned normally and provided data on the Earth's trapped radiation belts and on the radiation environment encountered by the spacecraft in transit to and near the Moon. Data obtained from the two dosimeters is shown in Table 3.2-22.

Dosimeter 1 (DF04), located near the film cassette, had a sensitivity of 0.25 rad per count with a capacity of 0 to 255 counts. Dosimeter 2 (DF05), located near the camera loop-er, had a sensitivity of 0.5 rad per count and a similar capacity of 0 to 255 counts.

Table 3.2-21: Lunar Orbiter II SPAC Program Execution

Program	Successful Executions	Input Errors	Unsuccessful Executions		Total
			System Errors	SPAC Software Errors	
CEUL	1038	14	7	0	1,059
DATL	597	30	11	0	638
TRBL	202	18	4	0	224
COGL	206	12	14	0	232
SGNL	43	3	0	0	46
GASL	109	7	1	0	117
HUBL	141	7	2	0	150
QUAL	99	4	0	0	103
SIDL	22	0	0	0	22
CORL	11	2	1	0	14
COOL	50	8	0	11*	69
UTAB	81	0	2	0	83
TIML	580	53	9	0	642
SEAL	135	2	0	0	137
Totals	3314	160	51	11	3,536
Percent of Totals	93.69%	4.56%	1.44%	0.31%	100%

Table 3.2-22: Radiation Data Record - Mission II

GMT	Radiation Counter	New Reading (RAD)
311:00:25:40.8 (Nov 7)	DF04	0.50
311:00:44:29.8 (Nov 7)	DF04	0.75
318:04:15:43.2 (Nov 14)	DF04	1.00
325:20:11:7.2 (Nov 21)	DF05	0.5
325:21:05:15.9 (Nov 21)	DF04	1.25
332:16:11:07 (Nov 28)	DF04	1.50
340:16: (03-13) (Dec 6)	DF05	1.00
348:06-10 (Dec 14)	DF04	2.00
355:09-10 (Dec 21)	DF05	1.50
356:09-357:0:57 (Dec 22)	DF04	2.25

Due to the inherent shielding of the spacecraft, the photo subsystem structure and the 2 grams-per-centimeter aluminum shielding provided the film supply cassette, it was estimated that solar flares of magnitude 2 or less would have negligible effect on the undeveloped film. Flares of greater magnitude could produce fog on the film.

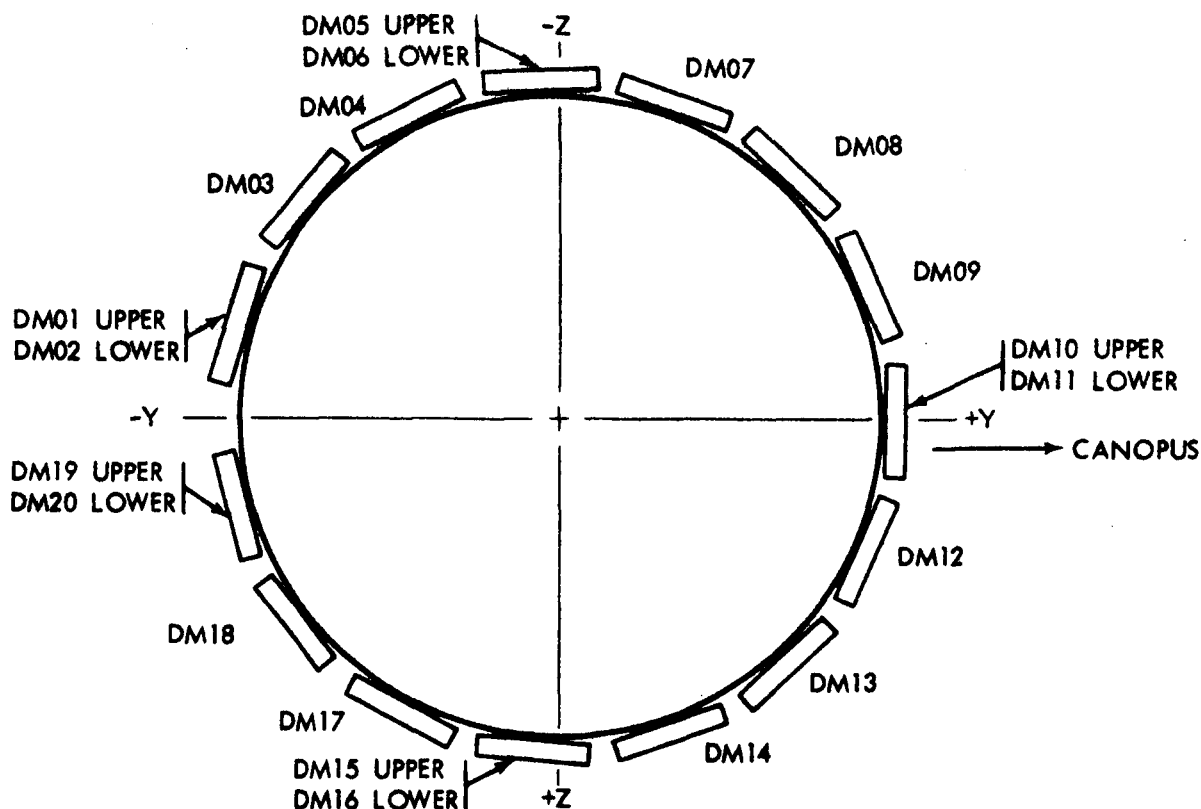


Figure 3.2-46: Micrometeoroid Detector Locations

The initial #1 dosimeter (DF04) readings indicate that the spacecraft penetrated the Van Allen Belts and received a total radiation dose of 0.75 rad at the film cassette. The #2 dosimeter (DF05) was not turned on until the Van Allen Belts were passed. From that time until January 4, the dosimeters have recorded a normal combination of galactic cosmic radiation and dosimeter noise.

If the dosimeter noise was constant, one could determine the galactic cosmic-ray background dose. However, the noise is a function of the temperature, and this dependence obscures the galactic radiation dose.

Before Mission II, it was suggested by Dr. Head of NASA- ERC that a proton event was highly probable about November 18. While the Sun was active during this portion of the mission, no proton event occurred.

3.2.5.2 Micrometeoroid Data

Three micrometeoroid hits, recorded during the photographic portion of Mission II, were recorded by discrete telemetry channel state changes recorded at:

Orbit 31 Day	319:12:45:40	DM04 (Detector 4)
Orbit 101 Day	329:17:22:55.9	DM05 (Detector 5)
Orbit 159 Day	338:02:04:47	DM13 (Detector 13)

See Figure 3.2-46 for locations of the micrometeoroid detectors. Figures 3.2-47, 3.2-48, 3.2-49 and 3.2-50 show the approximate locations of the Lunar Orbiter II when collision with meteoroids took place. Figure 3.2-51 plots true anomaly against time for convenience in calculations.

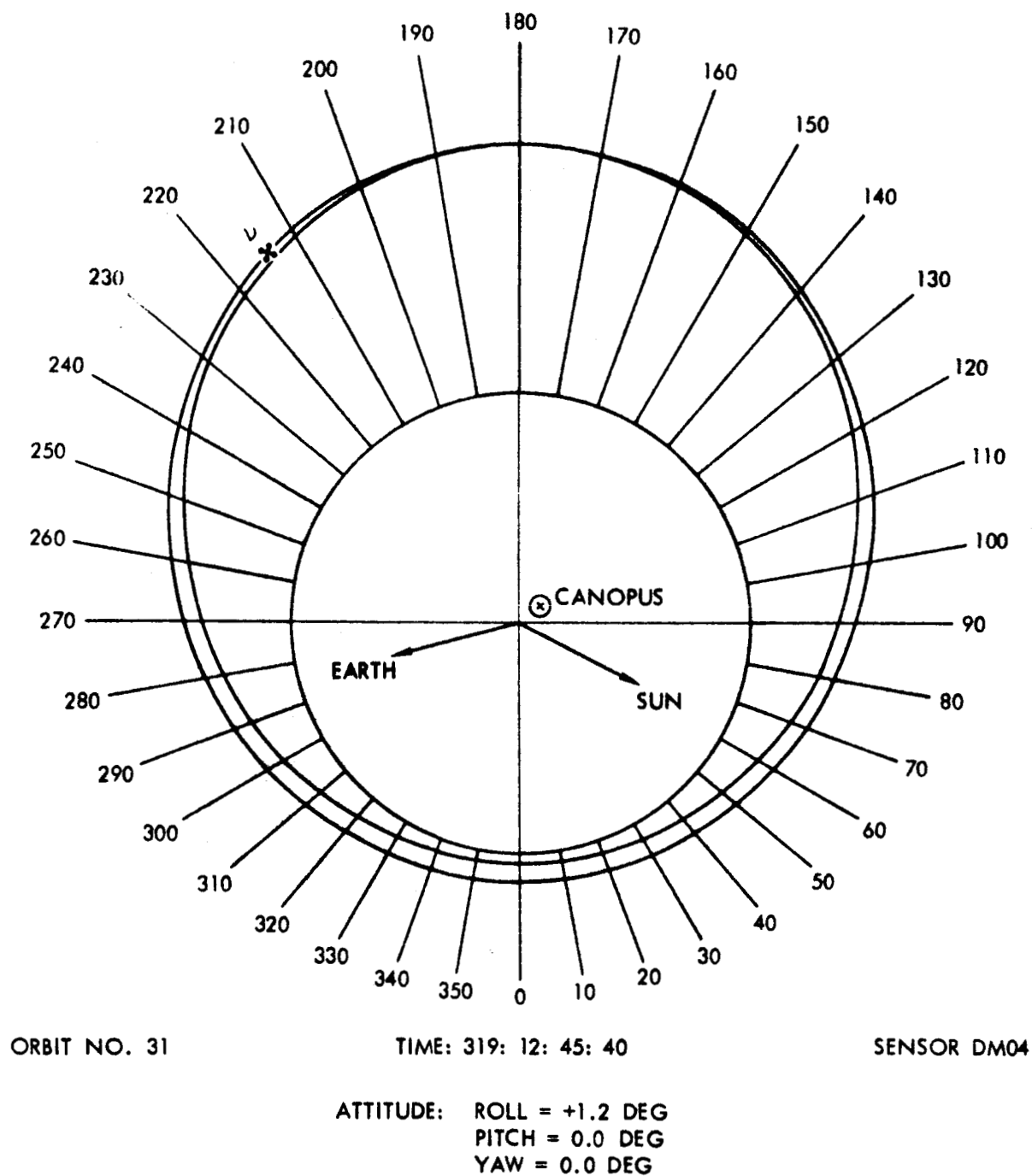


Figure 3.2-47: L.O. II Location at Meteoroid Collision—Detector 4

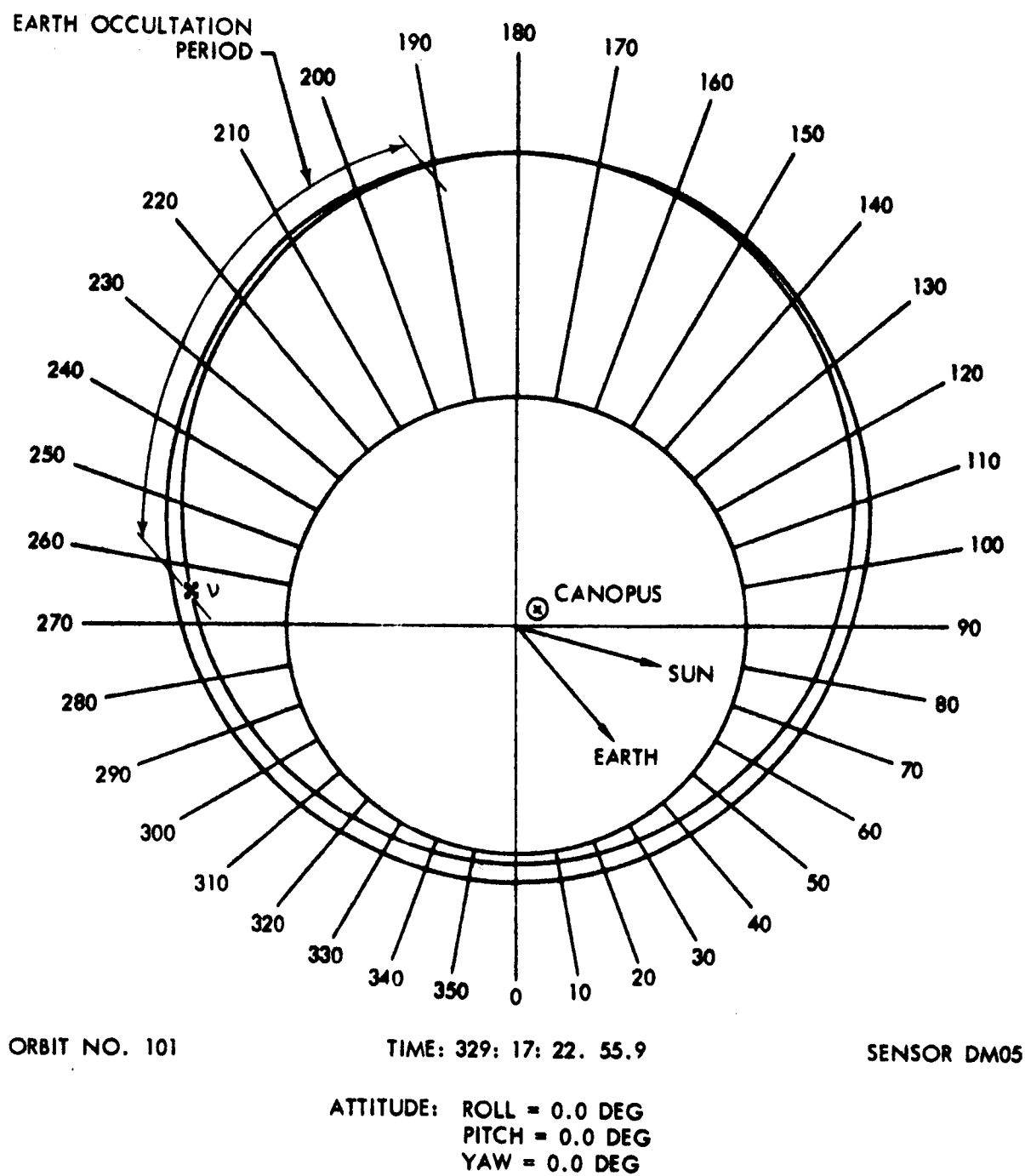
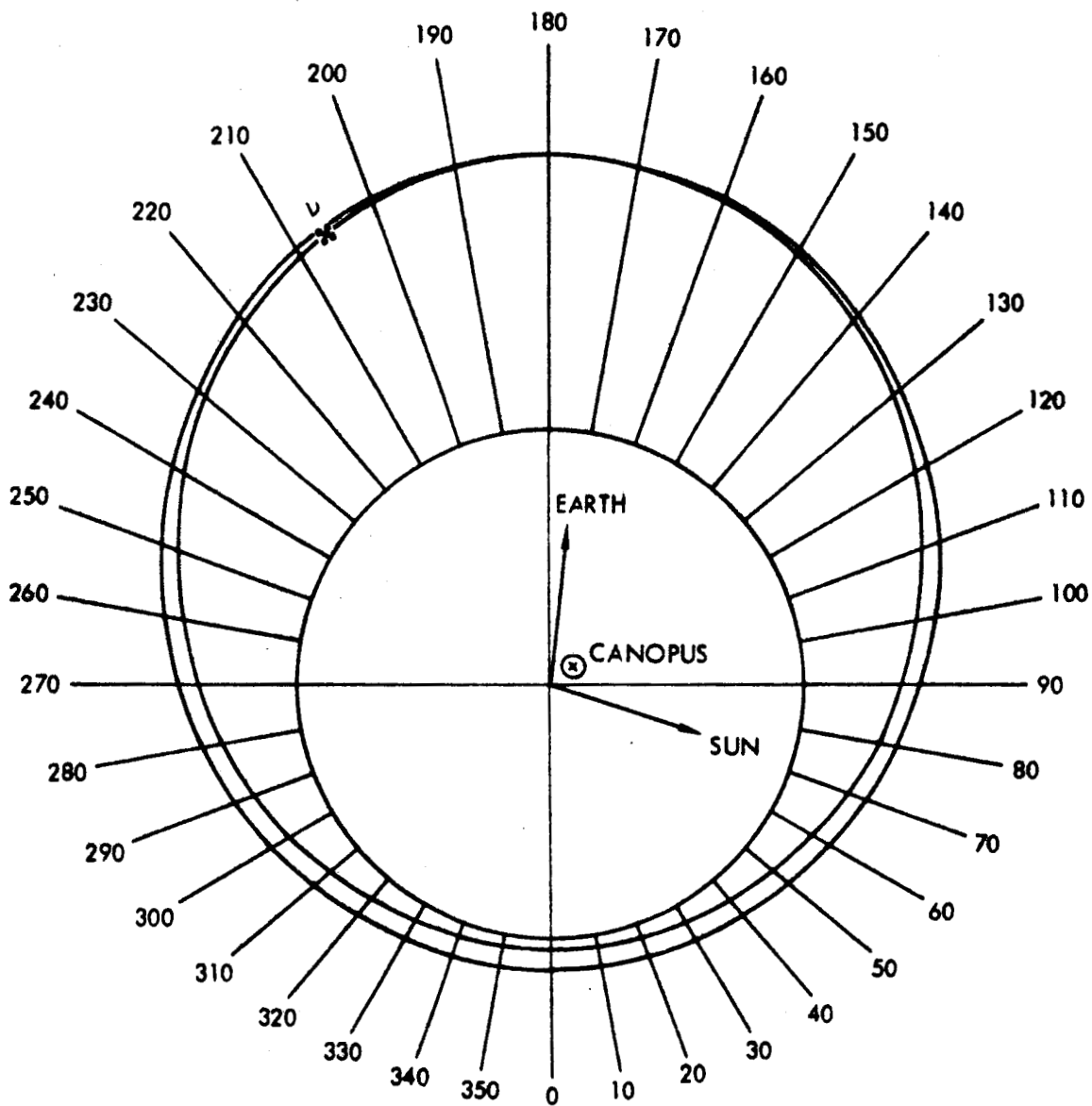


Figure 3.2-48: L.O. II Location at Meteoroid Collision—Detector 5



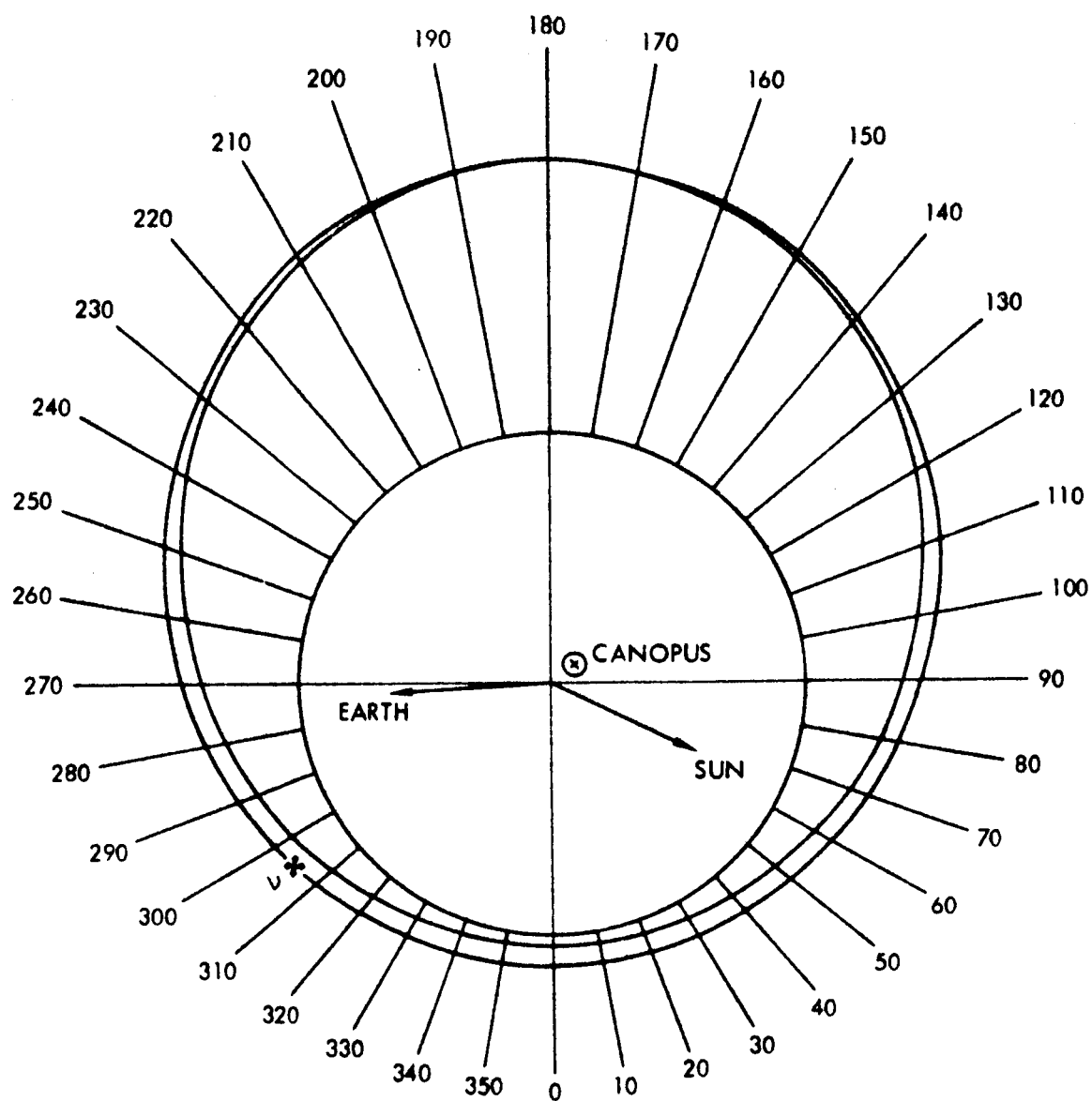
ORBIT NO. 159

TIME: 338: 02: 04: 07

SENSOR: DM13

ATTITUDE: ROLL = +3.0 DEG
 PITCH = +28.0 DEG
 YAW = +7.4 DEG

Figure 3.2-49: L.O. II Location at Meteoroid Collision—Detector 13



ORBIT NO.29

TIME: 319: 06: 24

SENSOR: ST04

ATTITUDE: ROLL = 0.0 DEG
PITCH = -23.0 DEG
YAW = +4.0 DEG

Figure 3.2-50: L.O. II Location at Suspected Meteoroid Collision—ST04 Thermistor

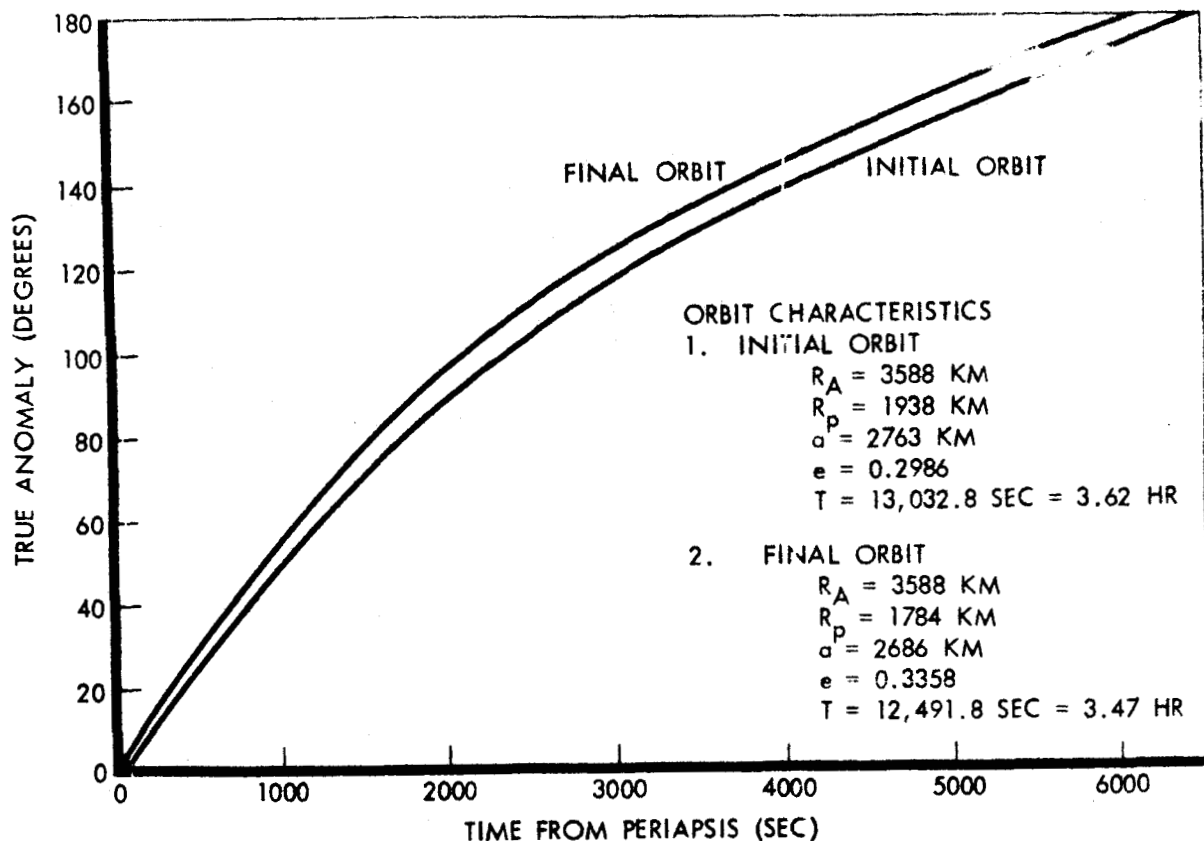


Figure 3.2-51: True Anomaly vs Time—Mission II Orbits

The actual time of impact on Detector 5 is not known since the event occurred during an Earth occultation period. No hit was indicated at earthset but at earthrise the detector recorded the impact.

Telemetered tank deck temperature data indicated a possible additional hit near the instrumentation thermistor. See Figure 3.2-41 for the history of the ST04 thermistor anomaly in Orbit 29. Figure 3.2-50 indicates the spacecraft location at the time of this inspected hit.

The increased micrometeoroid activity detected during Mission II may be related to the annual meteoric shower attributed to the Leonid meteor swarm. This meteoric activity occurs in mid-November of each year.

Appendix A

SUMMARY OF LUNAR ORBITER II ANOMALIES

CONTENTS

	Page
Star Tracker Performance During L.O. Mission II	128
Random Firing of Reaction Control Jets	132
Photo Subsystem - Differential Exposure Levels	132
Photo Subsystem - Improper 610-mm Shutter Count	132
Photo Subsystem - Improper Processing	133
Photo Subsystem - Readout Command	133
Thermal Control	134
TWTA - Helix Current Variation	134
30 kc - Subcarrier Oscillation	135

STAR TRACKER PERFORMANCE DURING L.O. MISSION II

Day 312 (See Figure A-1)

The spacecraft was operating locked on Canopus. Propellant squibs were fired; the star map voltage dropped; Canopus star tracker roll error voltage went to -4 degrees, the spacecraft moved a little in all axes and netted approximately 1.7 degrees off Canopus in roll. It is theorized that the shock from the squibs shook a dust particle off the spacecraft. The sunlit dust particle drifted past the tracker and led it off Canopus. The tracker remained locked at the minus roll limit because the tracker was still receiving enough light (presumably off the baffles) to keep it in the track mode. An alternate theory is that the squib firing may have excited a tracker vibration of higher frequency than the tracker servo could follow.

Day 314 (See Figure A-2)

After initial orbit injection, and after a period of darkness in which the spacecraft was being controlled by the tracker, the spacecraft emerged into sunlight. Roughly 50 seconds after getting the "sun presence" signal the star map voltage peaked, then dropped to background level, while the Canopus star tracker roll error signal went to 4 volts. It is theorized that a speck of dust which may have been traveling with the spacecraft was illuminated and passed through the tracker field of view, unlocking it from Canopus and causing it to lock on the baffles as before. Sun glint is discounted as a cause because of the long history of successful tracking prior to orbit injection.

Day 315 (See Figure A-3)

The tracker had been turned on during the lunar night, was tracking Canopus, and had been left on after emergence into sunlight. The star map output dropped quite suddenly to background level and the roll error went to -4 degrees. In a period of approximately 8 minutes the Inertial Reference Unit roll error grew steadily to approximately -2 degrees and the star map voltage rose more or less proportionately to about 1-1/4 volts, and then suddenly showed peaks near 5 volts. The star map then resumed its upward trend for a short period but further evidence was lost due to earthset. The field of view of the tracker was approximately 31 degrees from the illuminated moon. It is theorized that the abrupt rise in tracker roll error was caused by a drifting dust particle or moon glint and that subsequent phenomena were caused by moon glint as the spacecraft drifted.

POSSIBLE MODIFICATIONS

International Telephone and Telegraph has submitted a proposal for a study which would limit the tracker scan such that it could not "lock on" the baffles as it now does. Although this "lock-on" is an undesirable characteristic in the design, in the present situation the advantage to be gained by redesign is too minute to justify the cost (and hazard) involved in the change. The lock-on can be corrected operationally by simply turning the tracker off, then on whenever this unwanted lock-on occurs.

One possible alternative (not formally proposed) is imposition of a field-limiting aperture which would cut out about half of the roll field (present capability exceeds absolute requirements). This would reduce the probability of tracker diversion by glint by some factor (as much as 50% under some circumstances) but probably would not significantly improve capability to operate near the illuminated moon.

The only correction that would really provide operational freedom from the "anomalies" described above would be a marked reduction in sensitivity to off-axis light. To illustrate the probably difficulty of accomplishing this, an obvious step would be to provide a longer "barrel" on the optics of the tracker. The benefits would probably be less than one would assume from a geometric comparison, so to achieve much improvement a long tube would be required. A collapsible tube which must be oriented with an accuracy of perhaps ± 1 degree and whose mechanism must have a high reliability would be a design problem of considerable proportions.

RECOMMENDATION

Since the Canopus tracker does perform its basic function of orienting the spacecraft in roll attitude this allows closed loop mode updating. The flight can then be accomplished mainly on inertial hold with occasional updating. This method has been proven to work well in both flights with reasonable nitrogen consumption and minimal operational problems. Accordingly, it is recommended that the operational techniques and updating be used for the remaining flights.

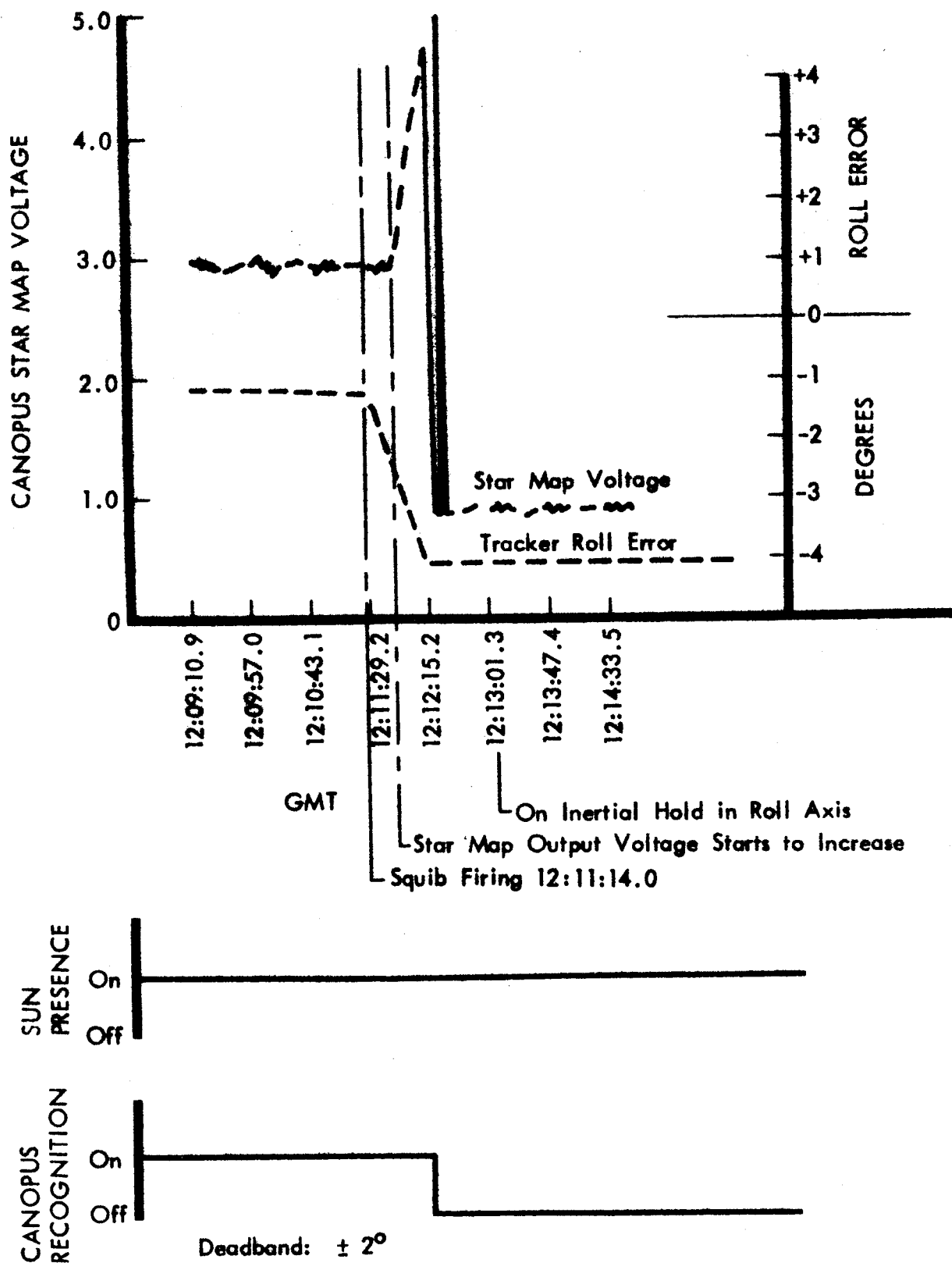


Figure A-1: LOSS OF CANOPUS AFTER FIRING SQUIB VALVES — DAY 312

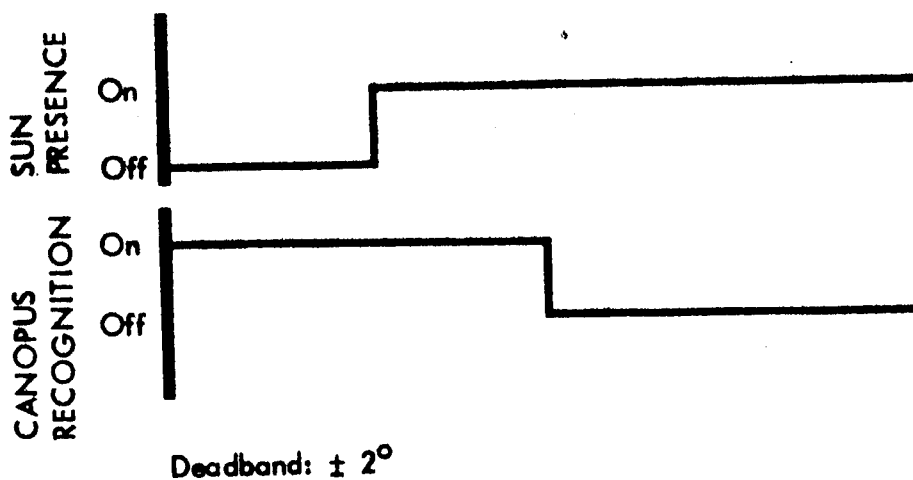
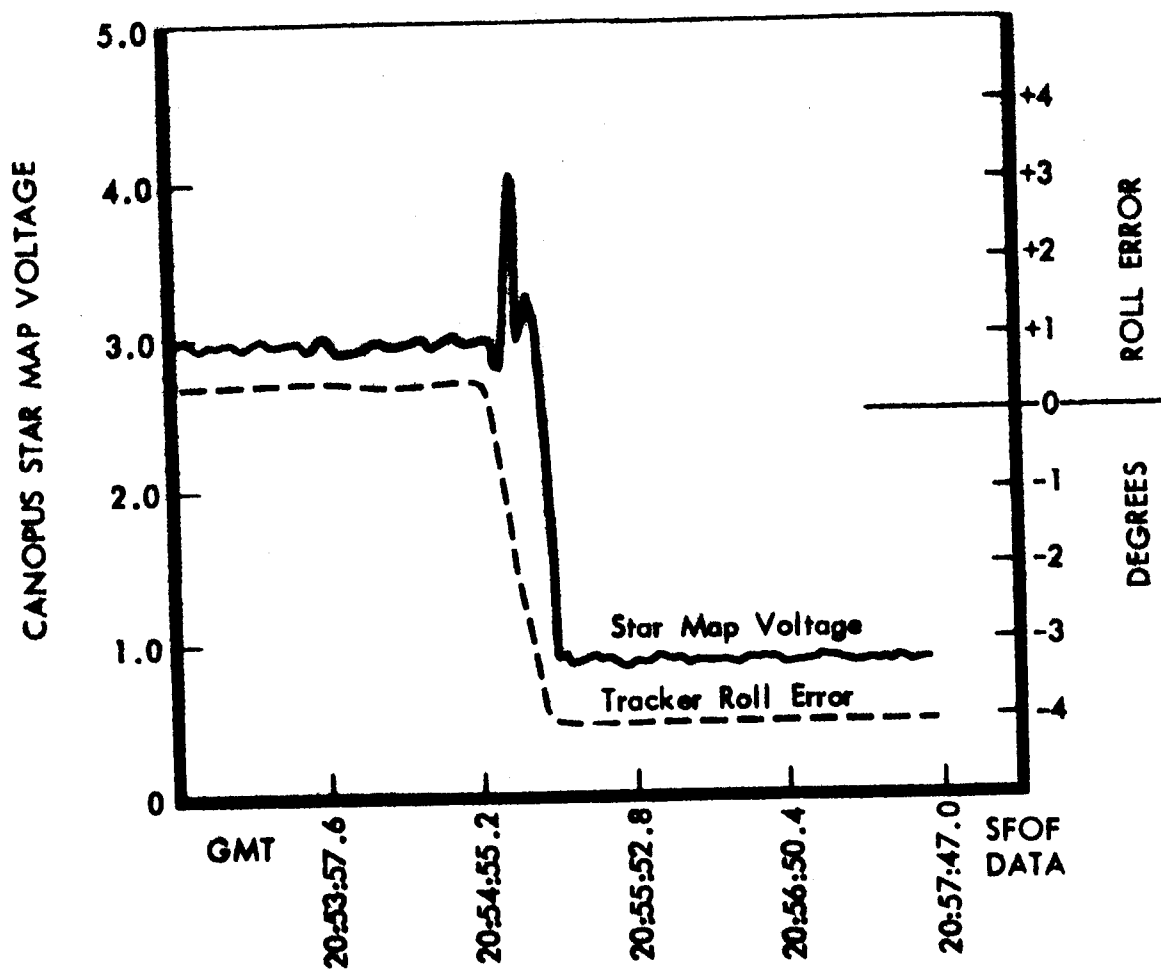


Figure A-2: LOSS OF CANOPUS AFTER INITIAL ORBIT INJECTION — DAY 314

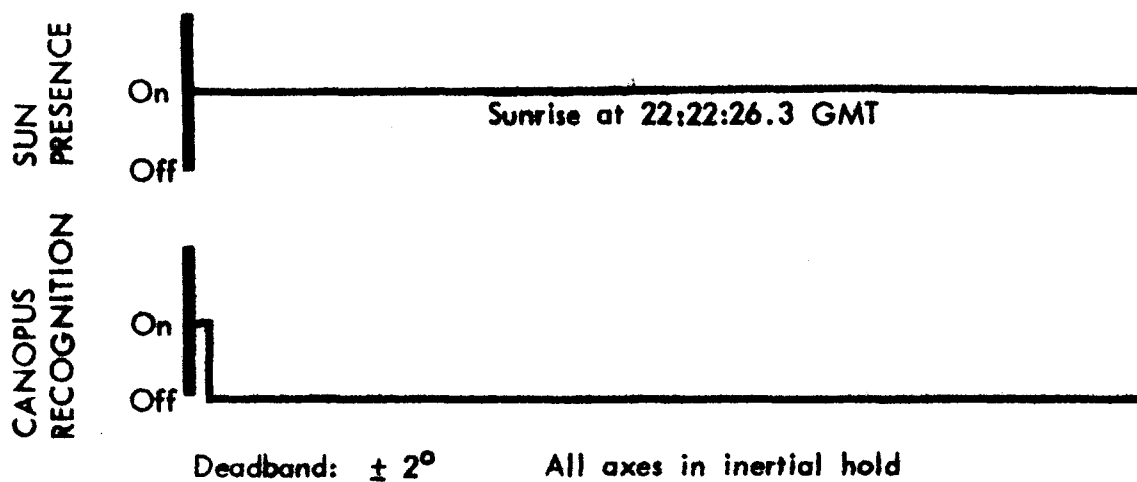
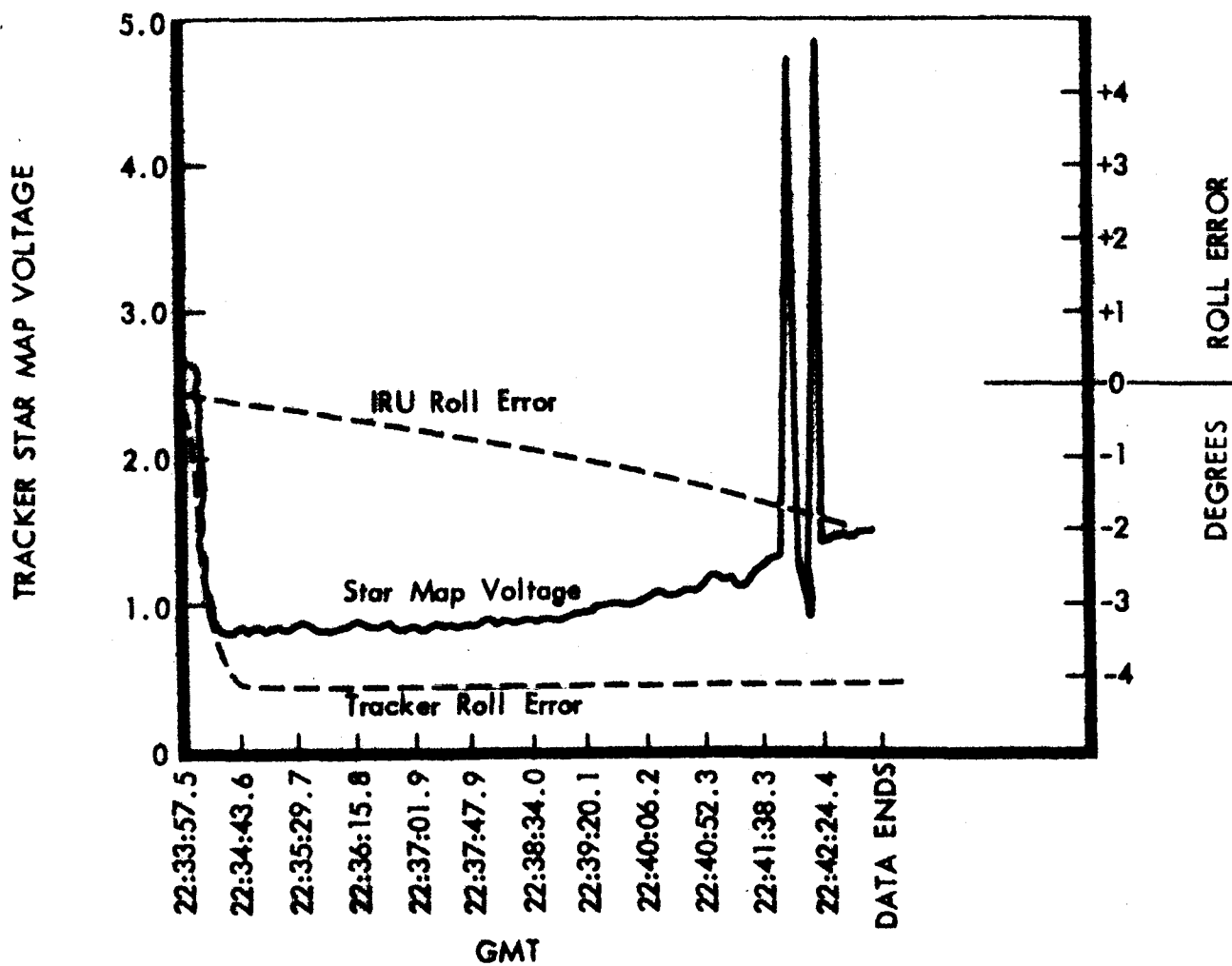


Figure H-3: LOSS OF CANOPUS WHILE TRACKING WITHIN 30° OF THE LIMB OF THE MOON. DAY 315

RANDOM FIRING OF REACTION CONTROL JETS

During Mission II orbits, it was noticed that whenever the Canopus tracker was turned on, a rate transient occurred somewhat randomly in all axes. The magnitudes were random between 0.0 and 0.04 degree per second. The sign is random but tends to be positive. Since this was measured by all gyros it was assumed that reaction control jets were actually firing as a result of the programmer signal to turn on the tracker.

The foregoing is not considered unusual. Whenever the Canopus tracker is turned on there is an error signal sent to the roll jets and the subsequent spacecraft movement caused by the roll thrusters may cause the other thrusters

to operate. The spacecraft inertial ref. unit is very sensitive to movement. This characteristic has been noted during the spacecraft ground testing wherein thrusters fired due to building vibration.

Although the foregoing random firing uses less than 0.2 pound of N₂ during a mission, this is offset by lower than predicted limit cycle rates resulting from single pulsing, rather than double or triple pulsing of the limit cycle control system.

This is not considered a failure.

PHOTO SUBSYSTEM - DIFFERENTIAL EXPOSURE LEVELS

On both PS-4 (Mission I) and PS-6 (Mission II) telephoto and wide-angle frames exposed simultaneously show density inequalities of approximately 0.3. This phenomenon was noticed during evaluation of Mission I photographs. The 80-mm frames had received more exposure than the corresponding 610-mm frames. This was discussed with Eastman Kodak and NASA in early October. Approximately October 18th, a test on PS-6 at ETR confirmed the numerical values of the transmission difference.

On the basis of the above and other Boeing-Kodak telecons, a Kodak proposal was submitted to Boeing on November 4 for the installation of a neutral-density filter on the 80-mm camera for exposure equalization. On December 1, NASA directed Boeing to present technical and cost proposals with schedule for the above by De-

cember 9. NASA further directed Boeing to proceed with filter preparation. A January 5, 1967, NASA letter further directed installation and test of the filters on the remaining photo subsystems.

The filter installed was a screw-in type using the threads already available on the front cell of the 80-mm lens. A small hole in the metal mount was provided to prevent pressure differential from building up during flight. The filter itself was evaporated inconel on a glass substrate with a nominal density of 0.20. The inconel side of the filter faced away from the 80-mm lens and the other side was coated with an anti-reflector.

This filter installation will be used on future L.O. missions.

PHOTO SUBSYSTEM - IMPROPER 610-MM SHUTTER COUNT

Telemetered indication of shutter counts (telemetry channel PB 04) showed erratic operation of the 610-mm shutter as follows:

Orbit of First Occurrence	Camera Frames	Shutter Counts
51*	8	17
51	1	2
60*	8	4
61	8	0
62	8	8
66*	8	3

*These phenomena occurred only once - the others occurred more than once.

Analysis of other flight data showed proper exposure and correct number of film advances for commanded number of exposures.

Kodak analysis of the failure, including results of special tests on Photo Subsystem 1A, indicated the failure was of a random nature, a degradation or intermittent failure of one or more of the several components or connections in the first flip-flop of the shutter counter circuitry. Approximately two dozen nearly identical flip-flop circuits performed satisfactorily during the first two Lunar Orbiter missions. Since shutter

operation was normal, the malfunction was not an operational or mission-critical failure. No

redesign or rework of follow-on units is contemplated.

PHOTO SUBSYSTEM - IMPROPER PROCESSING

Available prints, equivalent to approximately 90% of the flight film, were examined for processing defects other than that associated with processor stop.

Frame Affected	Site	Photo Orbit
19 T	IIP-1	52
27 T	IIS-2a	53
67 T	IIP-5	62
71 T	IIP-5	62
75 T	IIS-5	64
101 T	IIP-7a	76
101 WA	IIP-7a	76
102 T	IIP-7a	76
103 T	IIP-7a	76
118 WA	IIP-8a	80
119 T	IIP-8a	80
131 T	IIP-8c	82
185 T	IIP-12a	93
188 T	IIP-12b	94
215 T	IIS-17	102

In particular the film of Site IIP-7a (Orbit 76 photos) was improperly processed. Numerous underdeveloped areas are apparent, appearing as a mottled or lace effect. There are also two to four streaks lengthwise that detract from the appearance of the photos. It is suspected that these undeveloped areas are caused by defects in the bimaf due to manufacturing defects, bubbles, dryout, or improper contact with the film.

No problems in the photo subsystem instrumentation were noticed at any time during the processing of this area.

The quality and quantity of photo data was not significantly decreased.

PHOTO SUBSYSTEM - READOUT COMMAND

At the end of seven final readout sequences the readout electronics did not turn off with the normal stored program commands, but required a real-time command for turnoff.

Termination of the readout sequence at the end of each of the following seven orbits did not occur in response to the stored program command, but required execution of one additional real-time command, RTC 16, "readout drive on." In each case the readout sequence terminated in response to the first supplemental command.

The anomalous occurrences were as follows:

Orbit No.	Day & Time of Termination (GMT)
127	333 14:29:43
128	333 17:52:14
131	334 04:18:01
150	336 22:24:10
176	340 16:47:40
180	341 06:41:58
181	341 10:09:08

This is similar to problems occurring in the engineering model which were caused by the backing off (reversing) of the OMS drum after power was removed, as is explained fully in EK Engineering Note L-016957-KU dated December 15, 1965. The pressure of the spot stop cam on the ramp (when the OMS stops prior to the dwell area) can cause a reverse rotation which allow the readout electronics to turn back on as the encoder position changes.

The focus lines were visible in the video output, verifying that the OMS was not in the spot stop position.

The real-time command executed caused the video signal to turn off soon after initiated, which verifies that the OMS had reversed and had been stopped only slightly ahead of the normal stop position. This can be caused by a slight wear on the cam, bearings, motor-calculated drift, slight binding of the OMS in this location, changes in the encoder band, wear on the encoder brushes, or a shift in the encoder setting.

Kodak analysis, based upon available flight data is that the phenomenon is most likely due to a time/temperature effect on the mechanism and lubrication, produced by the long readout periods, resulting in a back-sliding of the gate cam follower on the front side of the OMS cam, causing the readout electronics to turn back on. The failure occurred only after extended readout

periods (more than two frames), and had never occurred after shorter test or limited flight readout periods.

Operational procedures for Mission III will provide real-time backup commands for readout turnoff, similar to Mission II.

THERMAL CONTROL SUMMARY

The equipment mounting deck (EMD) temperatures on Mission I increased during flight at a rate higher than anticipated. Since the increased solar intensity for the Mission II flight would be approximately 6°F higher, it was apparent that Mission II should be altered to fly "off-Sun" and/or the paint on the EMD should be improved to accomplish the basic photographic mission. After investigating several possibilities, it was decided to overcoat the EMD on the Mission II spacecraft with 2 mils of S-13G paint, based on 350 equivalent sun hours of in situ testing by Hughes Aircraft Co. on a B-1056 paint coupon overcoated with S-13G. The Hughes test data indicated that approximately a 10°F improvement in spacecraft temperatures could be expected with the S-13G overcoat. Also Mission II would basically be flown "off-Sun," except during the picture-taking phase of the mission, to retard the degradation of the EMD paint. In addition to the EMD overcoating, the Mission II spacecraft was instrumented with four paint coupons to obtain flight data on the following coatings:

- 1) B-1056 coupon.
- 2) B-1056 coupon with 2 mils B-1059 overcoat.
- 3) B-1056 coupon with 2 mils S-13G overcoat.
- 4) B-1056 coupon with second surface mirror.

The S-13G overcoating on the EMD resulted in approximately a 9°F improvement in the EMD temperatures on Mission II as compared to Mission I EMD temperatures. The S-13G over B-1056 coupon was approximately 7°F cooler

than the B-1056 coupon and the B-1059 over B-1056 coupon was approximately 3°F cooler than the B-1056 coupon. The second surface mirror temperature varied between -77°F and +4°F during the initial orbits and between -69°F and +21°F by the 90th orbit. The EMD temperature by the IRU (STO3) and the transponder (STO2) had reached 93°F by the end of the picture taking phase of the mission.

The improved thermal control on Mission II has resulted in CCN 105 which overcoats the EMD on Mission III with S-13G. CCN 105 also authorizes installation of paint coupons on remaining spacecraft (four paint coupons per spacecraft). The paint coupons on Missions III and IV are:

- 1) B-1056 coupon with 2 mils S-13G overcoat.
- 2) B-1060 coupon (same as S-13G except uses TMC catalyst).
- 3) S-13-G coupon.
- 4) Surveyor white coupon.

The paint coupons to be flown on Mission V will be determined at a later date.

In summary, flight data demonstrates that overcoating the EMD with S-13G and flying the spacecraft "off-Sun" does provide adequate thermal control capability to accomplish the photographic mission on future flights. Also, the solar intensity will be less for all flights between now and November 1967, providing up to approximately 12°F improvement in thermal control.

TWTA FAILURE INVESTIGATION

TWTA Serial Number 18 used in Mission II failed to operate when commanded "on" in Orbits 179 and 181. Prior to failure the helix current had exhibited growth, and indication of

step changes similar to conditions noted during ground testing.

On December 6, at approximately 5:30 pm PST,

the "TWTA on" command (RTC 115) was executed. The collector current (telemetry indication) should change from -20 to 0.6 ma, and approximately 1 minute later should rise to approximately 40 ma. This time the first three T/M frames after the "execute" command showed 0.61 ma, but on the fourth frame the collector current changed to 8 ma and continued at this level. Bus current increased 0.5 amp at time of the execute (approximately normal); a normal jump of 1.3 amps 1 minute after execute did not occur. Deck temperature (ST-01) was 59°F at turn-on.

After approximately 8 minutes "TWTA off" (RTC 116) was executed. The collector current did not change until seven frames later. After seven frames following the "TWTA off" execute, all TWTA T/M indications changed to the normal off readings.

The "TWTA on" (RTC-115) command was executed a total of four times and "TWTA off" (RTC-116) was executed twice, without detectable change.

Command RTC-7, "rotate antenna plus one degree," was executed and performed to prove that the command link was operating normally.

Station 41 reported a "glitch" in receiver AGC after the RTC 115 "execute" command on Orbit 178. Normal condition is a rise from -138 to -99 dbm. In this case there was a momentary 10-db drop before the power rose. In Orbit 179 there was a momentary 5-db drop and the signal strength returned to -138 dbm.

Tests on Spacecraft 1 and bench tests on components show that the initial turn-on current has a peak of 8 to 11 amperes, which has a duration of approximately 2 milliseconds, followed by a low steady-state value for approximately a minute until the high-voltage turn-on. At this time six rather sharp triangular spikes, each of

roughly 2 milliseconds duration and having 6 amp peaks, occur. (This is believed to be normal; however, there is no ready explanation of why it occurs.) This is followed by a steady-state current of approximately 1.7 amps.

Transponder power output remained within 437 to 447 mw during the period of interest.

	Orbit 178	Orbit 179
EE-07 (bus current, amps)		
frame # 1	3.75	3.75
2	4.12	3.75
3	5.23	3.68
4		4.00
5		4.06 Commanded Off
6		4.00
7		4.00
13		3.56
CE-05 (Coll. current, ma)		
frame # 1		-20.79
2		0.61
3		0.61
4		0.61
5		8.00
6		8.00
7		8.00
13		-20

CONCLUSIONS

(Conclusions must be recognized as tentative and unsubstantiated.)

There was an initial internal failure of the TWTA power supply caused by rapid voltage rise; this caused full bus voltage to be applied to the transformers which supply the tube (normally regulated to 24 volts). Complete failure ensued.

30-KC SUBCARRIER OSCILLATOR OFFSET FAILURE REPORT LO-II-4 (05009)

Two 30-kc subcarrier oscillators are provided in the modulation selector for use in different modes of operation. During L. O. Mission II the Mode 1 and 3 oscillator was offset in center frequency by a maximum of 110 cycles. The specification on the component permits 90 cycles; however, the ground system was suf-

ficiently flexible to enable continued reception of all signals without significant difficulty. This change of frequency was later shown to have occurred during ground testing of Spacecraft 5 but was not cause for rejection because measurement of this frequency was not specified as a spacecraft level test.

Spacecrafts 6 and 7 have been checked for this characteristic and both are well within specification requirements (within 15 cps of nominal). Review of FAT data indicates that the frequency change on Serial Number 09 (in Spacecraft 5)

was the progressive, occurred during successive high-temperature exposures, and apparently was stabilizing. No further action is expected (except to check frequency before flight for all future launches).